

CHALMERS TEKNISKA HÖGSKOLA



CHALMERS UNIVERSITY OF TECHNOLOGY
GÖTEBORG
SWEDEN

SHIP FLOW CALCULATIONS AND RESISTANCE MINIMIZATION

Keun Jae Kim

CHALMERS UNIVERSITY OF TECHNOLOGY

SHIP FLOW CALCULATIONS AND RESISTANCE MINIMIZATION

by

Keun Jae Kim



Submitted to the School of Mechanical Engineering,
Chalmers University of Technology in partial
fulfillment of the requirements for the degree
of Doctor of Philosophy.

DIVISION OF MARINE HYDRODYNAMICS
CHALMERS UNIVERSITY OF TECHNOLOGY
S-412 96 GÖTEBORG, SWEDEN.

Göteborg 1989

ISBN 91-7032-443-3
BIBLIOTEKETS REPROSERVICE
Chalmers University of Technology
Göteborg, Sweden, 1989

Ship Flow Calculations and Resistance Minimization

Keun Jae Kim

**Division of Marine Hydrodynamics
1989**

DISSERTATION

This dissertation is based on the following four appended papers:

- Paper A: Kim, Keun-Jae, 1988 "Calculation of ship viscous resistance using boundary layer theory based on first or higher order approximations", Report No 72, Department of Marine Hydrodynamics, Chalmers University of Technology, Gothenburg, Sweden
- Paper B: Kim, Keun-Jae, 1989 "A higher order panel method for calculating free surface potential flows with linear free surface boundary conditions", SSPA Report 2966-2, SSPA Maritime Consulting AB, Gothenburg, Sweden
- Paper C: Kim, Keun-Jae, 1989 "A higher order panel method for calculating free surface potential flows with non-linear free surface boundary conditions", SSPA Report 2966-1, SSPA Maritime Consulting AB, Gothenburg, Sweden
- Paper D: Kim, Keun-Jae, Esping, Björn and Holm, Dan, 1989 "Numerical method for minimizing ship resistance", SSPA Report 2964-1, SSPA Maritime Consulting AB, Gothenburg, Sweden

CONTENTS

	page
DISSERTATION	2
CONTENTS	3
LIST OF SYMBOLS	4
ABSTRACT	7
ACKNOWLEDGEMENTS	9
I. INTRODUCTION	11
II. MATHEMATICAL STATEMENT OF THE PROBLEM	18
II-1. The Formulation of the Viscous Flow Problem	19
II-2. The Formulation of the Potential Flow Problem	20
II-3. The Formulation of the Optimization Problem	22
III. NUMERICAL SOLUTION OF THE PROBLEM	25
III-1. The Solution of the Viscous Flow Problem	25
III-2. The Solution of the Potential Flow Problem	30
III-3. The Solution of the Optimization Problem	33
IV. CONCLUSIONS	39
V. FUTURE APPLICATIONS AND DEVELOPMENTS	41
VI. SUMMARY OF APPENDED PAPERS	42
REFERENCES	46

APPENDED PAPERS

Paper A: Calculation of ship viscous resistance using boundary layer theory based on first or higher order approximations

Paper B: A higher order panel method for calculating free surface potential flows with linear free surface boundary conditions

Paper C: A higher order panel method for calculating free surface potential flows with non-linear free surface boundary conditions

Paper D: Numerical method for minimizing ship resistance

LIST OF SYMBOLS

$[A], A_{ij}$	Coefficient matrix for the linear equation system
$\{B\}, B_i$	Right hand side vector for the linear equation system
C_B	Block coefficient
C_E	Entrainment coefficient
C_F	Skin friction coefficient (total)
C_f	Skin friction coefficient (local) in x-direction
C_p	Pressure coefficient
C_v	Viscous resistance coefficient
C_W	Wave resistance coefficient
E	Entrainment rate
F_n	Froude number V_s/\sqrt{gL}
g	Acceleration of gravity
g_i, \bar{g}_i	Geometrical constraints and their upper bound
H_1	Head's shape factor for the velocity profile
H_{12}	Shape factor for velocity profiles in boundary layer
$h=Z(X,Y)$	Wave elevation
h_1, h_2, h_3	Metric coefficients
I_{px}, I_{pz}	Pressure integrals
I_{k1x}, I_{k3x}	Curvature integrals
I_{k1z}, I_{k3z}	
K_{12}, K_{32}	Normal curvatures of surfaces $y=\text{const}$ along lines $z=\text{const}$ and $x=\text{const}$ respectively
K_{120}, K_{320}	As above, but for $y=0$
K_{13}, K_{31}	Geodesic curvatures of lines $z=\text{const}$ and $x=\text{const}$ on surfaces $y=\text{const}$
K_{130}, K_{310}	As above, but for $y=0$
M	Number of adjacent panels
NC	Number of constraints
ND	Number of design variables
NE	Total number of panels
NF	Number of panels on the free surface
NH	Number of panels on the body
\bar{N}	Unit normal vector with components (N_x, N_y, N_z) in reference co-ordinates

\vec{N}^E	Unit normal vector with components (N_ξ, N_η, N_ζ) in panel co-ordinates
p	Static pressure
R_F	Skin friction resistance
R_N	Reynolds number
R_P	Pressure resistance
R_T	Total resistance of ship
R_V	Viscous resistance
R_{VP}	Viscous pressure resistance
R_W	Wave resistance
s	Arc length along the streamline
S_{FC}	Area of free surface covered by source panel
U_B	Component of the induced velocity at the free surface by hull source
U, V, W	Mean velocity components
u', v', w'	Fluctuating velocity components
U_e, V_e, W_e	Mean velocity components at the edge of the boundary layer
U_∞	Magnitude of the uniform onset flow velocity
\bar{V}	Flow velocity with components (ϕ_x, ϕ_y, ϕ_z) or (u, v, w)
V_S	Ship speed
V_H	Displacement volume of ship
$[X], [Y]$	Matrices of induced velocities
$[Z]$	
X, Y, Z	Global reference co-ordinates
x, y, z	Local coordinates
α	Linking factor to governing point
β_k	Linking factor for master design variable k
β_0	Wall cross flow angle
δ	Boundary layer thickness
$\bar{\delta}$	Generalized boundary layer thickness
δ_1, δ_2	Displacement thickness
$\bar{\delta}_1, \bar{\delta}_2$	Generalized displacement thickness

θ_{11}, θ_{12}	Momentum thickness
θ_{21}, θ_{22}	
$\bar{\theta}_{11}, \bar{\theta}_{12}$	Generalized momentum thickness
$\bar{\theta}_{21}, \bar{\theta}_{22}$	
$\theta_{11\infty}$	Momentum thickness in the far wake
θ_{11t}	Momentum thickness at the trailing edge
ϵ	Convergence parameter for sensitivity analysis
ϵ_1	Convergence tolerance for optimization procedure
ϵ_2	Convergence tolerance for optimization procedure
σ	Source density
ϕ	Total velocity potential
Φ	Velocity potential
ν	Kinematic viscosity
ρ	Density
τ_{xy}, τ_{zy}	Wall shear stress in x and z direction respectively
γ	Design variable
λ	Lagrange multipliers
ξ, η, ζ	Panel co-ordinates

ABSTRACT

A numerical procedure for the analysis of the hydrodynamic performance of ships and the design of optimized hull forms is presented. The emphasis of the paper lies on two essential aspects of the problem: (i) how the hydrodynamic performance of a ship can be predicted in a more accurate way, and (ii) how the performance can be improved through systematic variation of the shape of the hull form in a more efficient way.

A boundary layer method of the integral type is developed based on the first and higher order approximations to predict the viscous resistance and flow properties around ship hulls and different levels of approximation are compared to find the most suitable one for a hull form optimization procedure.

A higher order panel method for calculating free surface potential flows is developed based on the Hess-Smith-Dawson theory. Source singularities are distributed on the hull and part of the free surface and the strengths of these sources are determined to satisfy the hull and free surface boundary conditions. In contrast to a first-order panel method that uses flat panels, usually with constant source density, the present method uses curved panels generated by polynomials of the second degree with linearly varying source density. Other improvements, as compared to the original Dawson method, are that the panel grid on the free surface is independent of the streamlines and that the resistance is computed in a more accurate way.

Promising results are obtained for the method based on linearized free surface boundary conditions. An improvement, over first order linear methods, in the prediction of wave resistance has been achieved.

A more accurate method, based on non-linear free surface boundary conditions has also been developed. The variable strength of

source singularities is adjusted to satisfy the normal velocity boundary condition on the wetted hull surface and the non-linear form of the free surface condition on the wavy surface. An exact solution is obtained through iterations and in each iteration the free surface boundary condition is linearized based on the small perturbation principle, about the previous solution. Much better converged solutions have been achieved.

Having all the numerical tools for hydrodynamic analysis, a mathematical procedure for optimizing hull forms is developed. The optimal hull form design system enables the designer to include advanced hydrodynamic performance predictions at an early stage of the design process, allowing a systematic evaluation of the hydrodynamic performance characteristics as a function of the hull geometry. This system is based on a rapid design oriented first order boundary layer method and the linear type of wave resistance theory for hydrodynamic analysis. The objective function is taken as a linear combination of viscous and wave resistance. The resulting large, highly constrained non-linear optimization problem is solved by a dual method of mathematical programming.

The entire process of hydrodynamic analysis, geometrical modelling and optimization thus attempts to imitate the traditional hull form design procedure. The system of computer programs can be used to develop mathematically faired and hydrodynamically desirable hull forms from an existing ship.

Keywords:

Ship flow, viscous resistance, wave resistance, resistance minimization, viscous flow, wake, boundary layer theory, integral method, potential flow, free surface boundary condition, panel method, optimization, objective function, constraints, mathematical programming, dual technique

Footnote: The term "hydrodynamic performance" used in the present paper identifies "resistance performance".

ACKNOWLEDGEMENTS

It is a great pleasure to me to thank all the people who have influenced my thinking and contributed to my research work during my years at the Department of Marine Hydrodynamics, CTH and at the Department of Fluid Mechanics, SSPA.

I wish to express my genuine respect and sincere gratitude to Prof Lars Larsson for his inspiring guidance and invaluable encouragement during the course of my studies. His advice and suggestions are always valuable and the arrangement for cooperative work on Paper D with ALFGAM Optimizing AB is much appreciated.

Grateful thanks are also due to Prof Gilbert Dyne for his deep understanding and spiritual encouragement, and to Prof Jan Bäcklund of the Royal Institute of Technology for his great interest and support during the course of the work on Paper D.

I am also most grateful to Dr K-S Min of Daewoo Shipbuilding & Heavy Machinery Ltd, Korea for his important suggestion on Paper D of the thesis.

Thanks are expressed to Dr Björn E D Esping and Dr Dan Holm of ALFGAM Optimizing AB, who worked together with me on the resistance minimization project of Paper D and who kindly permitted the use of the OASIS-ALADDIN optimization system and their computer facilities.

Further I wish to express my thanks to all my colleagues at Chalmers and SSPA, particularly Dr L Broberg, who has given his valuable time in discussions of great interest, Mr John Olofson who has provided good working environment in SSPA's computer. I wish to thank Prof C-O Larsson, Mr D-H Zhang and Miss Eira Samuelsson for their constructive advice and help in many respects.

I also repeat my thanks to the people mentioned in the appended papers, who have helped me in many ways with the preparation of the thesis. In addition I would like to thank Mrs Brita Svanberg for her careful preparation of all the figures. I also thank Mrs Elisabeth Algar who typed Papers C and D of the thesis, and Mrs Barbara Karsberg for her excellent typing and for correcting my linguistic errors.

Finally, but foremost, I wish to dedicate this thesis to my father, Eui-Hyun Kim, and my wife, Eun-Mee Kim, as a small acknowledgement of their everlasting love and affection.

The work was funded by the Swedish Board for Technical Development, financial support for living expenses being provided by Daewoo Shipbuilding & Heavy Machinery Ltd, Korea for the first four years and thereafter by SSPA.

I am very grateful for this support and for the provision of typing and computing facilities.

I. INTRODUCTION

An optimal design of a hull form may be defined as the rational establishment of a hull form that is the best of all possible designs within a prescribed objective and a given set of geometrical limitations. This topic is intellectually attractive as well as technically significant, since it combines a comprehensive mathematical model for the evaluation of the hydrodynamic performance and the important sensitivity analysis and the capability of geometrical modelling and optimization with respect to the governing design variables. The development of each element has taken place particularly over the last 20-25 years, and has been strongly boosted by the availability of large, high speed computers.

Until recently, the only way to evaluate ship performance was through experiment. Although computational ship hydrodynamics including a free surface has a long history, its usefulness has been limited due to the rather drastic simplifications required for an analytical approach to the problem. The past 10 years have, however, seen major achievements not only in the free surface potential flow prediction but also in the ability to predict the viscous flow in the boundary layer and wake. Numerical predictions of ship performance have become an important part of the design procedure.

Currently, research on the prediction of ship performance may very roughly be said to follow two main paths. Along the first one, research is primarily devoted to the development of calculation methods of ship viscous resistance.

Boundary layer theory has been frequently applied to investigate the flow properties around ships and to predict the viscous resistance. Many methods are found in the literature; a number of good ones were tested at the SSPA-ITTC WORKSHOP in 1980, [1], and more have been presented since then [2, 3]. These include

integral types of boundary layer calculation methods, more complicated methods based on partial differential equations, and higher order modifications of these.

Successful predictions have been made of the flow over a large part of the hull. However, most boundary layer calculations usually fail to give sufficient accuracy in the prediction of the stern flow. This failure is due to a number of reasons, including the neglect of the higher order effects, such as the curvature effect, the normal pressure gradient effect and the viscid/inviscid interaction effect, the possibility of a local region of separated flow and the existence of the free surface. Several attempts, based on partial differential equations, have been made to overcome these difficulties in total or in part [2, 3]. At SSPA such a method has recently been developed by Broberg & Zhang, [4]. Methods of this kind are, however, too expensive to be used in an optimization process where systematic changes of the hull form are to be made.

Paper A describes four numerical methods, which are capable of determining the local flow properties and overall drag on ship hulls. The simplest one is of first order and represents a simplification of Larsson's method [5] to enable very rapid calculations. Three methods are of higher order, incorporating a varying number of higher order effects to find the best trade off between accuracy and computational effort [6].

Along the other main path of research, the emphasis is laid on the free surface potential flow around ships.

This problem is very well defined in a purely mathematical sense, but a number of numerical methods based on different approximations are found in the literature; a number of good ones were tested on several well specified test cases at the DTNSRDC WORKSHOPS in 1979 [7] and 1983 [8], and many interesting papers have also been presented at international seminars [9] and

conferences [10-13]. A major break-through was the paper presented by C W Dawson at the Second Conference on Numerical Hydrodynamics in 1977 [14]. As had been suggested by Gadd two years earlier [15] the free surface boundary condition could be approximately satisfied by covering part of the undisturbed surface close to the hull with simple Rankine sources. In Dawson's method the free surface boundary condition is linearized along the streamlines of the double model solution and a backward difference scheme in the implementation of the free surface condition is used to satisfy the radiation condition. This method turned out to be very successful and was adopted by many organizations. Many Dawson-like methods, which are variations and extensions of the original Dawson method, have been published [16-18]. Considerable effort has been made also at SSPA in the past five years to extend and improve the theory. Much of this work is described in the two PhD theses by Xia in 1986 [19] and Ni in 1987 [20].

Xia developed a first order linear panel method based on Dawson's approach for treating the linear free surface condition and the Hess-Smith method [21] with flat panels covered by constant source density for the solution procedure. This program is one of the family of Dawson-like methods, but has a number of special features of its own for ship flow with a transom stern and lifting surfaces [22]. It has been used extensively in commercial work and has given reasonably good predictions for simple types of hull forms. However, some tests for more complex types of hull forms with bulbous bows and bluff stern shapes indicate that certain improvements would be desirable. Ni improved the accuracy by introducing higher order (curved) panels of the second degree with linearly varying source density, as suggested by Hess [23]. The higher order panel method has been applied to the linear free surface problem [24]. The principal disadvantage of this method or any three-dimensional panel method is that of computing expense. The computing cost for a flow calculation increases as the square of the panel number or

faster and the major expenses are due to the calculation of the velocity influence coefficient matrix and the routine for inverting it. These calculations take about 95% of the total computation costs for a larger number of panel elements than 800. Accordingly, there is a need for an increase in efficiency and this has been the aim of the work described in Paper B [25]. A higher order linear panel method with a better overall efficiency of the solution procedure and better accuracy has been developed and used in the optimization procedure.

Considerable improvements, both in increasing the accuracy and efficiency, and in reducing the amount of work required for the input preparations have been obtained for many cases of interest. Other improvements, as compared to the original Dawson method, are that the panel grid on the free surface is independent of the streamlines and that the resistance is computed in a more accurate way.

It should be noticed that the free surface panels are still flat and that linear free surface boundary conditions are considered. This is clearly an oversimplification in the bow and stern regions of the free surface.

Further attempts to improve the accuracy have been made by taking the non-linear effects into account in the free surface boundary condition.

Ogiwara took the non-linear effect into account iteratively by using relaxation factors in 1985, [26] and Xia proposed an iterative procedure in 1986, [27]. In his method the free surface boundary condition is linearized about the initial wavy surface, using the small perturbation principle and new wave elevations and source distributions are solved in the next iteration. It was found that the convergence problem for the iterative procedure is quite severe.

A higher order global algorithm was applied to the non-linear three-dimensional free-surface problem by Ni [28]. The results of the test computations were always convergent if a relaxation factor was used for the wave elevation modification. A single model with a new panelling to fit the wavy free surface was used and the vertical derivatives of the induced velocity were kept in the free surface boundary condition.

In order to fulfill the basic requirements of generality, economy and accuracy for the application to practical hull form design, some improvements and modifications have been made in Paper C, based on the earlier work by Xia [27] and Ni [28]. An exact solution is obtained through iterations and in each iteration the free surface boundary condition is linearized, based on the small perturbation principle, about the previous solution. The iteration starts from the linear solution. In each iteration the hull and free surface panels are adjusted according to the new wavy surface and the sources are moved accordingly to simulate the boundary condition more exactly. In the new solution the kinematic and dynamic boundary conditions are satisfied simultaneously, i.e. the new source strength as well as the new wave elevation are obtained at the same time.

One of the major improvements is that the hull panels just below the wavy surface are generated in a more accurate way by considering the hull shape above the designed load waterline. In the early work on this method by Ni the hull was considered wall-sided. This simplification may lead to some limitation in its application to ships with barge-type stern sections, or inclined bows and sterns. This restriction is now removed.

Currently there is also a development towards the use of optimization methods in the ship design process. One example is the development of optimization procedures for ship structures. Another example is the application of the optimization procedure in the routine design of a propeller to suit a given radially

varying axial wake and having maximum efficiency while producing a given thrust at a given ship speed and rate of revolution.

Optimization procedures have been studied, which can optimize the ship hull form and general layout, taking resistance and transportation capacity into account. Traditionally such design procedures are mainly based on empirical relations between resistance and the principal hull characteristics. The design of such a preliminary optimization procedure is relatively uncertain due to very approximate empirical functional relations.

More recently optimal hull form design studies based on an analysis procedure have been made by many investigators. Among the more significant research work on the optimization of hull forms, reference can be made to work at shipyards in Japan and Korea. An attempt was made by Nagamatsu & Baba in 1983 [29] to minimize the viscous resistance of three-dimensional full form ships by means of the Hook and Jeeves direct search method. Other attempts to minimize the wave resistance were made by Min & Kim [30] and Suzuki [31] using a similar type of direct search method with a penalty function technique. These methods suffer from some computational disadvantages and are not entirely efficient for non-linear multivariable constrained problems. Nowaki [32] applied a mathematical optimization technique of the non-linear programming type to the minimum viscous drag design of axisymmetric bodies.

A numerical method for the design of optimized hull forms with respect to the total resistance is described in Paper D. The main objective is to obtain an integrated computer system which will enable the designer to include advanced hydrodynamic performance predictions at an early stage of the design process, allowing a systematic evaluation of the hydrodynamic performance characteristics as a function of the hull geometry. This system of computer programs is based on a synthesis of hydrodynamic and sensitivity analysis, geometrical modelling and optimization. The

hull surface is represented mathematically using a boundary variation technique as a function of governing design variables and all of the geometry descriptions (for instance, panel element mesh) and hydrostatic computations (wetted surface area, volume, etc) needed for the hydrodynamic predictions are generated. Then the hydrodynamic performance is estimated using a rapid design oriented first order boundary layer method [33] described in Paper A for viscous resistance and a linear type wave resistance method [25, 34] described in Paper B. An optimum hull form is obtained through a systematic variation of the shape by changing the design variables. The optimum value of the design variables is determined in order to minimize the total resistance of the ship subject to a number of geometrical constraints. The general optimization code ALIBABA [35], which is based on the dual technique of mathematical programming, is used to find an optimum hull form in combination with a shape description module ALADDIN [36].

This system of computer programs has been tested to develop an optimized shape of hull forms for two relatively simple design test cases. The study had to be rather restricted due to computer speed and core memory size limitations, but the present method can be used to develop mathematically faired and hydrodynamically desirable hull forms for more commercial types of ships starting from an existing ship.

The optimal hull form design system (SINDBAD) based on subsystems for hydrodynamic analysis, geometrical modelling, design and optimization has thus attempted to imitate the traditional hull form design procedure.

II. MATHEMATICAL STATEMENT OF THE PROBLEM

As in the usual analysis, the flow is considered steady, irrotational and incompressible and a right-handed coordinate system OXYZ is employed with the origin on the mean free surface, X positive in the direction of the uniform flow, and Z positive in the upward direction. A ship, piercing the free surface, is assumed to be in a uniform onset flow of velocity U_∞ . Then the flow field around the ship may be divided into two principally different regions: the potential flow, where viscosity may be neglected, and the boundary layer-wake flow, close to and behind the body, where viscosity is important. The reason why this division may be made even though the physical properties of the flow may be the same everywhere, is that the velocity gradients, responsible for the shear stress generation are different. Close to the body the flow is very much dominated by the no-slip condition on the surface, and the velocity changes rapidly within the relatively thin boundary layer, which extends into a wake behind the body. Outside the boundary layer/wake velocity gradients are very small and the generated shear stress is negligible.

Due to the differences in flow characteristics stated above, the flows are governed by different equations and have to be solved by a different method.

The governing equations for viscous and potential flow are described in the following two subsections and the basic principle of optimization theory is discussed briefly in section II-3. Section III is devoted to the solution methods, which are an essential feature of the present paper.

II-1. The Formulation of the Viscous Flow Problem

1. Boundary Layer Equations

The boundary layer equations for a three-dimensional turbulent flow in a curvilinear orthogonal coordinate system are given by Nash and Patel [37].

Continuity equation:

$$\frac{1}{h_1} \frac{\partial U}{\partial x} + \frac{\partial V}{\partial y} + \frac{1}{h_3} \frac{\partial W}{\partial z} + K_{31}U + (K_{12}-K_{32})V + K_{13}W = 0 \quad (1)$$

x - Momentum equation:

$$\begin{aligned} \frac{U}{h_1} \frac{\partial U}{\partial x} + V \frac{\partial U}{\partial y} + \frac{W}{h_3} \frac{\partial U}{\partial z} + K_{12}UV + (K_{13}U - K_{31}W)W + \frac{1}{h_1} \frac{\partial (p/\rho)}{\partial x} \\ - \frac{1}{h_1 h_3} \frac{\partial}{\partial x} (h_1 h_3 \tau_{xy}/\rho) = 0 \end{aligned} \quad (2a)$$

y - Momentum equation:

$$\frac{U}{h_1} \frac{\partial V}{\partial x} + V \frac{\partial V}{\partial y} + \frac{W}{h_3} \frac{\partial V}{\partial z} - K_{12}U^2 - K_{32}W^2 + \frac{\partial}{\partial y} (p/\rho) = 0 \quad (2b)$$

z - Momentum equation:

$$\begin{aligned} \frac{U}{h_1} \frac{\partial W}{\partial x} + V \frac{\partial W}{\partial y} + \frac{W}{h_3} \frac{\partial W}{\partial z} + (K_{31}W - K_{13}U)U + K_{32}VW \\ + \frac{1}{h_3} \frac{\partial}{\partial z} (p/\rho) - \frac{1}{h_1 h_3} \frac{\partial}{\partial y} (h_1 h_3 \tau_{zy}/\rho) = 0 \end{aligned} \quad (2c)$$

Here h_1 and h_3 denote the metric coefficients which are a measure of the stretching of the corresponding x- and z-axes; h_2 is assumed to be identically equal to unity and this has already

been introduced in the derivation of the governing equations.

The parameters K_{13} and K_{31} are known as the geodesic curvature of the curve $z = \text{const}$ and $x = \text{const}$ respectively. They are given by

$$K_{13} = \frac{1}{h_1 h_3} \frac{\partial h_1}{\partial z}$$

$$K_{31} = \frac{1}{h_1 h_3} \frac{\partial h_3}{\partial x}$$
(3a)

and the normal curvatures K_{32} and K_{12} are defined by

$$K_{32} = \frac{1}{h_2 h_3} \frac{\partial h_3}{\partial y}$$

$$K_{12} = \frac{1}{h_1 h_2} \frac{\partial h_1}{\partial y}$$
(3b)

U , V and W represent the velocity components in x , y and z directions respectively. The parameters p , ρ and ν are the fluid static pressure, density and kinematic viscosity; τ_{xy} and τ_{zy} are the components of the shear stress.

$$\tau_{xy} = \rho \left(\nu \frac{\partial u}{\partial y} - \overline{u'v'} \right)$$
(4)

$$\tau_{zy} = \rho \left(\nu \frac{\partial w}{\partial y} - \overline{v'w'} \right)$$

The prime quantities u' , v' and w' are the fluctuating parts of the components of the velocity vector.

II-2. The Formulation of the Potential Flow Problem

The flow field around the ship may be described by a velocity potential ϕ which is generated by a certain distribution of

sources on a surface S and by the uniform onset flow in the X -direction

$$\phi(X,Y,Z) = \int \sigma(q)/r(p,q)dS + U_{\infty}X \quad (5)$$

where $\sigma(q)$ is the source density on the surface element dS and $r(p,q)$ is the distance from the point q to the field point $p(X,Y,Z)$ where the potential is being evaluated.

The potential ϕ is given in Eq (5) is governed by the Laplace equation.

$$\nabla^2\phi = 0 \quad (6)$$

in the fluid domain and satisfies the regularity condition at infinity

$$\nabla\phi \Rightarrow (U_{\infty}, 0, 0) \quad \text{as } r \rightarrow \infty \quad (7)$$

The source density σ should be determined from the boundary conditions on the hull and free surface. On the wetted hull surface the solid boundary condition is

$$\phi_n = 0 \quad (8)$$

where n denotes the outward normal to the hull surface. At the free surface, two boundary conditions must be imposed, i.e. the flow must be tangent to the free surface

$$\phi_X h_X + \phi_Y h_Y - \phi_Z = 0 \quad (9)$$

and the pressure should be constant

$$gh + \frac{1}{2}(\nabla\phi \cdot \nabla\phi - U_\infty^2) = 0 \quad (10)$$

Further, no upstream waves should be generated.

II-3. The Formulation of the Optimization Problem

The mathematical formulation of the present design oriented problem which finds an optimum shape of the ship with a minimum resistance subject to geometric constraints can be expressed as

$$\begin{array}{llll} P : & \text{Find} & \gamma^* \in R^n & \\ & \text{Minimize} & R_T(\gamma_j) & j = 1, \text{ ND} \\ & \text{Subject to} & h_k(\gamma_j) = 0 & k = 1, \text{ EC} \\ & & g_i(\gamma_j) \leq 0 & i = 1, \text{ IC} \end{array} \quad (11)$$

Where γ^* is a vector representation of ND design variables defining the hull surface and hull form characteristics. The total ship resistance, which includes the wave and/or viscous resistance component, is used as an objective function R_T . The geometrical and practical design constraints about the hull are contained in $h_k(\gamma_j)$ and $g_i(\gamma_j)$. EC and IC are the numbers of equality and inequality constraints.

The functions R_T , h_k and g_i depend both on design and state, and the equality constraints comprise the state equations. Under the assumption that R_T , h_k and g_i are continuous and differentiable functions of γ_j , the Lagrangian function L may be expressed as:

$$L(\gamma_j, \mu_k, \lambda_i) = R_T(\gamma_j) + \sum \mu_k h_k(\gamma_j) + \sum \lambda_i [g_i(\gamma_j) + s_i^2] \quad (12)$$

where the equality and inequality constraints in (11) are adjoined by means of the Lagrangian multipliers μ_k and λ_i

respectively, after the inequality constraints have been converted into the equalities $g_i(\gamma_j) + s_i^2 = 0$ by introducing the real slack variables s_i . The conditions of stationarity of L with respect to an arbitrary admissible variation of γ_j lead to a number of ND so called optimality conditions,

$$\frac{\partial R_T}{\partial \gamma_j} + \sum \mu_k \frac{\partial h_k}{\partial \gamma_j} + \sum \lambda_i \frac{\partial g_i}{\partial \gamma_j} = 0 \quad (13)$$

and stationarity with respect to the Lagrangian multipliers μ_k recovers the equality constraints in (11),

$$h_k(\gamma_j) = 0 \quad (14)$$

The stationarity of L with respect to s_i yields the so called switching conditions $\lambda_i \cdot s_i = 0$, and the necessary conditions $\partial^2 L / \partial s_i^2 \geq 0$ for a minimum of L imply that the Lagrangian multipliers λ_i must be non-negative, i.e. $\lambda_i \geq 0$. A combination of the latter result with the switching conditions and the defining equations for s_i yields the conditions

$$\begin{aligned} \lambda_i &= 0 \quad \text{if } g_i(\gamma_j) < 0 \\ \lambda_i &\geq 0 \quad \text{if } g_i(\gamma_j) = 0 \end{aligned} \quad (15)$$

which are seen to imply simplification in (13) if one or more of the inequality constraints are not tight.

Equations (13)-(15) constitute the formal set of governing equations for the present hull form optimization problem and are called the generalized Kuhn-Tucker conditions. Mathematically these governing equations must be solved since the ND optimality conditions (13) and EC+IC constraint equations (14) and (15) form a set of (ND+EC+IC) simultaneous equations for the solution of

ND unknown variables γ_j and EC+IC unknown Lagrange multipliers μ_k and λ_1 . A characteristic feature is, however, that the governing equations can only be solved analytically for relatively simple problems, because the optimality conditions are in general implicit and nonlinear in design variables, and a non-negative value is required for the Lagrange multipliers in the solution. Thus an iterative numerical method has to be applied for the solution of the present resistance minimization problem.

III. NUMERICAL SOLUTION OF THE PROBLEM

III-1. The Solution of the Viscous Flow Problem

To solve the boundary layer equations given in (1-2) in a more efficient way, an integral type of method rather than a method based on finite difference is employed. The momentum integral equations based on the streamline coordinate system are obtained by integrating the equation (2) with respect to y from the wall, $y=0$ to some point $y>\delta$ in the potential flow outside the boundary layer and solved together with empirical correlations by the Runge-Kutta-Gill procedure along the streamlines. Different levels of approximation are made to investigate the generality, accuracy and efficiency for the application to practical hull form design.

To develop the most simple solution procedure the first order momentum integral equations and entrainment equation are derived under the small cross flow approximation. They are given by the following equations. See Larsson [5].

$$\frac{1}{h_{10}} \frac{\partial \theta_{11}}{\partial x} + (2\theta_{11} + \delta_1) \frac{1}{U_e h_{10}} \frac{\partial U_e}{\partial x} + K_{310} \theta_{11} = \frac{1}{2} C_f \quad (16a)$$

$$\begin{aligned} \frac{1}{h_{10}} \frac{\partial \theta_{21}}{\partial x} + 2\theta_{21} \left(\frac{1}{U_e h_{10}} \frac{\partial U_e}{\partial x} + K_{310} \right) - K_{130} (\theta_{11} + \delta_1) = \\ \frac{1}{2} C_f \cdot \tan \beta_0 \end{aligned} \quad (16b)$$

$$\frac{1}{h_{10}} \frac{\partial}{\partial x} \{U_e (\delta - \delta_1)\} + U_e K_{310} \delta_2 = E \quad (17)$$

Subscripts e and o are used to denote values at the edge of the

boundary layer ($y=\delta$) and on the surface ($y=0$). C_f and β_0 are the skin friction coefficient and wall cross flow angle defined by

$$C_f = \tau_{0x} / \frac{1}{2} \rho U_\infty^2 \quad (18)$$

$$\beta_0 = \tan^{-1} \tau_{0z} / \tau_{0x} \quad (19)$$

where $\tau_0 = (\tau_{0x}, 0, \tau_{0z})$ is the wall shear stress vector.

h_{10} and h_{30} denote the metric coefficients, which are measures of the stretching of the corresponding x and z co-ordinates on the surface.

The parameters K_{130} and K_{310} are the geodesic curvatures of the curves $z=\text{const}$ and $x=\text{const}$, respectively on the surface. They are given by

$$K_{130} = \frac{1}{h_{10}h_{30}} \frac{\partial h_{10}}{\partial z} \quad (20)$$

$$K_{310} = \frac{1}{h_{10}h_{30}} \frac{\partial h_{30}}{\partial x}$$

The influence of higher order terms is neglected in the above derivations, but will be considered later for the higher order equations.

The higher order momentum integral and entrainment equations are derived by retaining the first order terms of δ/R and the larger. δ/R is the ratio of the boundary layer thickness to the radius of the surface curvature R . The equations are as follows. See Larsson [38].

$$\frac{1}{h_{10}} \frac{\partial \bar{\theta}_{11}}{\partial x} + (2\theta_{11} + \delta_1) \frac{1}{U_e h_{10}} \frac{\partial U_e}{\partial x} + K_{310} \cdot \theta_{11} =$$

$$\frac{1}{2} C_f + I_{px} + I_{k1x} + I_{13x} \quad (21a)$$

$$\frac{1}{h_{10}} \frac{\partial \bar{\theta}_{21}}{\partial x} + 2\theta_{21} \left(\frac{1}{U_e h_{10}} \frac{\partial U_e}{\partial x} + K_{310} \right) - K_{130} (\theta_{11} + \delta_{11}) =$$

$$\frac{1}{2} C_f \tan \beta_0 + I_{pz} + I_{k1z} + I_{k3z} \quad (21b)$$

$$\frac{1}{h_{10}} \frac{\partial}{\partial x} \{ U_e (\bar{\delta} - \bar{\delta}_1) \} + U_e K_{310} (\bar{\delta} - \bar{\delta}_1) - U_e K_{130} \bar{\delta}_2 =$$

$$(1 + K_{120} \delta) \cdot (1 + K_{320} \delta) E \quad (22)$$

The equations (21) and (22) differ from the corresponding first order ones (16) and (17) in three respects: the pressure and curvature integrals on the right hand side and the bars over certain quantities.

The "I" quantities on the right hand side members are integrals, which appear due to the inclusion of, on the one hand, pressure gradients through the layer (I_{px} , I_{pz}) and, on the other hand, normal curvature of the surface (I_{kx} , I_{kz}).

In the present work Head's entrainment relations are used for the boundary layer

$$C_E = \frac{E}{U_e} = 0.0306(H_1 - 3.0)^{-0.653} \quad (23a)$$

$$H_1 = 1.535(H_{12} - 0.7)^{-2.715} + 3.3$$

A relation due to Kang is employed in the wake

$$C_E = \frac{E}{U_e} = 0.11299 - 0.048275 \ln(H_1) + 0.0051395 \cdot \{\ln(H_1)\}^2 \quad (23b)$$

For the tangential velocity components the well known power-law and Mager assumptions are made.

$$\frac{U}{U_e} = \left(\frac{y}{\delta}\right)^{\frac{1}{n}} = \left(\frac{y}{\delta}\right)^{\frac{H_{12}-1}{2}} \quad (24a)$$

$$\frac{W}{U_e} = \left(\frac{y}{\delta}\right)^{\frac{H_{12}-1}{2}} \left\{1 - \frac{y}{\delta}\right\}^2 \tan\beta_0 \quad (24b)$$

For the normal velocity component a linear variation is assumed.

$$\frac{V}{V_e} = \frac{y}{\delta} \quad (24c)$$

In the wake calculation, an approximation of Coles' wake function is employed for the streamwise velocity profile, while Mager's assumption is used for the cross flow.

$$\frac{U}{U_e} = 1 - \lambda \cos^2\left(\frac{\pi}{2} \frac{y}{\delta}\right) \quad (25a)$$

$$\frac{W}{U_e} = \left\{1 - \frac{y}{\delta}\right\}^2 \frac{U}{U_e} \tan\beta_0 \quad (25b)$$

Introducing these expressions in the definitions of the basic integral parameters, the following relations appear

$$\begin{aligned}
 \delta_1 &= \delta A_1 \\
 \theta_{11} &= \delta(A_1 \lambda - A_2 \lambda^2) \\
 \delta_2 &= -\delta \tan \beta_0 (A_3 - A_4 \lambda) \\
 \theta_{12} &= \delta \tan \beta_0 (A_4 \lambda - A_5 \lambda^2) \\
 \theta_{22} &= -\delta \tan^2 \beta_0 (A_6 - A_7 \lambda + A_8 \lambda^2) \\
 \theta_{21} &= \delta_2 + \theta_{12}
 \end{aligned} \tag{26}$$

By definition $H_{12} = \delta_1 \cdot \theta_{11}$, which yields

$$\begin{aligned}
 H_{12} &= \frac{A_1}{A_1 - A_2} \\
 \lambda &= \frac{A_1}{A_2} \frac{H_{12}^{-1}}{H_{12}}
 \end{aligned} \tag{27}$$

The constants $A_1 - A_8$ attain the following numerical values

$$\begin{aligned}
 A_1 &= 0.5 & A_2 &= 0.375 & A_3 &= 0.333 \\
 A_4 &= 0.268 & A_5 &= 0.233 & A_6 &= 0.200 \\
 A_7 &= 0.359 & A_8 &= 0.165
 \end{aligned} \tag{28}$$

Finally, Ludwig-Tillmann's law is used for the skin friction

$$C_f = 0.246 \cdot (10.0)^{-0.678 H_{12}} \left(\frac{\nu}{U_e \cdot \theta_{11}} \right)^{0.268} \tag{29}$$

In the present calculation, the viscous resistance is calculated by computing the momentum loss in the far wake. This momentum area can be determined either from the continuation of the boundary layer calculation along the streamlines extending into the wake region, or from the Squire & Young method [39]. Both have been tried in the present work. Applying the Squire & Young formula, and extending it to three dimensional boundary layer flow, the momentum thickness $\theta_{11\infty}$ in the far wake may be given by:

$$\theta_{11\infty} = \theta_{11t} \cdot \left\{ \frac{U_e}{U_\infty} \right\}^{(H_{12}+5)/2} \quad (30)$$

where θ_{11t} represents the momentum thickness at the trailing edge.

The integration of equation (30) over the girth of a cross section therefore gives the resistance due to the momentum loss which is accumulated in the upstream portion of the body.

$$R_V = \rho U_\infty^2 \int \theta_{11\infty} dq \quad (31)$$

Despite of the relative simplicity the method is known to give a fair estimation of the viscous resistance.

III-2. The Solution of the Potential Flow Problem

The exact problem described in section II-2 is nonlinear, since the free surface boundary condition itself is nonlinear and should be exactly satisfied on the wavy surface $Z=h(X,Y)$, which is unknown, and must be computed as a part of the solution. Thus, numerical methods, which have been applied to solve the problem usually entail some kind of linearization procedure.

Unknown sources σ on the hull and wavy surface $Z=h(X,Y)$ will

induce a potential ϕ and a wave elevation h which satisfy the boundary conditions (9) and (10).

$$D_1(\sigma, h) = \phi_X h_X + \phi_Y h_Y - \phi_Z = 0$$

$$D_2(\sigma, h) = h - \frac{1}{2g} [U_\infty^2 - (\phi_X^2 + \phi_Y^2 + \phi_{ZZ}^2)] = 0$$

These non-linear forms of the free surface boundary conditions can be linearized by introducing small perturbations $\delta\sigma$ and δh with respect to the previous solution in a first order Taylor expansion.

$$D_1(\sigma, h) \approx D_1(\sigma^\circ, h^\circ) + \Delta D_1(\sigma, h^\circ) + \Delta D_1(\sigma^\circ, h) \approx$$

$$D_1(\sigma^\circ, h^\circ) + \frac{\partial}{\partial \sigma} D_1(\sigma, h^\circ) \cdot \delta\sigma + \frac{\partial}{\partial h} D_1(\sigma^\circ, h) \cdot \delta h \approx 0$$

(32)

$$D_2(\sigma, h) \approx D_2(\sigma^\circ, h^\circ) + \Delta D_2(\sigma, h^\circ) + \Delta D_2(\sigma^\circ, h) \approx$$

$$D_2(\sigma^\circ, h^\circ) + \frac{\partial}{\partial \sigma} D_2(\sigma, h^\circ) \delta\sigma + \frac{\partial}{\partial h} D_2(\sigma^\circ, h) \cdot \delta h \approx 0$$

It is a fundamental assumption of the present method that the perturbations of source ($\delta\sigma$) and wave elevation (δh) are small in certain senses. In a Taylor series, higher order terms in these quantities then become very small and can be neglected.

Here the superscript, $^\circ$, corresponds to the previous solution which is assumed to be known a priori.

$$D_1(\sigma^\circ, h^\circ) = \phi_X h_X^\circ + \phi_Y h_Y^\circ - \phi_Z = 0$$

(33)

$$D_2(\sigma^\circ, h^\circ) = h^\circ - \frac{1}{2g} [U_\infty^2 - (\phi_X^2 + \phi_Y^2 + \phi_Z^2)] = 0$$

where ϕ_X , ϕ_Y and ϕ_Z mean the velocity components induced by σ° on the free surface $Z=h^\circ(X, Y)$.

The partial increments of D_1 and D_2 should be found in such a way that a new velocity potential $\phi=\phi+\delta\phi$ induced by introducing

small perturbations $\delta\sigma$ and δh should satisfy Eqs (9) and (10) on the new wave surface $h=h^\circ+\delta h$. ΔD_1 and ΔD_2 can be linearly expanded based on σ° and h°

$$\Delta D_1(\sigma, h^\circ) = \delta\phi_X h_X^\circ + \delta\phi_Y h_Y^\circ - \delta\phi_Z \quad (34)$$

$$\Delta D_1(\sigma^\circ, h) = \phi_X \delta h_X + \phi_Y \delta h_Y + (\phi_{XZ} h_X^\circ + \phi_{YZ} h_Y^\circ - \phi_{ZZ}) \delta h$$

$$\Delta D_2(\sigma, h^\circ) = \frac{1}{g} (\phi_X \delta\phi_X + \phi_Y \delta\phi_Y + \phi_Z \delta\phi_Z) \quad (35)$$

$$\Delta D_2(\sigma^\circ, h) = \delta h + \frac{1}{g} (\phi_X \phi_{XZ} + \phi_Y \phi_{YZ} + \phi_Z \phi_{ZZ}) \delta h$$

Therefore the linearized free surface boundary conditions are

$$\begin{aligned} &\phi_X h_X^\circ + \phi_Y h_Y^\circ - \phi_Z + \phi_X \delta h_X + \phi_Y \delta h_Y \\ &+ (\phi_{XZ} h_X^\circ + \phi_{YZ} h_Y^\circ - \phi_{ZZ}) \delta h = 0 \end{aligned} \quad (36)$$

$$\begin{aligned} &\{1 + \frac{1}{g} (\phi_X \phi_{XZ} + \phi_Y \phi_{YZ} + \phi_Z \phi_{ZZ})\} \delta h = \\ &\frac{1}{2g} \{u_\infty^2 - \phi_X^2 - \phi_Y^2 - \phi_Z^2 - 2(\phi_X \delta\phi_X + \phi_Y \delta\phi_Y + \phi_Z \delta\phi_Z)\} - h^\circ \end{aligned} \quad (37)$$

In the linear solution, a linearization of the free surface condition is performed with respect to the flow at zero Froude number, i.e. the flow with an undisturbed flat free surface and the terms containing the second derivative of velocity potential (ϕ_{XZ} , ϕ_{YZ} , ϕ_{ZZ}) are not included, based on the assumption that these terms are relatively small and can be neglected. Therefore the free surface boundary conditions for the linear solution are further approximated as:

$$\phi_X h_X^\circ + \phi_Y h_Y^\circ - \phi_Z + \phi_X \delta h_X + \phi_Y \delta h_Y = 0 \quad (38)$$

$$\delta h = \{ U_\infty^2 + \phi_X^2 + \phi_Y^2 - 2(\phi_X \phi_X + \phi_Y \phi_Y) \} / 2g - h^\circ \quad (39)$$

Here the double model potential ϕ and the Bernoulli wave elevation h° are assumed to be known from the double model solution, and these conditions are to be applied at $Z=0$.

In the nonlinear solution an exact solution is obtained through iterations and in each iteration the free surface boundary condition is linearized, based on the small perturbation principle, about the previous solution. The iteration start from the linear solution. In each iteration the hull and free surface panels are adjusted according to the new wavy surface and the sources are moved accordingly to simulate the boundary condition more exactly. In the new solution the kinematic and dynamic boundary conditions are satisfied simultaneously, i e the new source strength as well as the new wave elevation are obtained at the same time. Upon convergence, which is usually obtained after 5-6 iterations, the non-linear terms go to zero and the solution is exact with respect to the boundary conditions.

Once the final source density σ and wave height h are determined the flow velocity and pressure may be calculated at any point. With known pressure and velocity distributions, the wave pattern and the wave resistance can be predicted

$$R_w = \rho U_\infty^2 \int C_p N_X dS \quad (40)$$

III-3. The Solution of the Optimization Problem

The minimization problem formulated in section II-3 is a nonlinear programming problem, and it can be solved using a standard mathematical optimization algorithm with possible gradients estimated numerically. But such a procedure (for

instance, an iterative mathematical programming method) can be expected to be fairly computer-time consuming, because it will require an accurate evaluation, at each iteration, of the objective and constraint functions and their gradients. These evaluations are very expensive as each evaluation involves a flow calculation which leads to the solution of a large system of linear equations. Therefore the resulting solution method must have the essential features of accuracy and efficiency.

The method to be presented in the following is based on the Kuhn-Tucker conditions (13), which state that at optimum the gradient of the objective function is a linear combination of the active constraint gradients.

$$\frac{\partial R_T}{\partial \gamma_j} + \sum_{i=1}^{NC} \lambda_i \frac{\partial g_i}{\partial \gamma_j} = 0 \quad j = 1, ND$$

$$\lambda_i (g_i - \bar{g}_i) = 0 \quad i = 1, NC \quad (41)$$

$$\lambda_i \geq 0$$

where the equality constraints $h_k(\gamma_j)=0$, $k=1$, EC, and inequality constraints $g_i(\gamma_j) \leq 0$, $i=1$, IC in (11) are converted into inequalities $g_i(\gamma_i) \leq \bar{g}$, $i=1$, NC, by introducing the following relations with very small positive real variables δ_k

$$h_k(\gamma_j) = 0 \quad \longleftrightarrow \quad -\delta_k \leq h_k(\gamma_j) \leq \delta_k$$

then the total number of constraints NC become $2*EC+IC$ and their upper bounds \bar{g}_i are newly introduced.

To solve the optimization problem P in (11), an iterative application of sequential convex programming is employed. The

optimization starts at an arbitrary initial design estimate, which can be one of the best existing ships selected from a hull form data base. The geometry of the initial hull form is modelled mathematically with a number of design variables and exposed to uniform onset flow at design speed. A systematic evaluation of the hydrodynamic performance characteristics is performed as a function of the hull geometry. With an objective hull form and knowing its hydrodynamic performance, a convex subproblem $P^{(k)}$, which converges to the solution of the optimization problem P , is created. Linear approximations of nonlinear functions $R_T(\gamma_j)$ and $g_i(\gamma_j)$ are obtained first by replacing the nonlinear function of the problem by their first order Taylor series approximations expanded at the preceding design point $\gamma_j^{(k)}$.

$$R_T(\gamma_j) = R_T(\gamma_j^k) + \sum_{j=1}^{ND} \frac{\partial R_T}{\partial \gamma_j} (\gamma_j - \gamma_j^k)$$

$$g_i(\gamma_j) = g_i(\gamma_j^k) + \sum_{j=1}^{ND} \frac{\partial g_i}{\partial \gamma_j} (\gamma_j - \gamma_j^k)$$
(42)

The derivatives needed to get the Taylor series approximation can be estimated numerically as differences obtained by recalculation or by a quasi-analytically based procedure

$$\frac{\partial R_T}{\partial \gamma_j} = \frac{R_T(\gamma_j) - R_T(\gamma_j^k)}{\Delta \gamma_j}$$

$$\frac{\partial g_i}{\partial \gamma_i} = \frac{g_i(\gamma_j) - g_i(\gamma_j^k)}{\Delta \gamma_j}$$
(43)

By this approach, the original nonlinear problem P is now reduced to a sequence of linear subproblems $\tilde{P}^{(k)}$ which is given by

$$\tilde{p}(k) : \quad \min \tilde{R}_T(\gamma_j) = R_T(\gamma_j^k) + \sum_{j=1}^{ND} \frac{\partial R_T}{\partial \gamma_j} (\gamma_j - \gamma_j^k)$$

Subject to

(44)

$$\tilde{g}_i(\gamma_j) = g_i(\gamma_j^k) + \sum \frac{\partial g_i}{\partial \gamma_j} (\gamma_j - \gamma_j^k) \leq \bar{g}_i$$

$$\underline{\gamma}_j \leq \gamma_j \leq \bar{\gamma}_j \quad i = 1, NC, \quad j = 1, ND$$

The design variables γ_j are modified so that the current design moves towards a design satisfying the applicable optimality criteria. The $\Delta\gamma_j$ are restricted to be less than some move limits so that the design remains in the neighbourhood of the initial design. Thus there is a relationship between the nonlinearity of the functions $R_T(\gamma_j)$ and $g_i(\gamma_j)$ and the appropriate values of the move limit which will allow an efficient solution.

In the solution made in paper D, a strictly convex approximate subproblem $p(k)$ is generated in each step of the iterative process based on Method of Moving Asymptotes (MMA).

In the MMA approximation, both the objective function R_T and the constraints g_i are linearly approximated by a first order Taylor series expansion in variables of the type $1/(\gamma_j - L_j)$ or $1/(U_j - \gamma_j)$ depend on the signs of the derivatives of R_T (or g_i) around the preceding design point, where L_j and U_j are the lower and upper asymptotes to γ_j , and γ_j will always lie somewhere in between. Then a more complicated subproblem $\tilde{p}(k)$ can be generated, but the detail derivations will not be given here. See Svanberg [40].

The approximated subproblem $\tilde{p}(k)$ is explicit, convex and separable, so this may be solved by using dual methods of mathematical programming [41-42]. The Lagrangian function

corresponding to $\tilde{p}(k)$ is given by

$$L(\gamma, \lambda) = \tilde{R}_T(\gamma) + \sum_i \lambda_i (\tilde{g}_i(\gamma) - \bar{g}_i) \quad \lambda_i \geq 0 \quad (45)$$

L is separable which implies

$$L(\gamma, \lambda) = \sum_{j=1}^{ND} L_j(\gamma_j, \lambda) \quad (46)$$

The minimization of the Lagrangian function can be obtained from:

$$\frac{\partial L_j(\gamma_j, \lambda)}{\partial \gamma_j} = 0 \Rightarrow \gamma_j = \gamma_j(\lambda) \quad j=1, ND \quad (47)$$

The resulting equations are uncoupled, due to the separability, and of second degree which implies that γ_j can be expressed explicitly by the Lagrangian multipliers.

Let $\psi(\lambda) = L(\gamma(\lambda), \lambda)$. It can be shown that $\psi(\lambda)$ is concave. λ is found from the solution of the dual problem D.

$$\begin{aligned} D: \quad & \max \psi(\lambda) \\ & \text{subject to } \lambda_j \geq 0 \end{aligned} \quad (48)$$

D can be solved by an arbitrary method for unconstrained maximization, for instance the quasi-Newton method [43], which OASIS uses. The method has to be modified to handle the simple non-negative constraints on λ . It should be noticed that the value of the dual function is equal to the value of the objective function at optimum, i e:

$$\max \psi(\lambda) = \min R_T(\gamma) \quad (49)$$

Min $L(\gamma, \lambda)$ implies:

$$\frac{\partial \tilde{R}_T(k)}{\partial \gamma_j} + \sum_{i=1}^{NC} \lambda_i \frac{\partial \tilde{g}_i(k)}{\partial \gamma_j} = 0 \quad (50)$$

which is the Kuhn Tucker condition for optimum. A new design point, at which the Kuhn-Tucker conditions would be satisfied, can be generated directly. Naturally, because of the approximations of the Taylor series expansion, the solution procedure developed in this manner still requires some steps of iteration. After each approximate subproblem is solved, a full hydrodynamic analysis is conducted to calculate the object function, constraints and their gradients for the next approximated problem. This iteration procedure is repeated until a convergence criterion is met and an optimum hull form, with a design satisfying the optimum criterion is guaranteed to be at least a local minimum, is finally generated.

IV. CONCLUSIONS

A numerical procedure for the analysis of the hydrodynamic performance of ships and the design of optimized hull forms is presented in the present thesis. Special emphasis has been laid on two essential aspects of the problem: (i) how the hydrodynamic performance of a ship can be predicted in a more accurate way, and (ii) how the performance can be improved through a more efficient systematic variation of the shape of the hull form. According to the studies presented in the appended papers, the following conclusions can be drawn:

- Four methods for calculating the viscous resistance and flow properties around ship hulls of arbitrary shape have been developed, based on different levels of approximation, to investigate the efficiency and accuracy for application to practical hull form design. The simplest method is accurate enough to predict differences due to changes in the hull form and can therefore be used in the optimization procedure. The higher order methods predict the absolute value of the viscous resistance with acceptable accuracy and provide a reasonable quantitative prediction of local flow properties, including skin friction and pressure coefficients.
- A higher order panel method for calculating the potential flow about ships has also been developed, based on linear and non-linear free surface boundary conditions. The linear method is efficient for evaluating the wave pattern and the wave resistance of practical ship hull forms. The non-linear method provides a possibility of obtaining more accurate results for relatively simple hull forms, but further investigations on the numerical procedure should be carried out for more complicated hull forms.

- To improve the traditional hull form design procedure, a numerical method for the design of an optimum hull form with minimum resistance has been developed by synthesis of hydrodynamic analysis, geometrical modelling and optimization. The system of computer programs can be used to develop mathematically faired and hydrodynamically desirable hull forms, starting from an existing ship.

V. FUTURE APPLICATIONS AND DEVELOPMENTS

The method presented here is only the first step in a more comprehensive effort to develop a complete Optimum Hull Form Design System (SINDBAD). All of the important factors for determining ship performance have not yet been incorporated in this system. In particular, it is important in the design of ships that the considerations of propulsion and seakeeping have to be included at a very early stage of the design. (Furthermore, the minimum weight design procedure should be an integral part of the design process.)

Future work will integrate the ship resistance program SINDBAD with the structural optimization system OASIS in order to solve problems with mixed objective or constraint functions. An example of this is: minimize a combination of ship resistance and weight with constraint on load volume, stresses, displacements, eigenfrequencies etc.

With significant advances in computer technology and successful development at SSPA of a numerical code for solving the Navier-Stokes equation with or without a propeller [44, 4], we are presently considering the inclusion of these numerical codes to extend the capability and generality of the Optimal Hull Form Design System (SINDBAD). The SINDBAD System has been constructed in a general form so that inclusion of other hydrodynamic computational methods can easily be made.

VI. SUMMARY OF APPENDED PAPERS

Paper A: Calculation of ship viscous resistance using boundary layer theory based on first or higher order approximations

Four methods for calculating the viscous resistance and flow properties around ship hulls of arbitrary shape are described. The methods are based on generalizations of Larsson's first and higher order boundary layer integral methods. Their generality, economy and accuracy for application to practical hull form design is investigated. The objective is thus to compare different levels of approximation to find the most suitable one for a hull optimization procedure.

The simplest method is based on the assumption of a thin boundary layer to enable fast computations. No higher order effects are taken into account and the choice of numerical scheme is made on the basis of simplicity and economy. The higher order version III takes full account of the influence of longitudinal and transverse surface curvatures and normal pressure gradients on the development of boundary layers, and also of the viscid/inviscid interaction in the stern region. In order to examine the effect of the higher order terms on the prediction of flow properties, the higher order version I with only surface curvature effects and the higher order version II with curvature and normal pressure gradient effects have also been developed.

The results of test computations for an SSPA 720 and an HSVA Tanker indicate that the simplest method is accurate enough to predict differences due to changes in the hull form and can therefore be used in an optimization procedure. The higher order versions predict the absolute value of the viscous resistance with acceptable accuracy and provide a reasonable quantitative prediction of local flow properties including skin friction and pressure coefficients.

Paper B: A higher order panel method for calculating free surface potential flows with linear free surface boundary conditions

A method for calculating the potential flow about ships is described.

The hull and part of the free surface are imagined to be covered with distributions of source singularities, and the source strengths are adjusted to satisfy boundary conditions. An exact boundary condition is satisfied on the hull, while on the free surface the boundary condition is linearized with respect to the double model solution. Higher order panels are used, so the panels are parabolic rather than flat and the source density distribution on each panel is not constant but varies linearly.

The objective is to increase the efficiency and accuracy of the method by introducing the higher order panels. Another improvement, as compared to the original Dawson method [14], is a body-fitted panel grid, which is independent of streamlines on the free surface. This is introduced to get better wave pattern predictions in the bow and stern and also the wave resistance is computed in a more accurate way.

A definite improvement over the first order method is achieved for several test cases in the prediction of the wave pattern and the wave resistance.

Paper C: A higher order panel method for calculating free surface potential flows with non-linear free surface boundary conditions

The linear method described in Paper B is extended to be fully non-linear.

An exact solution is obtained through iterations and in each iteration the free surface boundary condition is linearized, based on the small perturbation principle, about the previous solution. The iteration starts from the linear solution. In each iteration the hull and free surface panels are adjusted according to the new wavy surface and the sources are moved accordingly to simulate the boundary condition more exactly. In the new solution the kinematic and dynamic boundary conditions are satisfied simultaneously, i.e. the new source strength as well as the new wave elevation are obtained at the same time. Upon convergence, which is usually obtained after 5-6 iterations, the non-linear terms go to zero and the solution is exact with respect to the boundary conditions.

In order to fulfill the basic requirements of generality, economy and accuracy for the application to practical hull form design, some improvements and modifications have been made based on the earlier work by Xia [27] and Ni [28]. One of the major improvements is that the hull panels just below the wavy surface are generated in a more accurate way by considering the hull shape above the designed load waterline. In the early work on this method by Ni the hull was considered wall-sided. This simplification may lead to some limitation in its application to ships with barge-type stern sections, or inclined bows and sterns. This restriction is now removed.

It is believed that this is important for wave pattern prediction since the influence of the sources on hull panels just below the free surface is considerably greater than that of sources on the other parts of the hull. On the other hand, this might cause some problems of convergence due to the fact that the change of the panel location may be large enough to violate the validity of the small perturbation principle. In order to improve the convergence, special care has been taken to select the initial condition and also to compute the velocity potential and the associated derivative terms in the free surface equation.

The present method has been applied to compute the wave pattern, pressure distribution over the hull surface and wave resistance for the Wigley hull and SSPA Ro-Ro ship, and converged solutions were usually obtained after 5-6 iterations.

Paper D: Numerical method for minimizing ship resistance

The hydrodynamic performance prediction methods described in Papers A and B are integrated with an optimization procedure in order to develop a numerical method for the design of an optimum hull form with minimum resistance. The main objective is to obtain an integrated computer system which will enable the designer to include advanced hydrodynamic performance predictions at an early stage of the design process allowing a systematic evaluation of hydrodynamic performance characteristics as a function of the hull geometry.

In the optimum hull form design process the hull surface is represented mathematically by a number of design variables and a systematic evaluation of the hydrodynamic performance characteristics is performed as a function of the hull geometry. An optimum hull form is obtained through a systematic variation of the shape by changing the design variables. The optimum value of the design variables is determined in order to minimize the total resistance of the ship subject to a number of geometrical constraints. The general optimization code ALIBABA, which based on the dual technique of mathematical programming, is used to find an optimum hull form in combination with a shape description module ALADDIN. The entire process of hydrodynamic analysis, geometrical modelling and optimization has thus attempted to imitate the traditional hull form design procedure. The system of computer programs can be used to develop mathematically faired and hydrodynamically desirable hull forms starting from an existing ship.

REFERENCES

- [1] LARSSON, L (Editor): "SSPA-ITTC Workshop on Ship Boundary Layers 1980". Proceedings, Publication of the Swedish Maritime Research Centre, SSPA, No 90, 1981
- [2] LARSSON, L (Editor): "Proceedings of the Second International Symposium on Ship Viscous Resistance". SSPA, 1985
- [3] TANAKA, I (Editor): "Osaka International Colloquium on Ship Viscous Flow". Proceedings, Osaka, 1985
- [4] BROBERG, L, & ZHANG, D H: "Numerical Solution of the Reynolds-Averaged Navier-Stokes Equations for Ship Stern Flow". SSPA Report 2803-1, 1988
- [5] LARSSON, L: "A Calculation Method for Three-Dimensional Turbulent Boundary Layers on Ship-Like Bodies". First International Conference on Numerical Ship Hydrodynamics, Washington DC, 1975
- [6] LARSSON, L, & CHANG, M-S: "Numerical Viscous and Wave Resistance Calculations Including Interaction". 13th Symposium on Naval Hydrodynamics, Tokyo, 1980
- [7] BAI, K J, & MACARTHY, J H (Editors): "Proceedings of the First Workshop on Ship Wave Resistance Computations". David W Taylor Naval Ship Research and Development Center, 1979
- [8] NOBLESSE, F, & MACARTHY, J H (Editors): "Proceedings of the Second Workshop on Ship Wave Resistance Computations". David W Taylor Naval Ship Research and Development Center, 1983

- [9] The Society of Naval Architects of Japan: "Proceedings of the International Seminar on Wave Resistance". Tokyo, Japan, 1976
- [10] SCHOT, JOANNA W & SALVESEN, NILS (Editors): "Proceedings of the First International Conference on Numerical Ship Hydrodynamics", Maryland, USA, 1975
- [11] WEHAUSEN, JOHN V & SALVESEN, NILS (Editors): "Proceedings of the Second International Conference on Numerical Ship Hydrodynamics", University of California, Berkeley, 1977
- [12] DERN, JEAN-CLAUDE & HAUSSLING, HENRY J (Editors): "Proceedings of the Third International Conference on Numerical Ship Hydrodynamics", Paris, 1981
- [13] MCCARTHY, JUSTIN H (Editor): "Proceedings of the Fourth International Conference on Numerical Ship Hydrodynamics", Washington DC, 1985
- [14] DAWSON, C W: "A Practical Computer Method for Solving Ship-Wave Problems". Proceedings of the Second International Conference on Numerical Ship Hydrodynamics, Berkeley, 1977
- [15] GADD, G E: "A Method of Computing the Flow and Surface Wave Pattern around Full Forms". Transactions of the Royal Institution of Naval Architects, 1976
- [16] OGIWARA, S: "A Method to Predict Free Surface Flow around Ship by Means of Rankine Sources". Journal of the Kansai Society of Naval Architects, Japan, Vol 190, 1983
- [17] RAVEN, H C: "Variations on a Theme by Dawson". Proceedings of the Seventeenth Symposium on Naval Hydrodynamics, the Hague, 1988

- [18] MUSKER, A J: "A Panel Method for Predicting Ship Wave Resistance". Proceedings of the Seventeenth Symposium on Naval Hydrodynamics, the Hague, 1988
- [19] XIA, F: "Numerical Calculation of Ship Flows, with Special Emphasis on the Free Surface Potential Flow". PhD Thesis, Chalmers University of Technology, Gothenburg, 1986
- [20] NI, SHAO-YU: "Higher Order Panel Methods for Potential Flows with Linear on Non-Linear Free Surface Boundary Conditions". PhD Thesis, Chalmers University of Technology, Gothenburg, 1987
- [21] HESS, J L, & SMITH, A M O: "Calculation of Non-Lifting Potential Flow about Arbitrary Three-Dimensional Bodies". Douglas Report No E S 40622, 1962
- [22] XIA, F, & LARSSON, L: "A Calculation Method for the Lifting Potential Flow around Yawed, Surface-Piercing 3-D Bodies". Proceedings of the 16th Symposium on Naval Hydrodynamics, University of California, Berkeley, June, 1986
- [23] HESS, J L: "A Higher Order Panel Method for Three-Dimensional Potential Flow". Douglas Report N62269-77-C0437, 1979
- [24] NI, SHAO-YU: "A Higher Order Panel Method for Double Model Linearized Free Surface Potential Flows". SSPA Report No 2912-5, 1987
- [25] KIM, K J: "A Higher Order Panel Method for Calculating Free Surface Potential Flows with Linear Free Surface Boundary Conditions". SSPA Report No 2966-2, 1989

- [26] OGIWARA, S, & MARUO, H: "A Numerical Method of Non-Linear Solution for Steady Waves around Ships". Journal of the Society of Naval Architects of Japan, Vol 157, 1985
- [27] XIA, F: "A Study on the Numerical Solution of Fully Non-Linear Ship Wave Problems". SSPA Report No 2912-3, 1986
- [28] NI, SHAO-YU: "A Method for Calculating Non-Linear Free Surface Potential Flows Using Higher Order Panels". SSPA Report No 2912-6, 1987
- [29] NAGAMATSU, TETSUO & BABA, EIICHI: "Study on the Minimization of Ship Viscous Resistance". Journal of the Society of Naval Architects of Japan, Vol 154, Dec 1983
- [30] MIN, K-S & KIM, K-J: "A Study on the Optimum Hull Form Development Based on the Minimum Resistance Theory". Journal of the Society of Naval Architects of Korea, Vol 21, No 4, Dec 1984
- [31] SUZUKI, K & MARUO, H: "Application of Nonlinear Optimization Technique to Hull Form Design Based on Wave Resistance Theory". The Second International Symposium on Practical DEsign in Shipbuilding (PRADS 83), 1983
- [32] NOWAKI, H: "Optimization Methods Applied to Viscous Drag Reduction", Osaka International Colloquium on Ship Viscous Flow, Japan, October 1985
- [33] KIM, K-J & LARSSON, L: "Comparison between First and Higher Order Methods for Computing the Boundary Layer and Viscous Resistance of Arbitrary Ship Hulls". International Symposium on Resistance and Powering Performance, Shanghai, 1989

- [34] NI, S-Y, KIM, K-J, XIA, F & LARSSON, L: "A Higher Order Panel Method for Calculating Free Surface Potential Flows with Linear Free Surface Boundary Conditions", International Symposium on Resistance and Powering Performance, Shanghai, 1989
- [35] ESPING, B: "The ALIBABA Nonlinear Optimization Package". Computer and Structures, Vol 24, No 2, 1986
- [36] ESPING, B & HOLM, D: "A CAD Approach to Structure Optimization". Presented at the Conference 'Computer Aided Optimal Design', Portugal, and published in 'Computer Aided Optimal Design: Structure and Mechanical Systems'. editor C A Mota Soares, Springer-Verlag, 1987
- [37] NASH, J F & PATEL, V C: "Three Dimensional Boundary Layers". SBC Technical Books, Atlanta, 1972
- [38] LARSSON, L & LÖFDAHL, L: "A Method for Calculating Thick Three-Dimensional Turbulent Boundary Layers. Part I: Equations and General Principles". SSPA Report No 2360-1, 1979, 23 p
- [39] SQUIRE, H B & YOUNG, A D: "The Calculation of the Profile Drag of Airfoils", ARC Report and Mem No 1838, 1938
- [40] SVANBERG, K: "MMA - Method of Moving Asymptotes - A New Method for Structure Optimization", TRITA MAT-1985-RIT, Stockholm, Sweden, 1985
- [41] FLEURY, C & SCHMIT, L A: "Dual Methods and Approximation Concepts in Structure Analysis", NASA Contractor Report 3326, 1980

- [42] SVANBERG, K: "An Algorithm for Optimum Structure Design Using Duality", Mathematical Programming Study 20, pp 161-177, 1982

- [43] FLETCHER, R: "Practical Methods of Optimization", Vol 1, Unconstrained Optimization, John Wiley & Sons, 1982

- [44] ZHANG, D H: "Numerical Prediction of Propeller-Hull Interaction in Viscous Flow", SSPA Report No 2963-1, 1989

PAPER A

Chalmers University of Technology
Division of Marine Hydrodynamics
Report No 72

and

SSPA Report No 8018-1

Calculation of Ship Viscous Resistance
Using Boundary Layer Theory Based on
First or Higher Order Approximations

by

Keun Jae Kim

1988-01-07

FOREWORD

This paper describes one phase of the work done in the development of a general design procedure for the optimization of the ship hull form with respect to resistance.

It is well-known that the ship's resistance in still water is made up of two components, namely wave making resistance and viscous resistance, of which the viscous resistance component becomes the major part of the total resistance with the increase of fullness and the decrease of design speed. At the initial design stage of the ship hull form, the exact understanding of the characteristics of the boundary layer flow field around the ship is very important, not only for the prediction of the ship's hydrodynamic performance but also to improve the ship form.

In this paper we address ourselves to the problem of computing the boundary layers near the stern region and wake; this is essential for the calculation of the viscous resistance and for the prediction of the momentum deficit in the far wake.

ABSTRACT

This paper will describe a general method for calculating the viscous resistance and flow properties around ship hulls of arbitrary shape. The method developed is based on a generalization of Larsson's first, [1], and higher order integral method, [2], to fulfil the basic requirements of generality, economy and accuracy for the application to practical hull form design.

The simple version of the method developed is based on the assumption of a thin boundary layer for fast computation in the hull form optimization routine. No higher order effects are taken into account and the choice of numerical scheme is made on the basis of simplicity and economy, while the higher order version III, developed for the purpose of final evaluation of optimized hull forms, takes full account of the influence of longitudinal and transverse surface curvatures and normal pressure gradients on the development of boundary layers, and also of the viscid-inviscid interaction in the stern region. In order to examine the effect of the higher order terms on the prediction of flow properties, the higher order version I with surface curvature effects and the higher order version II with curvature and normal pressure gradient effects have been developed.

Numerical predictions have been made for two cases - an SSPA Model 720 at Reynolds number $5.0 \cdot 10^6$ and an HSVA Tanker at $6.6 \cdot 10^6$. The results demonstrate that the simple version of the method is accurate enough to predict differences due to changes in the hull form and can therefore be used in an optimization procedure. The higher order versions predict the absolute value of the viscous resistance with an acceptable accuracy and provide a reasonable quantitative prediction of local flow properties including skin friction and pressure coefficients.

ACKNOWLEDGEMENTS

The author wishes to express his deep gratitude to his advisor Professor L Larsson for his valuable suggestions and continual guidance, and cordial thanks to Professor G Dyne and Professor C-O Larsson for their constant encouragement during the course of the work.

The author is also most grateful to Dr K-S, Min for his deep understanding and spiritual encouragement.

Thanks are expressed to all my colleagues at Chalmers and SSPA, particularly Mr L Broberg, Mr D-H Zhang and Miss E Samuelsson for their constructive advice and help in many respects.

Finally, the author would like to express his appreciation to his family for their understanding, patience and everlasting love.

The work was funded by the Swedish Board for Technical Development and Hugo Hammar's Fund for Maritime Research, financial support for living expenses being provided by Daewoo Shipbuilding & Heavy Machinery Ltd in Korea.

CONTENTS	
	PAGE
FOREWORD	1
ABSTRACT	2
ACKNOWLEDGEMENTS	3
CONTENTS	4
LIST OF SYMBOLS	5
I. INTRODUCTION	8
II. COORDINATE SYSTEM	11
II-1. Mathematical Model of Hull Forms	12
II-2. Streamline Coordinate System	13
III. BASIC EQUATIONS	16
III-1. Governing Boundary Layer Equations	16
III-2. Momentum Integral Equations	17
III-3. Empirical Correlations	21
IV. NUMERICAL METHOD AND CALCULATION STRATEGY	24
IV-1. First Order Method	25
IV-2. Higher Order Method	26
IV-3. Numerical Calculation Procedure	31
V. RESULTS AND DISCUSSION	36
V-1. Results for an SSPA Model 720	36
V-2. Results for an HSVA Tanker Model	39
V-3. Computation Time	41
VI. CONCLUDING REMARKS AND FUTURE WORK	43
REFERENCES	45
LIST OF FIGURES	48

LIST OF SYMBOLS

A	Area
A_{mn}	Surface equation coefficient matrix
B	Half-beam of ship
C_B	Block coefficient
C_E	Entrainment coefficient
C_F	Skin friction coefficient (total)
C_f	Skin friction coefficient (local) in x-direction
C_p	Pressure coefficient
C_v	Viscous resistance coefficient
E	Entrainment rate
F_n	Froude number V_s/\sqrt{gL}
g	Acceleration of gravity
H_1	Head's shape factor for the velocity profile
H_{12}	Shape factor for the velocity profile
h_1, h_2, h_3	Metric coefficients
I_{px}, I_{pz}	Pressure integrals defined by (18a) and (18c)
I_{k1x}, I_{k3x}	Curvature integrals defined by (18)
I_{k1z}, I_{k3z}	
K_{12}, K_{32}	Normal curvatures of surfaces $y=\text{const.}$ along lines $z=\text{const.}$ and $x=\text{const.}$ respectively
K_{120}, K_{320}	As above, but for $y = 0$
K_{13}, K_{31}	Geodesic curvatures of lines $z=\text{const.}$ and $x=\text{const.}$ on surfaces $y=\text{const.}$
K_{130}, K_{310}	As above, but for $y = 0$
L	Ship length
$M-1$	Degree of polynomials fitted in X-direction
N	Number of terms in mapping of individual sections
\vec{N}	Unit normal vector of the coordinate lines
p	Static pressure
p_0	Static pressure on the surface
p_e	Static pressure at the edge of the boundary layer
q	Arc length along the girth line
R	Radius of curvature of the surface
R_n	Reynolds number $V_s \cdot L/\nu$

R_V	Viscous resistance
S	Wetted surface area
s	Arc length along the streamline
\vec{T}	Unit tangent vector of the coordinate lines
U, V, W	Mean velocity components
u', v', w'	Fluctuating velocity components
U_e, V_e, W_e	Mean velocity components at the edge of the boundary layer
U_∞	Freestream velocity
V	Displacement volume of ship
V_N	Transpiration velocity
V_S	Ship speed
X, Y, Z	Global coordinate system (X downstream, Z upwards)
x, y, z	Local coordinate system (x along U_e , y normal)
Y_r	Correction to the aft end of the hull
Z_k	Z coordinate of keel line at station
β_0	Wall cross flow angle
ΔC_p	Pressure change across the boundary layer
ΔC_{pk}	Contribution to the pressure change by the normal curvature of the surface
ΔC_{pv}	Contribution to the pressure change by the first acceleration term in the y-momentum equation
ΔC_{pv2}	Contribution to the pressure change by the second acceleration term in the y-momentum equation
δ	Boundary layer thickness
$\bar{\delta}$	Generalized boundary layer thickness, eq. (13)
δ_1, δ_2	Displacement thickness, eq. (14)
$\delta^*, \delta_1^*, \delta_2^*$	Defined by eq. (14)
$\bar{\delta}_1, \bar{\delta}_2$	Generalized displacement thickness, eq. (13)
θ_{11}, θ_{12}	Momentum thickness, eq. (14)
θ_{21}, θ_{22}	
$\theta_{11}^*, \theta_{12}^*$	Defined by eq. (14)
$\theta_{21}^*, \theta_{22}^*$	
$\bar{\theta}_{11}, \bar{\theta}_{12}$	Generalized momentum thickness, eq. (13)
$\bar{\theta}_{21}, \bar{\theta}_{22}$	

θ_{11t}	Momentum thickness at trailing edge
$\theta_{11\infty}$	Momentum thickness at far wake
ν	Kinematic viscosity
ρ	density
τ_{xy}, τ_{zy}	Wall shear stress in x and z direction respectively
ϕ	Polar coordinates of mapped plane
γ_{xy}, γ_{xz}	Velocity directional coefficients

I. INTRODUCTION

This paper describes one phase of the work done in the development of a numerical method for hull form optimization with respect to resistance. The work of hull form optimization contains four basic elements: a procedure for representing the hull mathematically, a method for calculating the viscous flow, a potential flow (wave resistance) and an optimization method. The present paper treats the first two parts of the work with special focus on the second one, concerning the problem of computing the boundary layer near the stern region and wake: this is very important for the calculation of viscous resistance and also for the prediction of momentum deficit in the far wake.

Boundary layer theory has been conveniently applied to investigate the flow properties around the ship and to predict the ship's viscous resistance. A great many methods are to be found in the literature; a number of good ones were tested at the SSPA-ITTC WORKSHOP in 1980, [4], and more have been presented since then, [3, 5, 6]. These include largely integral types of boundary layer calculation methods, such as simple first order methods, higher order modifications of these, and also more complicated methods based on partial differential equations.

Successful predictions have been made of the flow over a large part of the hull. However, most boundary layer calculations usually fail to give sufficient accuracy in the prediction of the stern flow. This failure is due to a number of reasons, including the neglect of the higher order effects, such as the curvature effect, the normal pressure gradient effect and the viscid-inviscid interaction effect, the possibility of a local region of separated flow and the existence of the free surface. Several attempts, based on partial differential equations, have been made to overcome these difficulties in total or in part, [5, 6]. So far no complete success has, however, been reported.

Although these difficulties may be overcome, the resulting complicated methods require considerable effort and enormous computing time. Consequently, and in addition to being hard to compute, these calculation methods are uneconomical when the influence of hull form parameters on the overall drag of the ship is to be systematically examined.

This paper describes a general practical purpose numerical method, which is capable of determining the local flow properties and overall drag on ship hulls. The method is developed on the basis of a generalization of Larsson's first, [1], and higher order integral method, [2], to fulfil the basic requirements of generality, economy and accuracy for the application to practical hull form design.

Several versions of a computer program have been developed under the concept of different numerical strategies. The simple version of the method is developed on the assumption of a thin boundary layer for fast computation in the hull form optimization process. No higher order effects are taken into account and the choice of numerical scheme is made on the basis of simplicity and economy. One of the main reasons for the development of such a simple method is that a convenient method, capable of providing a reasonable qualitative prediction of the relative change of the hull performance due to the change of the frame lines, is most desirable, particularly in the hull form optimization process, while the higher order versions of the computer program have been developed for the final evaluation of the boundary layer characteristics of the optimized hull form. The choice of the numerical scheme is made on the basis of generality and accuracy. The higher order version III takes full account of the influence of longitudinal and transverse surface curvatures and normal pressure gradients on the development of boundary layer and wake, and also of the viscous-inviscid interaction in the stern region.

In order to examine the effect of the higher order terms on the prediction of flow properties, higher order version I, containing surface curvature effects only, and higher order version II, containing curvature and normal pressure curvature effects have been developed.

The coordinate system and the practical calculation method for the general geometrical properties are described in detail in the following section. In section III, the governing boundary layer equations in a streamline coordinate system and the required empirical correlations are described. The numerical method is briefly discussed in section IV and the calculated results of different versions of the computer program are presented in section V, which includes comparisons with the measurements for two hull forms: an SSPA Model 720 and an HSVA Tanker Model. A demonstration of the ability of the method to represent the geometry of different hull configurations analytically is also made. A summary and conclusions are presented in section VI. A description of the computer boundary layer program is given in Kim, [28].

II. COORDINATE SYSTEM

The generation of a suitable coordinate system is one of the most important tasks in ship boundary layer calculation, since the accuracy of the numerical solutions is greatly dependent of the coordinates used. This is also one of the most difficult tasks as, in general, a ship's hull is a complicated non-developable surface. Most existing commercial-purpose ships have a bulbous bow, a flat bottom and a sharply curved stern section shape. In addition, the problem is further complicated by the existence of the free surface. The chosen coordinate system must be sufficiently general to allow these various features to be represented in the boundary layer calculation.

There are several numerically generated coordinates available, which fulfil all the requirements noted above. The most popular one is body-fitted and quite attractive because of its generality, but the determination of control functions and the associated geometrical parameters requires considerable effort. This coordinate system is uneconomical to use for the present purpose.

In the present study, a streamline coordinate system has been adopted to handle the geometry and the boundary condition more simply.

The major advantage of the coordinate system is its simplicity in the boundary layer equation, due to the fact that one coordinate direction coincides with the predominant direction of the flow, and the surface of the hull is the coordinate surface. The coordinate system also has other desirable features including the possibilities of treating arbitrary shapes and the continuous evolution of the coordinates from the stern to the near wake. On the other hand, there are several disadvantages. The system is dependent on Froude number and also Reynolds number

if the displacement effect is taken into account. To remove these difficulties, double model solutions only are considered and a fixed coordinate is used under the assumption that the change of coordinate between successive iteration steps is negligible in the present calculation.

II-1. Mathematical Model of Hull Forms

To make it possible to couple the present method with hull form optimization routines and also to make it easier to determine geometrical properties, such as metric coefficients and surface curvatures, a modified mathematical hull form representation method, very similar to that developed by von Kerczek & Tuck, [9], is employed. According to the new method the hull surface can be expressed by the mathematical equation in the parametric form as

$$Y = Y(X, \phi) = Y_r + \sum_{n=1}^N \sum_{m=1}^M A_{mn} X^{m-1} \cdot \cos\{(3-2n)\phi\}$$

$$Z = Z(X, \phi) = Z_c \sum_{n=1}^N \sum_{m=1}^M A_{mn} X^{m-1} \cdot \sin\{(3-2n)\phi\}$$
(1)

where

$$Z_c = 1 + \frac{T - Z_k}{Z_k} \frac{1 - e^{\frac{2}{\pi} c \phi}}{1 - e^{-c}}$$

Y_r = correction to the aft end of the hull (constant)

ϕ = angle between positive y-axis and position vector \bar{R}

c = constant

T = design draught

Z_k = z-coordinate of keel line at each section

Here the matrix coefficient A_{mn} can be determined from the off-sets in such a way that each cross section of the ship is fitted by a conformal mapping function in a least squares sense. Thereafter each coefficient, corresponding to a given term in the mapping function, is fitted with a lengthwise polynomial,

also in a least squares sense. A modified version of the Newton (Broyden-Fletcher-Goldfarb-Shanno) method with the golden section line search technique is used to determine the matrix coefficient A_{mn} . Two additional terms, Y_r and Z_c , are introduced in the hull surface equation to give a better representation in the bow and stern regions. This is in contrast to the method of von Kerczek, which is limited either to ship's hulls with conventional types of sections or to ships with small bulbous bows.

II-2. Streamline Coordinate System

Fig 1 depicts the streamline coordinate system (x,y,z) together with Cartesian coordinates (X,Y,Z) . The parametric curves $z = \text{const}$ and $x = \text{const}$ on the ship surface are chosen to coincide with the potential flow streamlines and the equipotential lines respectively. The y -axis is locally normal to the hull surface. These lines are obtained from a potential flow solution using the Hess & Smith (Douglas) method, [10]. The details of this coordinate system are described briefly in the following paragraph.

From the output of the potential flow computation, the direction cosines of the velocity and hence also of the streamlines at a large number of points on the hull surface are known. By means of spline functions these direction cosines are interpolated along the girth at certain sections. Then streamlines may be traced section by section along the hull. No equipotential lines have to be traced, however.

In the present version of the streamline tracing method, the tracing is carried out by numerically integrating the relation

$$\frac{d\phi}{dx} = (\gamma_{xy} - \frac{dy}{dx}) / \frac{dy}{d\phi} \quad (2a)$$

or

$$\frac{d\phi}{dX} = (\gamma_{XZ} - \frac{dZ}{dX}) / \frac{dZ}{d\phi} \quad (2b)$$

where the directional cosine of the velocity, γ_{XY} and γ_{XZ} , are known over the whole hull surface and the other derivative terms are easily calculated from the hull surface equation (1).

$$\frac{dY}{dX} = \sum_{n=1}^N \sum_{m=1}^M (m-1) A_{mn} X^{m-2} \cos\{(3-2n)\phi\}$$

$$\frac{dY}{d\phi} = - \sum_{n=1}^N \sum_{m=1}^M (3-2n) A_{mn} X^{m-1} \sin\{(3-2n)\phi\}$$

$$\frac{dZ}{dX} = Z_c \cdot \sum_{n=1}^N \sum_{m=1}^M (m-1) A_{mn} X^{m-2} \sin\{(3-2n)\phi\}$$

(3)

$$\begin{aligned} \frac{dZ}{d\phi} = \frac{dZ_c}{d\phi} \cdot \sum_{n=1}^N \sum_{m=1}^M A_{mn} X^{m-1} \sin\{(3-2n)\phi\} + \\ + Z_c \cdot \sum_{n=1}^N \sum_{m=1}^M (3-2n) A_{mn} X^{m-1} \cos\{(3-2n)\phi\} \end{aligned}$$

$$\frac{dZ_c}{d\phi} = \frac{T - Z_k}{Z_k} \cdot \frac{-\frac{2}{\pi} c e^{\frac{2}{\pi} c \phi}}{1 - e^{-c}}$$

The integration of equation (2) is carried out using the Runge-Kutta-Gill procedure. All streamlines are traced simultaneously with the same step size. The major advantage of the present streamline tracing method is its simplicity and generality. To use this method to find the coordinate system, it is only necessary to solve one of equation (2). The remaining one provides a check on the numerical accuracy of the mathematical expression of the ship's hull given by equation (1). Once the angle ϕ is determined at a certain step, the corresponding coordinates Y and Z are obtained from equation (1), so there is a guarantee

that the traced streamline points always are located on the hull surface. This is in contrast to many previous streamline tracing methods, for example that of Engevall (1984), [12]. Another advantage is that streamlines can be traced on the upper part of a bulbous bow. This is not possible in Larsson's method (1975), [11], for instance.

III. BASIC EQUATIONS

The three dimensional boundary layer equations and their boundary conditions for streamline coordinate system are well known, so the detail derivation will not be given here. See references [13] and [14].

III-1. Governing Boundary Layer Equation

The governing higher order boundary layer equation for a steady, incompressible turbulent flow are given by:

Continuity equation:

$$\frac{1}{h_1} \frac{\partial U}{\partial x} + \frac{\partial V}{\partial y} + \frac{1}{h_3} \frac{\partial W}{\partial z} + K_{31}U + (K_{12} + K_{32})V + K_{13}W = 0 \quad (4)$$

x - Momentum equation:

$$\begin{aligned} \frac{U}{h_1} \frac{\partial U}{\partial x} + V \frac{\partial U}{\partial y} + \frac{W}{h_3} \frac{\partial U}{\partial z} + K_{12}UV + (K_{13}U - K_{31}W)W + \frac{1}{h_1} \frac{\partial (p/\rho)}{\partial x} \\ - \frac{1}{h_1 h_3} \frac{\partial}{\partial x} (h_1 h_3 \tau_{xy}/\rho) = 0 \end{aligned} \quad (5a)$$

y- Momentum equation:

$$\frac{U}{h_1} \frac{\partial V}{\partial x} + V \frac{\partial V}{\partial y} + \frac{W}{h_3} \frac{\partial V}{\partial z} - K_{12}U^2 - K_{32}W^2 + \frac{\partial}{\partial y} (p/\rho) = 0 \quad (5b)$$

z - Momentum equation:

$$\begin{aligned} \frac{U}{h_1} \frac{\partial W}{\partial x} + V \frac{\partial W}{\partial y} + \frac{W}{h_3} \frac{\partial W}{\partial z} + (K_{31}W - K_{13}U)U + K_{32}VW \\ + \frac{1}{h_3} \frac{\partial}{\partial z} (p/\rho) - \frac{1}{h_1 h_3} \frac{\partial}{\partial y} (h_1 h_3 \tau_{zy}/\rho) = 0 \end{aligned} \quad (5c)$$

Here h_1 and h_3 denote the metric coefficients which are a measure of the stretching of the corresponding x and z axes; h_2 is assumed to be identically equal to unity and this has already been introduced in the derivation of the governing equations.

The parameters K_{13} and K_{31} are known as the geodesic curvature of the curve $z=\text{const.}$ and $x=\text{const.}$, respectively. They are given by

$$\begin{aligned} K_{13} &= \frac{1}{h_1 h_3} \frac{\partial h_1}{\partial z} \\ K_{31} &= \frac{1}{h_1 h_3} \frac{\partial h_3}{\partial x} \end{aligned} \quad (6)$$

and the normal curvatures K_{32} and K_{12} are defined by

$$\begin{aligned} K_{32} &= \frac{1}{h_2 h_3} \frac{\partial h_3}{\partial y} \\ K_{12} &= \frac{1}{h_1 h_2} \frac{\partial h_1}{\partial y} \end{aligned} \quad (7)$$

U, V and W represent the velocity components in x, y and z directions respectively. The parameters p, ρ and ν are the fluid static pressure, density and kinematic viscosity; τ_{xy} and τ_{zy} are the components of the shear stress.

$$\begin{aligned} \tau_{xy} &= \rho \left(\nu \frac{\partial u}{\partial y} - \overline{u v'} \right) \\ \tau_{zy} &= \rho \left(\nu \frac{\partial w}{\partial y} - \overline{v w'} \right) \end{aligned} \quad (8)$$

The prime quantities u', v' and w' are the fluctuating parts of the components of the velocity vector.

III-2. Momentum Integral Equations

The momentum integral equations based in the streamline coordinate system are obtained by integrating the equation (5) with respect to y from the wall, $y=0$ to some point $y>\delta$ in the potential flow outside the boundary layer. The first order momentum integral equations and entrainment equation are derived under small cross flow approximation. They are given by the following equations. See Larsson [1].

Streamwise momentum integral equation:

$$\frac{1}{h_{10}} \frac{\partial \theta_{11}}{\partial x} + (2\theta_{11} + \delta_1) \frac{1}{U_e h_{10}} \frac{\partial U_e}{\partial x} + K_{310} \theta_{11} = \frac{1}{2} C_f \quad (9a)$$

Crosswise momentum integral equation:

$$\frac{1}{h_{10}} \frac{\partial \theta_{21}}{\partial x} + 2\theta_{21} \left(\frac{1}{U_e h_{10}} \frac{\partial U_e}{\partial x} + K_{310} \right) - K_{130} (\theta_{11} + \delta_1) = \frac{1}{2} C_f \cdot \tan \beta_0 \quad (9b)$$

Entrainment equation:

$$\frac{1}{h_{10}} \frac{\partial}{\partial x} \{ U_e (\delta - \delta_1) \} + U_e K_{310} (\delta - \delta_1) - U_e K_{130} \delta_2 = E \quad (10)$$

The influence of higher order terms are neglected for the first order equations, but will be considered later for the higher order equations.

The higher order momentum integral and entrainment equations are derived by retaining the first order terms of δ/R and the larger. δ/R is the ratio of the boundary layer thickness to the radius of surface curvature R . They are given by the following equations. See Larsson [2].

Streamwise momentum integral equation:

$$\begin{aligned} & \frac{1}{h_{10}} \frac{\partial \bar{\theta}_{11}}{\partial x} + (2\theta_{11} + \delta_1) \frac{1}{U_e h_{10}} \frac{\partial U_e}{\partial x} + \frac{1}{h_{30}} \frac{\partial \bar{\theta}_{12}}{\partial z} + (\theta_{12} + \theta_{21}) \\ & \left(\frac{1}{U_e h_{30}} \frac{\partial U_e}{\partial z} + K_{130} \right) + K_{310} (\theta_{11} - \theta_{22}) = \frac{1}{2} C_f + I_{px} + I_{k1x} + I_{k3x} \end{aligned} \quad (11a)$$

Crosswise momentum integral equation:

$$\begin{aligned} & \frac{1}{h_{10}} \frac{\partial \bar{\theta}_{21}}{\partial x} + 2\theta_{21} \left(\frac{1}{U_e h_{10}} \frac{\partial U_e}{\partial x} + K_{310} \right) + \frac{1}{h_{30}} \frac{\partial \bar{\theta}_{22}}{\partial z} + \theta_{22} \left(\frac{1}{U_e h_{30}} \frac{\partial U_e}{\partial z} + K_{130} \right) \\ & - K_{130} (\theta_{11} + \delta_1 - \theta_{22}) = \frac{1}{2} C_f \tan \beta_0 + I_{pz} + I_{k1z} + I_{k3z} \end{aligned} \quad (11b)$$

Entrainment equation:

$$\begin{aligned} & \frac{1}{h_{10}} \frac{\partial}{\partial x} \{ U_e (\delta - \delta_1) \} + U_e K_{310} (\delta - \delta_1) - \frac{1}{h_{30}} \frac{\partial}{\partial z} (U_e \delta_2) - U_e K_{130} \delta_2 = \\ & (1 + K_{120} \delta) \cdot (1 + K_{320} \delta) E \end{aligned} \quad (11c)$$

The small cross flow approximation has not been applied when deriving the higher order momentum integral equation (11), however, in the computations to be presented in this paper it has been applied throughout. The six bar quantities are newly introduced in the higher order equations (11) and (12). They are defined with the relation $\delta^* = \delta^2/2$ by

$$\begin{aligned}
 \bar{\theta}_{11} &= \theta_{11} + K_{320} \theta_{11}^* \\
 \bar{\theta}_{12} &= \theta_{12} + K_{120} \theta_{12}^* \\
 \bar{\theta}_{21} &= \theta_{21} + K_{320} \theta_{21}^* \\
 \bar{\theta}_{22} &= \theta_{22} + K_{120} \theta_{22}^* \\
 \bar{\delta - \delta_1} &= \delta - \delta_1 + K_{320} (\delta^* - \delta_1^*) \\
 \bar{\delta_2} &= \delta_2 + K_{120} \delta_2^*
 \end{aligned} \tag{13}$$

Where the integral parameters are defined by

$$\begin{aligned}
 \delta_1 &= \int_0^\delta \left(1 - \frac{U}{U_e}\right) dy & \delta_2 &= \int_0^\delta -\frac{W}{U_e} dy \\
 \theta_{11} &= \int_0^\delta \left(1 - \frac{U}{U_e}\right) \frac{U}{U_e} dy & \theta_{12} &= \int_0^\delta \left(1 - \frac{U}{U_e}\right) \frac{W}{U_e} dy \\
 \theta_{21} &= \int_0^\delta -\frac{UW}{U_e^2} dy & \theta_{22} &= \int_0^\delta -\frac{W^2}{U_e^2} dy \\
 \delta_1^* &= \int_0^\delta y \left(1 - \frac{U}{U_e}\right) dy & \delta_2^* &= \int_0^\delta -y \frac{W}{U_e} dy \\
 \theta_{11}^* &= \int_0^\delta y \left(1 - \frac{U}{U_e}\right) \frac{U}{U_e} dy & \theta_{12}^* &= \int_0^\delta y \left(1 - \frac{U}{U_e}\right) \frac{W}{U_e} dy \\
 \theta_{21}^* &= \int_0^\delta -y \frac{UW}{U_e^2} dy & \theta_{22}^* &= \int_0^\delta -y \frac{W^2}{U_e^2} dy
 \end{aligned} \tag{14}$$

and two relations follow directly from the definitions

$$\begin{aligned}
 \theta_{12} &= \theta_{21} - \delta_2 \\
 \theta_{12}^* &= \theta_{21}^* - \delta_2^*
 \end{aligned} \tag{15}$$

Subscripts e and o are used to denote values at the edge of the boundary layer ($y=\delta$) and on the surface ($y=0$). C_f and β_0 are the skin friction coefficient and cross flow angle defined by

$$C_f = \tau_{ox} / \frac{1}{2} \rho U_e^2 \quad (16)$$

$$\beta_0 = \tan^{-1} \tau_{oz} / \tau_{ox} \quad (17)$$

Where $\tau_o = (\tau_{ox}, 0, \tau_{oz})$ is the wall shear stress vector.

The equations (11) and (12) differ from the corresponding first order ones (9) and (10) in three respects: the pressure and curvature integrals on the right hand side and bars over certain quantities. The "I" quantities on the right hand side members are integrals, which appear due to the inclusion of, on the one hand, pressure gradients through the layer (I_{px}, I_{pz}) and, on the other hand, normal curvature of the surface (I_{kx}, I_{kz}).

They are defined as

$$I_{px} = \frac{1}{h_{10} h_{30} U_e^2} \int_0^\delta h_3 \frac{\partial}{\partial x} \left\{ \frac{p-p_e}{\rho} - \frac{V_e}{2} \right\} dy \quad (18a)$$

$$I_{kx} = \frac{1}{h_{10} h_{30} U_e^2} \int_0^\delta h_1 h_3 K_{12} UV \, dy \quad (18b)$$

$$I_{pz} = \frac{1}{h_{10} h_{30} U_e^2} \int_0^\delta h_1 \left\{ \frac{\partial}{\partial z} (p/\rho) - U_e^2 h_3 K_{13} \right\} dy \quad (18c)$$

$$I_{kz} = \frac{1}{h_{10} h_{30} U_e^2} \int_0^\delta h_1 h_3 K_{32} VW \, dy \quad (18d)$$

$$I_{k1x} = I_{kx} - K_{120} \left[(\theta_{12}^* + \theta_{21}^*) \left(\frac{1}{U_e h_{30}} \frac{\partial U_e}{\partial z} + K_{130} \right) \right] - \theta_{21}^* \frac{1}{h_{30}} \frac{\partial K_{120}}{\partial z} \quad (18e)$$

$$I_{k3x} = -K_{320} \left[(2\theta_{11}^* + \delta_1^*) \frac{1}{U_e h_{10}} \frac{\partial U_e}{\partial x} + K_{310} (\theta_{11}^* - \theta_{22}^*) \right] - \theta_{22}^* \frac{1}{h_{10}} \frac{\partial K_{320}}{\partial x} \quad (18f)$$

$$I_{k1z} = -K_{120} \left[\theta_{22}^* \left\{ \frac{2}{U_e h} \frac{\partial U_e}{\partial z} + K_{130} \right\} - K_{130} (\theta_{11}^* + \delta_1^* + \theta_{22}^*) \right] - (\theta_{11}^* + \delta_1^* + \theta_{22}^*) \frac{1}{h_{30}} \frac{\partial K_{120}}{\partial z} \quad (18g)$$

$$I_{k3z} = I_{kz} - K_{320} \left[2\theta_{21}^* \left(\frac{1}{U_e h_{10}} \frac{\partial U_e}{\partial x} + K_{310} \right) \right] - \frac{1}{h_{10}} \frac{\partial K_{320}}{\partial x} \theta_{21}^* \quad (18h)$$

III-3. Empirical Correlations

The solution of the system of equations given by (9) or (11) requires additional relations; a correlation is needed for the skin friction coefficient C_f , a velocity profile family and an auxiliary equation are necessary. The latter can be any one of a number of possibilities, but the most popular choice is the entrainment equation, given by (10) or (12), which is essentially an integral form of the continuity equation for the boundary layer. A recent report by Childs et al, [15], shows that this is the best choice among the equations in common use.

1. Entrainment Correlation

An empirical relation between the entrainment rate and the velocity profile form factor is needed. Several of these already exist, but Head's correlation [16] is one of the better ones available. In the present calculation, Head's correlation for the boundary layer and Kang's relation [17] for the wake calculation are employed. The Head's entrainment rate may be related to H_1 via relation

$$\begin{aligned} C_E = \frac{E}{U_e} &= 0.0306 (H_1 - 3.0)^{-0.653} \\ H_1 &= 1.535 (H_{12} - 0.7)^{-2.715} + 3.3 \end{aligned} \quad (19)$$

The relation due to Kang are given by

$$C_E = \frac{E}{U_e} = 0.11299 - 0.048275 \ln(H_1) + 0.0051395 \cdot \{\ln(H_1)\}^2 \quad (20)$$

2. Velocity Profile Family

In order to compute a number of relations between the unknowns, functional relationships for the velocity profile and static pressure have to be assumed. For the tangential velocity components the most well known power-law and Mager assumptions

are made.

$$\frac{U}{U_e} = \left(\frac{Y}{\delta}\right)^{\frac{1}{n}} = \left(\frac{Y}{\delta}\right)^{\frac{H_{12}-1}{2}} \quad (21a)$$

$$\frac{W}{U_e} = \left(\frac{Y}{\delta}\right)^{\frac{H_{12}-1}{2}} \left\{1 - \frac{Y}{\delta}\right\}^2 \tan\beta_0 \quad (21b)$$

For the normal velocity component a linear variation is assumed.

$$\frac{V}{V_e} = \frac{Y}{\delta} \quad (21c)$$

In the wake calculation, an approximation of Cole's wake function is employed for the streamwise velocity profile, while Mager's assumption is used for the cross flow.

$$\frac{U}{U_e} = 1 - \lambda \cos^2\left(\frac{\pi Y}{2\delta}\right) \quad (22a)$$

$$\frac{W}{U_e} = \left\{1 - \frac{Y}{\delta}\right\}^2 \frac{U}{U_e} \tan\beta_0 \quad (22b)$$

Introducing these expressions in the definitions of the basic integral parameters, the following relations appear

$$\begin{aligned} \delta_1 &= \delta A_1 \\ \theta_{11} &= \delta (A_1 \lambda - A_2 \lambda^2) \\ \delta_2 &= -\delta \tan\beta_0 (A_3 - A_4 \lambda) \\ \theta_{12} &= \delta \tan\beta_0 (A_4 \lambda - A_5 \lambda^2) \\ \theta_{22} &= -\delta \tan^2\beta_0 (A_6 - A_7 \lambda + A_8 \lambda^2) \\ \theta_{21} &= \delta_2 + \theta_{12} \end{aligned} \quad (23)$$

By definition $H_{12} = \delta_1 / \theta_{11}$, which yields

$$\begin{aligned}
 H_{12} &= \frac{A_1}{A_1 - A_2} \\
 \lambda &= \frac{A_1}{A_2} \frac{H_{12} - 1}{H_{12}}
 \end{aligned}
 \tag{24}$$

The constants $A_1 - A_8$ attain the following numerical values

$$\begin{aligned}
 A_1 &= 0.5 \\
 A_2 &= 0.375 \\
 A_3 &= 0.333 \\
 A_4 &= 0.268 \\
 A_5 &= 0.233 \\
 A_6 &= 0.200 \\
 A_7 &= 0.359 \\
 A_8 &= 0.165
 \end{aligned}
 \tag{25}$$

3. Skin - friction Correlation

Ludwig and Tillmann [18] proposed a semi-empirical law in which the skin friction is related to the boundary layer momentum thickness and velocity profile factor. This law is supposed to be valid for mild pressure gradients and employed here.

The Ludwig-Tillmann skin friction correlation reads:

$$C_f = 0.246 \cdot (10.0)^{-0.678 H_{12}} \left(\frac{v}{U_e \cdot \theta_{11}} \right)^{0.268}
 \tag{26}$$

IV. NUMERICAL METHOD AND CALCULATION STRATEGY

The numerical method developed in the present paper is based on a generalization of Larsson's first, [1], and higher order integral method, [2]. Larsson's first order method has so far been applied to several different types of ship hulls including the SSPA Model 720 and an HSVA Tanker at the SSPA-ITTC WORKSHOP in 1980, and the higher order method has been applied only to a simple mathematical Wigley model. These methods have been found to be efficient and accurate. However, they have a limitation in their application to practical hull form design due to the fact that the one of the first order requires relatively high computing costs for routine computation in the optimization process and the one of the higher order did not have a reliable procedure for calculating normal curvatures of the ship surface.

A general practical purpose numerical method for calculating the viscous resistance and flow properties around ship hulls is presented. Several versions of a computer program have been developed under the concept of different numerical strategies. A simple version of the method has been developed for fast computation in the hull form optimization routine, while higher order versions have been developed for the final evaluation of the boundary layer-wake characteristics of the optimized hull form. The choice of the numerical scheme is made on the basis of simplicity and economy for the simple version of the method, and on the basis of generality and accuracy for the higher order versions during the development of the computer program. The details of the different versions of the method are summarized in Table 1.

To illustrate the basic differences in calculation strategy of the numerical method, we shall at first consider the solution of the first order flow equation (9), and then the solution of the full flow equation given in (11).

IV-1. First Order Method (FITBL.F77)

A simple numerical method is developed under the assumption of a thin boundary layer for the prediction of global flow properties and overall drag on ship hulls. The most simple numerical schemes have been adopted for fast computation and several approximations have been made to make the calculation procedure as simple as possible. The first order boundary layer equation (9) expressed in a streamline coordinate system together with empirical correlations, which are given in section III-3, are solved by the Runge-Kutta-Gill procedure along the streamline. No higher order effects are taken into account and the pressure distribution at the boundary layer edge is assumed to be the same as the distribution at the hull surface. The metric coefficients and the curvatures are computed as follows.

$$h_1(i,j) = 1/U_e(i,j)$$

$$h_3(i,j) = \sqrt{(Y(i,j)-Y(i,j-1))^2 + (Z(i,j)-Z(i,j-1))^2}$$

$$K_{13} = \frac{1}{h_1} \frac{\partial h_1}{\partial q} = \frac{1}{h_1(i,j)} \cdot \frac{h_1(i,j) - h_1(i,j-1)}{q(i,j) - q(i,j-1)} \quad (27)$$

$$K_{31} = \frac{1}{h_3} \frac{\partial h_3}{\partial s} = \frac{1}{h_3(i,j)} \cdot \frac{h_3(i,j) - h_3(i-1,j)}{s(i,j) - s(i-1,j)}$$

where s and q represent the arc length along the streamline and the girthline respectively. The index i and j denote the i -th station and the j -th streamline.

One of the main reasons for the development of such a simple method is that a convenient method, capable of providing a reasonable qualitative prediction of the relative change of the hull performance due to the change of the frame lines, is most desirable, particularly in the hull form optimization process.

IV-2. Higher Order Method (HITBL.F77)

Successful predictions can be made by the previously described first order method over a large part of the hull. However, the accuracy in the stern region is relatively poor. The poor resolutions are due to a number of reasons, including the turbulent nature of the three-dimensional boundary layer, the complexity and wide range of geometrical configurations employed and the neglect of the higher order effects. In order to improve the accuracy and to examine the effects of the higher order terms on the prediction of the stern flow, three versions of the higher order method have been developed. The details of the higher order methods are described in the following subsections.

1. Surface Curvature Effects (HITBL-I)

In the present version of the higher order method, HITBL-I, a numerical investigation of the effect of normal curvatures on the development of the boundary layer has been made. The numerical method takes into account the variation of metric coefficients and curvatures across the boundary layer. In the first order method h_1 and h_3 are assumed to be independent of y , which is clearly an oversimplification in the stern region of a ship. In the present approximation they are now functions of all three coordinates and a linear dependence is assumed.

$$h_1 = h_{10}(x,z)(1+K_{120}y) : h_3 = h_{30}(x,z)(1+K_{320}y) \quad (28)$$

here K_{120} and K_{320} are taken as the normal curvature of the surface, and h_2 is still assumed identically equal to unity.

In using this method special care must be taken in obtaining normal curvatures of the coordinate system, since the prediction of the viscous resistance of a ship hull as a function of the hull form partly depends on our ability to evaluate these quantities. The curvatures may be computed as follows.

The geodesic curvatures :

$$\begin{aligned} K_{13} &= \frac{d\vec{T}_s}{ds} \cdot (\vec{T}_s \times \vec{N}) \\ K_{31} &= \frac{d\vec{T}_q}{dq} \cdot (\vec{T}_q \times \vec{N}) \end{aligned} \quad (29a)$$

and normal curvatures :

$$\begin{aligned} K_{32} &= \frac{d\vec{T}_s}{ds} \cdot \vec{N} \\ K_{21} &= \frac{d\vec{T}_q}{dq} \cdot \vec{N} \end{aligned} \quad (29b)$$

where \vec{T} and \vec{N} represent the unit tangent and normal vector of the coordinate lines.

Using the velocity profiles (21) and the relations given by (28), the curvature integrals defined in (18b) and (18d) can be written as

$$\begin{aligned} I_{K1x} &= \frac{2 K_{120} V_e \theta_{11}}{U_e} \frac{B(H_{12})}{(H_{12} + 3)} \\ I_{K3x} &= -K_{320} \theta_{11}^2 A(H_{12}) \cdot \left[\frac{H_{12} + 5}{2U_e h_{10}} \cdot \frac{\partial U_e}{\partial x} + K_{310} \right] \\ I_{K1z} &= 0.5 K_{120} K_{130} \theta_{11}^2 A(H_{12}) (H_{12} + 3) \\ I_{K3z} &= 0.0 \end{aligned} \quad (30)$$

Where $A(H_{12})$ and $B(H_{12})$ are functions of H_{12} .

$$A(H_{12}) = \frac{H_{12}^2 (H_{12} + 1)}{(H_{12} - 1)(H_{12} + 3)} \quad (31a)$$

$$B(H_{12}) = \frac{H_{12} (H_{12} + 1)}{H_{12} - 1} \quad (31b)$$

2. Normal Pressure Gradient Effects (HITBL-II)

In the present version of the higher order method, HITBL-II, a numerical investigation of the effects of normal curvature and also normal pressure gradient on the development of the boundary layer and wake has been made. The numerical method takes into account the variation of normal curvature and pressure across the boundary layer.

A quite complicated expression for the pressure variation is obtained by integrating equation (5b) with a velocity profile given by either eq. (21) for the boundary or eq. (22) for the wake. It may however be simplified considerably making an order of magnitude analysis of the different terms with the assumptions that x, z, U, h_1 and h_3 are of order unity while $y, v, w, K_{12}\delta$ and $K_{32}\delta$ are of order (δ/R) . Only terms of order unity and (δ/R) will be retained in the relations given in this section.

For the boundary layer:

$$\Delta C_p = \Delta C_{pv} \left[1 - \left(\frac{y}{\delta} \right)^{\frac{1}{n} + 2} \right] + \Delta C_{pv2} \left[1 - \left(\frac{y}{\delta} \right)^2 \right] - \Delta C_{pk} \left[1 - \left(\frac{y}{\delta} \right)^{\frac{2}{n} + 1} \right] \quad (32)$$

$$\text{Where } \Delta C_p = \frac{p - p_e}{\frac{1}{2} \rho U_e^2}$$

$$n = \frac{H_{12} - 1}{2}$$

ΔC_{pv} , ΔC_{pv2} , ΔC_{pk} are contributions from the first, second and fourth term respectively in equation (5b) and they are given by

$$\begin{aligned}
\Delta C_{pv} &= \frac{4\delta^2}{(H_{12} + 3)U_e} \frac{1}{h_{10}} \frac{\partial}{\partial x} \left(\frac{V_e}{\delta} \right) \\
\Delta C_{pv2} &= \left(\frac{V_e}{U_e} \right)^2 \\
\Delta C_{pk} &= \frac{2K_{120}\delta}{H_{12}}
\end{aligned} \tag{33}$$

The pressure integrals I_{px} and I_{pz} in equations (18a) and (18d) can be obtained by introducing the pressure given by equations (32) and (33).

$$\begin{aligned}
I_{px} &= \frac{1}{2U_e^2} \left[\frac{H_{12}+3}{H_{12}+5} \frac{\partial}{h_{10}\partial x} (U_e^2 \delta \Delta C_{pv}) - \frac{1}{3} \frac{\partial}{h_{10}\partial x} (U_e^2 \delta \Delta C_{pv2}) \right. \\
&\quad \left. - \left\{ \frac{H_{12}}{H_{12}+1} + \frac{K_{320}\delta H_{12}}{H_{12}+2} \right\} \frac{\partial}{h_{10}\partial x} (U_e^2 \delta \Delta C_{pk}) \right]
\end{aligned} \tag{34a}$$

$$\begin{aligned}
I_{pz} &= \frac{1}{2U_e^2} \left[\frac{H_{12}+3}{H_{12}+5} \frac{\partial}{h_{30}\partial z} (U_e^2 \delta \Delta C_{pv}) + \frac{2}{3} \frac{\partial}{h_{30}\partial z} (U_e^2 \delta \Delta C_{pv2}) \right. \\
&\quad \left. - \left\{ \frac{H_{12}}{H_{12}+1} + \frac{K_{320}\delta H_{12}}{H_{12}+2} \right\} \frac{\partial}{h_{30}\partial z} (U_e^2 \delta \Delta C_{pk}) \right] \\
&\quad + \frac{1}{2} \frac{\partial}{h_{30}\partial z} (K_{120}\delta^2) - \frac{1}{4} \frac{\delta}{h_{30}\partial z} (K_{120}\delta^2)
\end{aligned} \tag{34b}$$

and for the wake:

$$\begin{aligned}
\Delta C_p &= \Delta C_{pv} \left[\frac{1}{2} \left\{ 1 - \left(\frac{Y}{\delta} \right)^2 \right\} - \lambda \left\{ \frac{1}{4} \left(1 - \left(\frac{Y}{\delta} \right)^2 \right) - \frac{\left(\frac{Y}{\delta} \right) \cdot \sin \pi \left(\frac{Y}{\delta} \right)}{\pi} \right. \right. \\
&\quad \left. \left. - \frac{1}{2\pi^2} \left(1 + \cos \pi \left(\frac{Y}{\delta} \right)^2 \right) \right\} \right] + \Delta C_{pv2} \left[1 - \left(\frac{Y}{\delta} \right)^2 \right]
\end{aligned} \tag{35}$$

$$\text{Where } \Delta C_{pv} = \frac{2\delta^2}{U_e} \frac{1}{h_{10}} \frac{\partial}{\partial x} \left(\frac{V_e}{\delta} \right) \tag{36}$$

$$\Delta C_{pv2} = \left(\frac{V_e}{U_e} \right)^2$$

$$I_{px} = \frac{1}{2U_e^2} \left[\left\{ \frac{1}{3} - \lambda \left(\frac{1}{6} - \frac{1}{\pi^2} \right) \right\} \frac{\partial}{h_{10}\partial x} (U_e^2 \delta \Delta C_{pv}) - \frac{1}{3} \frac{\partial}{h_{10}\partial x} (U_e^2 \delta \Delta C_{pv2}) \right] \tag{37}$$

$$I_{pz} = 0$$

3. Viscid Inviscid Interaction (HITBL-III)

As well known, the interaction between the boundary layer and the external inviscid flow may become important near the stern. In the present version of the higher order method, HITBL-III, this viscid-inviscid interaction problem has been investigated. There are several methods available for calculating the mutual influence between the boundary layer and the potential flow. One of the more popular among them is the displacement surface method, which takes the boundary layer effect on the potential flow into account by adding the displacement thickness to the original hull surface. This is, however, quite difficult in a three-dimensional case, because the potential flow and boundary layer calculations are carried out for a fictitious hull surface and new hull lines would probably have to be faired in each iteration step. Therefore an alternative approach has been employed here. All the necessary calculations are carried out for the fixed original body surface and also the location of the sources is unchanged. However, the normal velocity at the centre of each element is no longer put equal to zero, but to some finite value which will displace the whole fluid outwards equally much as the displacement thickness.

This transpiration velocity is computed according to Lighthill, [19]. In principle his derivation could be extended to take into account higher order effects in a manner similar to the one of section III but this was not considered necessary, since the effect of the transpiration velocity is in itself of higher order. The normal velocity component can be obtained by integrating the continuity equation through the boundary layer.

$$V_N = \delta_1 U_e K_{310} + \frac{1}{U_e} \frac{\partial U_e}{h_{10} \partial x} + U_e \frac{\partial \delta_1}{h_{10} \partial x} + U_e \frac{\partial \delta_2}{h_{30} \partial z} \quad (38)$$

In accordance with the small cross-flow approximation, the last term has been dropped in the present calculation.

IV-3. Numerical Calculation Procedure

The general derivation of the momentum integral equations and a suitable iterative numerical procedure for its solution have been described in detail by Larsson, [2]. This procedure was utilized with some minor modifications in the present study. The details of the numerical procedure for the prediction of ship viscous resistance are described step by step in the following paragraph.

Step 1. Hull Form Representation (HULSEC.F77, HULGEN.F77)

A ship hull is represented by a mathematical hull surface equation with seven terms mapping coefficients and a nine degree polynomial curve fit of the coefficients in the longitudinal direction.

Step 2. Coordinate System (GEOM1H.F77)

A streamline system is constructed on the hull surface based on the potential flow solution of the Douglas program with the double model approximation.

Step 3. Geometrical Properties (GEOM2H.F77)

The metric coefficients and curvatures of the hull surface are obtained from the evaluation of either eq (27) for the first order version or eq (29) for the higher order version of the method.

Step 4. First Order Boundary Layer Calculation (FITBL.F77)

The boundary layer calculation is performed based on the coordinates of Step 2 and the values of C_p and U_e on the hull surface. In order to provide initial data for the higher order calculation, the first order boundary layer calculations are reperformed based on a new coordinate system, which is generated in such a way that

the streamlines are traced along the hull surface based on the potential flow solution at the boundary layer edge.

Step 5. Higher Order Boundary Layer Calculation (HITBL.F77)

The governing higher order boundary layer equations are basically three ordinary differential equations, namely two momentum integral equations and one entrainment equation, which have to be solved for three basic variables θ_{11} , θ_{21} and H_{12} . All other equations are simply inter-relationships between the various quantities occurring in these differential equations. Then the governing equations (11) and (12) can be simply expressed in terms of $\bar{\theta}_{11}$, $\bar{\theta}_{21}$ and $\overline{\delta-\delta_1}$ instead of θ_{11} , θ_{21} and $\delta-\delta_1$.

$$\begin{aligned} a_1 \frac{d\bar{\theta}_{11}}{ds} + f_1(\theta_{11}, H_{12}, \theta_{21}, s, \dots) &= 0 \\ a_2 \frac{d\bar{\theta}_{21}}{ds} + f_2(\theta_{11}, H_{12}, \theta_{21}, s, \dots) &= 0 \\ a_3 \frac{d(\overline{\delta-\delta_1})}{ds} + b_3 \frac{d\bar{\theta}_{11}}{ds} + f_3(\theta_{11}, H_{12}, \theta_{21}, s, \dots) &= 0 \end{aligned} \quad (39)$$

This system of simultaneous first order ordinary differential equations is solved using the Runge-Kutta-Gill procedure by marching downstream along a streamline.

Since the first order method is based on the unbarred variables, the necessary relations between the barred and unbarred variables must be provided. Introducing the velocity profiles (21) and the definition of the integral thickness (14) and (15), the initial value of the barred quantities may be obtained from θ_{11} , θ_{21} and H_{12} .

$$\begin{aligned} \bar{\theta}_{11} &= \theta_{11} + K_{320} A(H_{12}) \theta_{11}^2 \\ \bar{\theta}_{21} &= \theta_{21} + K_{320} A(H_{12}) \theta_{11} \theta_{21} \\ \overline{\delta-\delta_1} &= \delta-\delta_1 + 0.5 K_{320} \theta_{11}^2 \cdot \{ B(H_{12}) - A(H_{12}) \cdot (H_{12}+1) \} \end{aligned} \quad (40)$$

In the present version of higher order method, the "I" integrals have to be included. In the expression for I_{px} , I_{k1x} , I_{k3x} and I_{pz} , the derivative terms of U_e and δ have been retained. Inserting the velocity profiles (21) in (13), δ may be obtained from θ_{11} and H_{12} in the previous iteration and U_e , V_e may be assumed known from the off-body calculation. In this way the derivatives of U_e , δ and "I" integrals can be computed in advance.

In order to proceed with the calculations a further step, the inverse calculation from barred quantities to unbarred quantities is needed. It is thus possible to obtain a solution for θ_{11} , θ_{21} and H_{12} from the system of equations (36) knowing $\bar{\theta}_{11}$, $\bar{\theta}_{21}$ and $\bar{\delta}-\bar{\delta}_1$. The equations are, however, non-linear and special care has to be exercised. The gradient projection method, which is one of the constrained multi-dimensional non-linear optimization methods, is used in the present calculation. A simple interpretation of the method arises from the fact that the inverse solution of (36) is equivalent to a solution of the constrained optimization problem which might be formulated in the following mathematical statements.

$$\text{Minimize } F(H_{12}, \theta_{11}) = |\epsilon_1| + |\epsilon_2|$$

$$H_{12} \theta_{11}$$

$$\begin{aligned} \text{subject to } \theta_{11} &\geq \bar{\theta}_{11} & \text{when } K_{320} &\leq 0.0 \\ \theta_{11} &< \bar{\theta}_{11} & K_{320} &> 0.0 \\ H_{12} &\geq 1.0 \\ H_{12} &\leq 2.5 \end{aligned} \quad (41)$$

$$\begin{aligned} \text{where } \epsilon_1 &= \bar{\theta}_{11} - \theta_{11} + K_{320} A(H_{12}) \theta_{11}^2 \\ \epsilon_2 &= \bar{\delta} - \delta_1 - \bar{\delta} - \bar{\delta}_1 + 0.5 K_{320} \theta_{11}^2 \{B(H_{12}) - A(H_{12}) \cdot (H_{12} + 1)\} \end{aligned} \quad (42)$$

Knowing θ_{11} , H_{12} and $\bar{\delta}-\bar{\delta}_1$, a new calculation may be performed a further step down along the streamline to the far wake region. Although the gradient projection method works well even in the thick boundary layer region near the stern end, numerical break-down happens when K_{320} is extremely large in negative or poor resolution of $\bar{\theta}_{11}$ and $\bar{\delta}-\bar{\delta}_1$ is taken from the first order solution.

This means that there is no real solution to eqs. (40). In order to avoid this difficulty, an approximate solution procedure is proposed. θ_{11} is determined first from the following equation.

$$\theta_{11} = \bar{\theta}_{11} \cdot \{ 1 - K_{320} A(\hat{H}_{12}) \cdot (\hat{\theta}_{11} / \bar{\theta}_{11})^2 \cdot \bar{\theta}_{11} \} \quad (43)$$

Where the superscript $\hat{}$ denotes the value in the previous iteration step. With the computed θ_{11} , H_{12} can be solved from the same calculation procedure.

Step 6. Viscid-Inviscid Interaction (HITBL-III)

A set of transpiration velocities for simulating the boundary layer effect on the potential flow is computed from eq (34) based on the displacement thickness distribution obtained using the solution of the higher order version II. The potential flow is then recalculated taking the transpiration velocities as the boundary condition and the higher order version II is used to obtain a new boundary layer solution.

Step 7. Calculation of the Viscous Resistance (FITBL.F77, HITBL.F77)

The most obvious way to obtain the viscous resistance from the boundary layer is to integrate the skin friction and pressure all over the surface to get the frictional and viscous pressure resistance. This method gives fair predictions for tangential force, however, the difficult part is the estimation of viscous pressure drag. The viscous pressure drag is calculated by allowing for the displacement effect of boundary layer on the pressure distribution. It is difficult to do accurately because in the region of very close to the stern, the accuracy of the pressure distribution becomes less reliable and such a estimation is very sensitive to small errors in stern region.

In the present calculation, the viscous resistance is calculated by computing the momentum loss in the far wake. This momentum

area can be determined either from the continuation of the boundary layer calculation along a streamline extending to the wake region or from the Squire & Young method. Both of them have been tried in order to demonstrate the difference in the prediction of viscous resistance. Applying the Squire & Young formula, [20], and extending it to three dimensional boundary layer flow, the momentum thickness θ_{11} in the far wake may be given by:

$$\theta_{11\infty} = \theta_{11t} \cdot \left\{ \frac{U_e}{U_\infty} \right\}^{(H_{12}+5)/2} \quad (44)$$

where θ_{11t} represents the momentum thickness at trailing edge.

The integration of equation (44) over the girth of a cross section therefore gives the resistance due to the momentum loss which is accumulated in the upstream portion of the body.

$$R_v = \rho U_\infty^2 \int \theta_{11\infty} dq \quad (45)$$

Despite of the relative simplicity the method is known to give a fair estimation of the viscous resistance [21,22].

V. RESULTS AND DISCUSSION

Several different versions of the computer program described in the previous sections have been tested to investigate the accuracy of the method and to define its limits of application. Two well-known hull forms, which have all the features of most commercial ships, have been used in the present study. The first one, discussed in section V-1, is the SSPA Model 720 and the other one, discussed in section V-2, is an HSVA Tanker with a rather complex shape.

V-1. Results for the SSPA Model 720

The body plan, represented by a mathematical hull surface equation with seven term mapping coefficients and nine degrees of polynomial curve fit, of $L:T:B = 2.0 : 0.11808 : 0.14167$ together with the streamlines on the hull surface is shown in Fig 2. The stern parts after $2x/L = 0.9$ have been modified so as to make variations of the normal curvature smoother and to avoid boundary layer edge interaction problems.

The modified sections are represented by solid lines, and the original ones by chain lines. The streamlines are traced on the basis of the potential flow solution of the Douglas computer program with the double model approximation. To obtain the solution 795 panel elements on the hull and wake are used. As can be seen from the figure, the uppermost streamlines are quite steep at the stern and merge into the waterline. In real flow, the waterline is a separation line and all upper streamlines at the stern merge into this line and separate. This happens fairly abruptly and quite large vertical velocity components may be found also very close to the waterline. Very similar flow patterns have been observed by Larsson, [23], in visualization tests (see Fig 3). Although significant separations are not observed, the effect of the separation is beyond the scope of the present study. To avoid this diffi-

culty and to keep the whole momentum area to the far wake, the uppermost streamlines at the stern part are modified. The modified streamlines are represented by solid lines and the original ones by chain lines.

The boundary layer-wake calculations are carried out at a Reynolds number, based on the length of the ship, equal to 5.0×10^6 , starting at $2x/L = -0.6$. The initial values are obtained from the measurements by Larsson, [24], which are given in Fig 4. A comparison of calculated and experimental values of the streamwise momentum thickness θ_{11} , the local skin friction coefficient c_f , the transverse distributions of the pressure coefficients c_p and the cross flow angle β_0 are shown in Figs 5-8 respectively, at (a) $2x/L = 0.5$, (b) $2x/L = 0.7$ and (c) $2x/L = 0.8$.

As can be seen from the figures, the boundary layer parameters vary greatly near the keel, where the curvatures and the pressure gradients are large and remain almost unchanged near the water surface, where the curvatures and pressure gradients are small. The most striking results for the keel line are the overprediction of the momentum thickness (Fig 5) and the irregular pressure distribution (Fig 7). This line is in the vertical plane of symmetry, where the boundary layer is thin and no longitudinal curvature effects appear. The main reason for the overprediction is probably small cross flow approximation, see Larsson, [4].

Judging from the girthwise distribution of the results in Figs 5-8 the boundary layer integral parameters are fairly well predicted by all the present methods, including first order theory at $2x/L = 0.5$, where the boundary layer still is thin.

At $2x/L = 0.7$ higher order effects have already started to play an important role. In general, the first order method produces a peak in the momentum thickness around $2G/L = 0.11$. Large cross flow angle gradients also appear around this position.

At $2x/L = 0.8$ the higher order methods seem to produce reasonable distributions, with some exception of the cross flow angle. The first order method produces too high a peak in the momentum thickness around $2G/L = 0.1$, resulting in an overprediction of the viscous resistance. Even though the results are not perfect, the higher order versions II and III give better predictions of momentum thickness and pressure distribution from the results of the inclusion of the effects of normal pressure gradients and viscous-inviscid interaction.

Fig 9.a shows the distribution of the boundary layer thickness at $2x/L = 0.7, 0.8$ and 0.9 , calculated by higher order theory with a comparison with measured values. The distribution does not seem unreasonable.

The calculated viscous resistance coefficients c_v are compared with measured ones in Table 2. The measurements were carried out by Freimanis & Lindgren, [25], in the SSPA towing tank. In the present calculations, the viscous resistance has been estimated by computing the momentum loss in the far wake ($2x/L = 2.0$). This momentum area was determined from the continuation of the boundary layer calculation along streamlines extending to the wake region and the Squire-Young method. There is a small quantitative difference between these two methods, but the qualitative agreement is fairly good. On the other hand, the viscous resistance calculated according to the simple version of first order theory differs considerably from the measured one, while the higher order versions produce reasonable predictions with 4-5%

difference. A probable reason for the difference in the first order theory is the overprediction of the momentum thickness in the stern region due to the neglect of higher order terms.

V-2. Results for the HSVA Tanker Model

The HSVA Tanker model, unlike the one discussed in section V-1, has a rather complex geometrical shape. The model possesses all the special features of a commercial ship, that is, a flat bottom and a sharply curved section shape in aftbody, and consequently serves an excellent case on which to investigate the accuracy of the methods and make clear their limit of application.

The bodyplan, represented by a mathematical hull surface equation with seven terms mapping coefficients and nine degrees of polynomial curve fit, of $L:T:B = 2.0 : 0.11228 : 0.15146$ together with the streamlines on the hull surface is shown in Fig 10. The streamlines are traced based on the potential flow solution with 741 panel elements for the Douglas program, treating the model as a double ship model.

The boundary layer calculations are carried out at a Reynolds number, based on the length L between perpendiculars, equal to 6.6×10^6 , starting at $2x/L = -0.790$. The initial values are obtained from measurements, which are given in Fig. 11. A comparison of computed results of θ_{11} , C_f , C_p and β_0 and Hoffmann's measurements [26] is shown in Figs 12-15 respectively, at (a) $2x/L = -0.744$, (b) $2x/L = 0.291$, (c) $2x/L = 0.502$ and (d) $2x/L = 0.884$.

As can be seen from the figures, similar tendencies as for the SSPA Model 720 case are observed. The correspondence between calculations and measurements is fairly good at $2x/L = -0.744$ as expected from the fact that this station is very close to the initial station.

Station $2x/L = 0.291$ is on the parallel middle body. As expected the measured variations in the integral parameters are very smooth compared with the first station. There is one marked peak, however. It occurs at the mid-girth for the momentum thickness. This was not observed in SSPA Model 720 case and all of the present methods miss it entirely. The only possible explanation is the existence of a bilge vortices in the boundary layer. It should be kept in mind that the hull is extremely full at the forebody and the radius of curvature of the bilges is quite small. If this explanation is correct, it is not surprising that no one of the present methods is able to predict the very high momentum thickness at the bilge, since the effect of a longitudinal vortex is not taken into account in the present calculation.

Also at station $2x/L = 0.502$, the same situation as for as the previous station occurs, but the variations are rather small. In fact even this station is not too far from the parallel part of hull.

At the final station $2x/L = 0.884$, similar tendencies as for the SSPA Model 720 are observed. The higher order methods seem to produce reasonable distributions for momentum thickness and pressure coefficients.

It should be noted that the deviation of the calculated skin friction from the measured one is relatively large, as can be seen from Fig 13. Possible reasons for this large deviation are the numerical errors in the computer program and/or measurement errors. The first explanation is not likely to be true, since the deviation is not to be found in the case of the SSPA Model 720 and the prediction of the other boundary layer parameters is reasonably good. A more possible reason is probably measurement errors, as indicated by the fact that the skin friction calculated by the Ludwig-Tillmann equation with the measured momentum thickness Reynolds number Re_θ and the shape factor H_{12} has almost the same magnitude as the one predicted by the present

calculation method.

Fig 16 shows the ditribution of the boundary layer thickness δ at $2x/L = 0.7, 0.8$ and 0.9 calculated by higher order theory with comparison with measured values. It seems to be reasonable.

The calculated viscous resistance coefficient C_v is shown in Table 2. In this case only the Squire-Young method is applied at station No 1 ($2x/L = 0.9$) to calculate the viscous resistance. It is noticed that the values predicted by different methods have almost the same magnitude. The measured value obtained from the towing test, [27], is shown in Table 2. The calculated viscous resistance is only 4-7 per cent lower than the measured one. It may therefore be concluded that the first order method is generally applicable to practical use with qualitative accuracy and the higher order versions of the present method predict the viscous resistance with acceptable accuracy.

V-3. Computation Time

The numerical procedure described in section IV was programmed for a Data General Computer at SSPA Maritime Consulting. The program was designed to be sufficiently general to allow it to be applied to practical hull form design and to be very flexible at the choice of numerical schemes in the boundary layer calculation. The details of the boundary layer computer program are given in reference [28].

One of the main advantages of the present calculation method compared to the method based on partially differential equations is the low computation time. Particularly the first order method is designed to be very simple and to be used in an optimization procedure. The necessary computation time for calculation of the viscous resistance depends much not only on the number of elements, streamlines and stations, but also on the numerical schemes chosen. The total CPU times for the HSVA Tanker case are as follows:

- Hull form representation (40 stations)	210 sec
- The basic potential flow (741 elements)	approx. 780 sec
- Coordinate system (17 streamlines)	250 sec
- Geometrical properties (17 x 40 points)	150 sec
- First order method	38 sec
- Higher order version I	278 sec
- Higher order version II	503 sec
- Higher order version III	1 623 sec

VI. CONCLUDING REMARKS AND FUTURE WORK

A general method for calculating the viscous resistance and flow properties around ship hulls is presented. A simple version of the method has been developed for fast computation in the hull form optimization routine, while higher order versions have been developed for the final evaluation of optimized hull forms. Numerical calculations of the boundary layer/wake have been made for two ship models at zero Froude number. According to these studies the following conclusions can be drawn:

- The first order method is accurate enough to predict the differences in hull performance due to changes in the hull form and can therefore be used in an optimization procedure with its essential features of numerical economy and qualitative accuracy.
- The higher order versions predict the viscous resistance with acceptable accuracy and provide a reasonable quantitative prediction of the local flow properties including skin friction and pressure coefficients.
- The importance of higher order effects becomes more dominant in the stern region. The only reasonable distributions of the momentum thickness and pressure coefficients were obtained with the method incorporating higher order effects. However, there is no big difference in the solutions with or without viscid-inviscid interaction. Stronger techniques may be necessary for the interaction problem, particularly in the presence of bilge vortices.

There is, however, a problem that needs to be considered and investigated before the present method can become a more effective tool in the design of ships, namely:

- The quality of the computed results is rather sensitive to the initial conditions, particularly to the initial distribution of cross flow angle. Additional work on the development of a general method for the generation of the initial conditions on arbitrary bow configurations is required.

REFERENCES

- [1] Larsson, L: A Calculation Method for Three-Dimensional Turbulent Boundary Layers on Ship-Like Bodies. First International Conference on Numerical Ship Hydrodynamics, Washington DC, 1975
- [2] Larsson, L & Chang, M-S: Numerical Viscous and Wave Resistance Calculations Including Interaction. 13th Symposium on Naval Hydrodynamics, Tokyo, 1980
- [3] Larsson, L (Editor): Proceedings of the First International Symposium on Ship Viscous Resistance. SSPA, 1978
- [4] Larsson, L (Editor): SSPA-ITTC Workshop on Ship Boundary Layers 1980. Proceedings, Publication of the Swedish Maritime Research Centre, SSPA No 90, 1981
- [5] Larsson, L (Editor): Proceedings of the Second International Symposium on Ship Viscous Resistance. SSPA, 1985
- [6] Tanaka, I (Editor): Osaka International Colloquium on Ship Viscous Flow. Proceedings, Osaka, 1985
- [7] Broberg, L: Calculation of Partially Parabolic Stern Flow. SSPA Report 2801-1, 1987
- [8] Chen H. C. & Patel V. C.: Calculation of Trailing-edge, Stern and Wake Flows by a Time-Marching Solution of the Partially-Parabolic Equations. IIHR Report No. 285, The University of Iowa, 1985
- [9] von Kerczek, C H & Tuck E O: The Representation of Ship Hulls by Conformal Mapping Functions. Journal of Ship Research, 1969
- [10] Hess J L & Smith A M O: Calculation of Potential Flow about Arbitrary Bodies. Progress in Aeronautical Sciences, Vol 8, Oxford, 1967

- [11] Larsson, L: Boundary Layers of Ships. Part IV: Calculations of the Turbulent Boundary Layer on a Ship Model. SSPA Allmän Rapport nr 47, 1974
- [12] Engevall, T: Strömlinjespråning Längs Fartygsskrov. (in Swedish), Examensarbete för civilingenjörsexamen 1984, Division of Marine Hydrodynamics, Chalmers University of Technology
- [13] Nash J F & Patel V C: Three Dimensional Boundary Layers, SBC Technical Books, Atlanta, 1972, 185p.
- [14] Larsson, L & Löfdahl L: A Method for Calculating Thick Three-Dimensional Turbulent Boundary Layers. Part I: Equations and General Principles, SSPA Report No 2360-1, 1979, 23p.
- [15] Childs et al: A Method of Prediction for Subsonic Compressible Diffusers. Report PD-24, Dept. of Mech. Eng. Stanford Univ., 1981
- [16] Head M R: Entrainment in the Turbulent Boundary Layer, Aeronautical Research Council, R&M No 3151, London 1958, 17p.
- [17] Kang S-H: Viscous Effects on the Wave Resistance of a Ship, Ph D Thesis, The University of Iowa, 1978
- [18] Ludwig, H & Tillmann, W: Investigation of the wall Shear Stress in Turbulent Boundary Layers (in German), Ingenieur-Archiv Vol. 17, 1949
- [19] Lighthill, M J: On Displacement Thickness. Journal of Fluid Mechanics 4(1958): p383-392.
- [20] Schlichting, H: Boundary Layer Theory. McGraw-Hill Book Co. Inc, Seventh Edition, p758.

- [21] Himeno Y: A Boundary-Layer Calculation on Ship Stern Wake Field and Viscous Resistance Including Vortex Resistance. US-JAPAN Cooperative Research on Viscous Flow Around Ships IIHR Report No. 265, The University of Iowa, 1983
- [22] Shirose, Y et al: Influence of Principal Particulars of Ships on Viscous Flow. Osaka International Colloquium on Ship Viscous Flow, 1985, p209-226
- [23] Larsson, L: An Experimental Investigation of the Three-Dimensional Turbulent Boundary Layer on a Ship Model. 11th Symposium on Naval Hydrodynamics, London, 1976
- [24] Larsson, L: Boundary Layers of Ships. Part III: An Experimental Investigation of the Turbulent Boundary Layer on a Ship Model. SSPA Allmän Rapport nr 46, 1974
- [25] Freimanis, E & Lindgren H: Systematic Tests with Ship Model with $\delta_{pp} = 0.675$, Part 1: Influence of Shape of Sections, SSPA Publication No. 39, 1957
- [26] Hoffmann, H P: Investigation of a Three-Dimensional Turbulent Boundary Layer on a Double Model of a Ship in a Wind Tunnel (in German). Institut für Schiffbau, University of Hamburg, Report No. 343, 1976
- [27] Naples Ship Model Basin Contribution to ITTC Resistance Committee Cooperative Experimental Program. CETENA Report 1887, Sept., 1983, Genoa, Italy
- [28] Kim K-J: A Description of a General Method for Calculating Three-Dimensional Boundary Layers on Ship Hull. SSPA Report 8081-1A, 1987

LIST OF FIGURES

- Fig 1 : General Coordinate System
- Fig 2 : Body plan and streamline coordinate system(SSPA Model 720)
- Fig 3 : Visualization of the flow around the stern of a double model (SSPA Model 720)
- Fig 4 . Initial values of θ_{11} , H_{12} and β_0 at station $2x/L=-0.6$
- Fig 5 : Comparison of computed momentum thickness θ_{11} with Larsson's measurement data at $2x/L=0.5, 0.7$ and 0.8
- Fig 6 : Comparison of computed skin friction C_f with measurements
- Fig 7 : Comparison of computed pressure coefficient C_p with measurement data
- Fig 8 : Comparison of computed cross flow angle β_0 with measurement data
- Fig 9 : Distribution of boundary layer thickness at $2x/L=0.7, 0.8$ and 0.9
- Fig 10: Body plan and streamline coordinate system(HSVA Tanker)
- Fig 11: Initial values of θ_{11} , H_{12} and β_0 at station $2x/L=-0.790$
- Fig 12: Comparison of computed momentum thickness θ_{11} with Hoffmann's measurement data at $2x/L=-0.744, 0.291, 0.502$ and 0.884
- Fig 13: Comparison of computed skin friction C_f with measurements
- Fig 14: Comparison of computed pressure coefficient C_p with measurement data
- Fig 15: Comparison of computed cross flow angle β_0 with measurement data
- Fig 16: Distribution of boundary layer thickness at $2x/L=0.7, 0.8$ and 0.9

Table 1. Summary of Numerical Methods

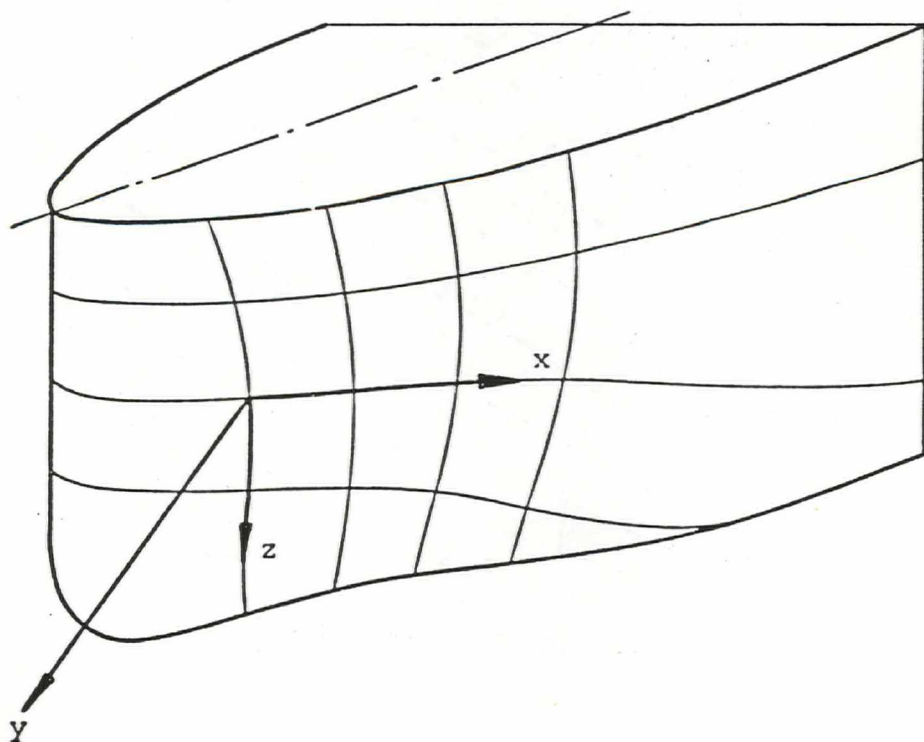
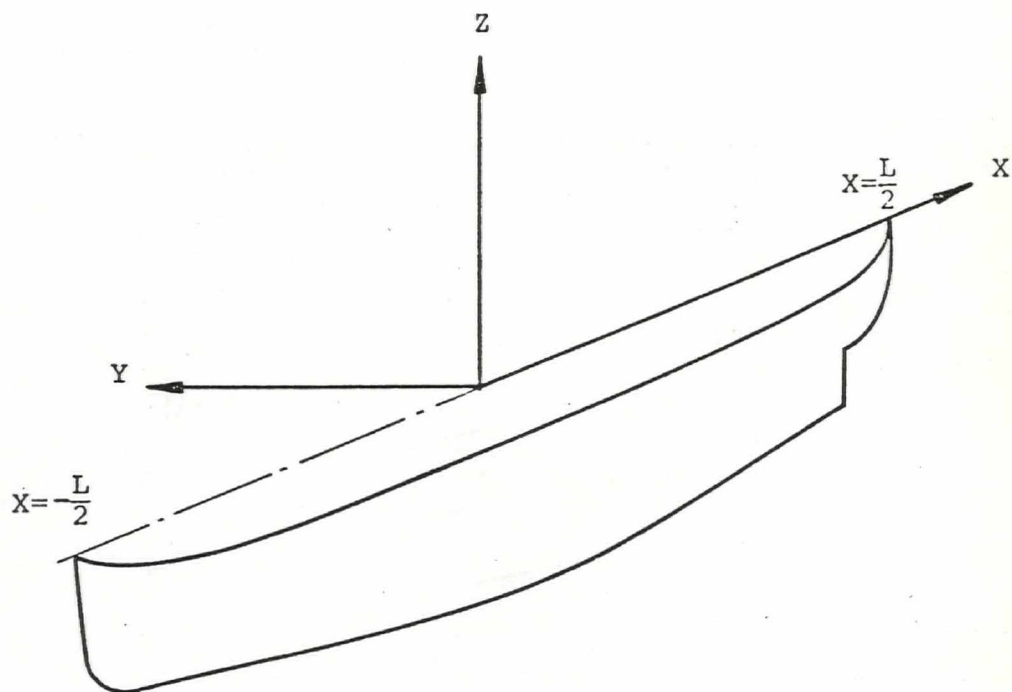
Methods	First Order Method (FITBL.F77)	Higher Order Method (HITBL.F77)		
		Version - I	Version - II	Version - III
Numerical Strategy	Simplicity Economy	Generality Accuracy	Generality Accuracy	Generality Accuracy
Higher Order Effects	No higher order effects	Surface curvature effect only	Surface curvature effect + Normal pressure gradient effect	Surface curvature effect + Normal pressure gradient effect + Viscid inviscid interaction
Accuracy	Qualitative prediction of the global flow properties	Quantitative prediction of the local flow properties including skin friction and pressure coefficients		
Application	Routine computation in optimization procedure	Final evaluation of the boundary layer characteristics of the optimized hull form		
Total CPU Time (HSVA Tanker)	38 sec	278 sec	503 sec	1623 sec

Table 2. Calculated Viscous Resistance Coefficients

Numerical Methods			SSPA Model 720	HSVA Tanker
Calculation (C_v*10^3)	FITBL	S-Y	2.929	3.490
		M-D	2.950	-
	HITBL-I	S-Y	2.530	3.499
		M-D	2.790	-
	HITBL-II	S-Y	2.270	3.521
		M-D	2.490	-
	HITBL-III	S-Y	2.250	3.560
		M-D	2.470	-
Measurement (C_v*10^3)			2.357	3.749

Note : M-D \Rightarrow Momentum area is determined from wake calculation.

S-Y \Rightarrow Momentum area is determined from Squire-Young formula

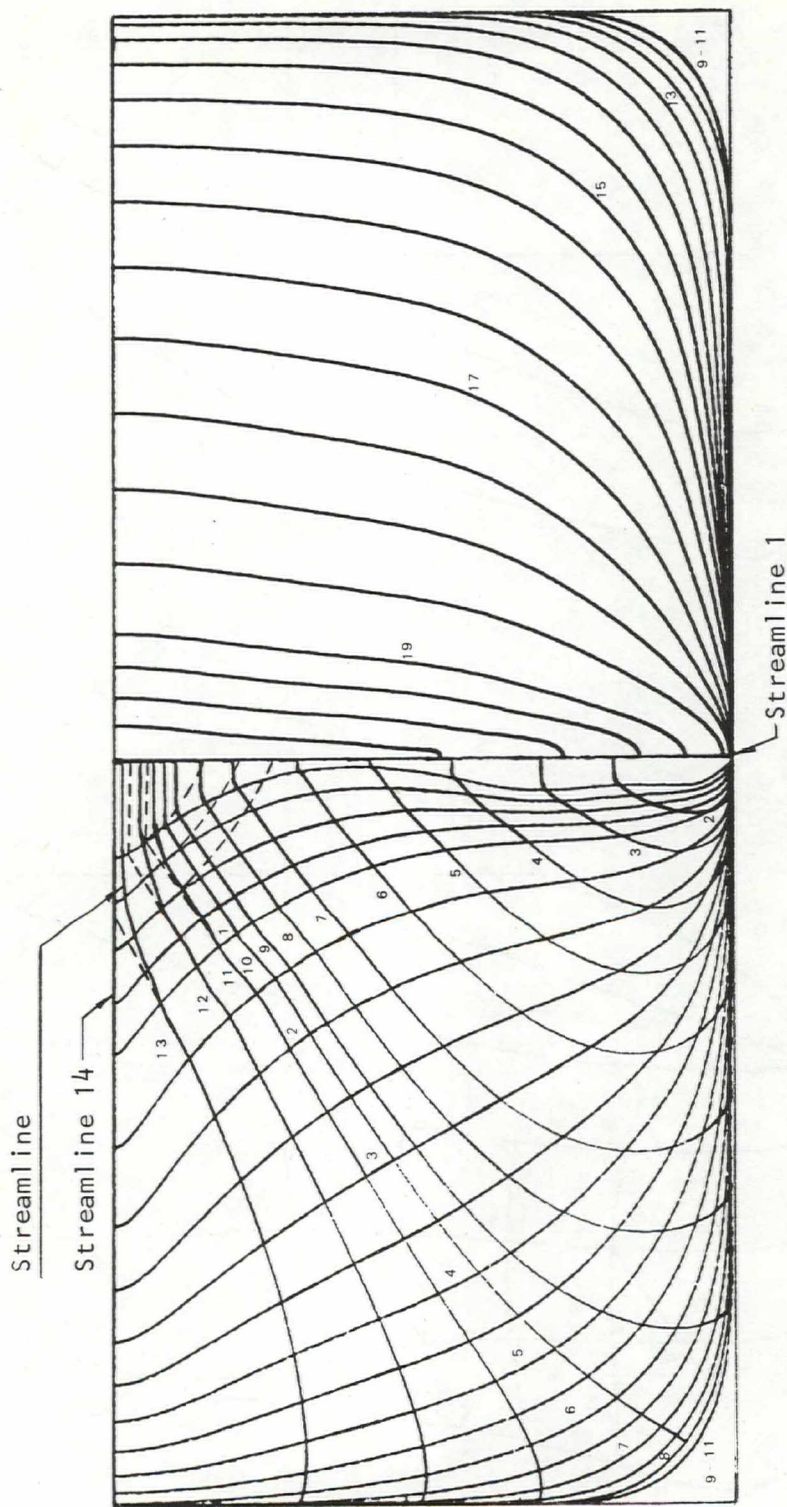


SSPA
&
CTH

BODY PLAN AND STREAMLINE COORDINATE

SSPA MODEL 720

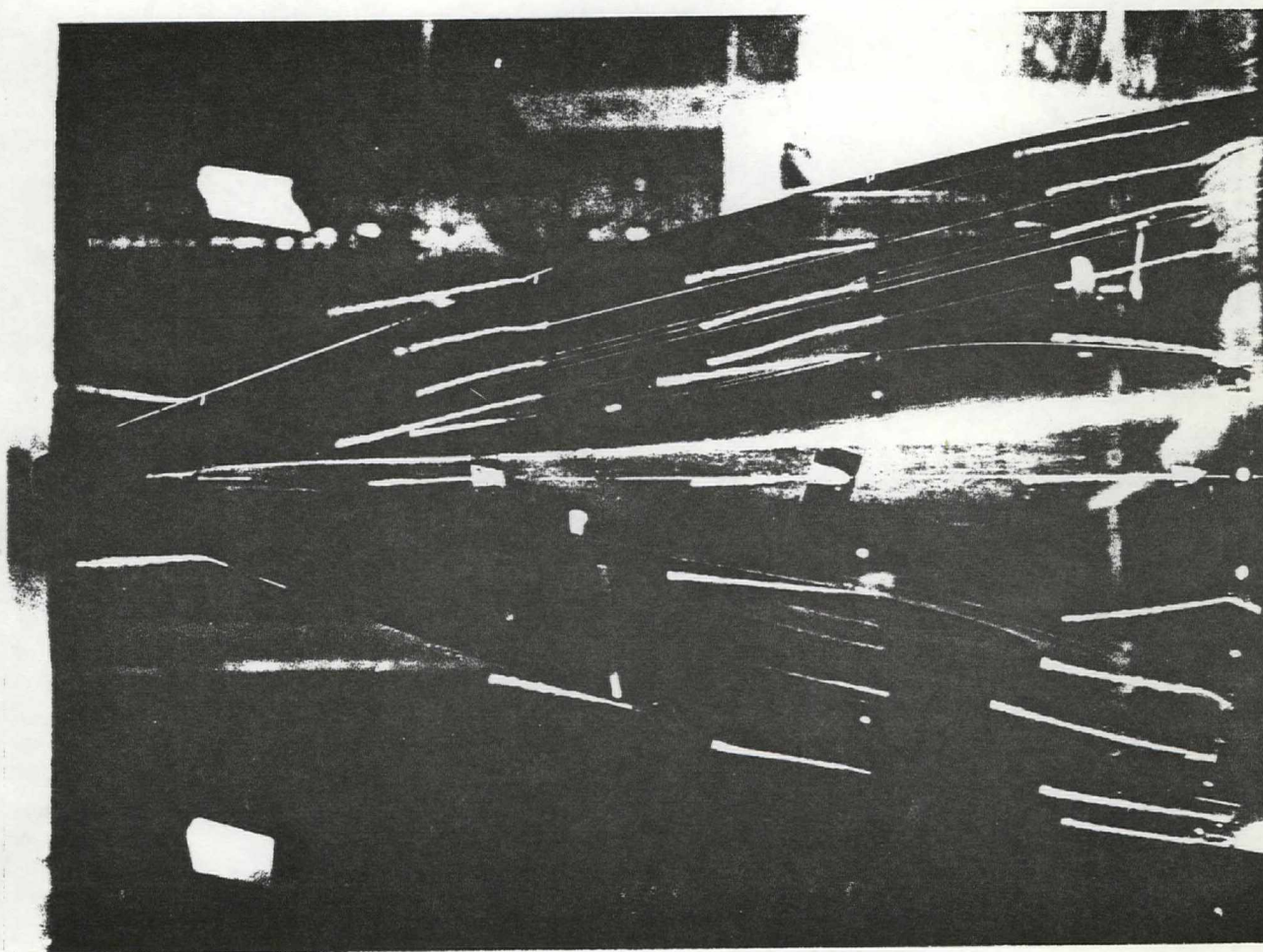
FIG. 2



**SSPA
&
CTH**

**VISUALIZATION OF THE FLOW AROUND
THE STERN OF A DOUBLE MODEL
SSPA MODEL 720 REF. [23]**

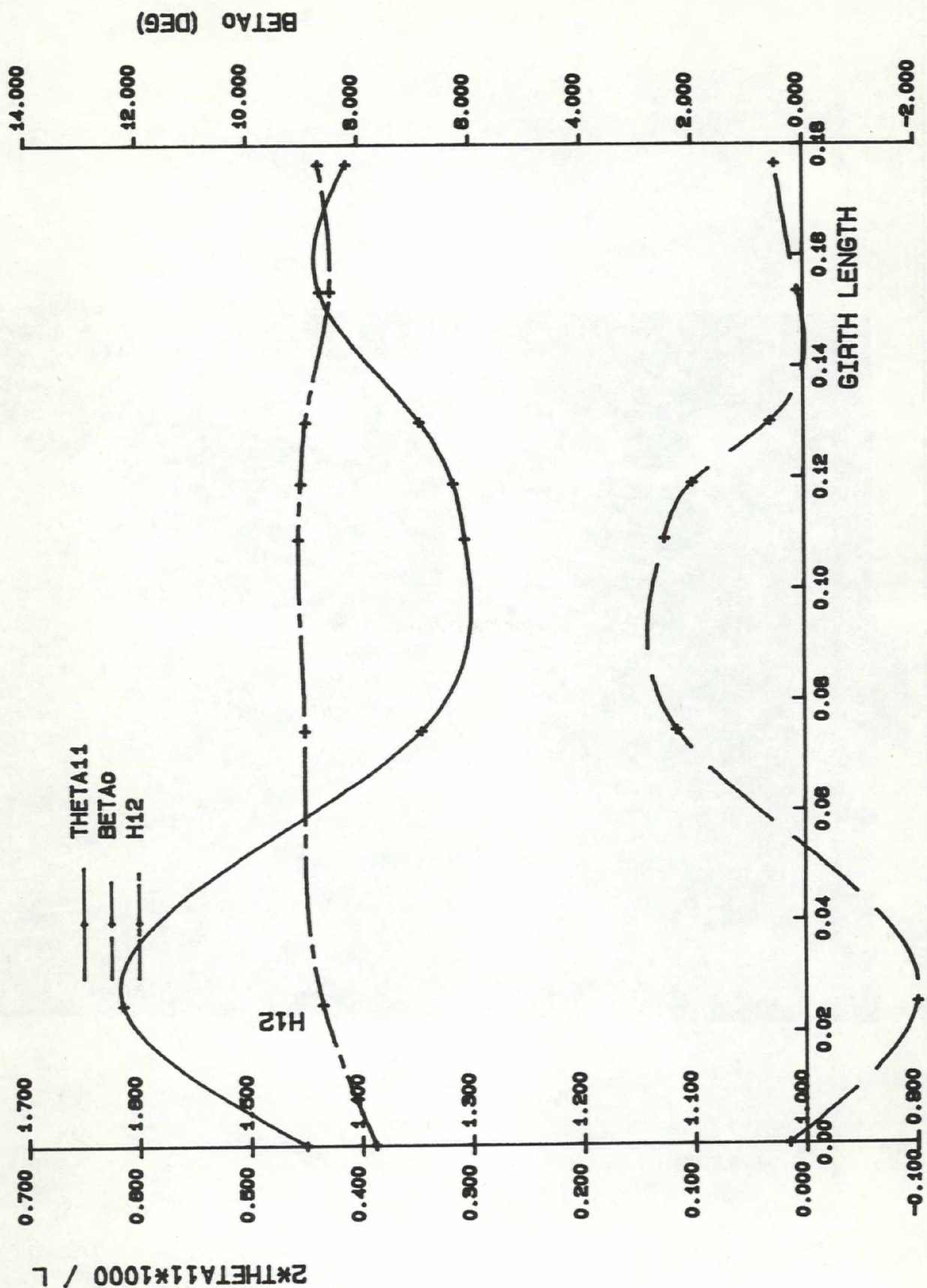
FIG. 3



SSPA & CTH

INITIAL VALUES OF THETA11, H12
AND BETA0 AT STATION $2X/L = -0.6$
SSPA MODEL 720

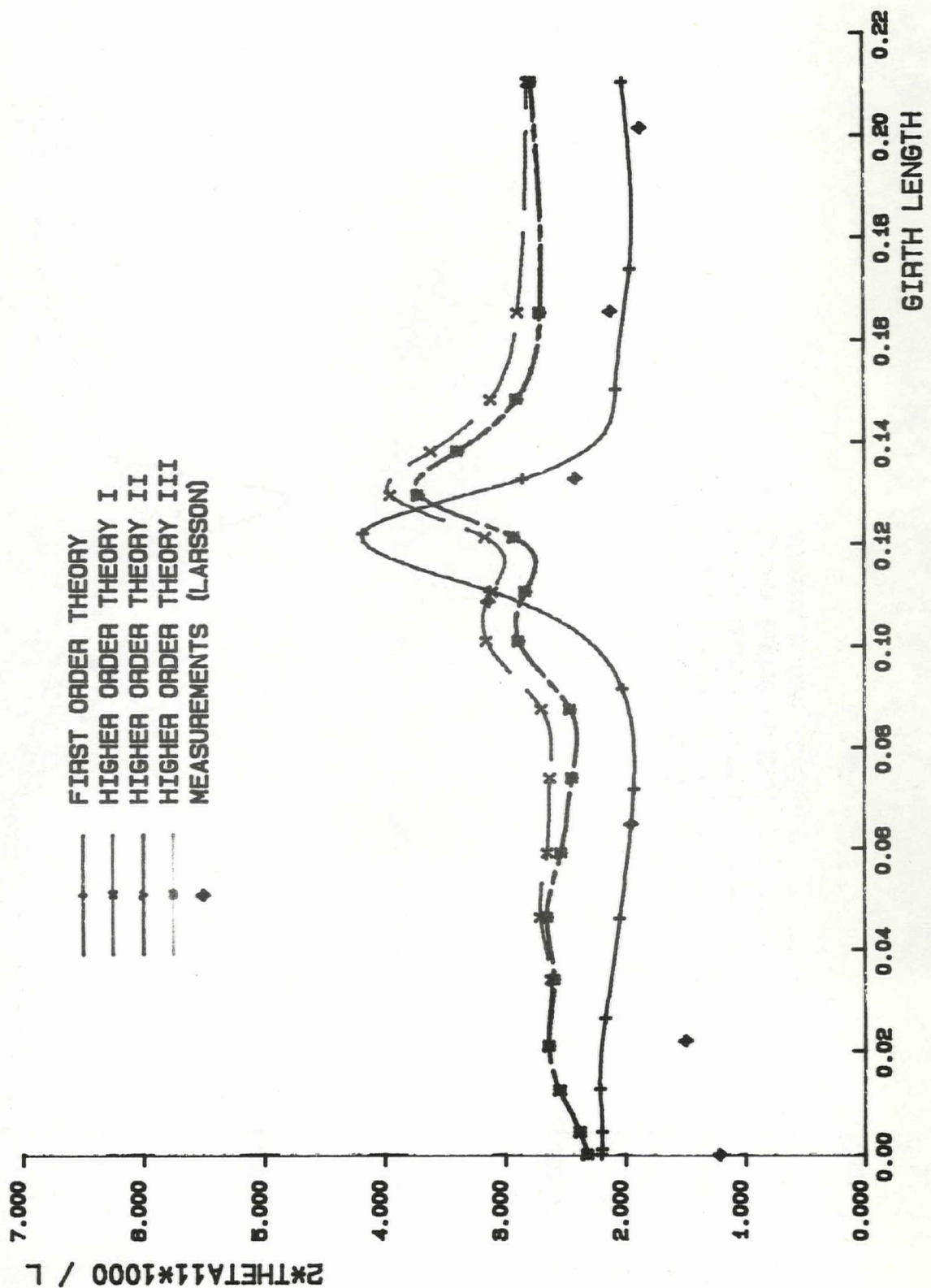
FIG. 4



SSPA
&
CTH

COMPUTED MOMENTUM THICKNESS
FOR RE=5.0E08 AT 2X/L = 0.5
SSPA MODEL 720

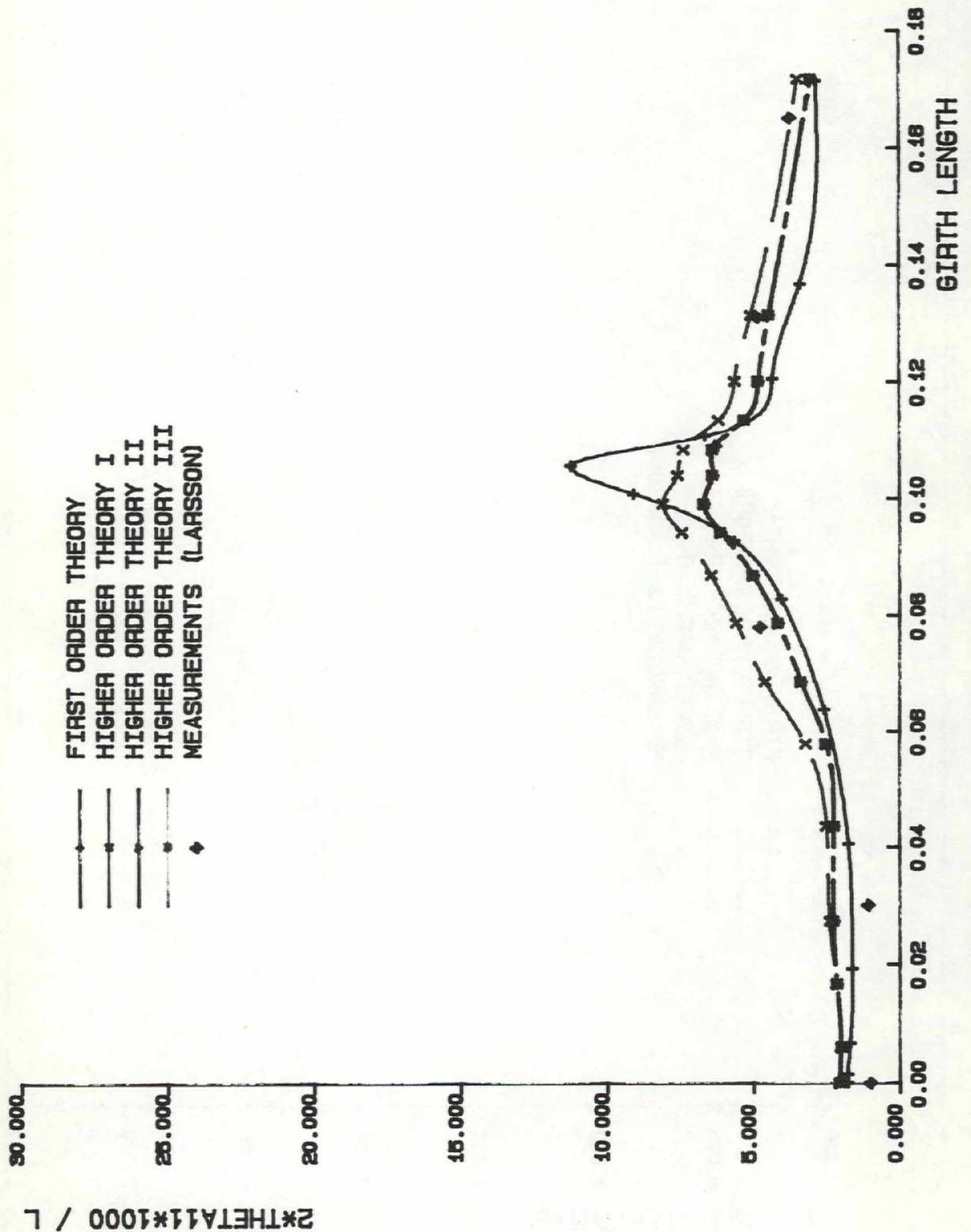
FIG. 5a



SSPA
&
CTH

COMPUTED MOMENTUM THICKNESS
FOR $RE=5.0E08$ AT $2X/L = 0.7$
SSPA MODEL 720

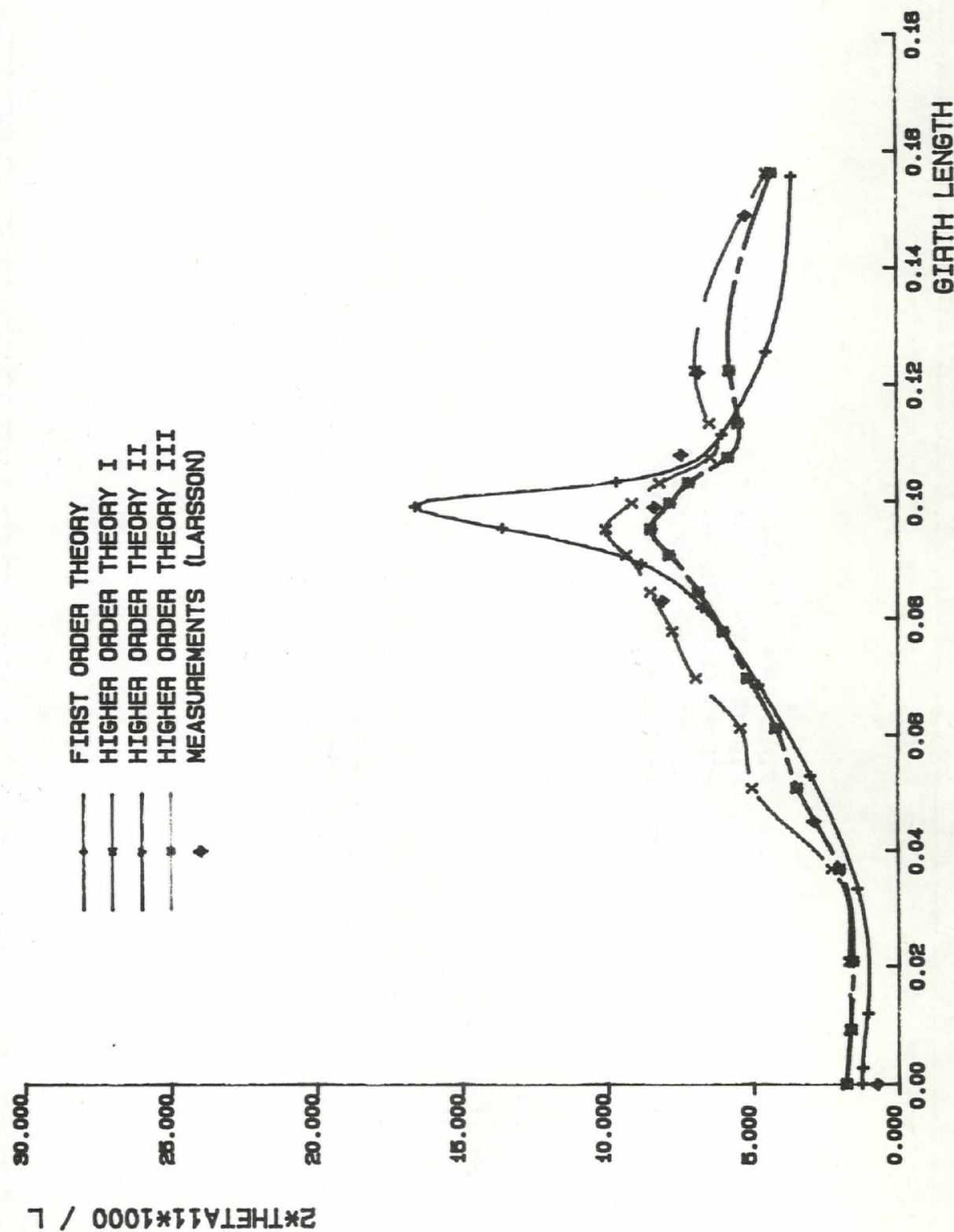
FIG. 5b



SSPA
&
CTH

COMPUTED MOMENTUM THICKNESS
FOR $RE=5.0E08$ AT $2X/L = 0.8$
SSPA MODEL 720

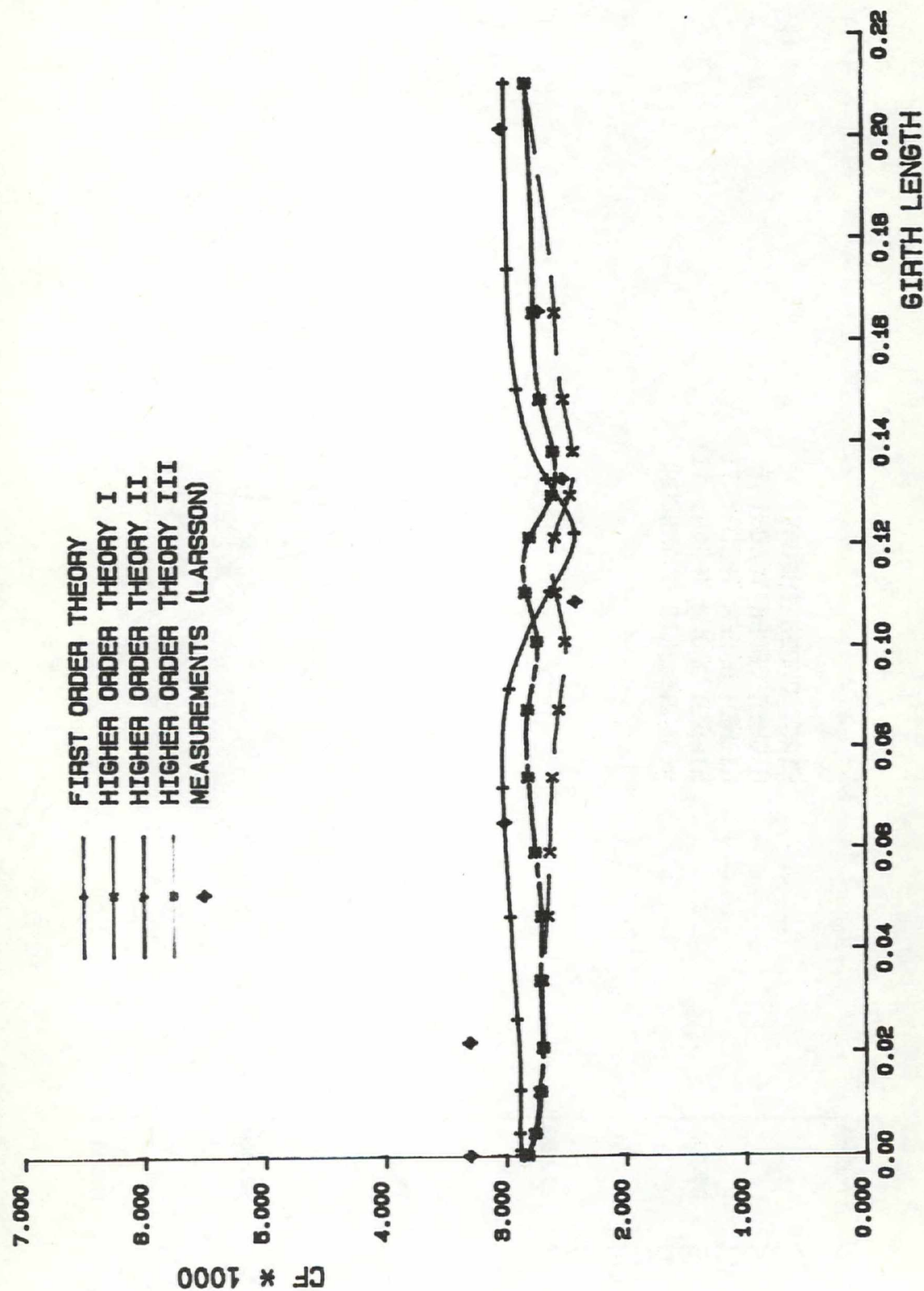
FIG. 5c



SSPA
&
CTH

COMPUTED SKIN FRICTION (CF)
FOR $RE=5.0E08$ AT $2X/L = 0.5$
SSPA MODEL 720

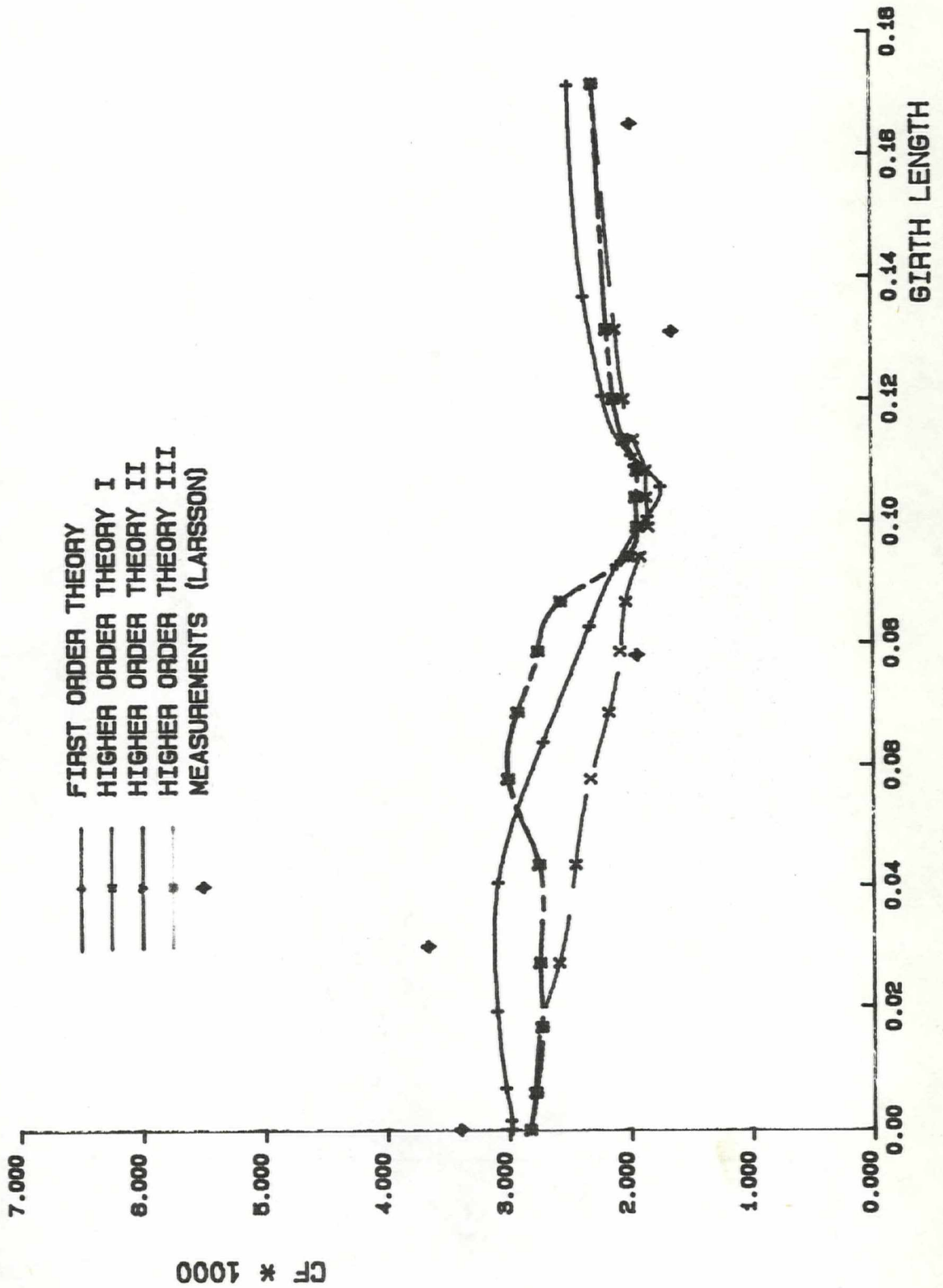
FIG. 6a



SSPA
&
CTH

COMPUTED SKIN FRICTION (CF)
FOR $RE=5.0E08$ AT $2X/L = 0.7$
SSPA MODEL 720

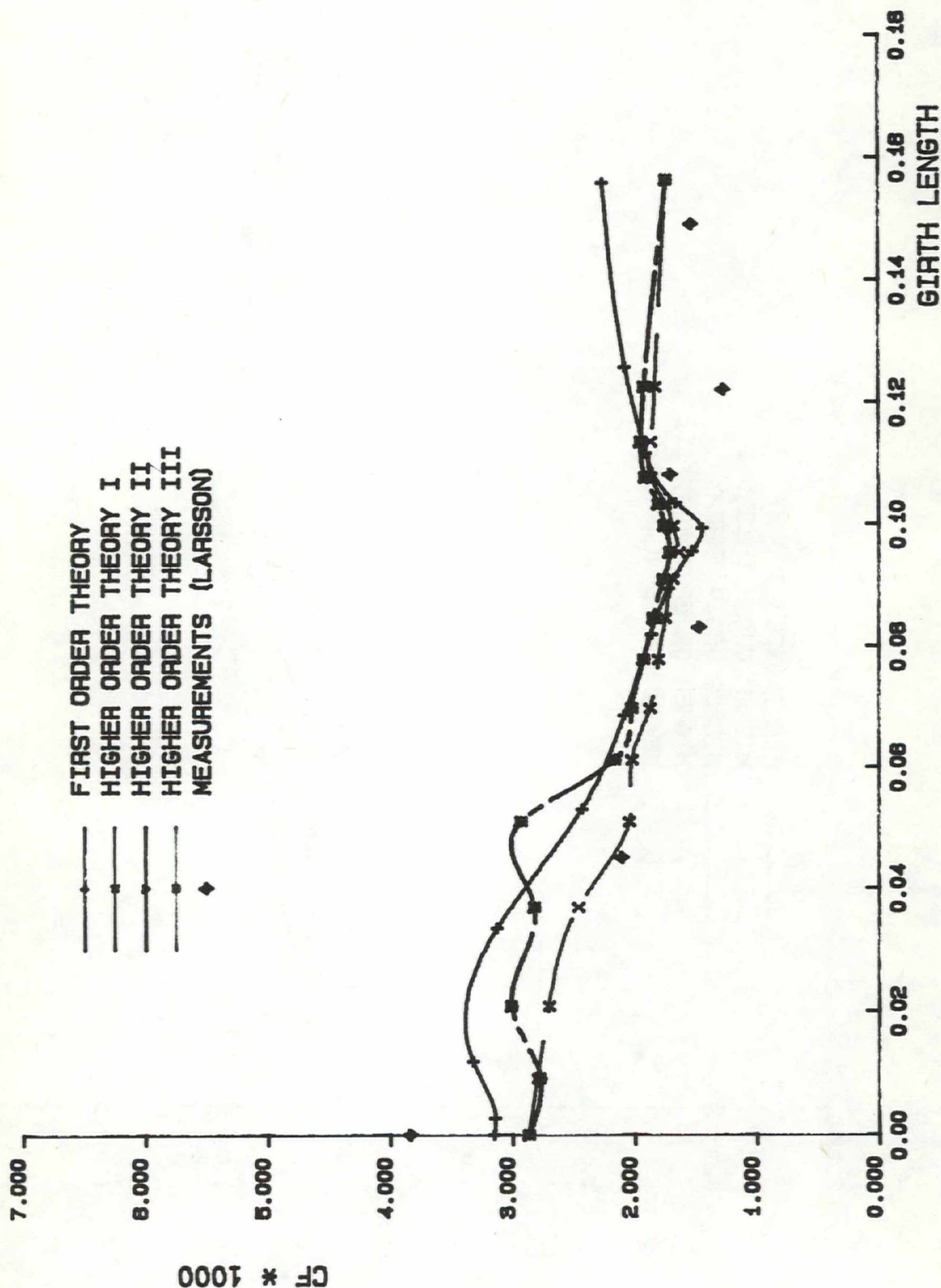
FIG. 6b



SSPA
&
CTH

COMPUTED SKIN FRICTION (CF)
FOR RE=5.0E08 AT 2X/L = 0.8
SSPA MODEL 720

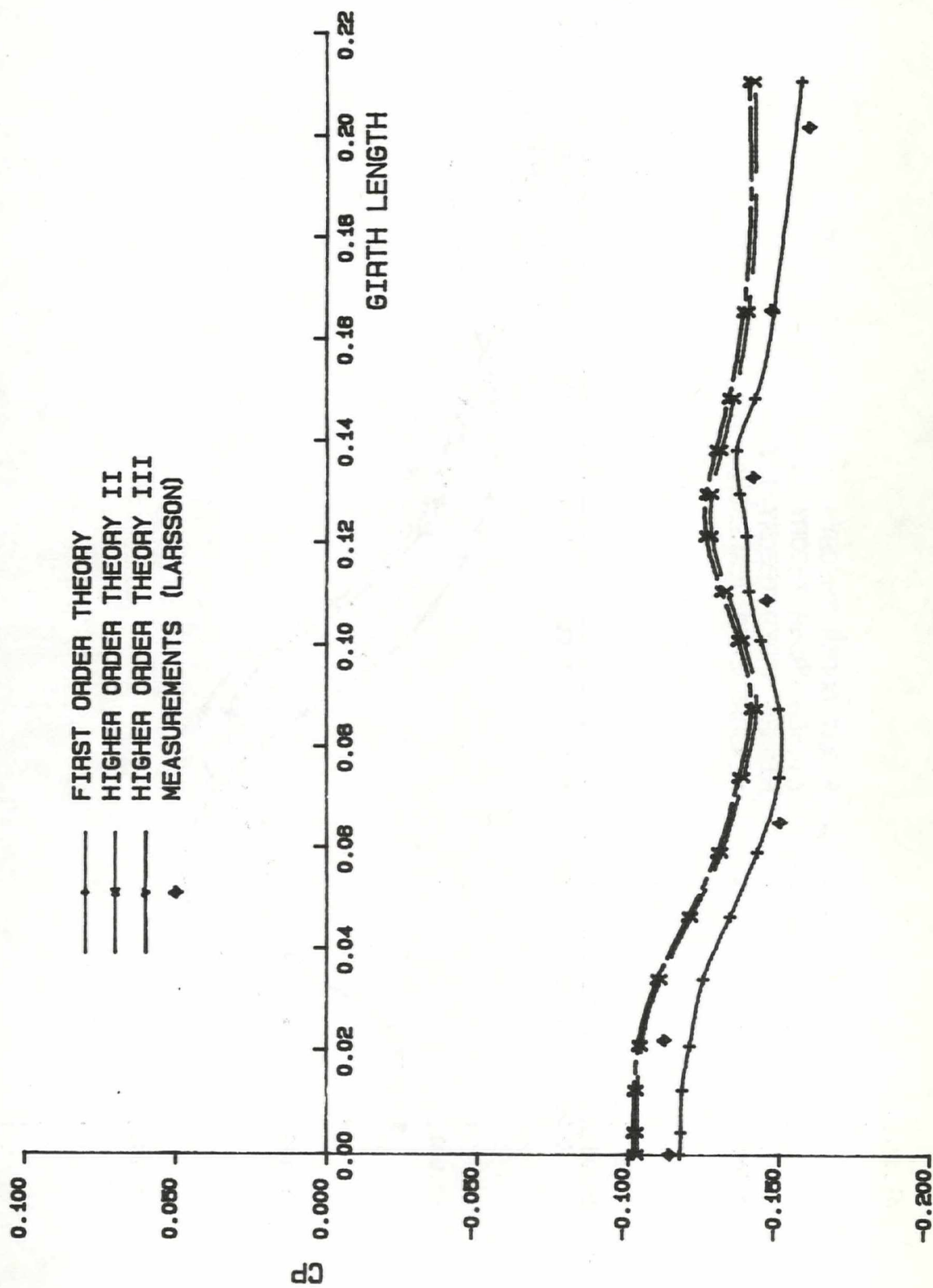
FIG. 6c

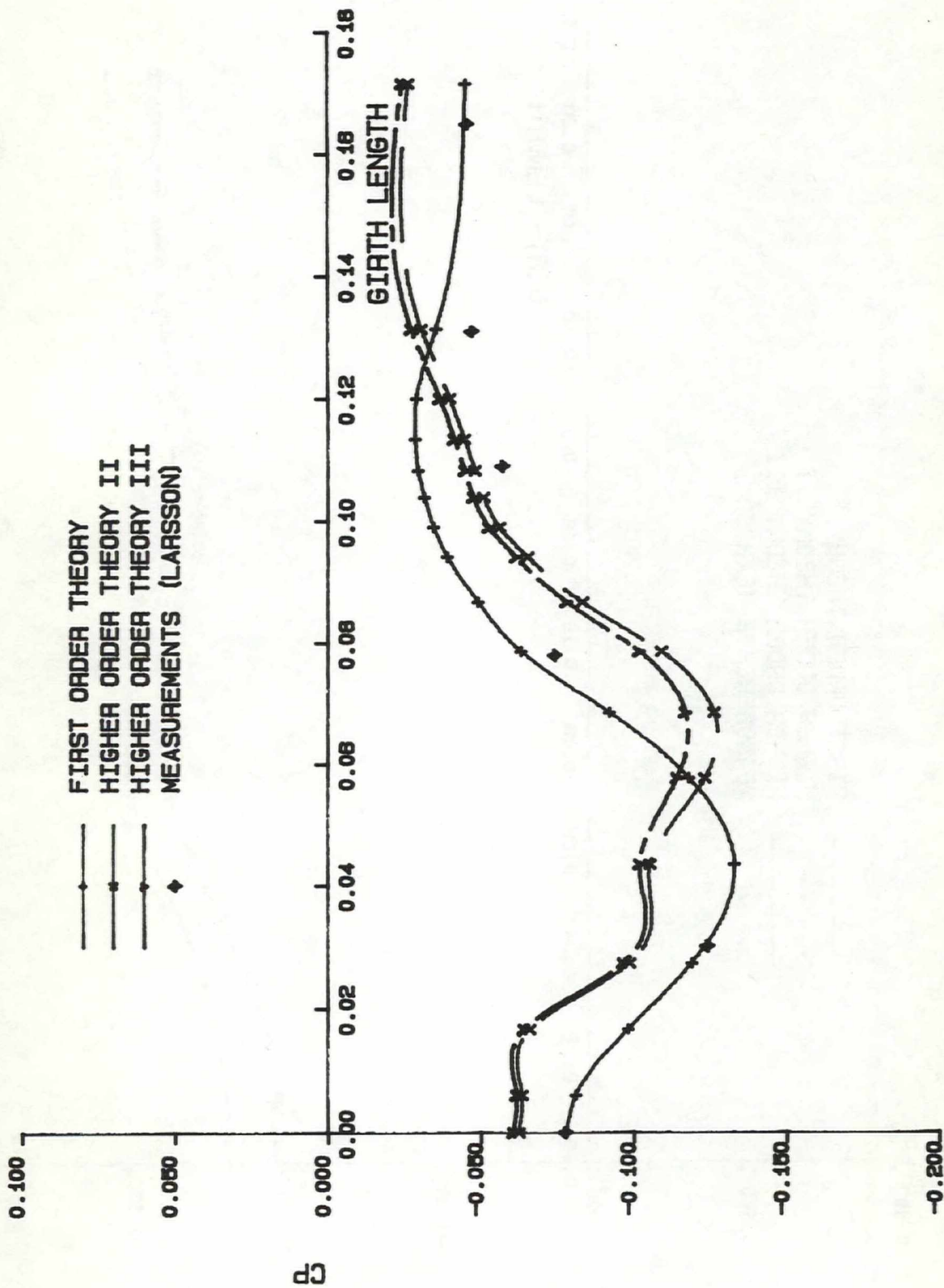


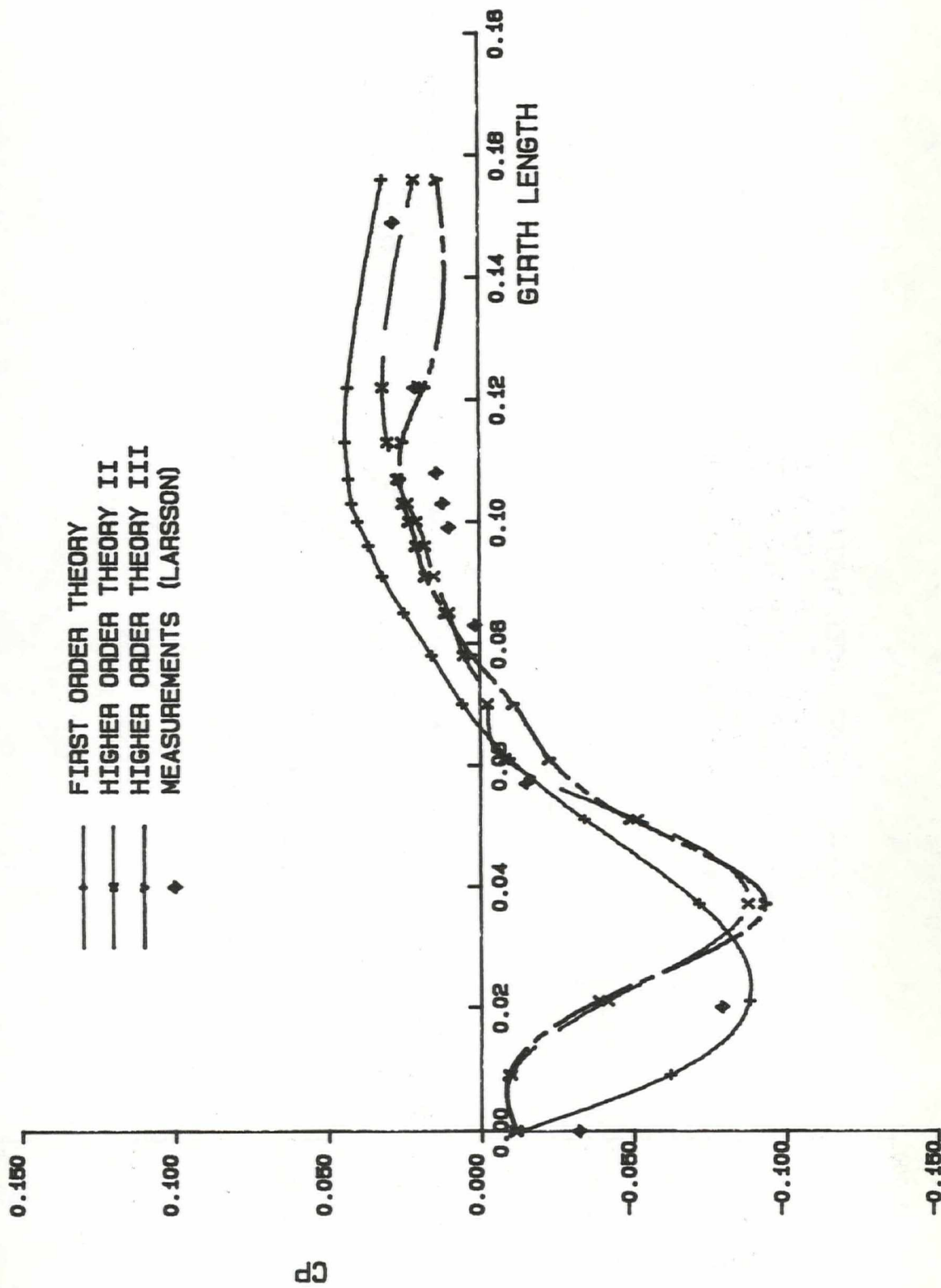
SSPA
&
CTH

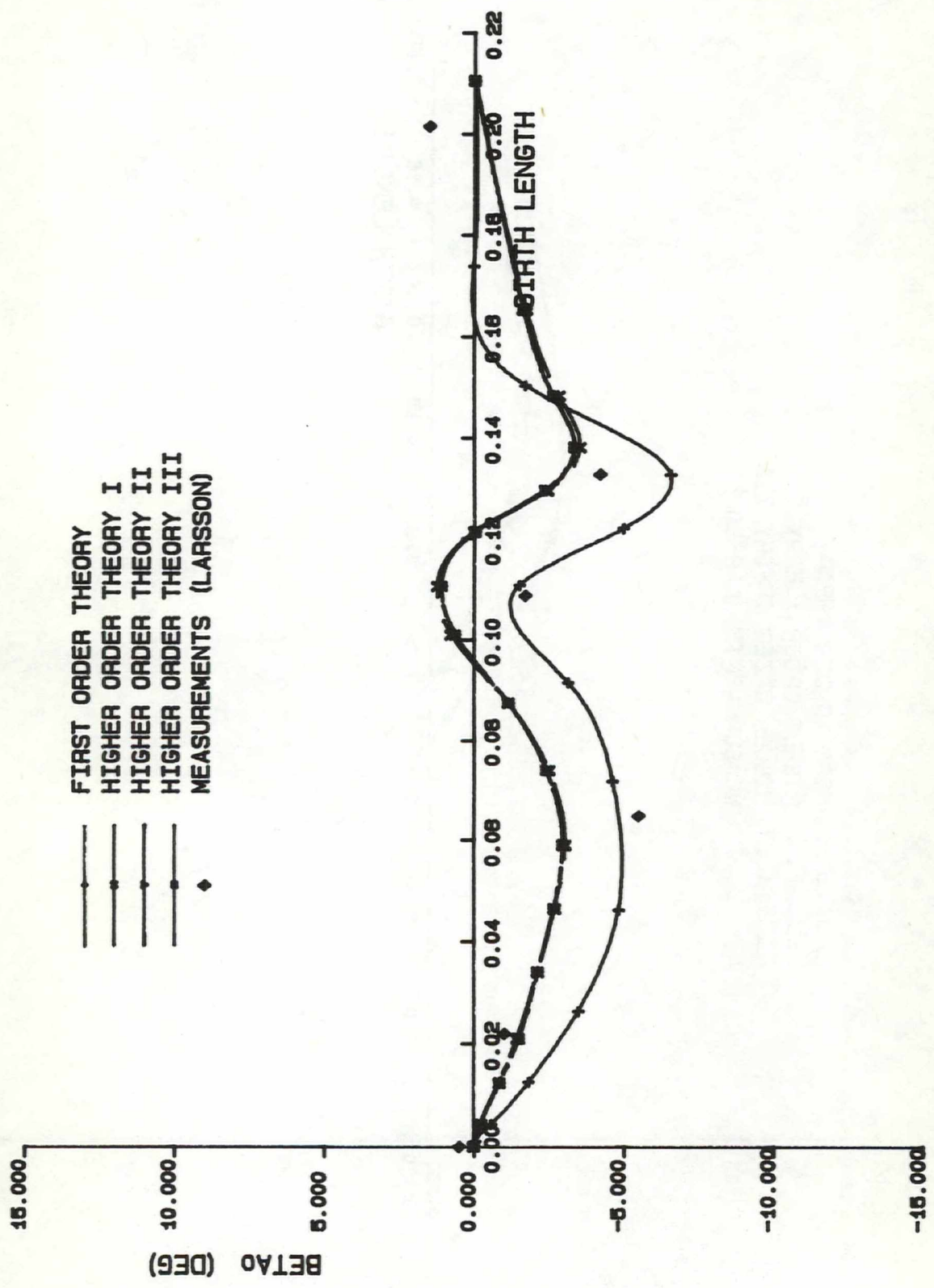
PRESSURE (CP) DISTRIBUTION
FOR RE=5.0E08 AT 2X/L = 0.5
SSPA MODEL 720

FIG. 7a





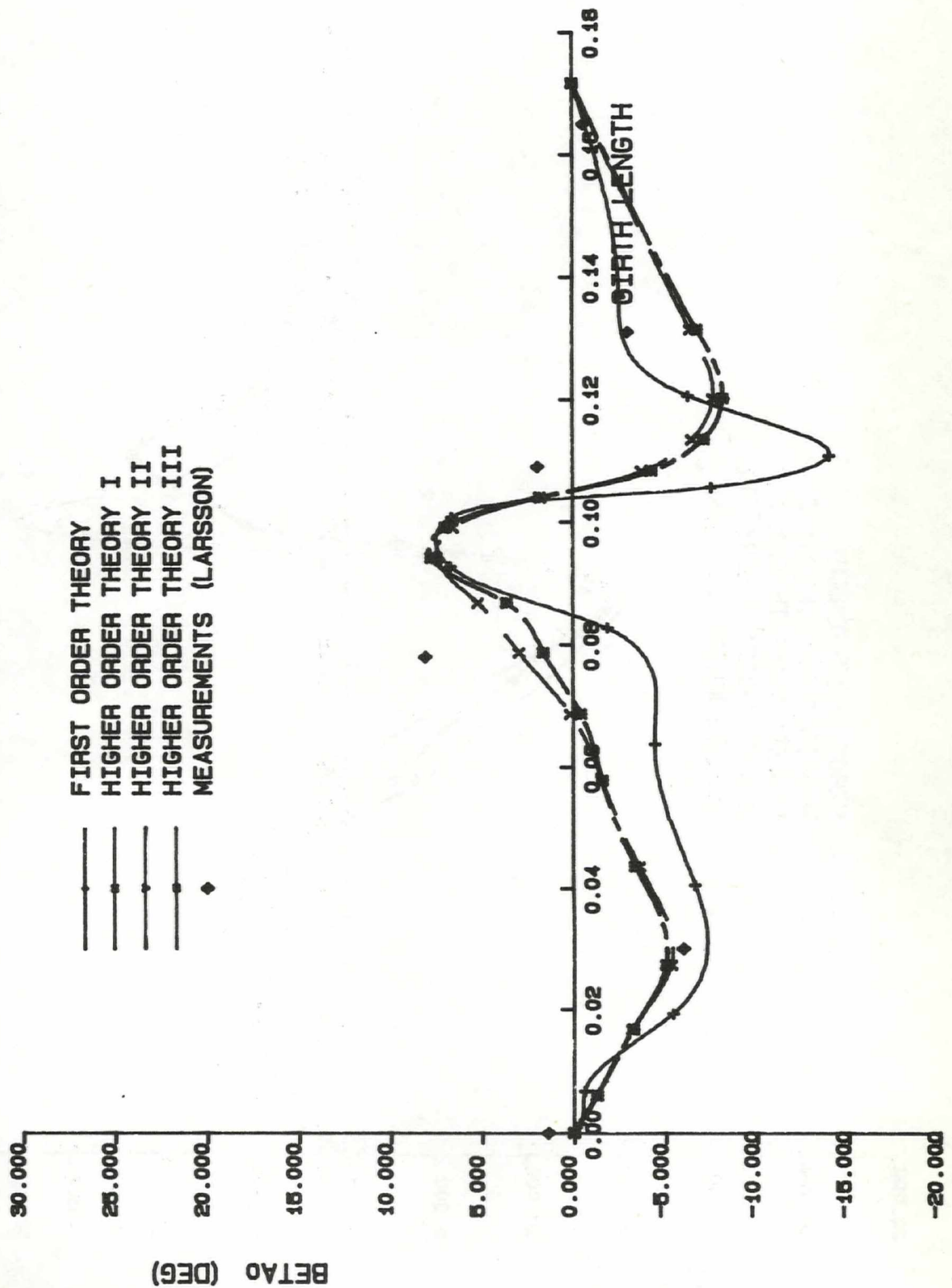


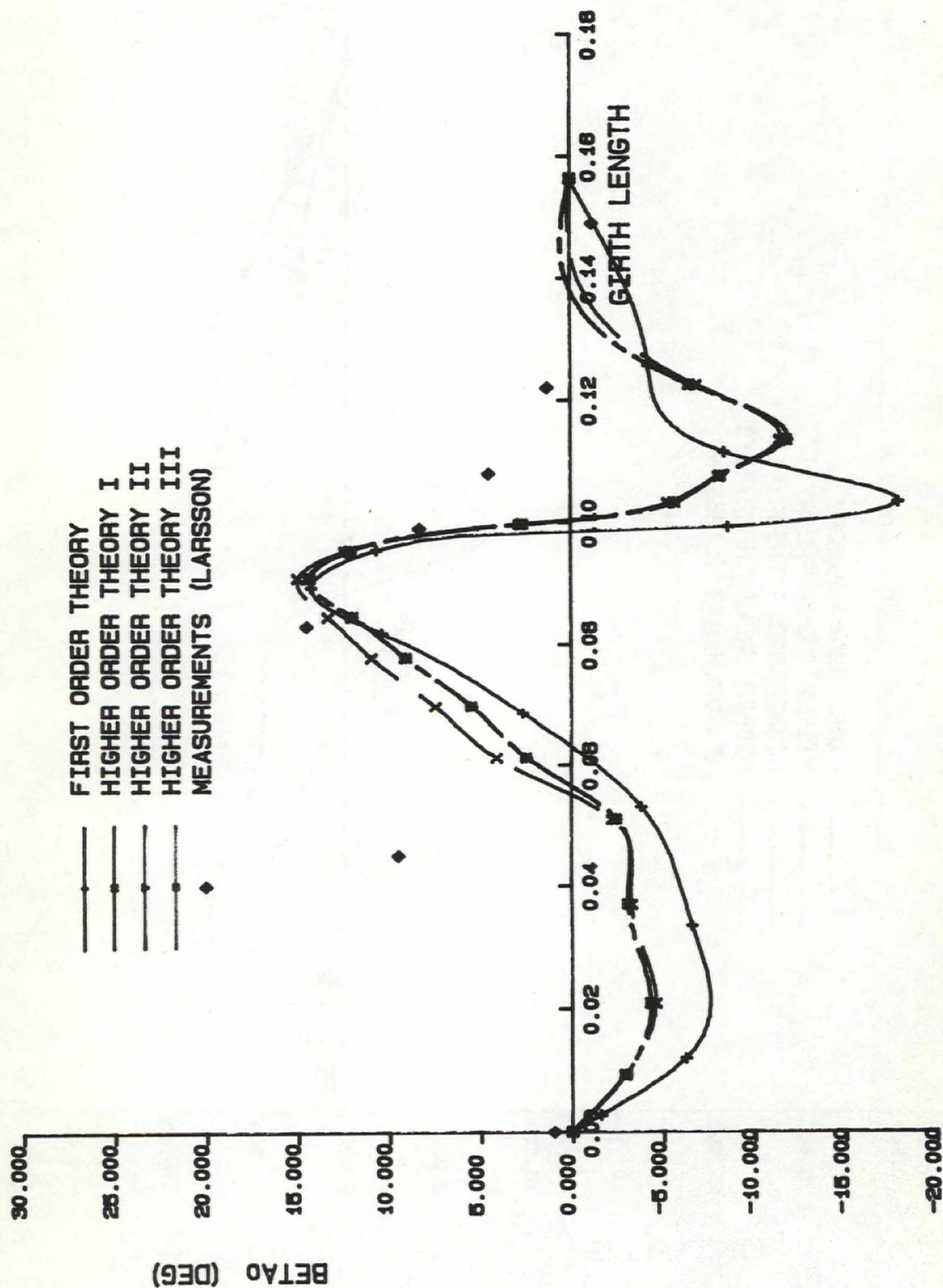


SSPA
&
CTH

COMPUTED CROSS FLOW ANGLE (BETA₀)
FOR RE=5.0E06 AT 2X/L = 0.7
SSPA MODEL 720

FIG. 8b

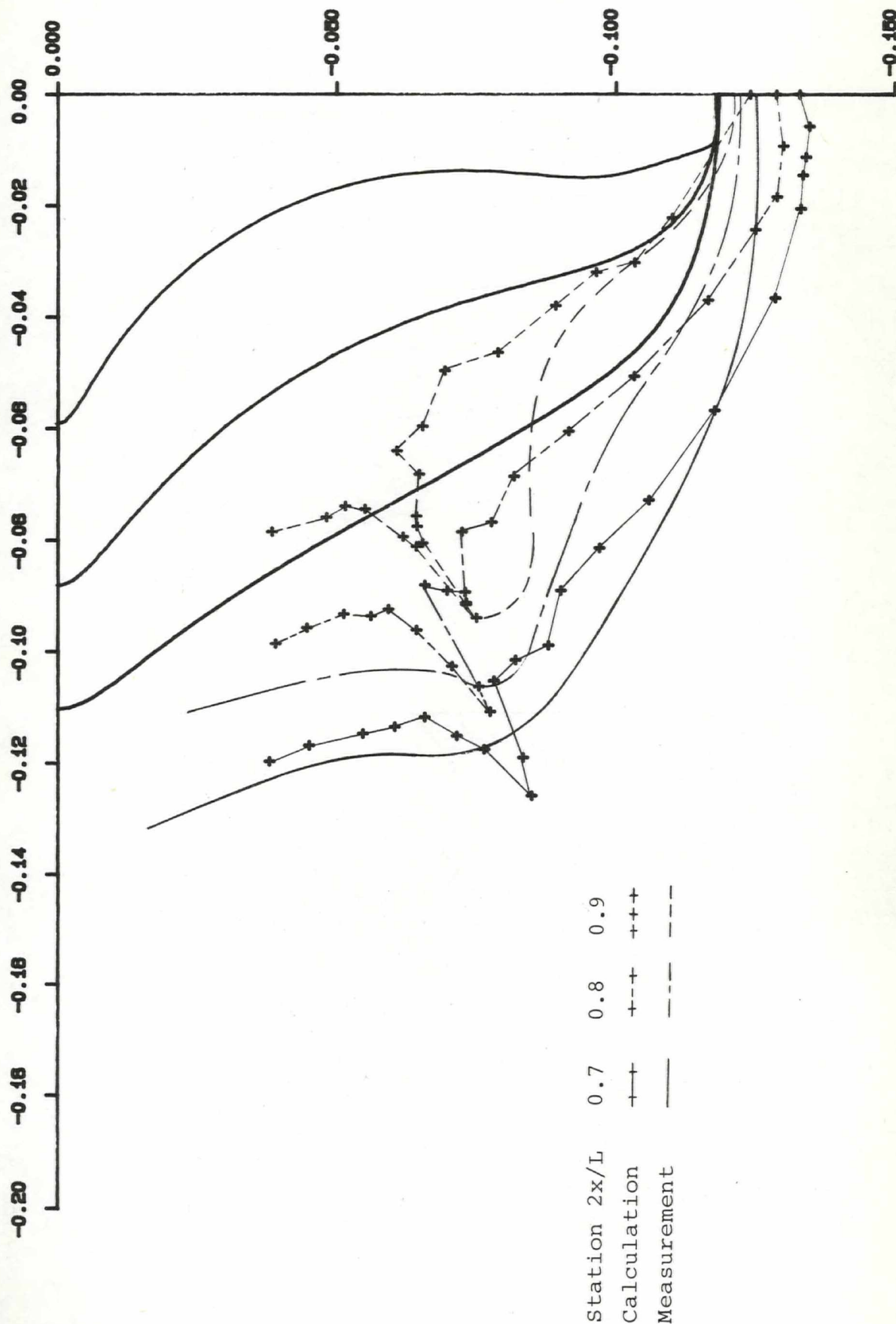




SSPA & CTH

BOUNDARY LAYER THICKNESS FOR SSPA
MODEL 720 AT X = 0.7, 0.8 AND 0.9
CALCULATED BY HIGHER ORDER THEORY

FIG. 9

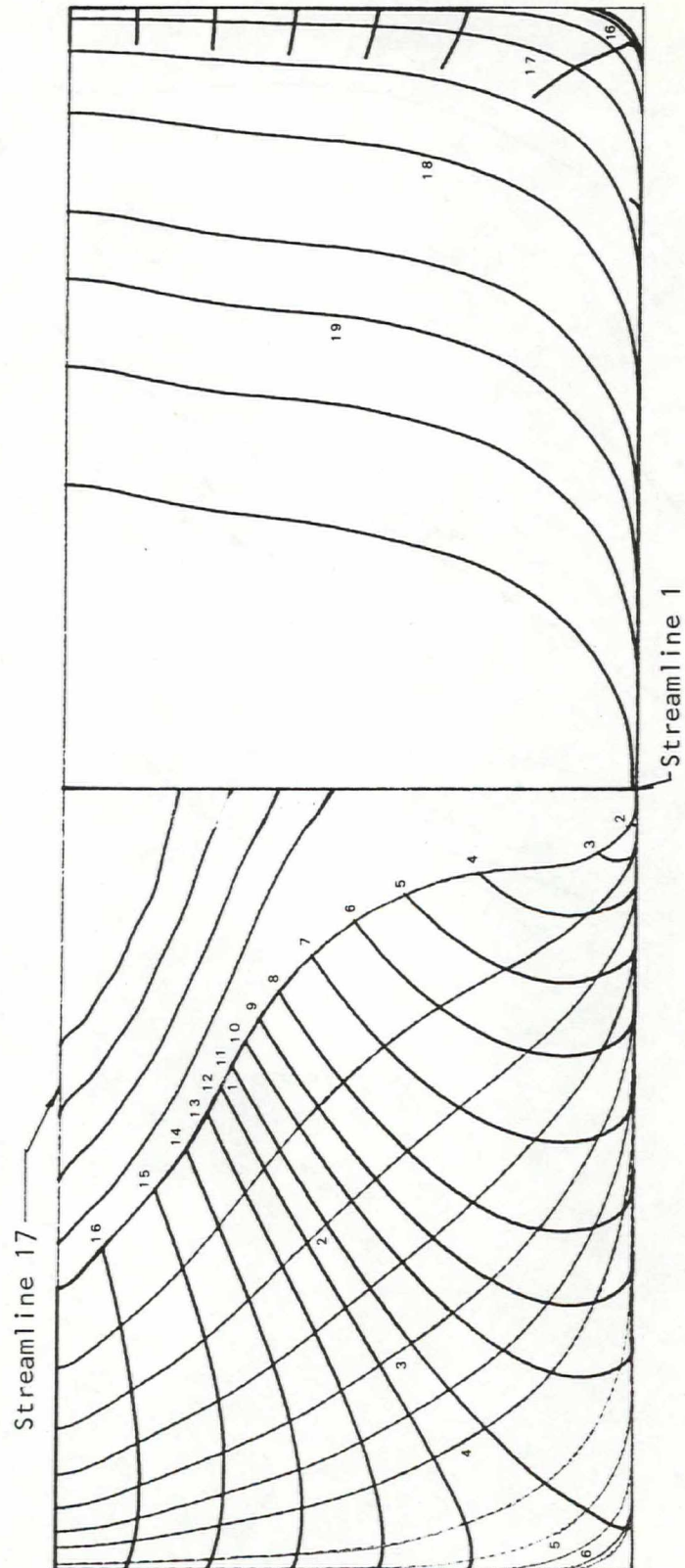


SSPA
&
CTH

BODY PLAN AND STREAMLINE COORDINATE

HSVA TANKER MODEL

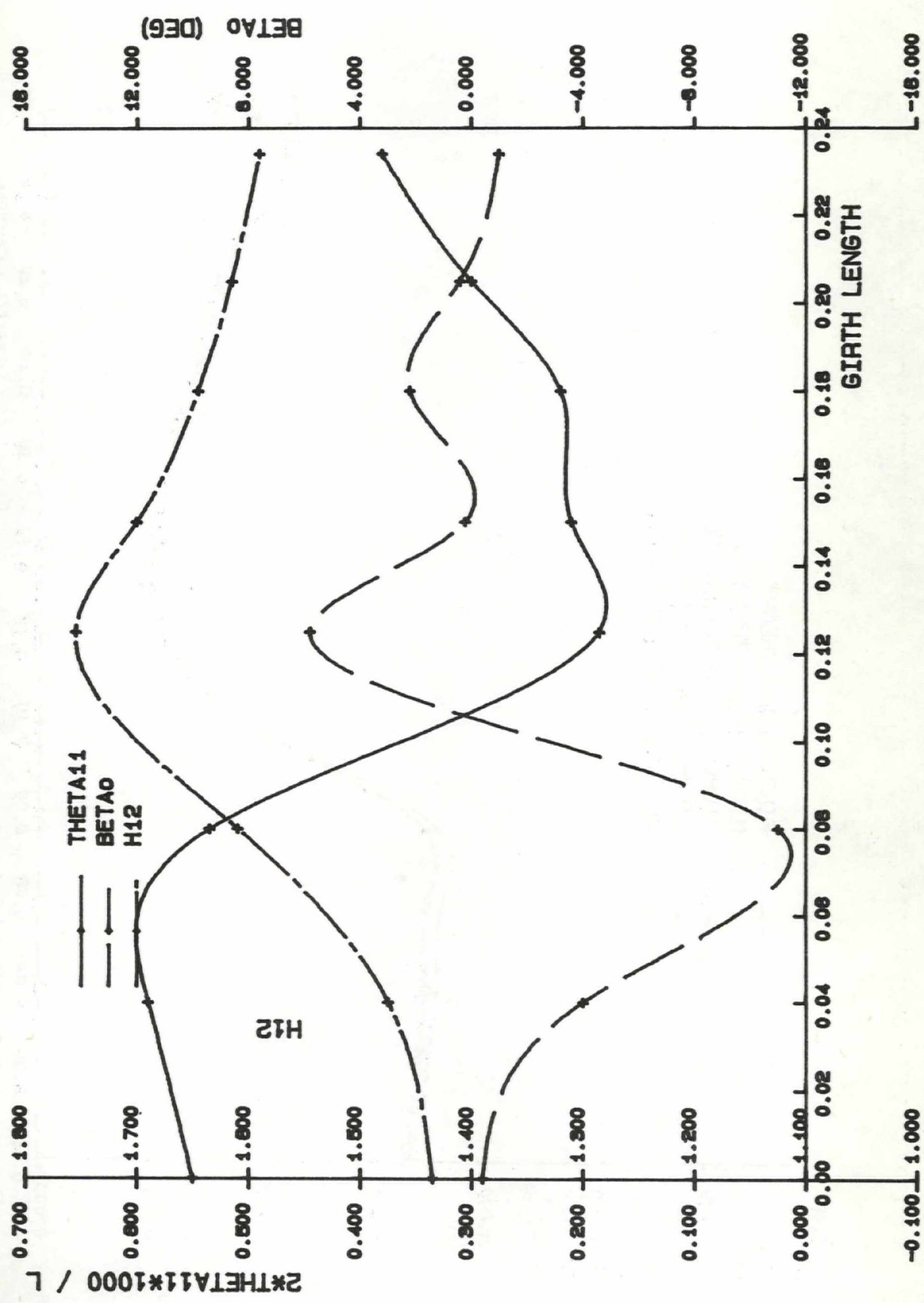
FIG. 10

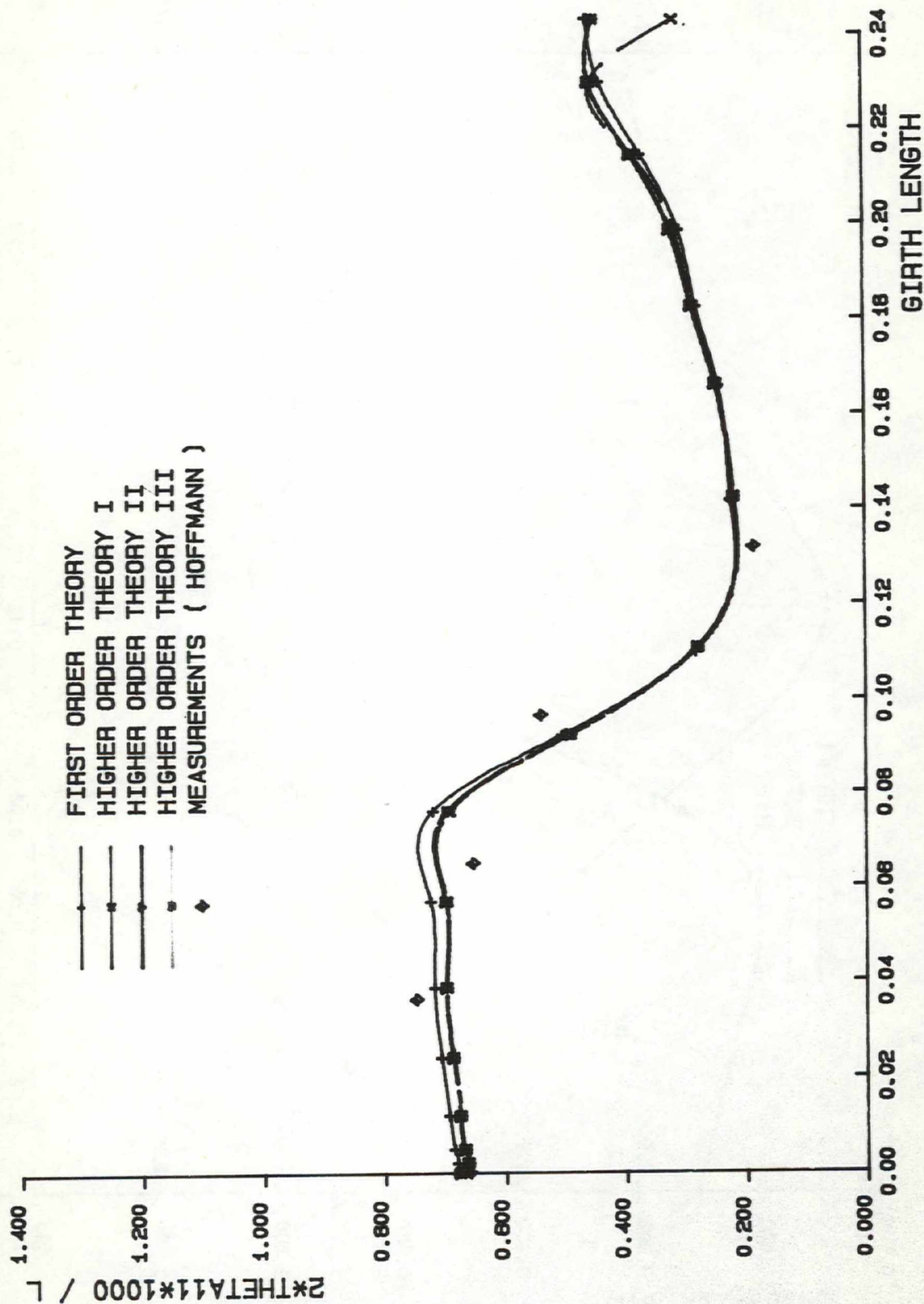


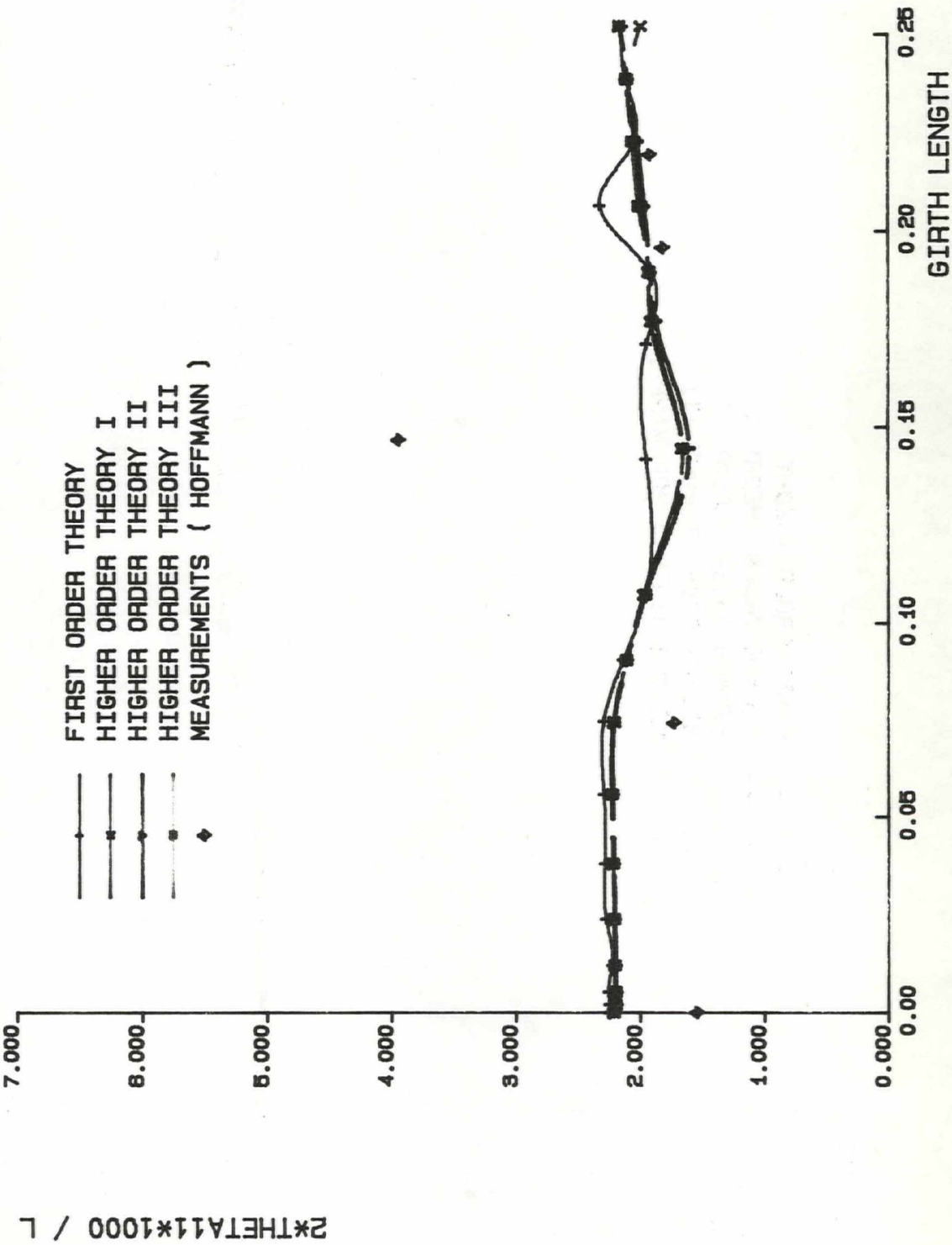
SSPA
&
CTH

INITIAL VALUES OF THETA11, H12
AND BETA0 AT STATION 2X/L= -0.790
HSVA TANKER MODEL

FIG. 11



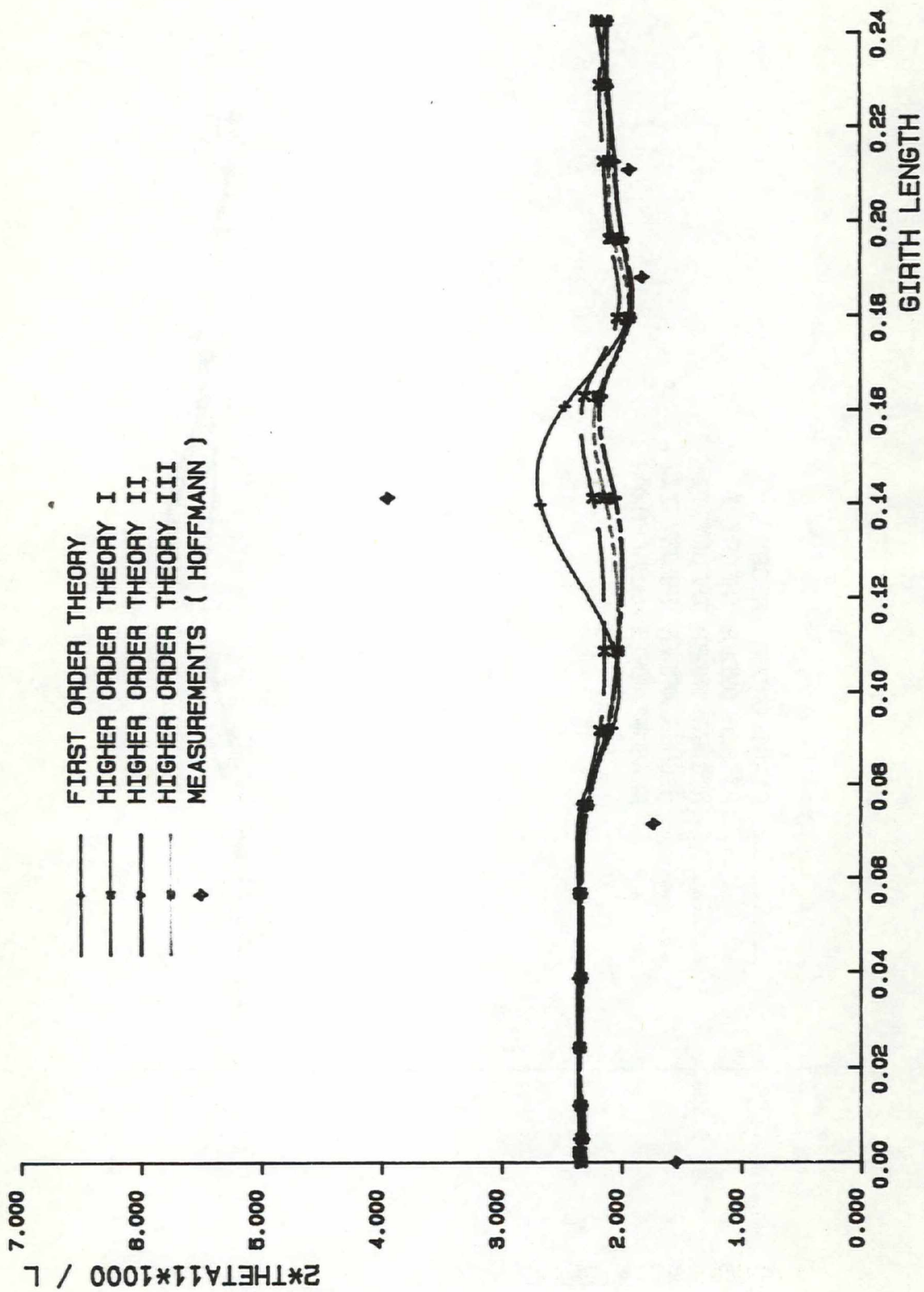




SSPA
&
CTH

COMPUTED MOMENTUM THICKNESS
FOR RE = 8.8E06 AT 2X/L = 0.502
HSVA TANKER MODEL

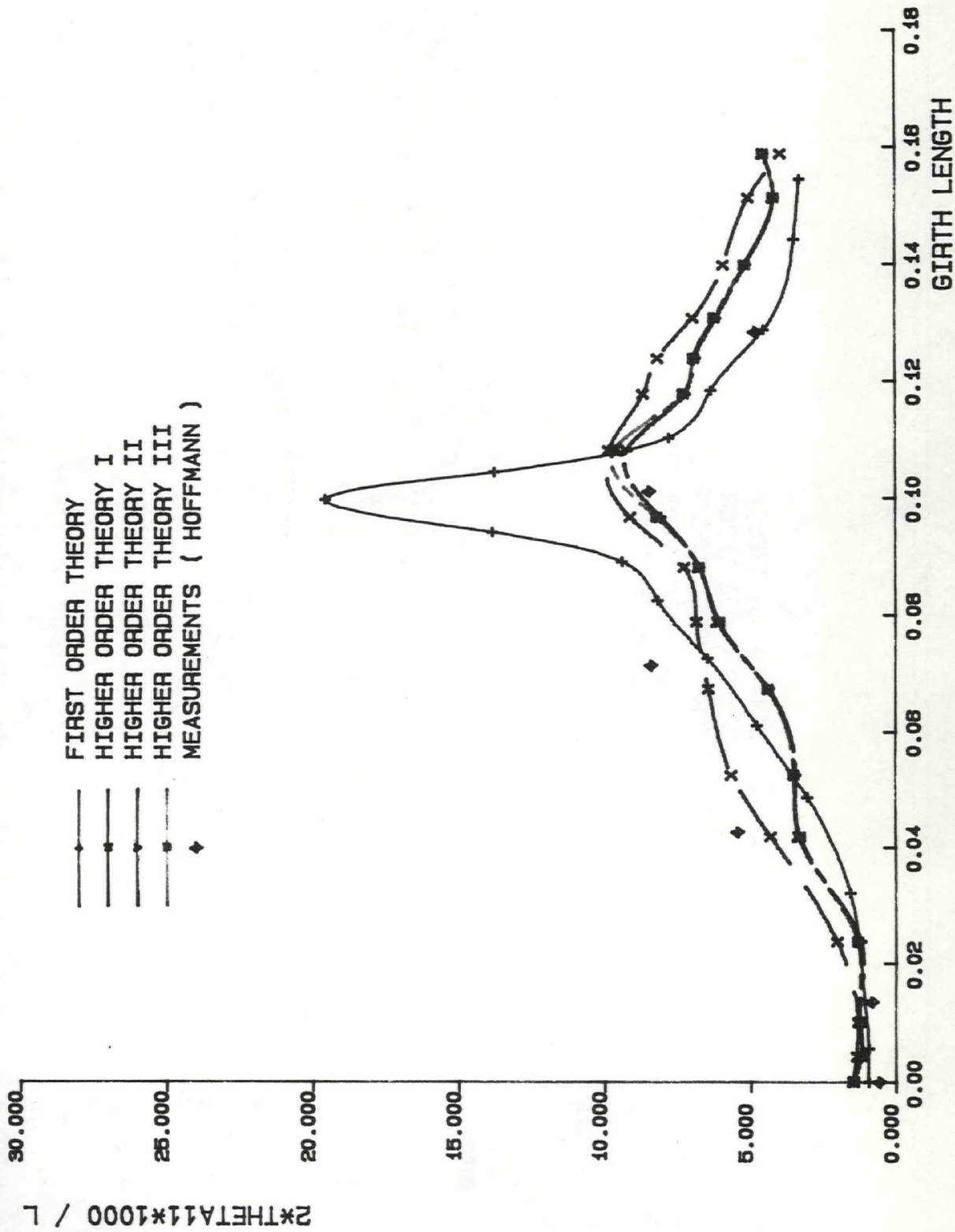
FIG. 12c



SSPA
&
CTH

COMPUTED MOMENTUM THICKNESS
FOR RE = 6.8E06 AT 2X/L = 0.884
HSVA TANKER MODEL

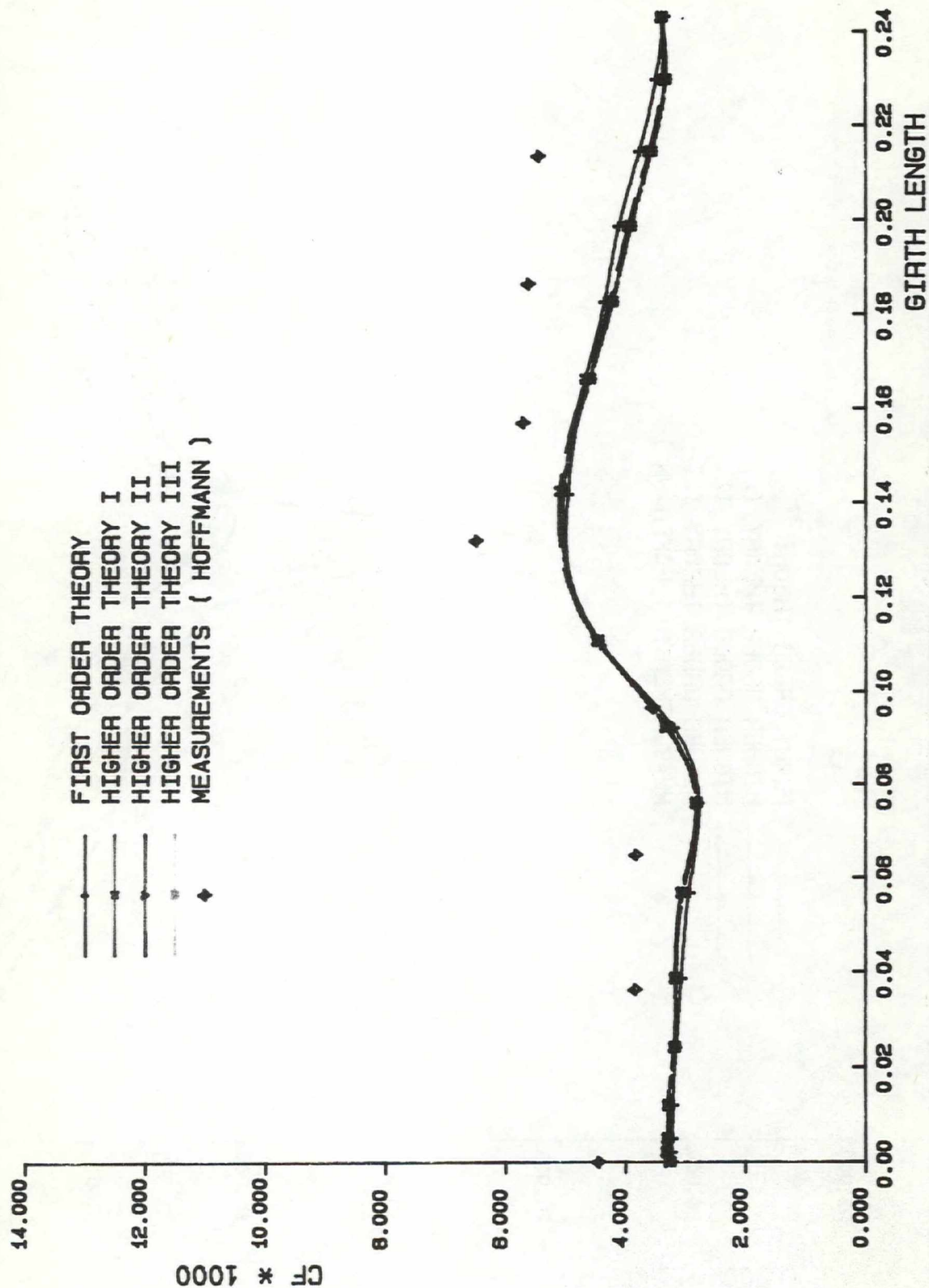
FIG. 12d

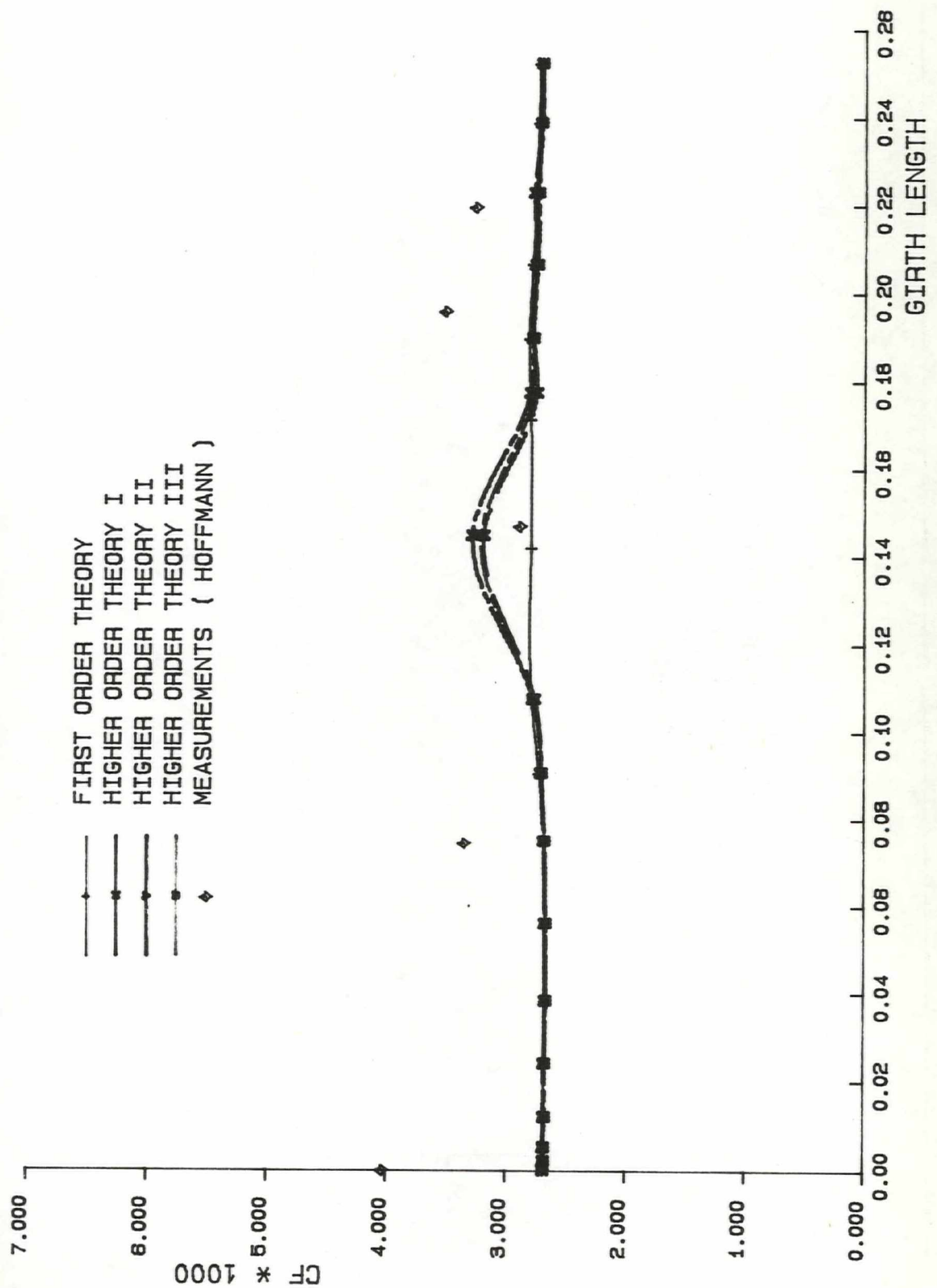


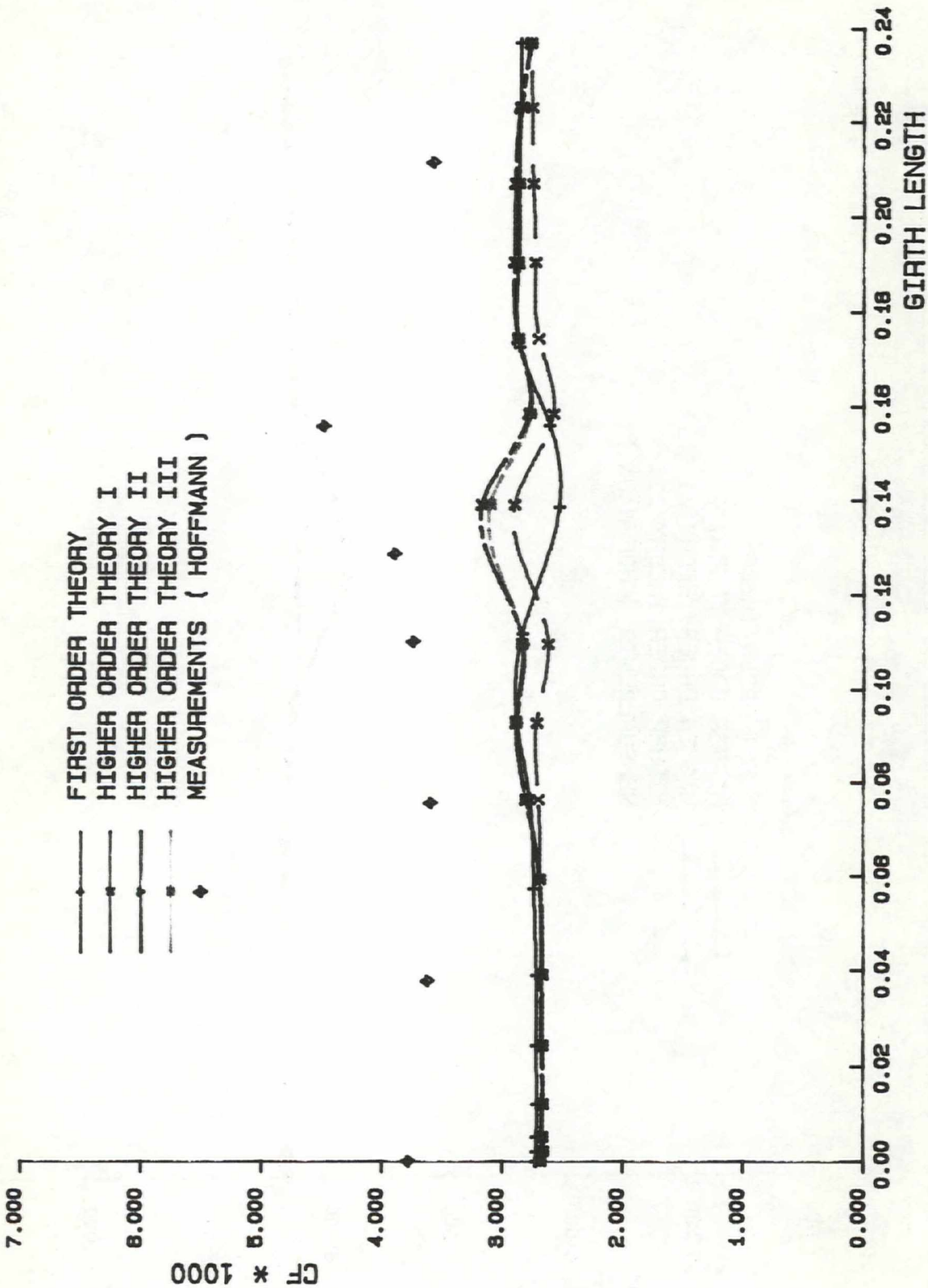
SSPA
&
CTH

COMPUTED SKIN FRICTION (CF) FOR
RE = 6.8E06 AT 2X/L = -0.744
HSVA TANKER MODEL

FIG. 13a



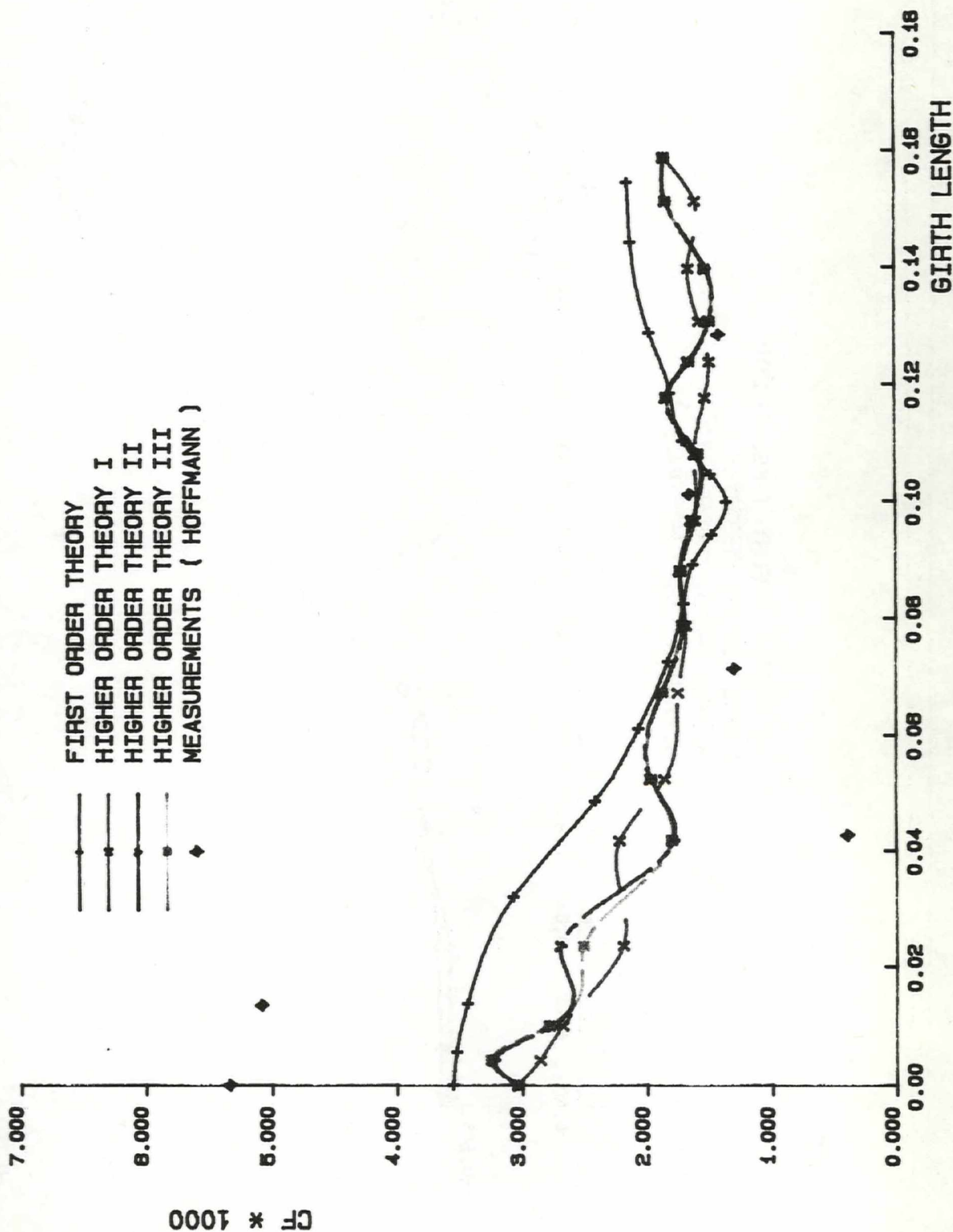


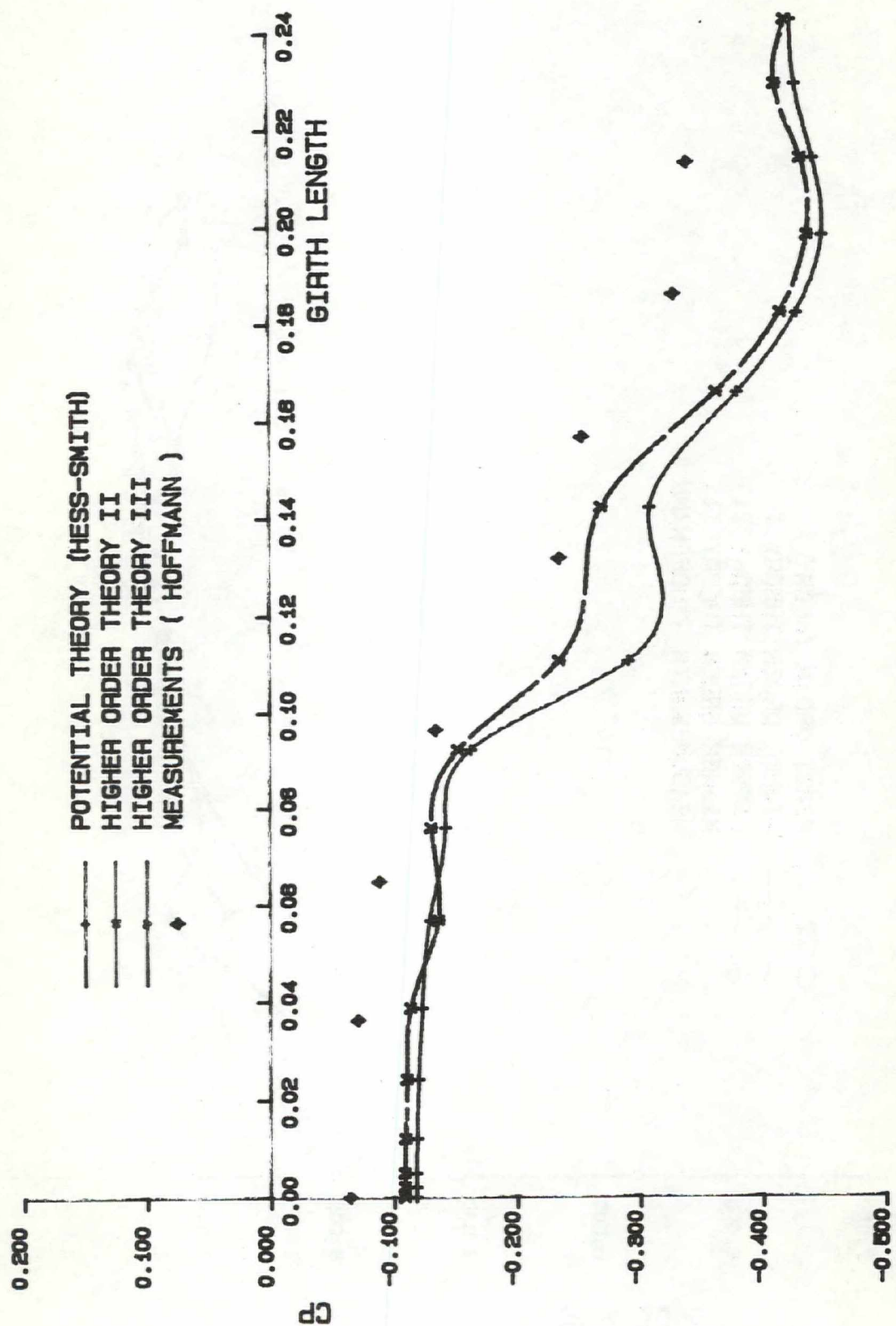


SSPA
&
CTH

COMPUTED SKIN FRICTION (CF)
FOR $RE = 8.8E08$ AT $2X/L = 0.884$
HSVA TANKER MODEL

FIG. 13d

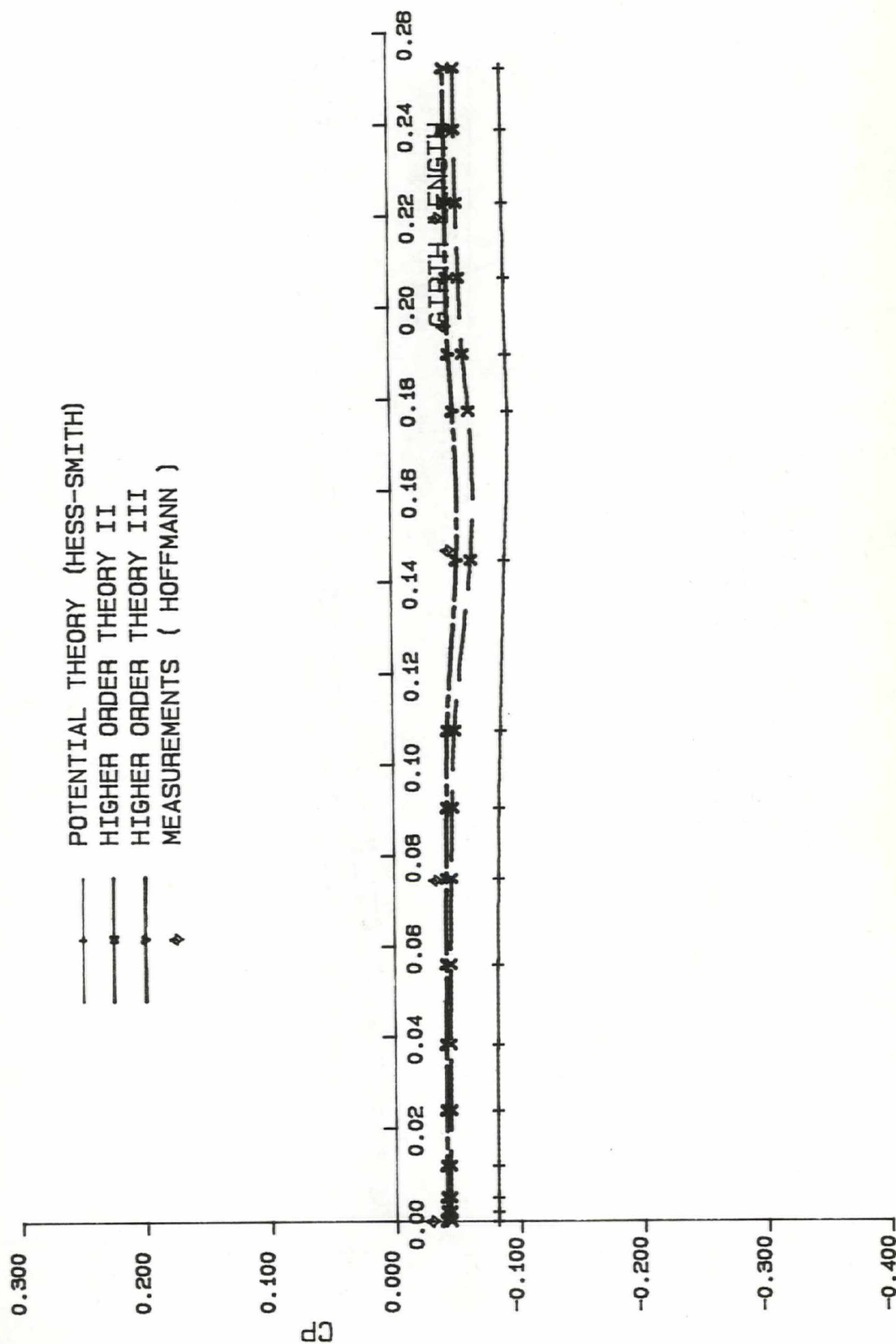




SSPA
&
CTH

PRESSURE (CP) DISTRIBUTION FOR
RE = 6.8E06 AT 2X/L = 0.291
HSVA TANKER MODEL

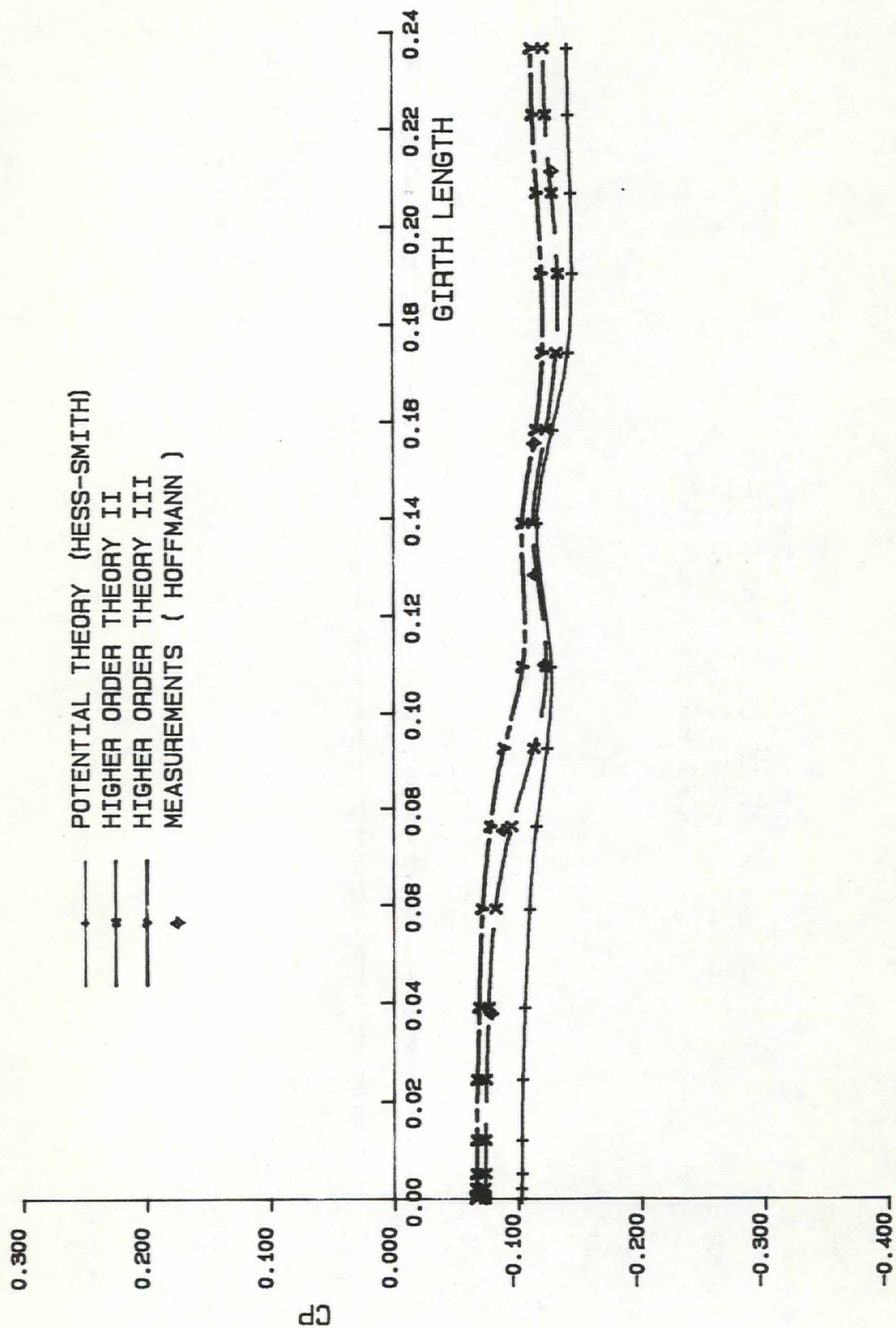
FIG. 14b

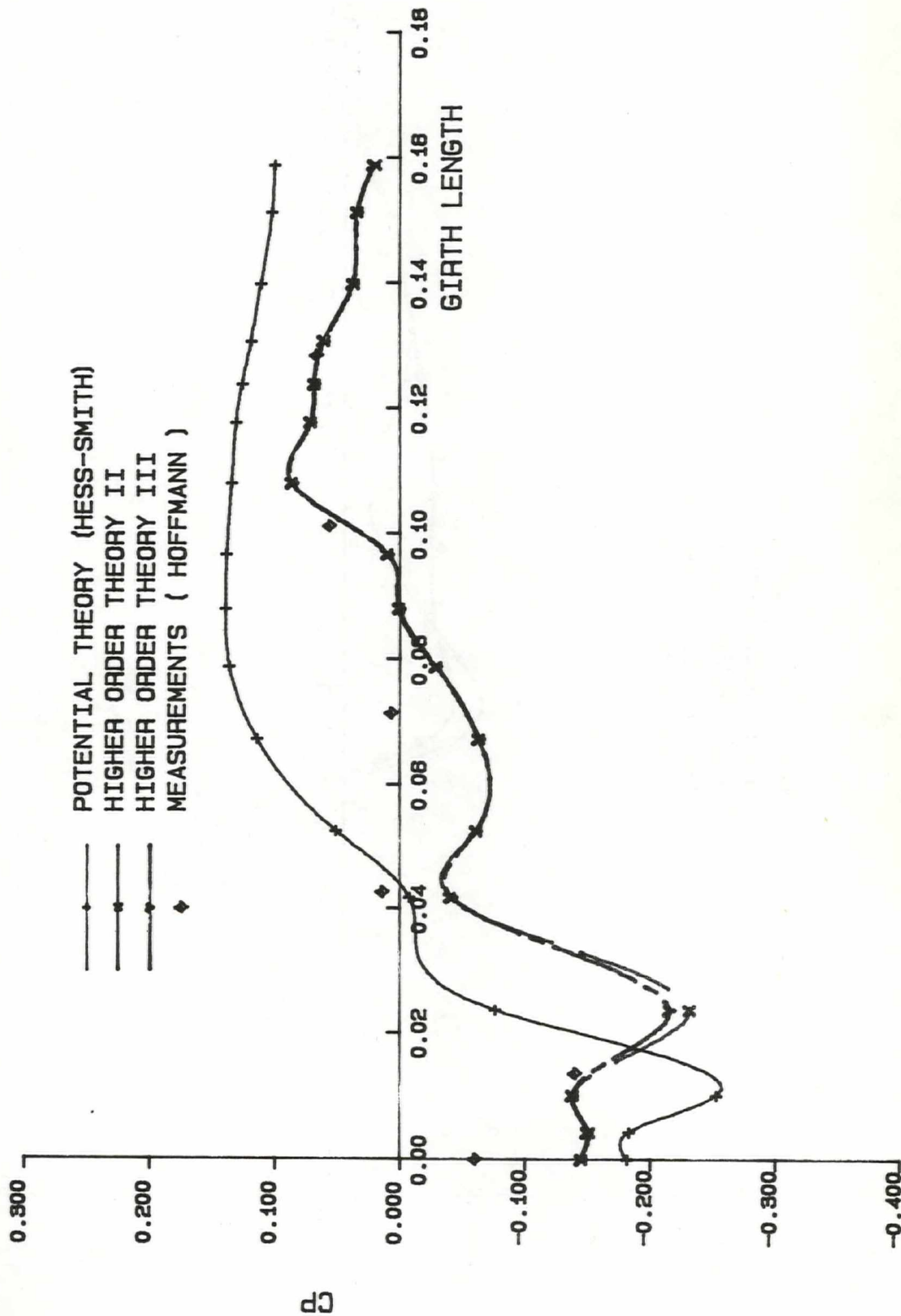


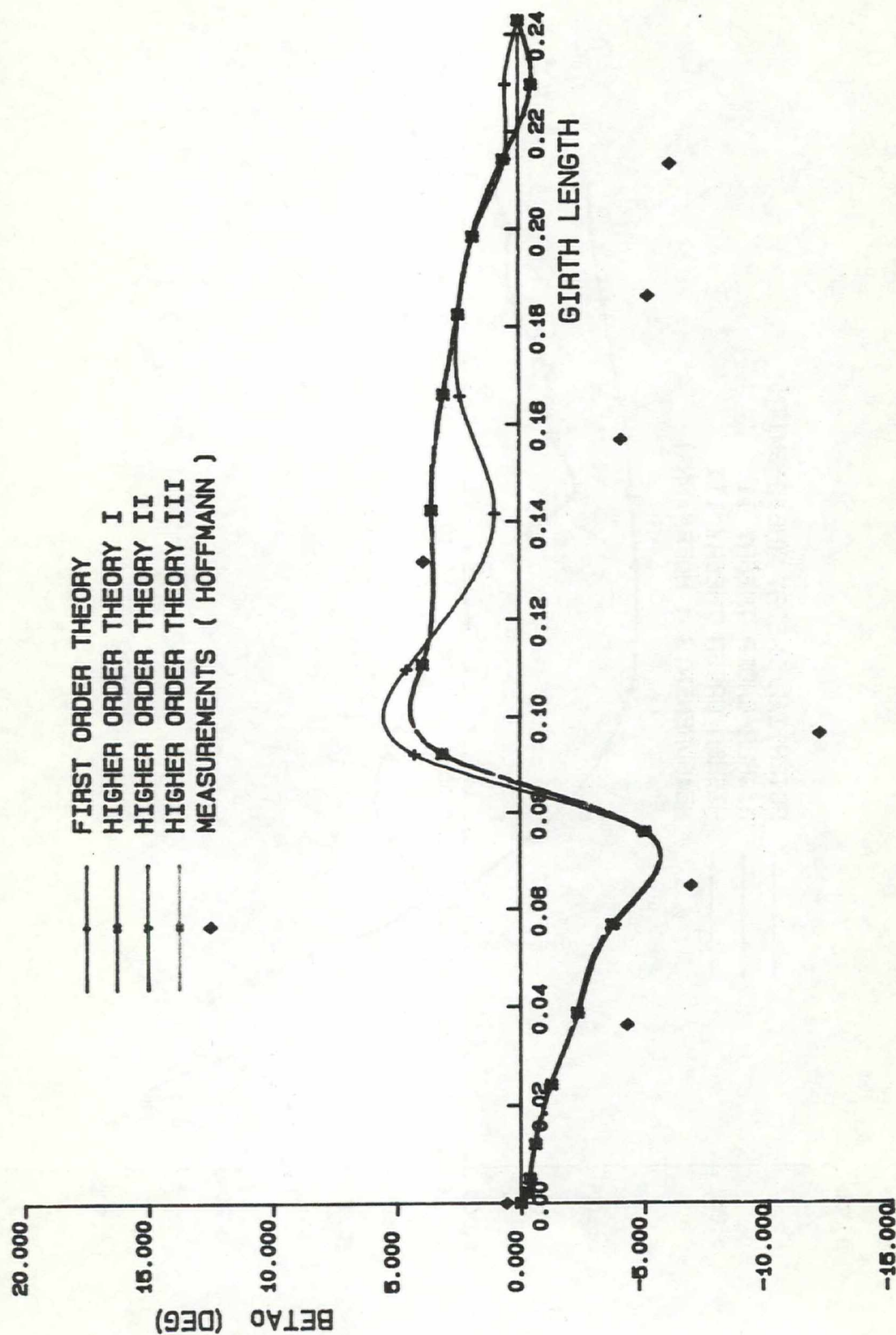
SSPA
&
CTH

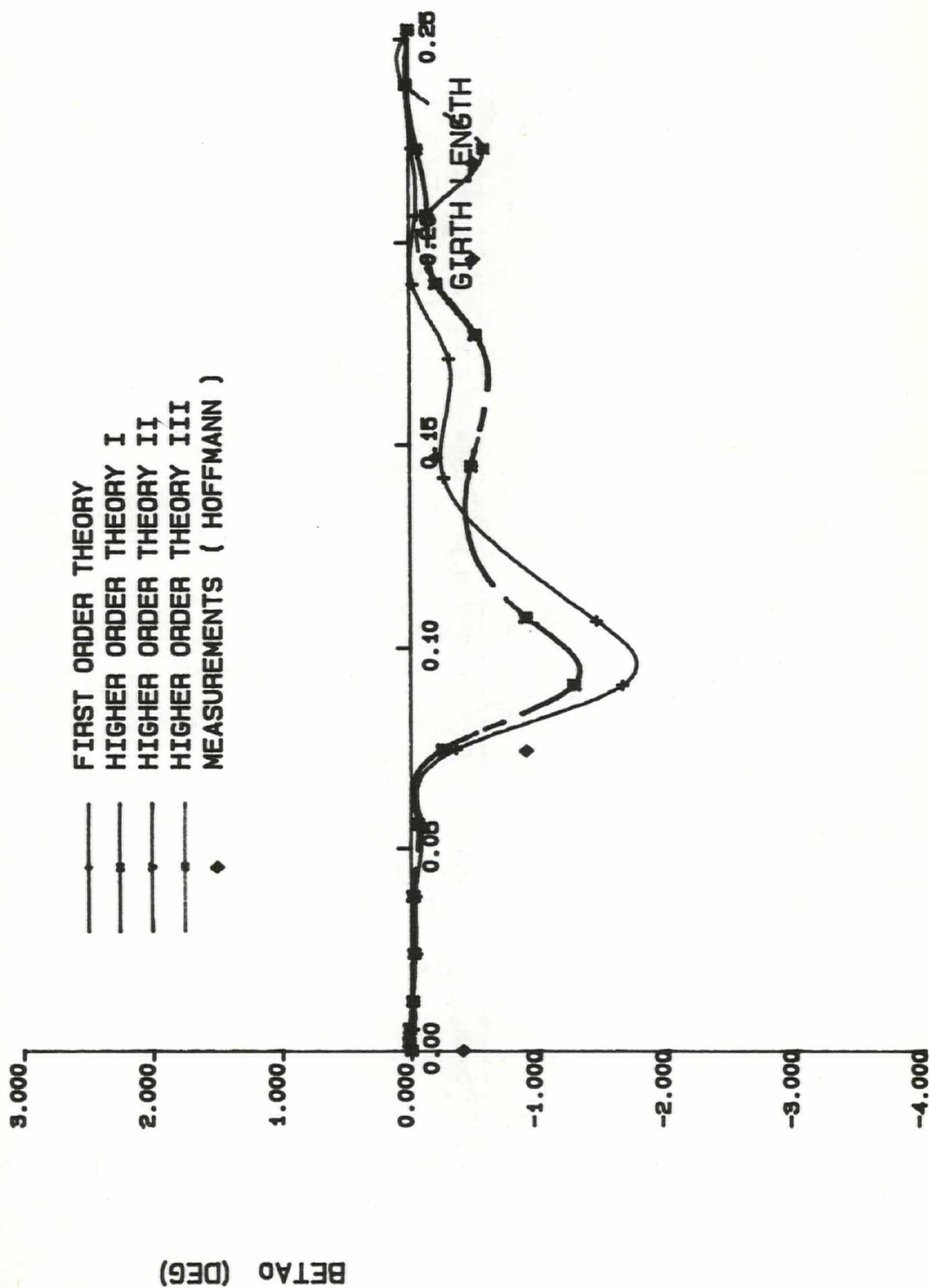
PRESSURE (CP) DISTRIBUTION
FOR $RE = 6.8E06$ AT $2X/L = 0.502$
HSVA TANKER MODEL

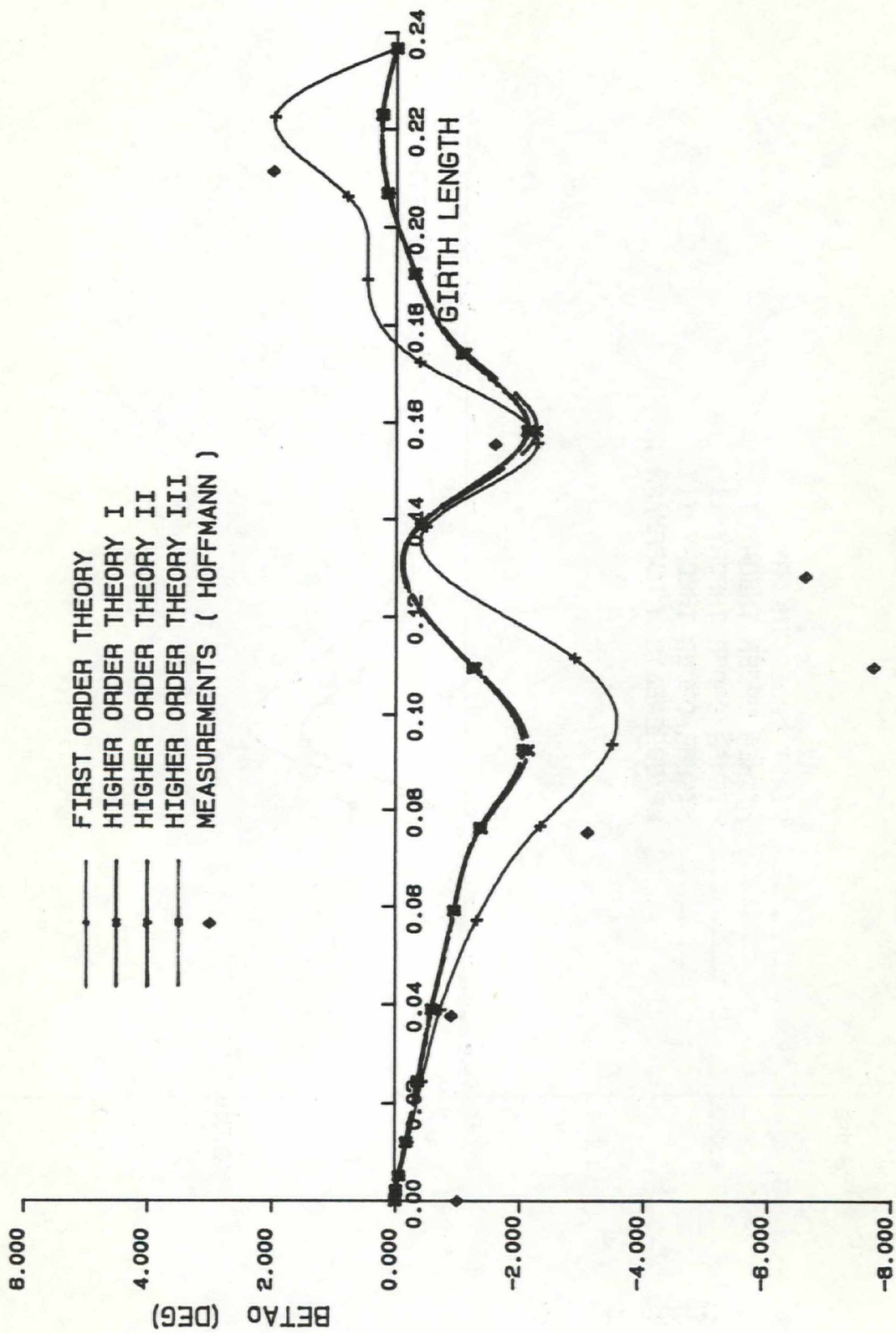
FIG. 14c

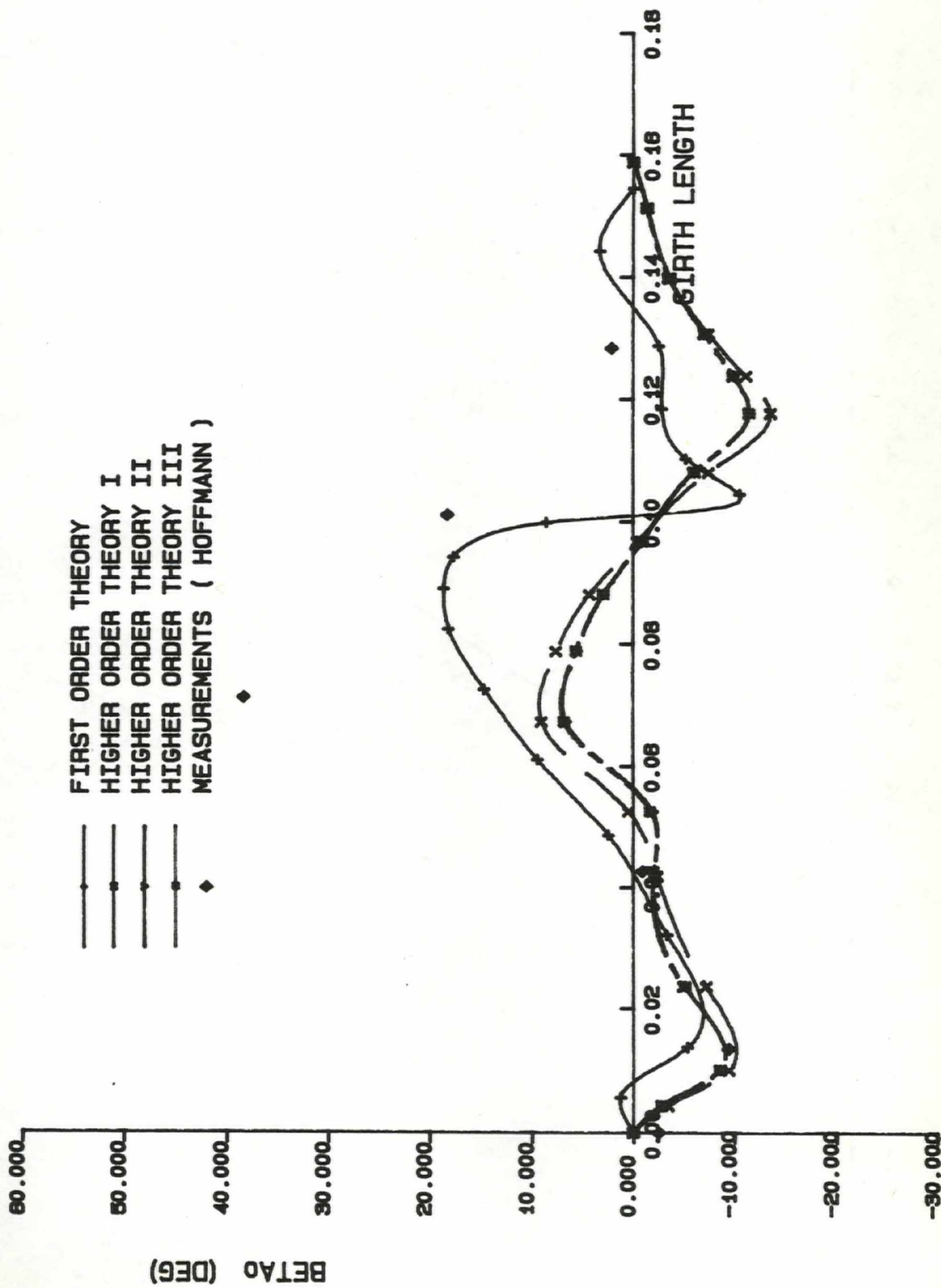








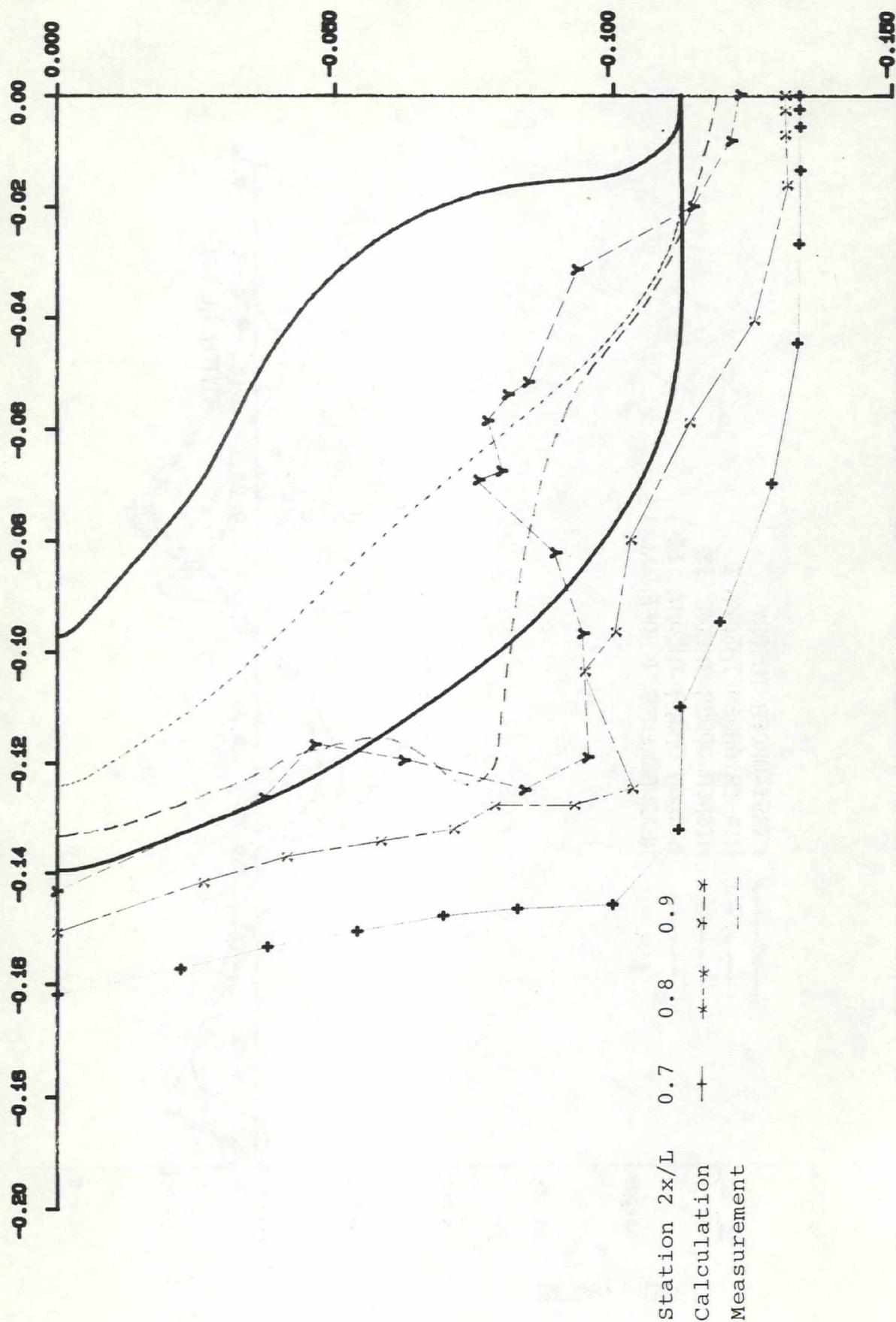




SSPA
&
CTH

BOUNDARY LAYER THICKNESS FOR HSVA
TANKER AT $2x/L = 0.7, 0.8$ AND 0.9
CALCULATED BY HIGHER ORDER THEORY

FIG. 16



PAPER B

SSPA Report No 2966-2

**A Higher Order Panel Method for Calculating
Free Surface Potential Flows with Linear
Surface Boundary Conditions**

by

Keun Jae Kim

1989-04-04

ABSTRACT

In the present paper a method for calculating the potential flow about ships is described. The problem is discretized by covering the hull and part of the free surface with panels. An exact boundary condition is satisfied on the hull, while on the free surface the boundary condition is linearized with respect to the double model solution.

The main difference between the present method and others of the same kind is that the panels are parabolic rather than flat and that the source density distribution on each panel is not constant but linearly varying. Other improvements, as compared to the original Dawson method, are that the panel grid on the free surface is independent of the streamlines and that the resistance is computed in a more accurate way.

A detailed description of the theory is given in the paper, which also presents results for several different cases, showing the improvement over first order methods.

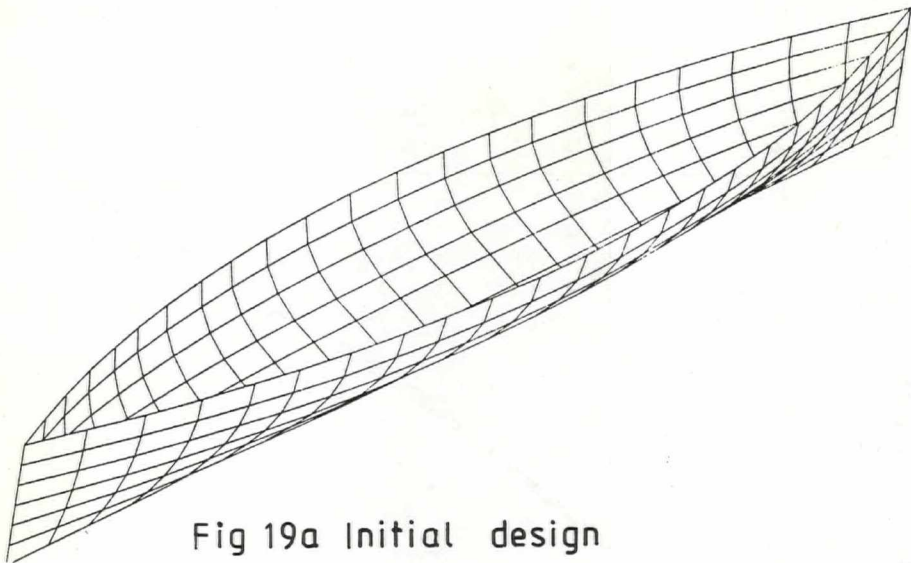


Fig 19a Initial design

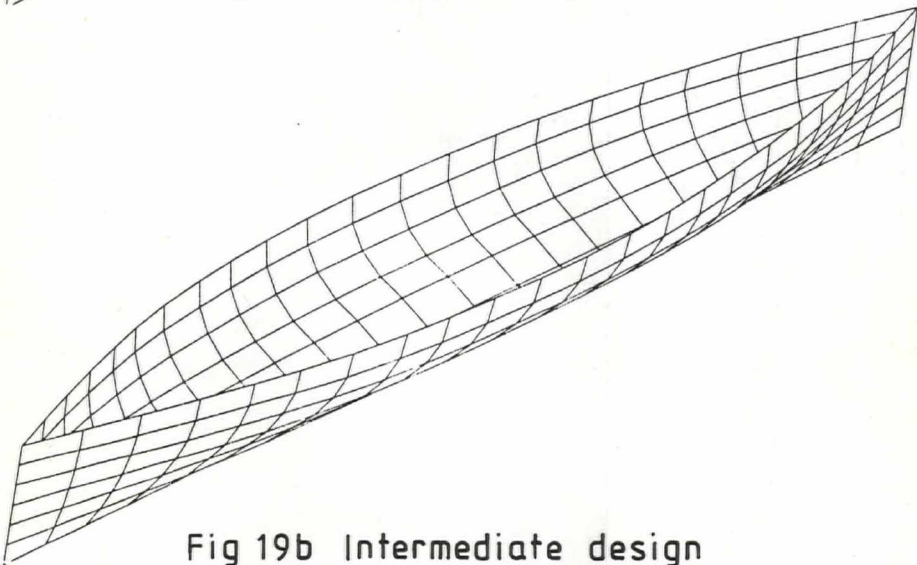


Fig 19b Intermediate design

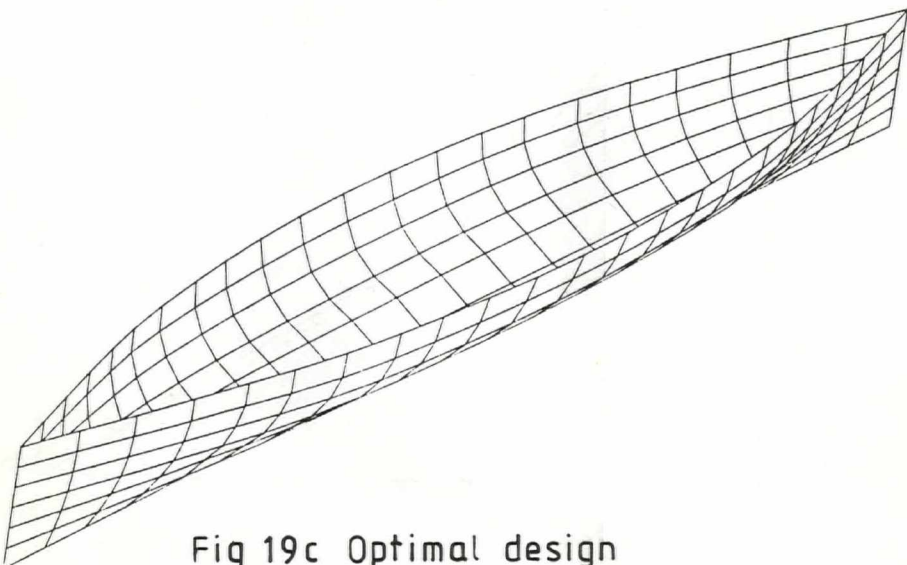
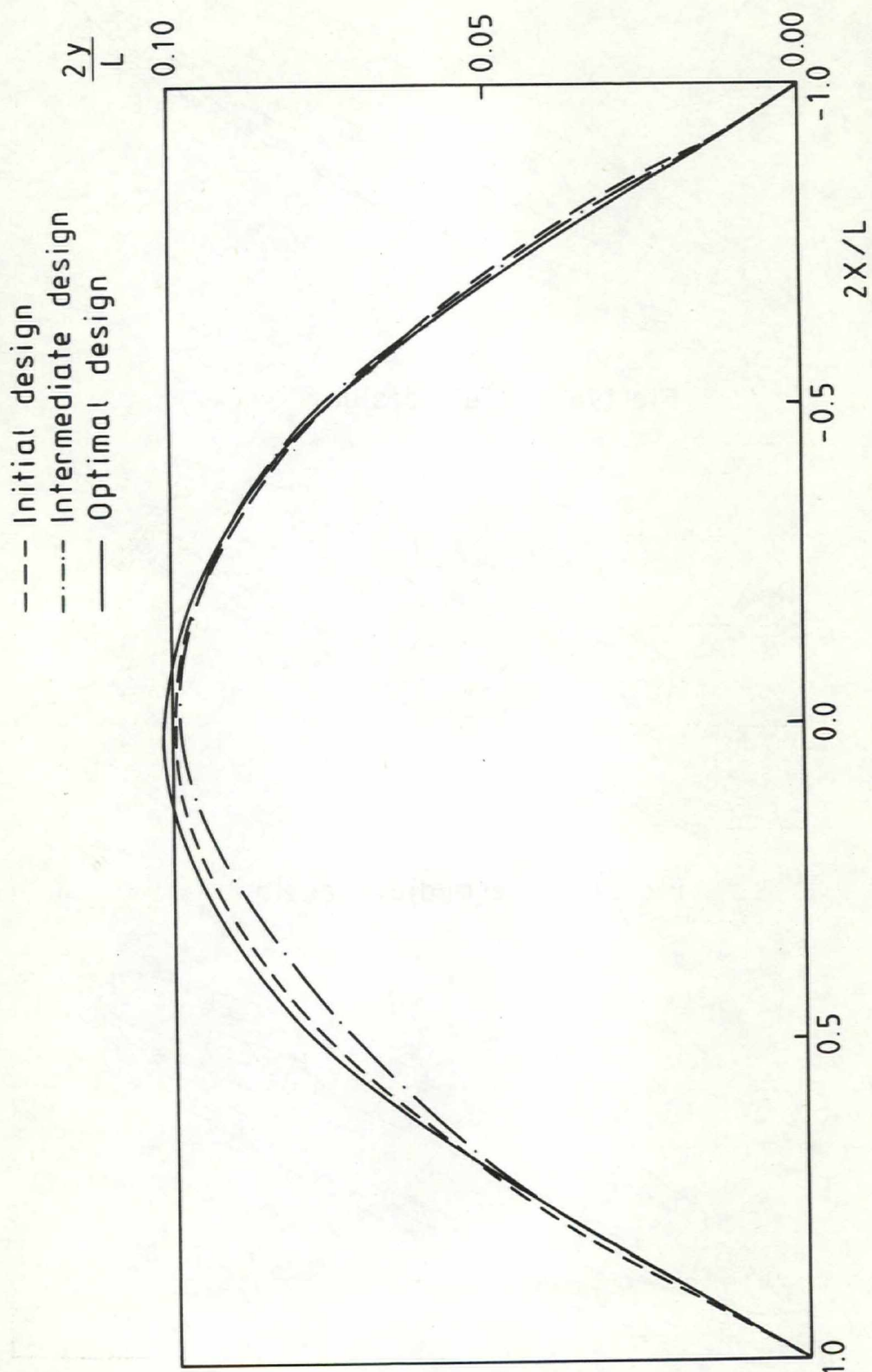


Fig 19c Optimal design

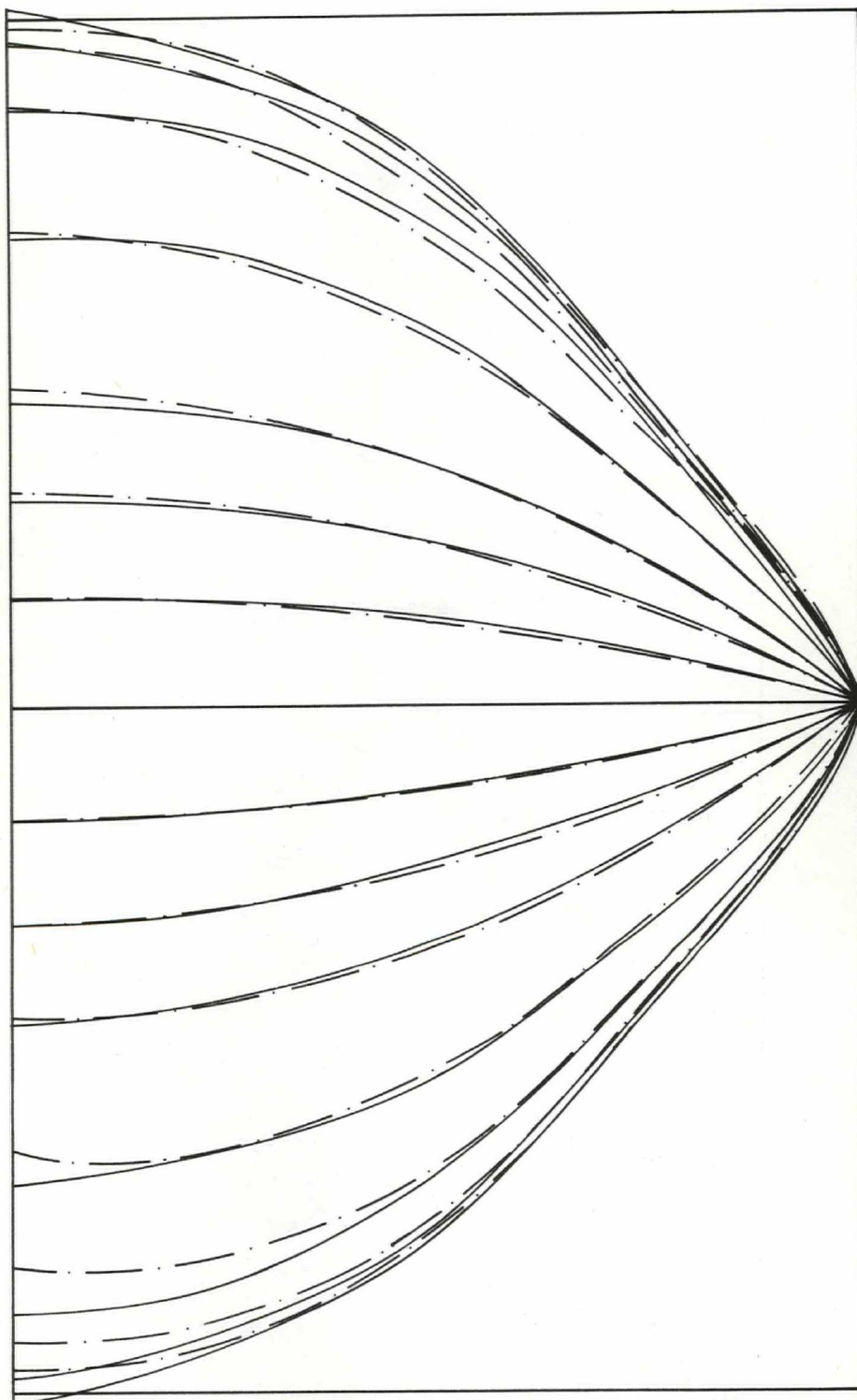


SSPA
&
CTH

Sectional view of optimized canoe
shape
(intermediate + optimal design)

FIG. 17b

----- Intermediate design
——— Optimal design

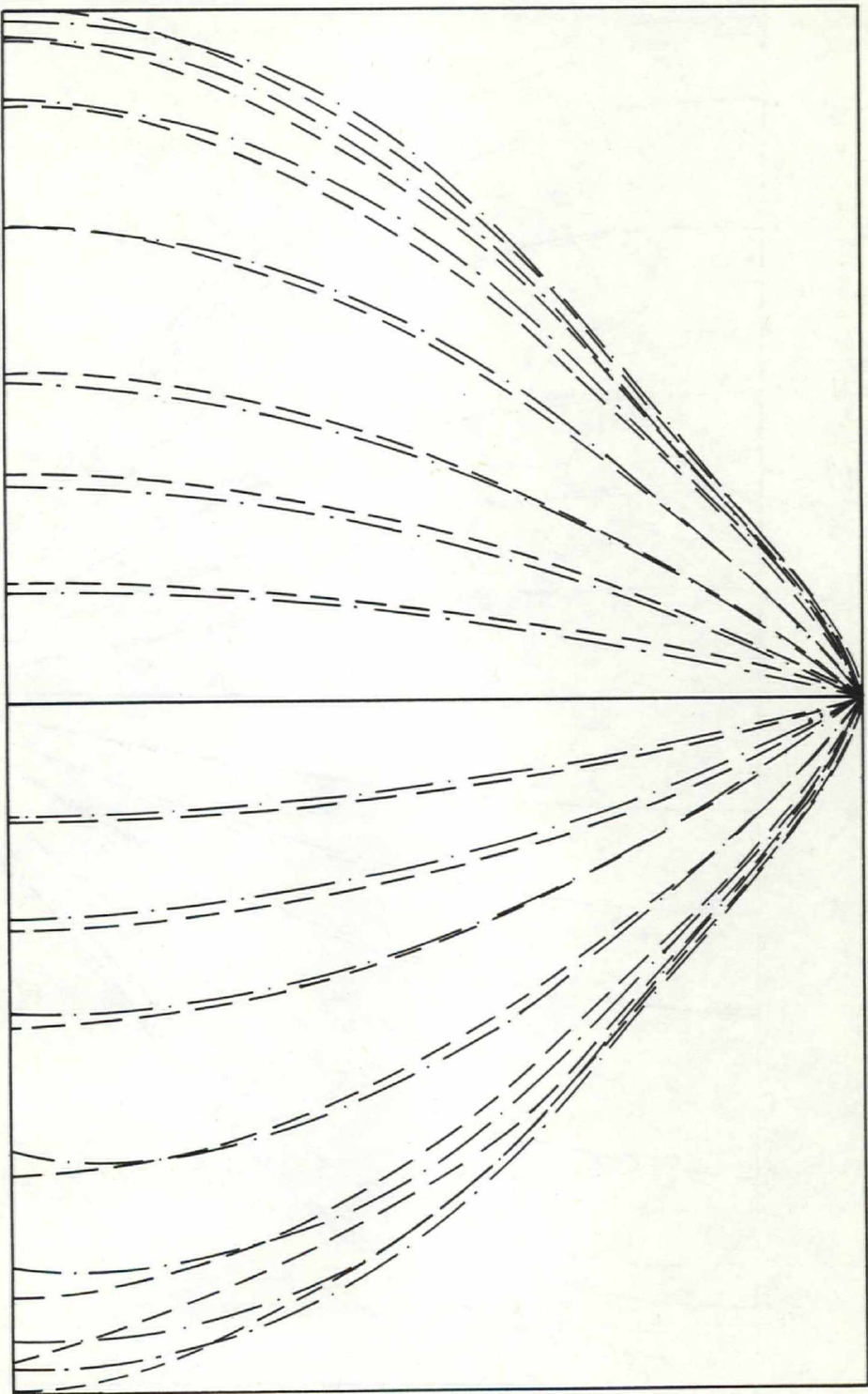


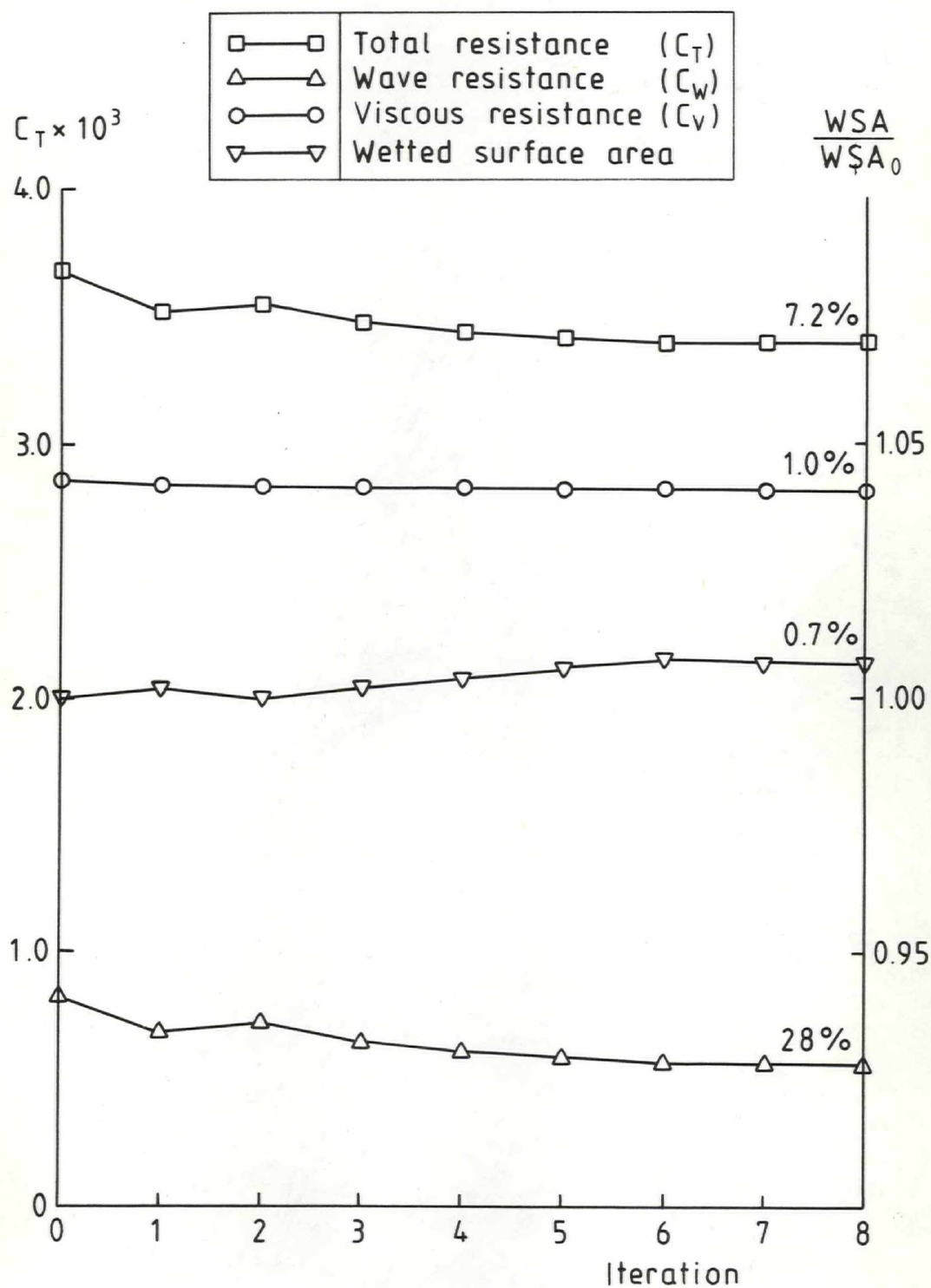
SSPA
&
CTH

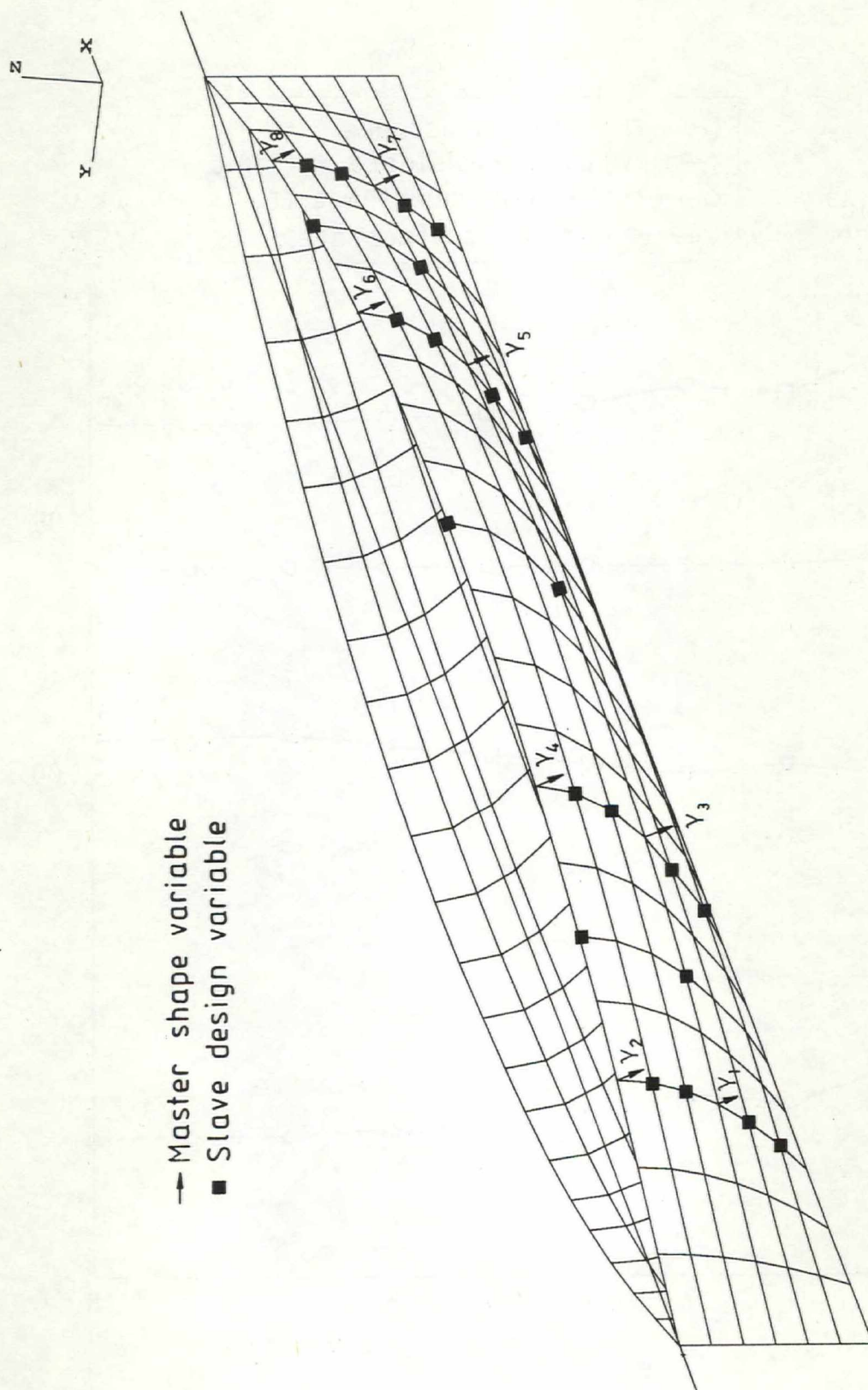
Sectional view of optimized canoe
shape
(initial + intermediate design)

FIG. 17a

--- Initial design
-.-.- Intermediate design







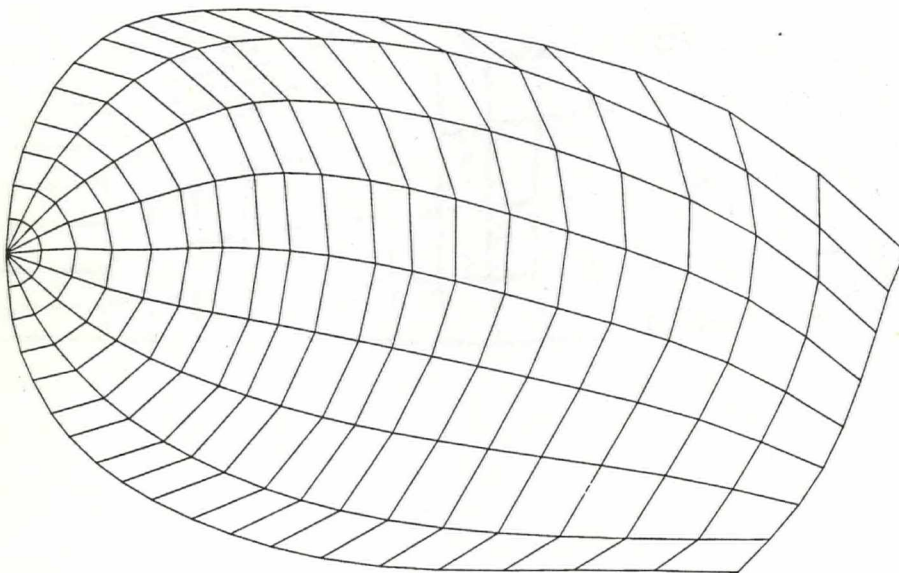


Fig 14a Initial design

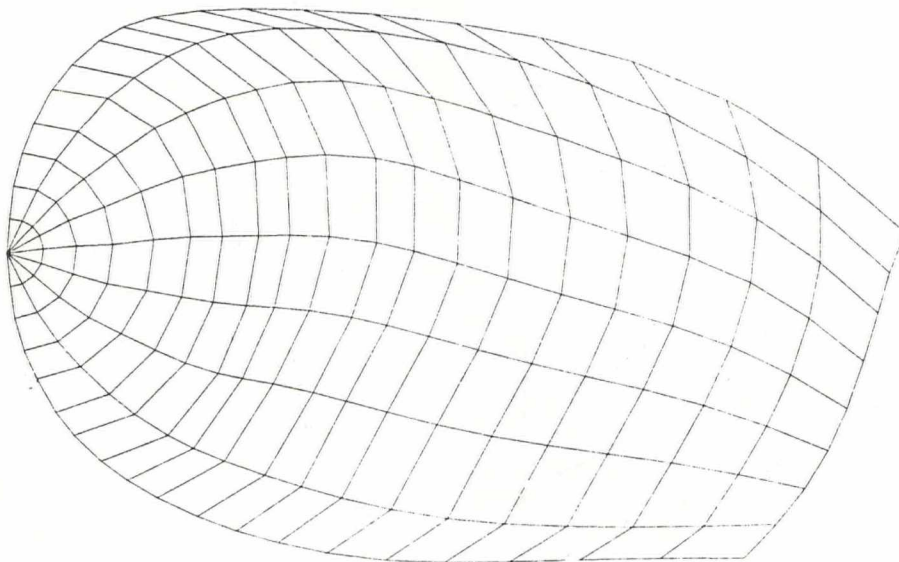
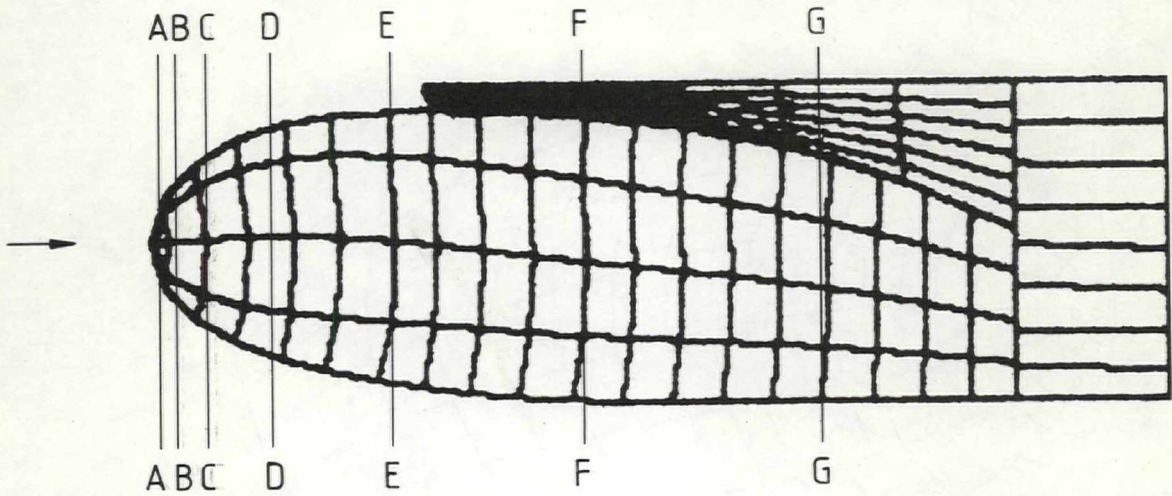
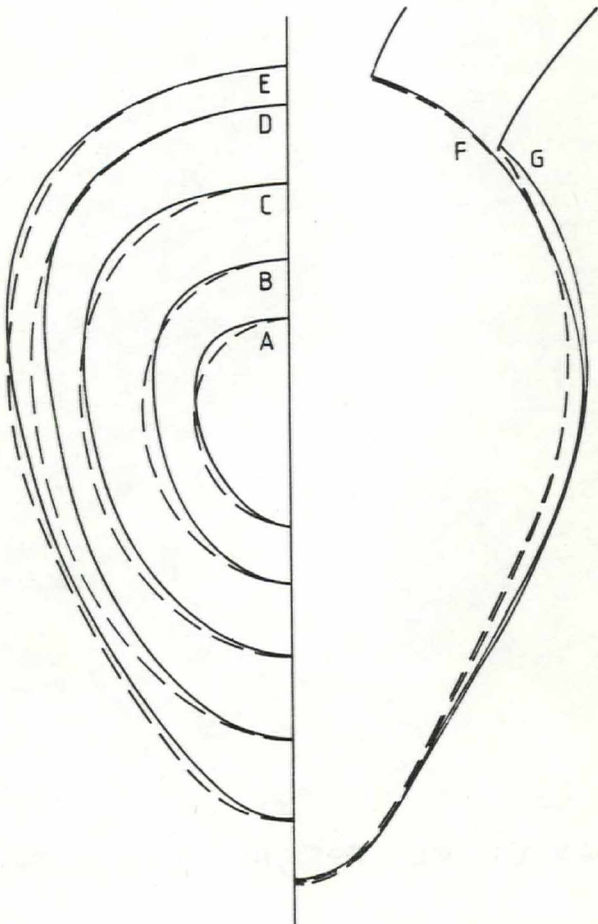
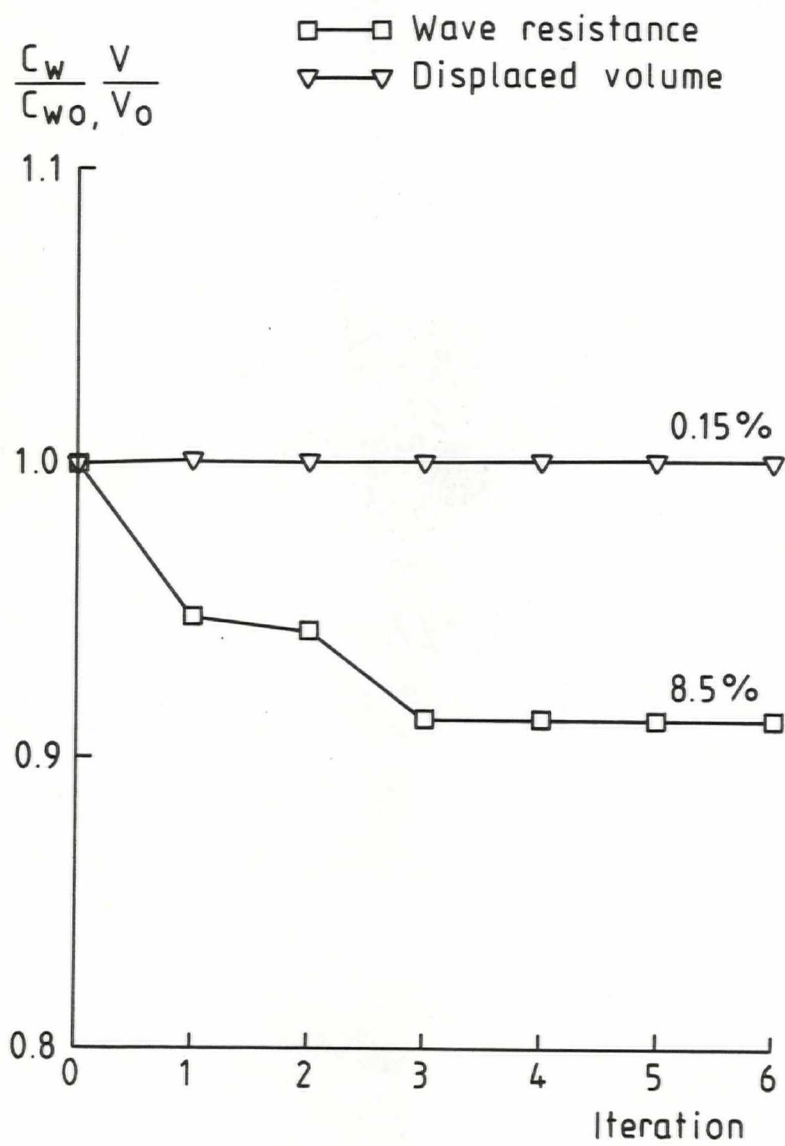


Fig 14b Optimal design



--- Original design
— Optimal design

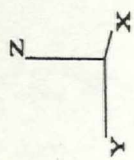




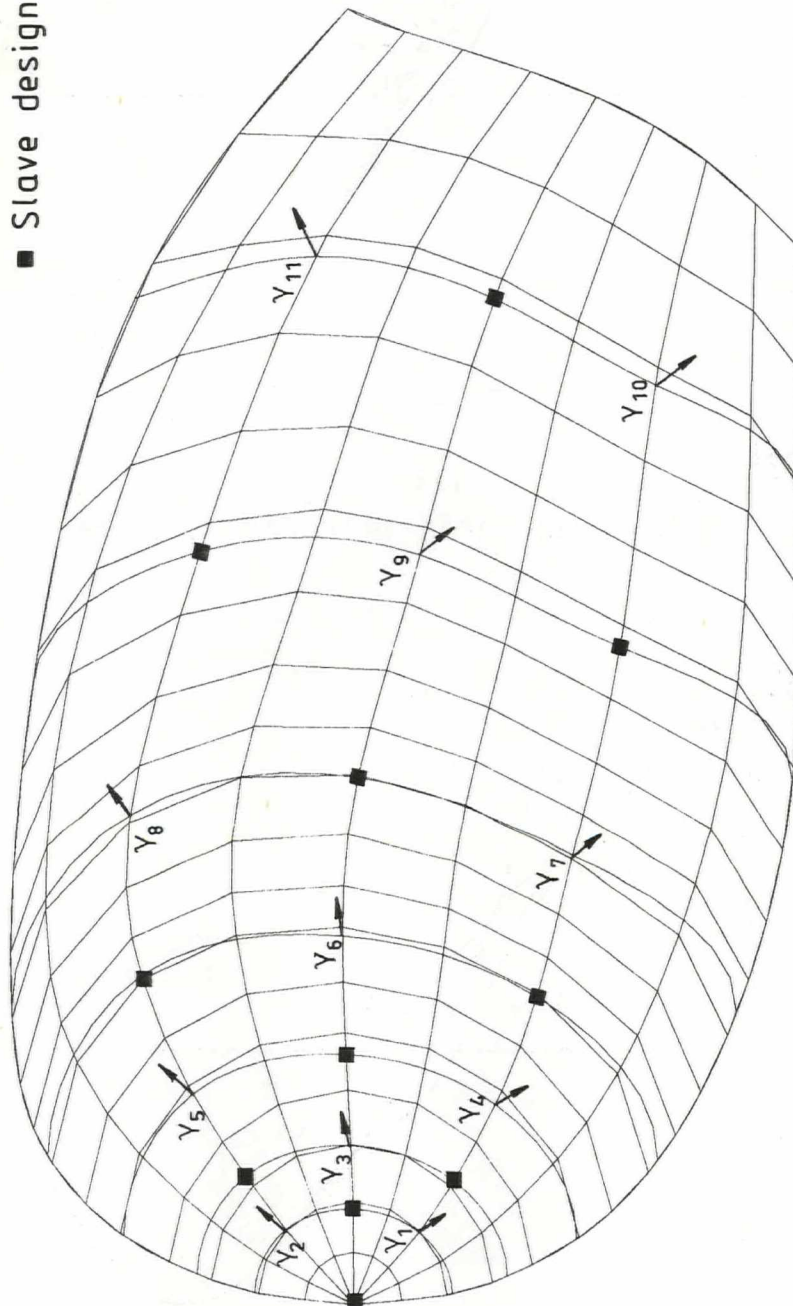
SSPA
&
CTH

Panel distribution with original
large bulb
the SSPA Ro-Ro ship

FIG. 11



→ Master shape variable
■ Slave design variable



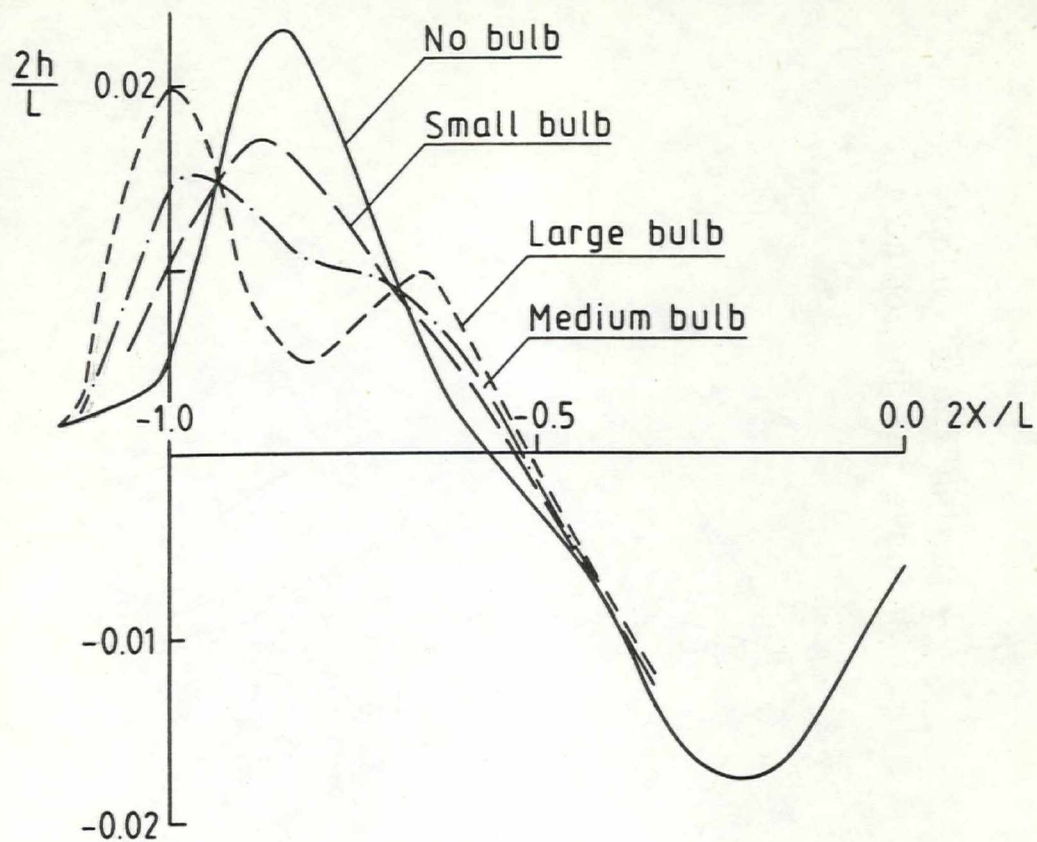


Fig 9a Calculated bow wave profile

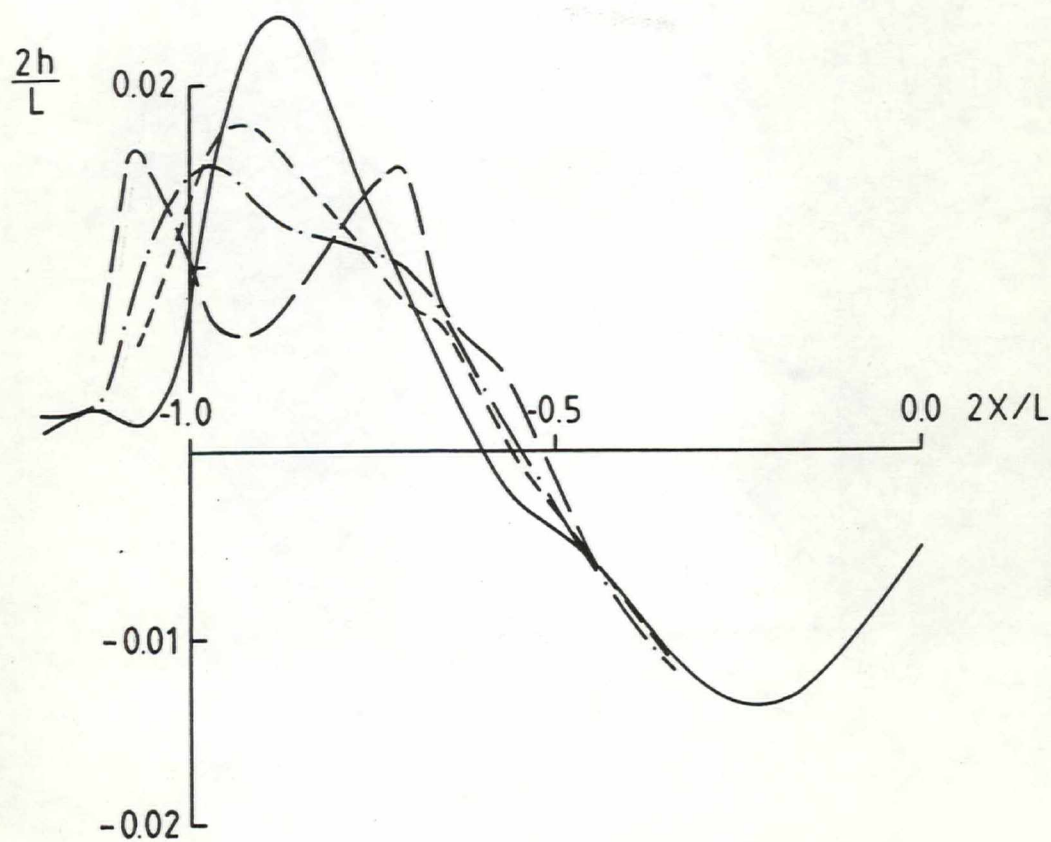


Fig 9b Measured bow wave profile

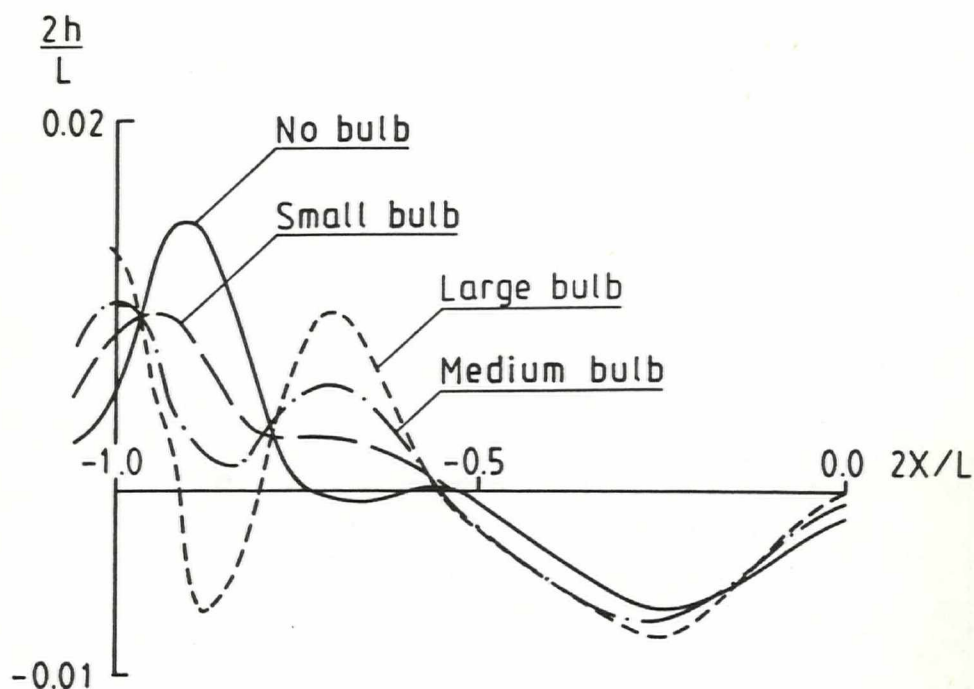


Fig 8a Calculated bow wave profile

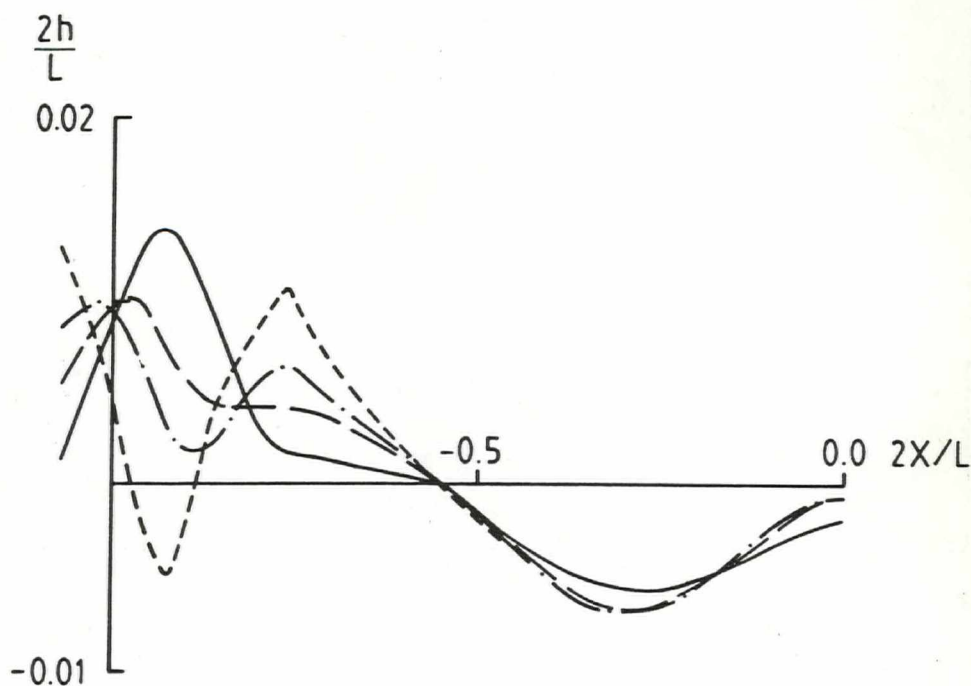


Fig 8b Measured bow wave profile

$C_w \times 10^{-3}$

3.0

Type	Measurement	Calculation
No bulb	————	▼
Small bulb	- - - - -	●
Medium bulb	- . - . -	▲
Large bulb	- - - - -	■

2.0

1.0

0

0

0.1

0.2

0.3

F_n

▼

●

▲

■

▼

●

▲

■

▼

●

▲

■

▼

●

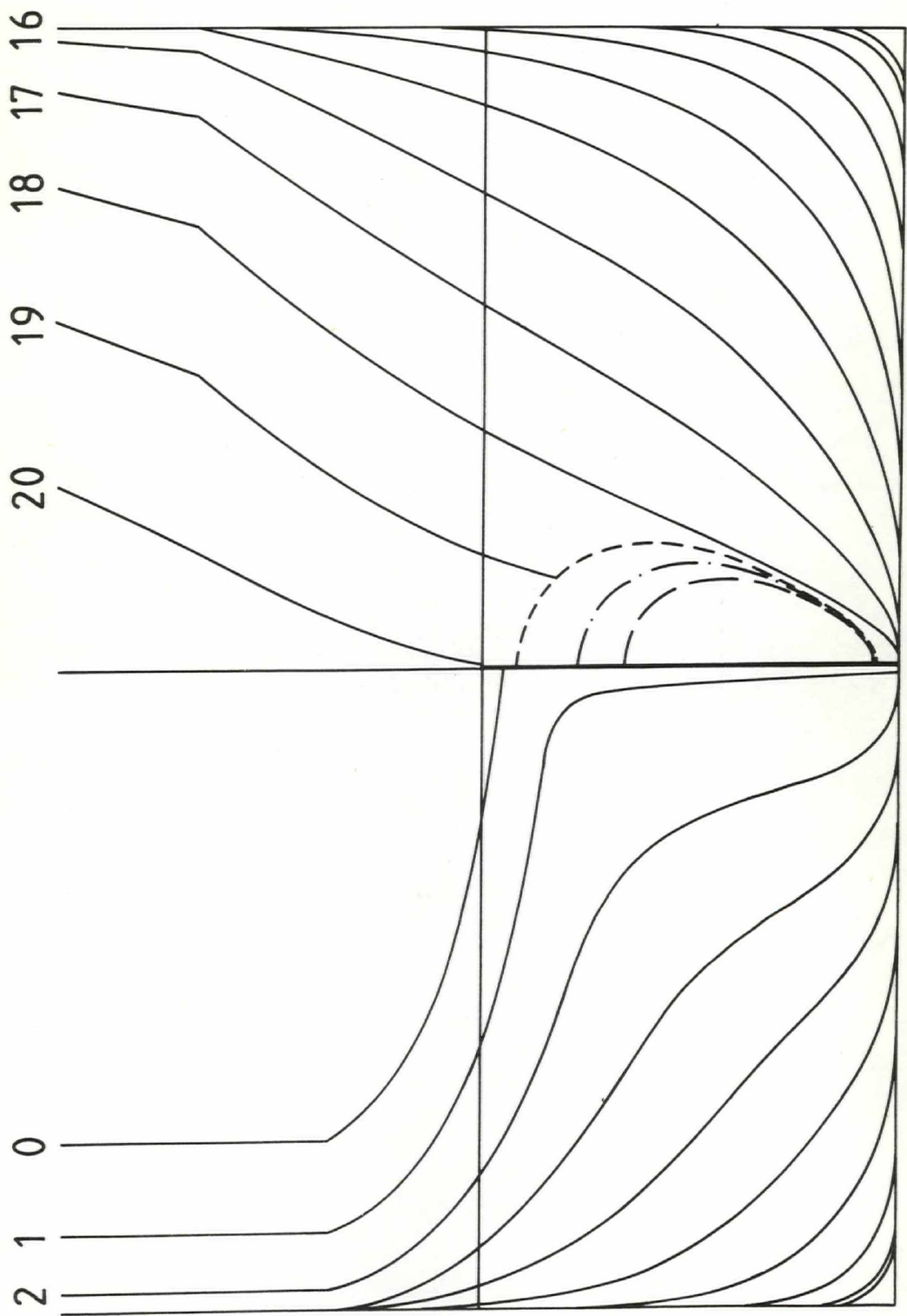
▲

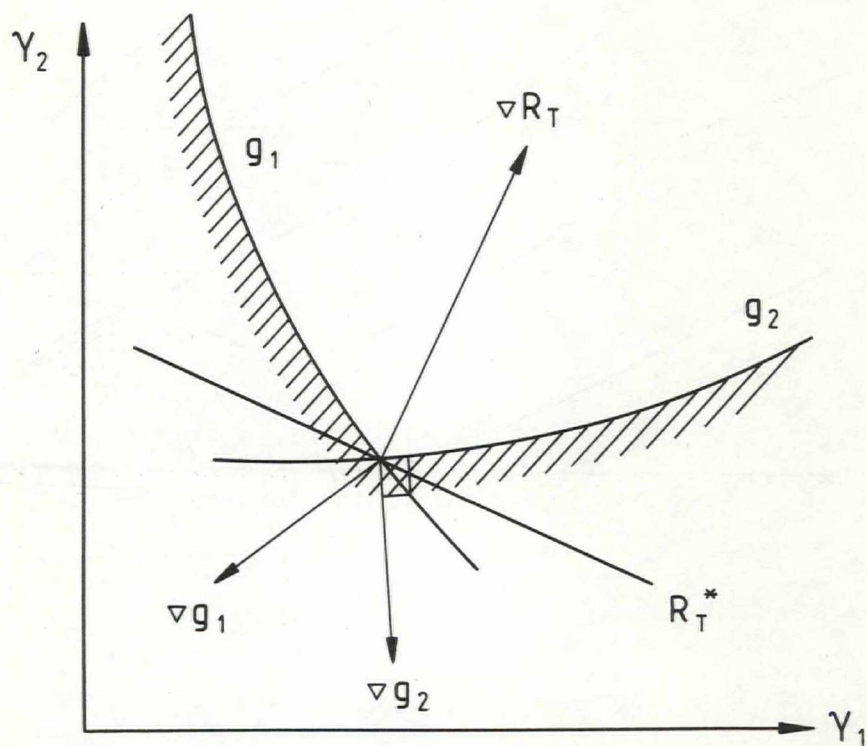
■

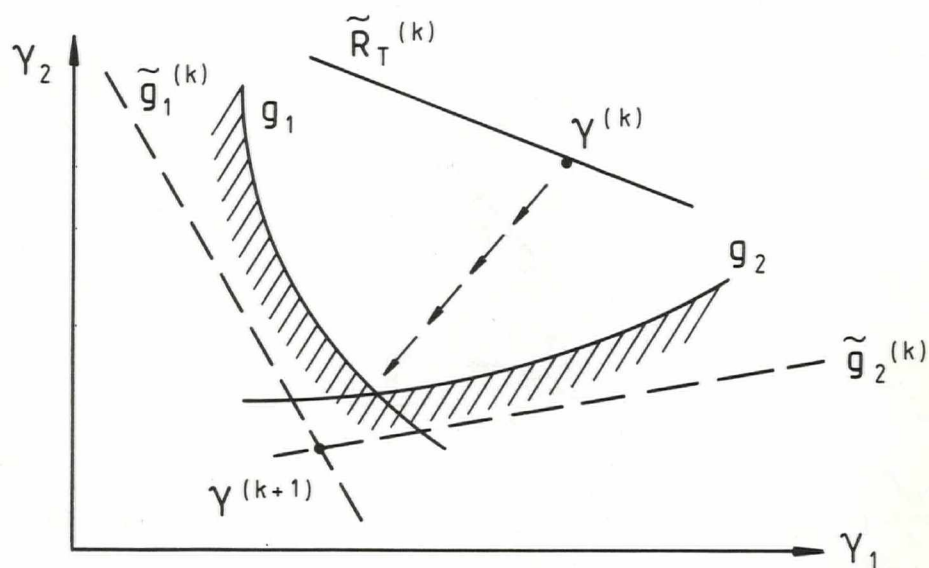
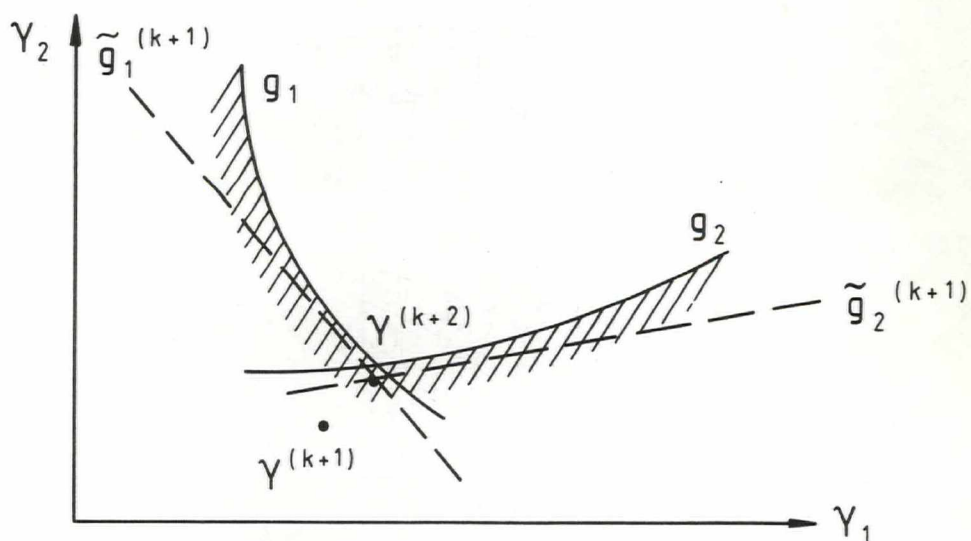
SSPA
&
CTH

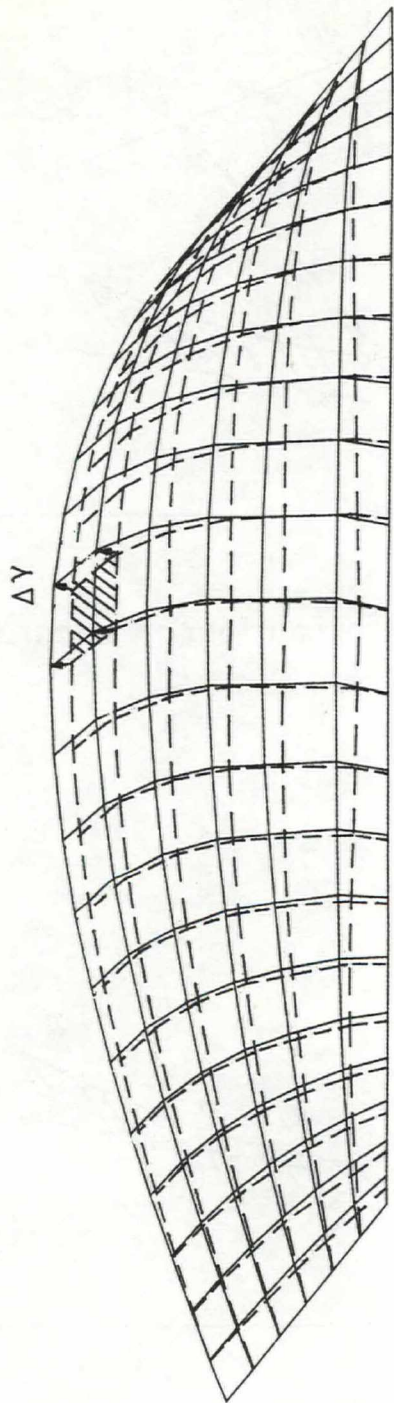
Body plan with bulbs
the SSPA Ro-Ro ship

FIG. 6





Fig 4a Linear approximation of subproblem $\tilde{p}^{(k)}$ Fig 4b Linear approximation of subproblem $\tilde{p}^{(k+1)}$



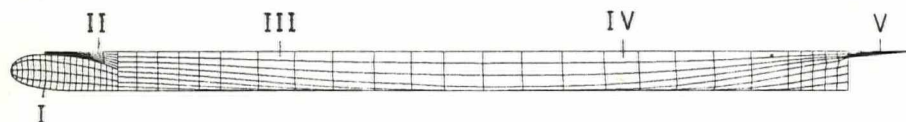


Fig 2a Side view

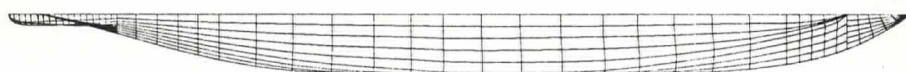


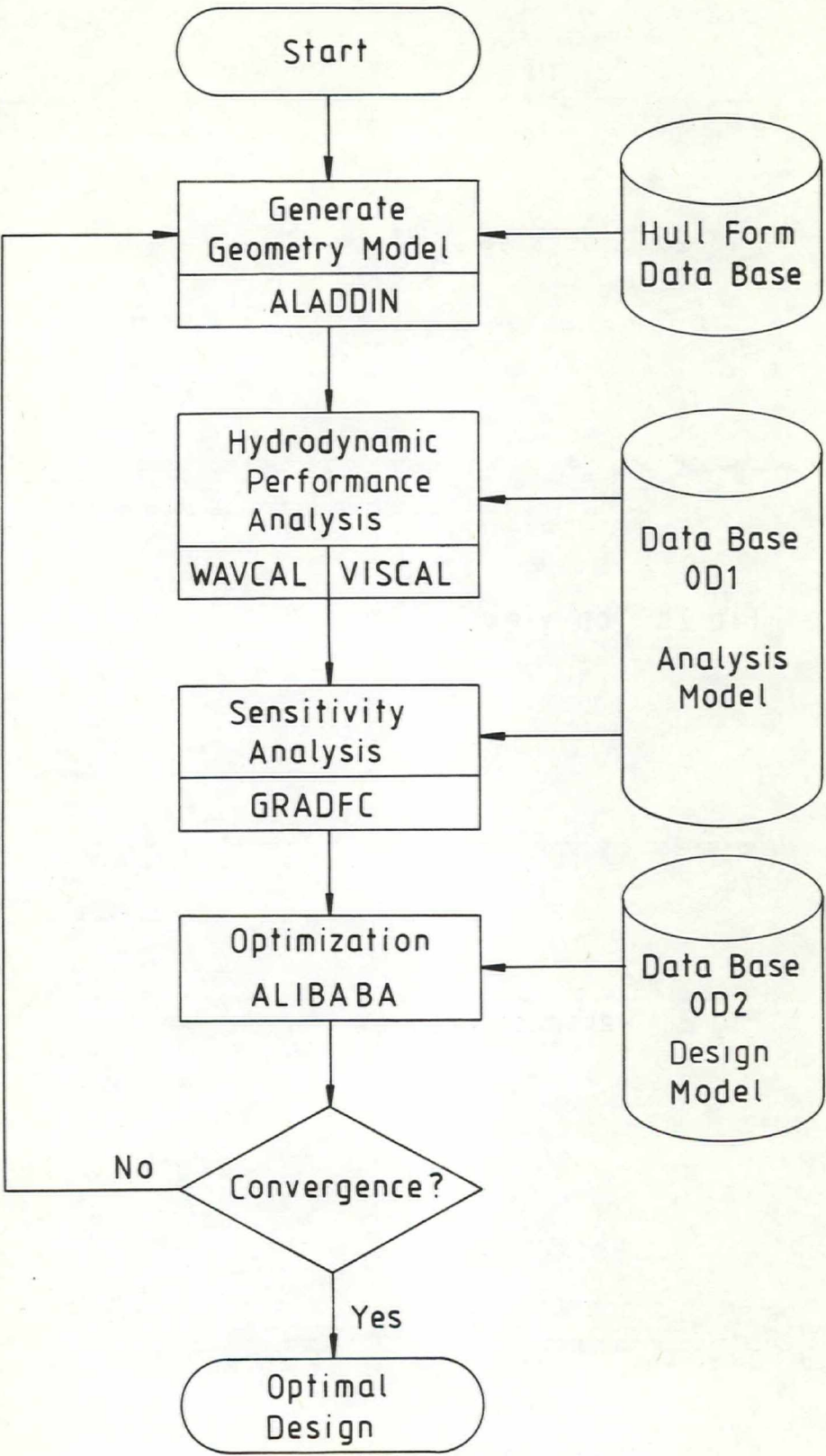
Fig 2b Top view



Fig 2c Perspective view



Fig 2d Perspective view



LIST OF FIGURES

- Figure 1 : Optimal Hull Form Design System (SINDBAD)
- 2 : Geometry modelling of SSPA Ro-Ro ship with large bulb using ALADDIN
- 3 : Interior node point variation
- 4 : Linear approximation with move limits
- 5 : Optimality condition (Kuhn-Tucker Criterion)
- 6 : Body plan with bulbs for the SSPA Ro-Ro ship
- 7 : Wave resistance for the SSPA Ro-Ro ship
- 8 : Wave profiles at $F_n = 0.21$ for the SSPA Ro-Ro ship
- 9 : Wave profiles at $F_n = 0.28$ for the SSPA Ro-Ro ship
- 10 : Optimization model with design variables
- 11 : Panel distribution with original large bulb
- 12 : Convergence history for the optimal bulb design
- 13 : Sectional view of the optimized bulb shape (initial + optimal design)
- 14 : Perspective view of the optimized bulb shape (initial + optimal design)
- 15 : Optimization model with design variables - canoe design
- 16 : Convergence history - canoe design
- 17 : Sectional view of the optimized canoe shape (initial, intermediate and optimal design)
- 18 : Waterline shape of the optimized canoe shape (initial, intermediate and optimal design)
- 19 : Perspective view of the optimized canoe shape (initial, intermediate and optimal design)

- [34] Hoyle, J W et al: "A Bulbous Bow Design Methodology for High Speed Ships", SNAME Annual Meeting, New York, November 1986
- [35] Esping, B J D: "A CAD Approach to the Minimum Weight Design Problem", International Journal of Numerical Method in Engineering, Vol 21, pp 1049-1066, 1985
- [36] Esping, B J D: "The OASIS Structural Optimization System", Computer & Structures, Vol 23, No 3, pp 365-377, 1986

- [25] Esping, B & Holm, D: " A CAD Approach to Structure Optimization", presented at the Conference 'Computer Aided Optimal Design: Structure and Mechanical Systems', editor C A Mota Soares, Springer-Verlag, 1987
- [26] Squire, H.B. & Young, A.D.: "The Calculation of the Profile Drag of Airfoils", ARC Rept and Mem No 1838, 1938
- [27] Schlichting, H.: Boundary Layer Theory, P764, 7th Edition, McGraw-Hill Book Company
- [28] Esping, B J D: "Minimum Weight Design of Membrane Structures Using Eight Node Isoparametric Elements and Numerical Derivatives", Computer & Structures, Vol 19, No 4, pp 591-604, 1984
- [29] Svanberg, K: "MMA - Method of Moving Asymptotes - A New Method for Structural Optimization", TRITA MAT-1985-RIT, Stockholm, Sweden, 1985
- [30] Fleury, C. & Schmit, L.A.: "Dual Methods and Approximation Concepts in Structural Analysis", NASA Contractor Report 3326, 1980
- [31] Svanberg, K.: "An Algorithm for Optimum Structure Design Using Duality", Mathematical Programming Study 20, pp 161-177, 1982
- [32] Fletcher, R: "Practical Methods of Optimization", Vol 1 Unconstrained Optimization, John Wiley & Sons, 1982
- [33] Esping, B J D: "The ALIBABA Non-Linear Optimization Package - Structural Optimization Using Numerical Techniques", PhD Thesis, Paper F, Report No 85-8, Department of Aeronautical Structures and Materials, the Royal Institute of Technology, Stockholm, Sweden, 1985

- [17] Inui, T.: "Study on Wave-Making Resistance of Ships", Chapter 11, Vol 2, Both Anniversary Series, The Society of Naval Architects of Japan, 1957
- [18] Yim, B.: "Minimum Wave Resistance of Bulbous Ships", Hydronautics Inc, Technical Report 117-3, 1963
- [19] Nagamatsu, T & Baba, E: "Study on the Minimization of Ship Viscous Resistance", Journal of the Society of Naval Architects of Japan, Vol 154, Dec, 1983
- [20] Min, K-S & Kim, K-J: "A Study on the Optimum Hull Form Development Based on the Minimum Resistance Theory", Journal of the Society of Navel Architects of Korea, Vol 21, No 4, Dec, 1984
- [21] Suzuki, K & Maruo, N: "Application of Nonlinear Optimization Technique to Hull Form Design Based on Wave Resistance Theory", The Second International Symposium on Practical Design in Shipbuilding (PRADS 83), 1983
- [22] Nowaki, H: "Optimization Methods Applied to Viscous Drag Reduction", Osaka International Colloquium on Ship Viscous Flow, October, Osaka, Japan, 1985
- [23] Kim, K-J & Larsson, L: "Comparison between First and Higher Order Methods for Computing the Boundary Layer and Viscous Resistance of Arbitrary Ship Hulls", International Symp on Resistance and Powering Performance, Shanghai, 1989
- [24] Kim, K-J: "A Higher Order Panel Method for Calculating Free Surface Potential Flows with Linear Free Surface Boundary Conditions", SSPA Report No 2966-2, 1989, also presented at International Symp on Resistance and Powering Performance, Shanghai, 1989

- [9] Kim, K-J & Larsson, L: "Comparison between First and Higher Order Methods for Computing the Boundary Layer and Viscous Resistance of Arbitrary Ship Hulls", International Symposium on Resistance and Powering Performance, Shanghai, P R China, 1989
- [10] Broberg, L: "Numerical Calculation of Ship Stern Flow, PhD Thesis, Division of Mechanics", Chalmers University of Technology, 1988
- [11] Xia, F: "Calculation of Potential Flow with a Free Surface", SSPA Report No 2912-1, Gothenburg, 1986
- [12] Ni, S-Y, Kim, K-J, Xia, F & Larsson, L: "A Higher Order Panel Method for Calculating Free Surface Potential Flows with Linear Surface Boundary Conditions", International Symp on Resistance and Powering Performance, Shanghai, P R China, 1989
- [13] Xia, F: "A Study on the Numerical Solution of Fully Non-Linear Ship Wave Problems", SSPA Report No 2912-3, 1986
- [14] Ni, S-Y: "A Method for Calculating Non-Linear Free Surface Potential Flows Using Higher Order Panels", SSPA Report No 2912-6, 1987
- [15] Kim, K-J: "A Higher Order Panel Method for Calculating Free Surface Potential Flows with Non-Linear Free Surface Boundary Conditions", SSPA Report No 2966-1, 1989
- [16] Taylor, D.W.: "Calculations for Ships' Forms and the Light Thrown by Model Experiments upon Resistance, Propulsion and Rolling of Ships", Trans Int Eng Congress, San Francisco, 1915

REFERENCES

- [1] Moor, D I & Parker, M N: "The BSRA Methodical Series - An Overall Presentation. Geometry of Forms with Block Coefficient and Longitudinal Center of Buoyancy", Trans RINA, Vol 103, 1961
- [2] Todd, F H: "Series 60 Methodical Experiments with Models of Single-Screw Merchant Ships", DTNSRDC Report No 1712, July 1963
- [3] Lackenby, H & Parker, M N: "The BSRA Methodical Series - An Overall Presentation Variation of Resistance with Breadth-Draught Ratio and Length-Displacement Ratio", Trans RINA, Vol 108, 1966
- [4] Clements, R E & Thomson, G R: "Model Experiments on a Series of 0.85 Block Coefficient Forms", Trans RINA, 1972
- [5] Della Loggia, B & Doria, L: "Methodical Series Tests for Fuller Ship Hull Forms, Ocean Engineering", Vol 7, 1980
- [6] Larsson, L: "A Calculation Method for Three-Dimensional Turbulent Boundary Layers on Ship-Like Bodies", First International Conference on Numerical Ship Hydrodynamics, Washington DC, 1975
- [7] Larsson, L & Chang, M-S: "Numerical Viscous and Wave Resistance Calculations Including Interaction", 13th Symposium on Naval Hydrodynamics, Tokyo, 1980
- [8] Kim, K-J: "Calculation of Ship Viscous Resistance Using Boundary Layer Theory Based on First or Higher Order Approximations", Department of Marine Hydrodynamics, Chalmers University of Technology, Report No 72, Gothenburg, Jan, 1988

V. CONCLUDING REMARKS AND FUTURE WORK

The objective has been to obtain an Optimum Hull Form Design System (SINDBAD), which will enable the designer to include advanced hydrodynamic performance predictions at an early stage of the design process, allowing a systematic evaluation of the hydrodynamic performance characteristics as a function of the hull geometry. The SINDBAD system has been applied to the bow shape optimization of a fine form, high speed ship and to the entire hull form optimization for a canoe type of vessel. Through the two optimum hull form design examples it has been demonstrated that the SINDBAD system can be used to develop mathematically faired and hydrodynamically desirable hull forms for commercial types of ships starting from an existing ship.

The method presented here is only the beginning of the work done in the development of a complete Optimum Hull Form Design System. All the important factors for determining a ship's performance have not yet been incorporated in this system. In particular, it is important in the design of ships that the considerations of propulsion and seakeeping are included at an early design stage. Furthermore, the determination of the optimal principal dimensions of the ship is also an integral part of the design process. Further development of the evaluation methods for ship motion, propulsion, manoeuvring characteristics have to be made and should be incorporated as they become available. However, this effort is not that simple, since it involves many different fields of ship hydrodynamics. Thus it seems that the most important next step is further improvement of the performance evaluation method.

The viscous flow method that is included in the present version of the Optimal Hull Form Design System (SINDBAD) is based on a first order integral method. A more advanced method for solving the Navier-Stokes equation will have to be incorporated to extend its capability and generality.

The optimization was performed starting from the Wigley hull and reduced the total resistance by 7.2% after eight iterations (see Fig 16). The sectional view of the optimized canoe design is compared with the initial design in Fig 17a and the intermediate one after two iterations in Fig 17b. The comparison of nondimensional design load waterline shapes for the optimal design with the initial one is made in Fig 18. Perspective comparisons are also made in Fig 19.

It can be seen from the convergence history curve presented in Fig 12 that a reduction of 8.5% in wave resistance is achieved after six iterations. The sectional and perspective views of the original and the optimal design are shown in Figs 13 and 14. It is interesting to note that the maximum section area is considerably increased, this being accomplished by reducing the volume in the lower part of the bulb. This indicates that the lower part of the bulb is not so important for the bow wave or wave resistance.

IV-3. Canoe Shape Optimization

As a more practical design example for the total resistance minimization, an optimization study of interest in the design of a racing canoe has been made. The entire hull form was optimized starting from the Wigley hull. Fig 15 shows the geometrical modelling of the original hull form with 132 panel elements. The hull surface is represented by using 8 master shape and 22 slave design variables.

The following design criteria were taken into account when optimizing the hull form with respect to total resistance:

- 1) The design speed for which the optimization is to be performed is 1.78 m/sec. This corresponds to $F_n = 0.25$ and $R_n = 9.28 \times 10^6$ based on LPP = 5.2 m.
- 2) Constant volume limitation ($C_B = 0.44$).
- 3) The geometrical shape changes are allowed along the y direction only, which means that the design draught is kept constant ($T = 0.325$ m) during the optimization process.

The resistance study with the SSPA Ro-Ro ship model 2062 has shown that a larger bulb size seems to increase a bulb's resistance reducing effect and the bow bulbs should be made as large as possible. There are, however, several practical constraints, associated with ship handling such as anchoring and dry docking, which have to be considered in the optimal bulb design.

An attempt to design an optimized bow shape has been made using the Optimal Hull Form Design System (SINDBAD) starting from the SSPA Ro-Ro ship with a large bulb. A symmetry half of the original bulb is modelled with 152 panel elements using 11 master shape and 10 slave design variables, as shown in Fig 11 and connected to the main hull. The wave resistance to be minimized is calculated from the momentum approach given in (11) with 726 elements (404 hull elements + 322 free surface panels).

The design criteria considered in the present optimization study are as follows:

- 1) The design speed for which the optimization is to be performed is $F_n = 0.28$. This corresponds to the ship speed 22.86 knots, based on LPP = 180 m
- 2) It is required that the bulb volume is kept constant, so that the location of the longitudinal centre of buoyancy should be maintained at the original position after optimization.
- 3) The original bulb contour on the XZ centreplane and the connection points between the bulb and the main hull are assumed not to be changed during the optimization process.
- 4) Zero transverse slope boundary conditions at points on the contour line are required.

As can be seen from the figure the present method predicted lower wave resistance than the measured residual resistance for the different bulb configurations at nearly all speeds. Although absolute quantitative differences are observed between computed wave and measured residual resistance curves, similar trends are evident and an identical ranking, large - medium - small - no bulb, can be obtained from the relative comparison of these curves. These rankings are arranged from best to worst, with best being a bulb which had the lowest resistance within the 15-22 knots speed range. These identical relative rankings indicate that the present method can be used with confidence to obtain the best bulb shape in the optimization procedure if minimizing a ship resistance is of main concern.

Another good indication in this respect can be found in the prediction of wave patterns as shown in Fig 8-9. The wave profiles vary greatly near the bow region depending on the bulb shape and remain almost unchanged on the remaining part of the free surface. The present method predicted this phenomenon very well.

IV-2. Optimal bulb design

The bulbous bow has been considered an effective means to reduce the resistance of the ship [34]. A bulb reduces wave resistance by lowering the bow wave system and it also reduces viscous resistance by smoothing the flow around the forebody.

For slender, fast hull forms such as a Ro-Ro ship, the primary reduction in resistance is due to the cancellation of the bow wave system, which is accomplished by interference, dependent upon the phase and amplitudes of the waves created by the bulb and the ship. At optimal conditions the two waves may cancel each other totally. The phase difference of the two wave systems is determined by the location of the bulb, and the amplitude of the bulb's wave determined by bulb volume.

IV. OPTIMIZATION EXAMPLE

In order to examine the validity of the optimization algorithm described in the previous section, the Optimal Hull Form Design System has been tested to develop mathematically faired and hydrodynamically desirable hull forms starting from an existing ship. As a first example, the method was applied to design an optimal bow shape of a Ro-Ro ship by minimizing the wave resistance. This design study was performed using the SSPA Ro-Ro ship model 2062 with a large bulb as the reference hull form. As a more practical design example, an attempt was made to optimize the entire hull form based on the Wigley hull for the application to the design of a canoe type of vessel. Each of these optimization examples will be discussed separately.

IV-1. Sample Resistance Calculation

Before proceeding to the optimization procedure, the hydrodynamic performance prediction method described in the previous section was tested to investigate the numerical accuracy and its applicability.

First the higher order linear free surface potential program (DHBHFL) was tested to evaluate its usefulness in bulbous bow design. DHBHFL computed the wave resistance based on the momentum approach and wave patterns of the SSPA RoRo ship model 2062 with and without bulb forms. Three different bulbous bow shape variations and the panel representation for the large bulb are presented in Fig 6 and Fig 11, respectively.

The computed wave resistance coefficient versus ship speed is presented in Fig 7 and a comparison with the measured residual resistance coefficient is made in a relative sense. It should be noted that the computed wave resistance is not comparable in an absolute sense to the measured residual resistance since this contains also other components like the viscous pressure resistance.

For the first two iterations ($k = 1, 2$):

$$\begin{aligned} L_j(k) &= \gamma_j(k) - (\bar{\gamma}_j - \gamma_j) \\ U_j(k) &= \gamma_j(k) + (\bar{\gamma}_j - \gamma_j) \end{aligned} \quad (39)$$

and for the following iterations ($k > 2$):

$$\begin{aligned} L_j(k) &= \gamma_j(k) - s*(\gamma_j(k-1) - L_j(k-1)) \\ U_j(k) &= \gamma_j(k) - s*(U_j(k-1) - \gamma_j(k-1)) \end{aligned} \quad (40)$$

where

$s = 0.7$ if $a \leq 0$, i.e. oscillating variables

$s = 1/\sqrt{0.7}$ if $a > 0$, i.e. monotonous variables

and

$$a = (\gamma_j(k) - \gamma_j(k-1)) * (\gamma_j(k-1) - \gamma_j(k-2)) \quad (41)$$

In the present calculation, the convergence tolerance for ϵ_1 and ϵ_2 are specified as 0.01 respectively and the optimum solution usually obtained after seven iterations.

III-5. Convergence

The iteration procedure described in the preceding sections is continued until the following convergence criterion is satisfied

$$\frac{R_T^{(k)} - R_T^{(k-1)}}{R_T^{(k)}} \leq \epsilon_1 \quad (37)$$

and

$$\frac{g_w^{(k)}}{\bar{g}_w} \leq 1 + \epsilon_2 \quad (38)$$

$R_T^{(k)}$ is the value of the objective function and $g_w^{(k)}$ is the worst constraint at iteration k .

The number of necessary subproblems to achieve convergence is in general rather small but strongly dependent on the quality of the chosen approximation. In the Method of Moving Asymptots used here, the solution of a subproblem is restricted to a small region in the vicinity of the current design by specifying move-limits on design variables and the upper U_j and lower limit L_j are arranged to be adjusted successively during the iteration to improve the approximations.

If the subproblem solutions are oscillating in a variable γ_j , L_j and U_j will be forced closer together. On the other hand, if the variable γ_j is monotonous, i.e. increasing or decreasing L_j and U_j will be pushed further apart.

the maximum perturbation are not included when computing the perturbed velocity influence matrix $A(\gamma + \Delta\gamma)$ in order to reduce the amount of required calculation without loss of numerical accuracy. With all derivative terms in eqs (30) and (31) known, the wave resistance gradient can now be estimated. This calculation procedure turned out to be very efficient and surprisingly stable considering the approximation involved.

2. Gradient of Constraints

The shape to be optimized is subject to geometric constraints which include bounds on form parameters, set limits on the principal dimensions and prevention of an undesired local shape. These restrictions have to be specified by the ship designer, but all of them are not always desirable. The designer has the option to impose these constraints or to allow the optimization to proceed without any constraints.

In this section, a volume constraint implemented on the Hull Form Optimization Design System (SINDBAD) is described and the additional constraints which have to be supplied by the designer are considered separately in section IV.

It is required that the volume of the hull, V_H , is kept constant during the optimization process. This requirement results in the following constraint:

$$V_H - \int_E Z N_Z dA = 0 \quad (35)$$

where N_Z is the Z component of the normal vector of a panel element.

The gradient of volume constraint is estimated by finite difference:

$$\frac{dV_H}{d\gamma} = \frac{V_H(\gamma + \Delta\gamma) - V_H(\gamma)}{\Delta\gamma} \quad (36)$$

The source strength derivative can also be approximated by the finite difference:

$$\frac{\partial \sigma}{\partial \gamma} = \frac{\sigma(\gamma + \Delta\gamma) - \sigma(\gamma)}{\Delta\gamma} \quad (31)$$

The source strength $\sigma(\gamma)$ for the hull shape of interest can be obtained from

$$\sigma_j(\gamma) = A_{ij}^{-1}(\gamma) \cdot B_i(\gamma) \quad (32)$$

To determine the perturbed source strength $\sigma(\gamma + \Delta\gamma)$, an iterative approach has been applied. The iteration scheme actually solves

$$\sigma_j^m(\gamma + \Delta\gamma) = A_{ij}^{-1}(\gamma) [B_i(\gamma + \Delta\gamma) - \Delta A_{ij}(\gamma) \sigma_j^{m-1}(\gamma) - \Delta A_{ij}(\gamma) \Delta \sigma_j^{m-1}(\gamma)] \quad (33)$$

The iteration is stopped when the following criterion is satisfied, where the superscript m represent iteration number and $\Delta \sigma_j^{m-1}(\gamma)$ is normally assumed to be zero at the first iteration

$$\sum_{j=1}^{NE} \left| \frac{\sigma_j^{(m-1)}}{\sigma_j^m} \right| /_{NE} \leq \epsilon \quad (34)$$

The prescribed convergence parameter ϵ has to be decided depending on the shape of the ship (here the default value of $\epsilon = 1.0E - 04$ is used) and the number of iterations needed is between 3 and 5.

The iteration method has its own feature of numerical efficiency. Only one determination of the inverse matrix A^{-1} for each subproblem is required and the perturbed source strength $\sigma(\gamma + \Delta\gamma)$ for each design variable can easily be calculated by changing the right-hand side only in eq (25). A filtering routine is introduced, so that smaller perturbed elements than 20% of

$$R_W = 4\pi \sum_{NH+1}^{NE} u_{Bi} \sigma_i S_i \quad (26)$$

Here u_{Bi} is the X component of induced velocity at the free surface panel by sources distributed on the hull and its image surfaces. This can be calculated from

$$u_{Bi} = \sum_{j=1}^{NH} X_{ij} \sigma_j \quad (27)$$

where X_{ij} is the X-wise velocity component induced at the control point on the i-th free surface panel by a unit source density at the control point of the j-th hull surface panel.

Then it can be shown that

$$\frac{dR_W}{d\gamma} = 4\pi \sum_{NH+1}^{NE} \left(\frac{\partial u_{Bi}}{\partial \gamma} \sigma_i S_i + u_{Bi} S_i \frac{\partial \sigma_i}{\partial \gamma} + u_{Bi} \sigma_i \frac{\partial S_i}{\partial \gamma} \right) \quad (28)$$

$$\frac{\partial u_{Bi}}{\partial \gamma} = \sum_{j=1}^{NH} \left(\frac{\partial X_{ij}}{\partial \gamma} \sigma_j + X_{ij} \frac{\partial \sigma_j}{\partial \gamma} \right) \quad (29)$$

The terms $\frac{\partial X_{ij}}{\partial \gamma}$ and $\frac{\partial S_i}{\partial \gamma}$ can easily be estimated from the finite difference

$$\begin{aligned} \frac{\partial X_{ij}}{\partial \gamma} &= \frac{X_{ij}(\gamma + \Delta\gamma) - X_{ij}(\gamma)}{\Delta\gamma} \\ \frac{\partial S_i}{\partial \gamma} &= \frac{S_i(\gamma + \Delta\gamma) - S_i(\gamma)}{\Delta\gamma} \end{aligned} \quad (30)$$

$$\left[\begin{array}{ccc|c} & & & \\ & & & \\ & & & \\ A_{ij} & & & \\ & & & \end{array} \right] \quad \left\{ \sigma_j \right\} = \left\{ B_i \right\} \quad (25)$$

In the numerical computations, the velocity influence coefficients A_{ij} have to be calculated accurately and inverted directly. The required number of induced velocity coefficient calculations due to only one disturbed node point can be up to $8 \times NE - 4^2$ as shown in (25). The number of disturbed panel elements (or node points) due to a small increment of the design variable $\Delta\gamma$ is almost the same as the total number of panel elements (or node points) within the surface, on which the point supported by the master design variable is located. This number can easily be increased up to the total number of panel elements if the design variable is supported on the common point between several surfaces.

This calculation procedure remains quite expensive and takes up to 95% of the total computation costs for larger numbers of panel elements than 800. Therefore, this direct approach becomes uneconomical when the wave resistance gradient is to be examined for all master design variables.

In the following it is described how the gradient of wave resistance can be effectively and quasi-analytically estimated. The wave resistance can be written in summation form

The optimization algorithms in this chapter are implemented in ALIBABA [33] which requires one evaluation of the objective and constraint functions and their gradients for each subproblem.

III-4. Sensitivity Analysis

1. Gradient of the Objective Function

The optimization algorithm described in the previous section requires an accurate evaluation of the gradient of the objective function R_T with respect to design variables. This can be derived analytically

$$\frac{dR_T}{d\gamma} = \frac{dR_V}{d\gamma} + \frac{dR_W}{d\gamma} \quad (23)$$

The gradient of viscous resistance is usually easily obtained by numerical differentiation

$$\frac{dR_V}{d\gamma} = \frac{R_V(\gamma + \Delta\gamma) - R_V(\gamma)}{\Delta\gamma} \quad (24)$$

On the other hand, a direct numerical differentiation for the wave resistance gradient is not usable in practice because it requires a large number of induced velocity coefficient calculations and the linear solution of a large system of equations. In the panel method used here, the source strength σ at every control point has to be solved first to determine the wave resistance. The source strength $\{\sigma\}$ is related to the boundary vector $\{B\}$ through the velocity influence coefficient matrix $[A]$

L is separable which implies

$$L(\gamma, \lambda) = \sum_j L_j(\gamma_j, \lambda) \quad (18)$$

The minimization of the Lagrangian function can be obtained from:

$$\frac{\partial L_j(\gamma_j, \lambda)}{\partial \gamma_j} = 0 \Rightarrow \gamma_j = \gamma_j(\lambda) \quad j=1, ND \quad (19)$$

The resulting equations are uncoupled, due to the separability, and of second degree which implies that γ_j can be expressed explicitly by the Lagrangian multipliers.

Let $\psi(\lambda) = L(\gamma(\lambda), \lambda)$. It can be shown that $\psi(\lambda)$ is concave.
is found from the solution of the dual problem D.

$$\begin{aligned} D: \quad & \max_{\lambda} \psi(\lambda) \\ & \text{subject to } \lambda_j \geq 0 \end{aligned} \quad (20)$$

D can be solved by an arbitrary method for unconstrained maximization, for instance the quasi-Newton method [32], which OASIS [36] uses. The method has to be modified to handle the simple non-negative constraints on λ . It should be noticed that the value of the dual function is equal to the value of the objective function at optimum, i e:

$$\max \psi(\lambda) = \min R_T(\gamma) \quad (21)$$

Min $L(\gamma, \lambda)$ implies:

$$\nabla R_T(\gamma) + \sum_i \lambda_i \nabla \tilde{g}_i(k) = 0 \quad (22)$$

which is the Kuhn Tucker condition for optimum, see Fig 5.

Subject to

$$\tilde{g}(\gamma) = g_i^{(k)}$$

$$- \sum \left(\frac{\partial g_i}{\partial \gamma_j} \right)^{(k)} (\gamma_j^{(k)} - L_j^{(k)})^2 \left[\frac{1}{(\gamma_j^{(k)} - L_j^{(k)})} - \frac{1}{(\gamma_j^{(k)} - L_j^{(k)})} \right]$$

$$+ \sum \left(\frac{\partial g_i}{\partial \gamma_j} \right)^{(k)} (U_j^{(k)} - \gamma_j^{(k)})^2 \left[\frac{1}{(U_j^{(k)} - \gamma_j^{(k)})} - \frac{1}{(U_j^{(k)} - \gamma_j^{(k)})} \right] \leq \bar{g}_i$$

$$\underline{\gamma}_j \leq \gamma_j \leq \bar{\gamma}_j \quad i = 1, NC, \quad j = 1, ND$$

in which \sum and \sum stand for the summation of those terms for which the gradients $(\partial R_T / \partial \gamma_j)$, $(\partial g_i / \partial \gamma_j)$ are negative and positive respectively.

The approximated subproblem $\tilde{p}^{(k)}$ is explicit, convex and separable, so this may be solved by using dual methods of mathematical programming [30,31].

The Lagrangian function corresponding to $\tilde{p}^{(k)}$ is given by

$$L(\gamma, \lambda) = R_T(\gamma) + \sum_i \lambda_i (g_i(\gamma) - \bar{g}_i) \quad \lambda_i \geq 0 \quad (16)$$

The solution of $\tilde{p}^{(k)}$ is obtained from

$$\max_{\lambda} (\min_{\gamma} L(\gamma, \lambda)) \quad (17)$$

In the present calculation, a strictly convex approximate subproblem $\tilde{P}^{(k)}$ is generated in each step of the iterative process based on Method of Moving Asymptots (MMA) [29], and solved using dual techniques. Generally, it is a very effective method where each iteration consists of two steps. The first step is the creation of the convex subproblem $\tilde{P}^{(k)}$ formed by a first order approximation of the objective function and the constraints at the preceding design point. The second step is the determination of the optimum design point by solving the subproblem using the duality theory for convex programming. The creation of $\tilde{P}^{(k)}$ requires one evaluation of the objective and constraint functions and their gradients.

In the MMA approximation, both the objective function R_T and the constraints g_i are linearly approximated by a first order Taylor series expansion in variables of the type $1/(\gamma_j - L_j)$ or $1/(U_j - \gamma_j)$ depend on the signs of the derivatives of R_T (or g_i) around the preceding design point, where L_j and U_j are the lower and upper asymptotes to γ_j , and γ_j will always lie somewhere in between.

By this approach, the original non-linear problem P is now reduced to a sequence of approximate subproblems $\tilde{P}^{(k)}$ which is given by

$$\begin{aligned} \tilde{P}^{(k)} : \quad \text{Min } \tilde{R}_T(\gamma) = R_T^{(k)} \\ - \sum \left(\frac{\partial R_T}{\partial \gamma_j} \right)^{(k)} (\gamma_j^{(k)} - L_j^{(k)})^2 \left[\frac{1}{(\gamma_j - L_j^{(k)})} - \frac{1}{(\gamma_j^{(k)} - L_j^{(k)})} \right] \\ + \sum \left(\frac{\partial R_T}{\partial \gamma_j} \right)^{(k)} (U_j^{(k)} - \gamma_j^{(k)})^2 \left[\frac{1}{(U_j^{(k)} - \gamma_j)} - \frac{1}{(U_j^{(k)} - \gamma_j^{(k)})} \right] \end{aligned} \quad (15)$$

require an accurate evaluation, at each iteration, of the objective and constraint functions and their gradients. These evaluations are very expensive as each evaluation involves a flow calculation which leads to the solution of a large system of linear equations.

Therefore, an alternative method [28] based on a sequence of linearized problems has frequently been used. In this technique, the minimization starts at an arbitrary initial design point and proceeds until a convergence criterion is met. Moreover both the objective function R_T and the constraints g_i are approximated by a first order Taylor expansion around the preceding design point $\gamma^{(k)}$:

$$\tilde{P}^{(k)} : \min \tilde{R}_T(\gamma) = R_T^{(k)} + \sum_{j=1}^{ND} \left(\frac{\partial R_T}{\partial \gamma_j} \right)^{(k)} (\gamma_j - \gamma_j^k)$$

Subject to

(14)

$$\tilde{g}_i(\gamma) = g_i^{(k)} + \sum \left(\frac{\partial g_i}{\partial \gamma_j} \right)^{(k)} (\gamma_j - \gamma_j^k) \leq \bar{g}_i \quad i = 1, NC$$

$$\underline{\gamma}_j \leq \gamma_j \leq \bar{\gamma}_j \quad j = 1, ND$$

By this approach, the original non-linear optimization problem is reduced to a sequence of linear subproblems, see Fig 4. In Fig 4a the objective function $\tilde{R}_T(\gamma)$ is now linear and the approximated subproblem $\tilde{P}^{(k)}$ is marked by a dashed line and its solution is $\gamma^{(k+1)}$. The procedure is repeated but now around $\gamma^{(k+1)}$ in Fig 4b. The new solution is $\gamma^{(k+2)}$ and the solution $\gamma^{(k)}$, $\gamma^{(k+1)}$ and $\gamma^{(k+2)}$ is moving closer to the optimum of the original problem P.

This is a regular linear programming (LP) problem which can be solved by using the Simplex method [32]. The sequence of linear approximations, however, may result in an unstable convergence.

No higher order effects are taken into account and the pressure distribution at the boundary layer edge is assumed to be the same as the distribution at the hull surface.

In the present calculation, the viscous resistance is calculated by computing the momentum loss in the far wake. This momentum area can be determined either from the continuation of the boundary layer calculation along a streamline extending to the wake region or from the Squire & Young method [26, 27]. Applying the Squire & Young formula, and extending it to three-dimensional boundary layer flow, the momentum thickness θ_{11} in the far wake may be given by:

$$\theta_{11\infty} = \theta_{11t} \cdot \left\{ \frac{U_e}{U_\infty} \right\}^{(H_{12}+5)/2} \quad (12)$$

where θ_{11t} represents the momentum thickness at the trailing edge. H_{12} is the shape factor for the velocity profile. U_e and U_∞ denote mean velocity components at the boundary layer edge and freestream velocity respectively.

The integration of equation (12) over the girth of a cross section therefore gives the resistance due to the momentum loss which is accumulated in the upstream portion of the body.

$$R_V = \rho U_\infty^2 \int \theta_{11\infty} dq \quad (13)$$

III-3. Optimization Method

In principle, the present optimization problem can be solved using a standard mathematical optimization algorithm with possible gradients estimated numerically. But such a procedure (for instance, an iterative mathematical programming method) can be expected to be fairly computer-time consuming, because it will

panels and required computing time (usually CPU time is proportional to third power of number of panels) seem to be possible in this approach.

Other advantages when compared to the original Dawson method are that a more convenient body-fitted grid on the free surface, which is independent of the double model streamlines, is introduced to improve the solution accuracy particularly at the end of the hull.

A momentum approach is employed to improve the numerical accuracy of the resistance calculation.

$$R_W = - \rho \int_{S_{FC}} U_B W_F \, dS \quad (11)$$

U_B and W_F are X and Z components of the induced velocity at the free surface panel by hull sources and free surface sources respectively. The integration domain S_{FC} is the part of the free surface covered by source panels.

In principle the free surface panel distribution should be extended over the entire region where there are significant waves. A limited region of free surface panels is only considered in the present calculation due to computer storage limitations.

2. Viscous Resistance

The first order integral type boundary layer method based on that described in reference [23] has been used to predict a viscous resistance component for the candidate hull in the optimization routine.

The first order boundary layer equations expressed in a streamline coordinate system together with empirical correlations are solved by the Runge-Kutta-Gill procedure along streamlines.

To avoid these difficulties, the total resistance is taken as a linear combination of wave and viscous resistance

$$(R_V = R_F + R_{VP}).$$

$$R_T = R_V + R_W \quad (10)$$

The first order boundary layer method and the linear wave resistance theory have been applied to predict the resistance components of ships. Quantitative prediction of ship resistance by these linear type methods may not be completely satisfactory due to the assumptions and simplifications involved. However, they are accurate enough to predict differences due to a small change of hull form and can therefore provide useful qualitative information regarding hull form improvement in the optimization procedure.

1. Wave Resistance

The linear higher order panel method based on that described in reference [24] has been used to predict a wave resistance component for the candidate hull in the optimization routine.

The hull surface and part of the free surface are imagined to be covered by a number of small panels with distributions of source singularities and the variable strengths of these distributions are adjusted to satisfy the boundary conditions. An exact boundary condition is satisfied on the hull while on the free surface the boundary condition is linearized with respect to the double model solution.

This method contains desirable features for the application to optimal hull form design compared to other methods of the same kind. In contrast to a first order panel method which uses flat panel usually with constant source density, the present method make use of parabolic panels with a linear variation of the source strength. A considerable reduction in the number of hull

III-2. Hydrodynamic Performance Prediction

The objective function in the present problem is the total resistance of the ship. The ship resistance in still water is made up of two major components, namely skin friction resistance R_F and pressure resistance R_P .

$$R_T = R_F + R_P \quad (8)$$

The pressure resistance mainly depends on the hull shape, while the skin friction is not sensitive to change of hull form but is proportional to the wetted surface area. Therefore a substantial reduction of the total resistance can only be achieved by reducing the pressure resistance. The pressure resistance may be further subdivided into components of viscous pressure resistance R_{VP} and wave resistance R_W

$$R_P = R_{VP} + R_W \quad (9)$$

For fine high speed ships, the wave resistance component dominates in the pressure resistance, while the viscous resistance dominates for full low speed ships.

The frictional and pressure resistance can be obtained directly from the hydrodynamic analysis by integrating skin friction and pressure all over the hull surface.

This gives fair predictions for the tangential force. The difficult part, however, is the estimation of viscous pressure drag. Separately this is calculated by allowing for the displacement effect of the boundary layer on the pressure distribution. This is difficult to do accurately because in the region very close to the stern, the accuracy of the pressure distribution becomes less reliable and such an estimation is very sensitive to small errors in the stern region.

Fig 3 shows how a variation of master variable γ_j influence the internal node points of the whole surfaces. Due to a small variation of master variable γ_j , the governing point $P_O(X_{Op}, Y_{Op}, Z_{Op})$ moved to $P(X_p, Y_p, Z_p)$ which coordinate is

$$\begin{aligned} X_p &= X_{Op} + a_x \gamma_j \\ Y_p &= Y_{Op} + a_y \gamma_j \\ Z_p &= Z_{Op} + a_z \gamma_j \end{aligned} \quad (4)$$

where a_x , a_y and a_z are linking factors to the coordinate of the point.

The coordinate of a point $Q(X_q, Y_q, Z_q)$ where a slave variable r is assigned, is calculated in a similar way.

$$\begin{aligned} X_q &= X_{Oq} + \beta_{xj} \gamma_j \\ Y_q &= Y_{Oq} + \beta_{yj} \gamma_j \\ Z_q &= Z_{Oq} + \beta_{zj} \gamma_j \end{aligned} \quad (5)$$

Then all internal node points variation can be calculated by defined interpolation functions such as straight lines, circular arcs, splines etc. within this restricted definition. It then follows that a variation of a master design variable γ_j causes a variation of all internal node points within the surface

$$\gamma_j + \Delta\gamma_j \Rightarrow r + \Delta r \quad (6)$$

This can be related in following equation

$$\frac{\partial r}{\partial \gamma_j} = \frac{\Delta r}{\Delta \gamma_j} \quad (7)$$

Once the hull surface is defined, hydrostatic quantities such as wetted surface area, displaced volume and center of buoyancy are calculated using the surface mesh described above.

With all different sets of body types defined, a geometry modelling of SSPA Ro-Ro ship with large bulb is made in Fig. 2 using ALADDIN to illustrate some of the versatility of the system. Since the shape of the upper hull above the waterline does not influence the hydrodynamic performance, the only starboard side of the wetted hull surface is modelled assuming symmetry about the centerplane. The hull surface is divided into five sections and each section is described with lofted surfaces. A simple fairing algorithm is used to connect two surfaces smoothly according to the specified fairing parameter (slope) by the designer. These four figures presented in Fig 2 demonstrate the flexibility of the fairing method used to connect the surfaces, particularly the bulb and fore hull surface.

This indicated that the disturbances due to change of design variable are to be confined to its own surface. This is one of the essential features of ALADDIN in connection with optimization. Another advantage is that an inverse routine for obtaining initial design variables from given geometric input data is not required in ALADDIN. The initial values of design variable are specified as zero and used to make corrections in the geometry without changing the coordinates.

The design variables are assigned to governing points and they affect the coordinates of the points. There are two types of design variables, namely master variables and slave variables. Master variables are used as main shape variation purpose while slave variables are linearly dependent on master variables and are used to reduce the number of master variables needed for a proper modelling. The slave variables r are connected with master variables according to the following principle:

$$r = r_0 + \sum \beta_k \gamma_k \quad (3)$$

where r_0 is original value and β_k is linking factor for master variable γ_k .

representation. These are also the most difficult tasks in general, since a ship hull is a complicated non-developable surface. Most existing commercial purpose ships have a bulbous bow, a flat bottom and a sharply curved stern section shape. Therefore, the hull surface generation method must be sufficiently general to allow these various features to be represented in the hull form design process.

In the Optimum Hull Form Design System the geometric definition of the hull form is represented by the interlinked program ALADDIN [25]. ALADDIN is a general three-dimensional preprocessor for creating input data to the optimum hull form design system. In ALADDIN the hull geometry is defined by a set of bodies of different types (points, lines, combined lines and surfaces). A set of governing points is a basic element in geometric modelling and directly linked to shape design variables. The lines are defined by a set of points and tangent vectors. Several different types of lines are used depending on which part of hull surface that is supposed to be generated. For more details see Ref [35].

- straight line in parallel middle body
- circle defined by three or four points in bilge keel area
- parabola defined by three points
- Ferguson spline defined by 0-2 tangent vectors and 2-9 points
- Bezier spline defined by 2-14 points

Three kinds of surfaces are used in ALADDIN. These are a four-sided Coon's surface, a three-sided Coon's surface and a four-sided lofted surface. On a Coon's surface (edge surface) the interior geometry is defined by the edge of the surface. The curvature of the surface will adjust to the angles and elevation of the edges. The lofted surface is used when the interior of the surface cannot be described by the edge line alone. By defining interior lines, the interior geometry becomes controlled by them, making it possible to define doubly curved surfaces.

III. OPTIMAL HULL FORM DESIGN PROCEDURE

The minimization problem formulated in the previous section can conveniently and efficiently be solved by using a mathematical programming method, where the optimality condition for the problem is solved directly through an iterative scheme. The optimization starts at an arbitrary initial design estimate which can be one of the best existing ships selected from a hull form data base. The geometry of the initial hull form is modelled mathematically with a number of design variables and exposed to uniform onset flow at design speed. A systematic evaluation of hydrodynamic performance characteristics is performed as a function of the hull geometry. Then the numerical form of Eq (2) is obtained at each iteration and used to compute new design variables. The new design variables are determined in order to minimize the total resistance of the ship subject to a number of geometrical constraints. This iteration procedure is repeated until a convergence criterion is met and an optimum hull form is finally obtained through a systematic variation of the shape by changing the design variables.

This optimum Hull Form Design System includes a comprehensive computer program module for the evaluation of the hydrodynamic performance characteristics and the important sensitivity analysis is mainly based on numerical derivatives of the resistance and the capability of the ship geometry modelling and optimization procedure. This design procedure is illustrated in Fig 1 and will be described in the following subsections.

III-1. Mathematical Modelling of Hull Geometry

A proper definition of the hull surface is one of the most important tasks in hull form design since most of the hydrodynamic performance prediction methods require a detailed surface geometry description and the accuracy of the numerical predictions is greatly dependent on the ability of hull surface

$$\nabla R_T + \sum_i \lambda_i \nabla g_i = 0$$

$$\lambda_i (g_i - \bar{g}_i) = 0 \quad i = 1, NC \quad (2)$$

$$\lambda_i \geq 0$$

∇R_T and ∇g_i are the gradients of R_T and g_i in a design point γ_j . The KT criterion is based on the assumption that at optimum the gradient of the objective function is a linear combination of the active constraint gradients. Active are those constraints for which $g_i = 0$. λ_i are the Lagrange multipliers.

Mathematically these ND+NC optimality conditions must be solved for ND unknown design variables and NC unknown Lagrange multipliers. However, it is difficult to solve directly, since this set of equations is implicit, highly nonlinear and a non-negative value is required for the Lagrange multiplier in the solution. An iterative approach has to be employed and the details of the solution procedure will be described in the following sections.

II. MATHEMATICAL FORMULATION OF THE PROBLEM

The mathematical formulation of the present design oriented problem which finds an optimum shape of the ship with a minimum resistance subject to geometric constraints can be expressed as

$$\begin{array}{llll}
 P : & \text{Find} & \gamma^* \in R^n & \\
 & \text{Minimize} & R_T(\gamma_j) & j = 1, ND \\
 & \text{Subject to} & g_i(\gamma_j) \leq \bar{g}_i & i = 1, NC
 \end{array} \quad (1)$$

Where γ^* is a vector representation of ND design variables defining the hull surface and hull form characteristics. The total ship resistance, which includes the wave and/or viscous resistance component, is used as an objective function R_T . The geometrical and practical design constraints about the hull are contained in $g_i(\gamma_j)$. NC is the number of constraints and \bar{g}_i are their upper bounds.

P is a nonlinear optimization problem since the objective function R_T and the constraints g_i are implicit, non-linear functions of the design variable γ_j . P is in many cases non-convex and has often multiple minima. In fact, there is no general reliable optimization method available to find a global minimum and no general agreement on the best approach to solve non-linear multivariable constrained problems. A method that works well on one problem may perform very poorly on another problem of the same kind.

In the present paper the optimization problem is solved by the general optimization code ALIBABA which uses the dual technique of mathematical programming. The mathematical programming method is based on the Kuhn Tucker (KT) criterion which states that at optimum the following conditions are satisfied:

problem and is solved using the dual technique of mathematical programming.

The derivatives needed to get the first order approximation (a Taylor series expansion) can be estimated numerically as differences obtained by recalculation or by a quasi-analytically based procedure.

The optimum values of the design variables are determined so as to minimize the total resistance of the ship, subject to a number of geometrical constraints, and an optimum hull form is obtained through a systematic variation of the shape by changing the design variables.

The entire process of hydrodynamic analysis, geometrical modelling, design and optimization has thus attempted to imitate the traditional hull form design procedure.

This system of computer programs has been tested to develop an optimized hull forms for two relatively simple design test cases. As a first example, the method was applied to design an optimal bow shape of a Ro-Ro ship by minimizing the wave resistance. This design study was performed using the SSPA Ro-Ro ship model 2062 with a large bulb as the reference hull form. As a more practical design example for the total resistance minimization an attempt was made to optimize the entire hull form starting from the Wigley hull. The present study had to be rather restricted due to computer speed and core memory size limitations, but the results indicate that the method can be used to develop mathematically faired and hydrodynamically desirable hull forms for more commercial types of ships starting from an existing ship.

on. Thus hull form optimization must compromise with other design features that it faces in order that the total design will meet its optimization goal. This kind of integrated system has not yet been developed, however.

In the present paper a numerical method for the design of optimized hull forms with respect to the total resistance is developed by integrating a numerical hydrodynamic prediction method with an optimization procedure. The interactive system enables the designer to include advanced hydrodynamic performance predictions at an early stage of the design process, allowing a systematic evaluation of hydrodynamic performance characteristics as a function of the hull geometry. This system of computer programs is based on a synthesis of hydrodynamics (WAVCAL, VISCAL), sensitivity analysis (GRADFC), geometrical modelling (ALADDIN) and optimization (ALIBABA).

In the geometry definition module, the hull surface is represented mathematically using a boundary variation technique as a function of the governing design variables, and the geometry description (for instance, panel mesh) and hydrostatic computations (wetted surface area, volume, etc) needed for the hydrodynamic predictions are generated. Then the hydrodynamic performance is estimated using a rapid design oriented first order boundary layer method [20] for viscous resistance and a linear type wave resistance method [21] in the hydrodynamic module.

Having all the numerical tools for geometrical definition and hydrodynamic analysis, a design procedure for an optimized hull form is developed. The optimized problem is very non-linear since the objective function and constraints are implicit and non-linear functions of the design variables. In order to solve this non-linear problem a series of convex separable subproblems is created using the method of Moving Asymptotes (MMA) [29]. Each subproblem is the first order approximation of the original

mathematical hull surface representation. Taylor D.W. in 1915 [16] mathematically generated the hull forms in his standard series, defining sectional area curve and design waterline by fifth-degree polynomials in accordance with form parameters, and experimentally investigated the systematic variations of resistance characteristic due to the change of form parameters and coefficients to find hydrodynamic optimization of hull forms.

Another origin based on theoretical approach can be referenced to Inui T. in 1957 [17]. In his work, based on Michell's thin ship approximation, an optimized hull form is obtained indirectly by determining the best polynomial singularity distributions in the ship centerplane to give a low wave resistance. Further investigations were made by Yim B. in 1963 [18]. In his work, the ship is represented as polynomial singularity distribution, and the doublet and quadruple distribution are also expressed in polynomials along the straight front perpendicular of the bow. Then optimum value of coefficients of the doublet and quadruple polynomials are determined under the condition that the bow wave resistance is minimum with a given ship polynomial.

More recently this goal has been pursued by numerous investigators. An attempt was made by Nagamatsu & Baba in 1983 [19] to minimize the viscous resistance of three-dimensional full form ships by means of the Hook and Jeeves direct search method. Other attempts to minimize the wave resistance were made by Min & Kim [20] and Suzuki & Maruo [21] using a similar type of direct search method with a penalty function technique. These methods suffer from some computational disadvantages and are not entirely efficient for non-linear multivariable constrained problems. Nowaki [22] applied mathematical optimization technique of non-linear programming type to minimum viscous drag design of hydrodynamic shapes of axisymmetric bodies.

In fact resistance minimization is only one aspect of the ship design in addition to propulsion, seakeeping, structure and so

I. INTRODUCTION

Traditionally the practical hull form design has been based on variation of existing hull forms, whose hydrodynamic characteristics are stored in a data base [1-5]. These methods may be adequate for the generation of the initial hull form at the conceptual design stage as long as the hull form variates lie within the limit of the data base. However, this traditional method has its own limitations in the application to practical hull form design due to the fact that most existing hull form data do not fully cover the design parameters and neither do they meet today's demand for fuel economy.

Today there exist numerical calculation methods capable of predicting the flow pattern and hydrodynamic performance of the ship hull. These methods are now used in many different stages of ship design. They are used for directing modifications of hull, as guidance for model testing, for calculation of scale effects and so on. These methods are the results of extensive work in the fields of computational fluid dynamics during the last 10 years. SSPA has developed a large number of computer programs to perform various ship design tasks as well as to analyse the hydrodynamic performance of ships. These include mainly boundary layer theory [6-9] and Navier-Stokes methods [10] for viscous flow and the linear [11, 12] and non-linear wave resistance methods [13, 14, 15].

Although the capabilities have been used in an individual manner for various research and commercial design purposes, their full potential within the context of a total design has until recently not been fully exploited.

Optimal hull form design procedures have been studied by many investigators, which can optimize the ship hull form taking part of the resistance into account. The resistance minimization can be traced back to the beginning of scientific developments in

α	Linking factor to governing point
β_k	Linking factor for master design variable γ_k
γ	Master design variable
λ	Lagrange multipliers
θ_{11}	Momentum thickness
$\theta_{11\infty}$	Momentum thickness in the far wake
θ_{11t}	Momentum thickness at the trailing edge
ϵ	Convergence parameter for sensitivity analysis
ϵ_1	Convergence tolerance for optimization procedure
ϵ_2	Convergence tolerance for optimization procedure
σ	Source density

LIST OF SYMBOLS

$[A], A_{ij}$	Coefficient matrix for the linear equation system
$\{B\}, B_i$	Right hand side vector for the linear equation system
F_n	Froude number
g_i, \bar{g}_i	Geometrical constraints and their upper bound
H_{12}	Shape factor for velocity profiles in boundary layer
L_j	Lower asymptotes for design variable
NC	Number of constraints
ND	Number of design variables
NE	Total number of panels
NF	Number of panels on the free surface
NH	Number of panels on the body
r	Slave design variable
R_F	Skin friction resistance
R_N	Reynolds number
R_P	Pressure resistance
R_T	Total resistance of ship
R_V	Viscous resistance
R_{VP}	Viscous pressure resistance
R_W	Wave resistance
S	Wetted surface area of ship
S_{FC}	Area of free surface covered by source panel
U_B	X component of the induced velocity at the free surface by hull source
U_e	x component of mean velocity at the boundary layer edge
U_j	Upper asymptotes for design variable
U_∞	Free stream velocity
V_H	Displacement volume of ship
W_F	Z component of the induced velocity at the free surface by free surface source
$[X], X_{ij}$	Matrices of induced velocities
X, Y, Z	Global reference co-ordinates
x, y, z	Local curvilinear orthogonal coordinates

LIST OF CONTENTS

	Page
ABSTRACT	D2
ACKNOWLEDGEMENTS	D3
LIST OF CONTENTS	D4
LIST OF SYMBOLS	D5
I. INTRODUCTION	D7
II. MATHEMATICAL FORMULATION OF THE PROBLEM	D11
III. OPTIMUM HULL FORM DESIGN PROCEDURE	D13
III-1. Mathematical Modelling of Hull Geometry	D13
III-2. Hydrodynamic Performance Prediction	D17
III-3. Optimization Method	D20
III-4. Sensitivity Analysis	D25
III-5. Convergence	D30
IV. OPTIMIZATION EXAMPLE	D32
IV-1. Sample Resistance Calculation	D32
IV-2. Optimal Bulb Design	D33
IV-3. Canoe Shape Optimization	D35
V. CONCLUDING REMARKS AND FUTURE WORK	D37
REFERENCES	D38
LIST OF FIGURES	D43

ACKNOWLEDGEMENTS

The authors wish to express their deep gratitude to Prof Lars Larsson, of the department of Marine Hydrodynamics, Chalmers University of Technology, Gothenburg and Prof Jan Bäcklund, Head of the Department of Aeronautical Structures and Materials, the Royal Institute of Technology, Stockholm, Sweden for their great interest and support.

The authors are also indebted to Dr Hans Groth for his help in the implementation of the VAX version of computer program on the FPS computer and to Mr Ingemar Sjörs for his translation of one of the important subroutines for solving nonsymmetric systems of large linear equations to the FPS computer.

The authors also wish to thank Mrs Barbara Karsberg, Mrs Elisabeth Algar, as well as Mrs Brita Svanberg who helped in plotting and typing the manuscript.

The project has been carried out in cooperation between SSPA Maritime Consulting AB, Gothenburg, and ALFGAM Optimizing AB, Stockholm, and has been sponsored by the Swedish Board for Technical Development.

ABSTRACT

A numerical method for the design of optimized hull forms with respect to the total resistance is presented. The main objective is to obtain an integrated computer system which will enable the designer to include advanced hydrodynamic performance predictions at an early stage of the design process allowing a systematic evaluation of hydrodynamic performance characteristics as a function of the hull geometry.

The Optimal Hull Form Design System (SINDBAD) contains four main modules. The first one generates a faired hull surface mathematically with a number of design variables, performs hydrostatic computations and generates geometry descriptions needed for the optimization process. The second and third modules compute total calm water resistance including viscous and wave resistance. The last module of the method produces a hull form of minimum resistance through a systematic variation of the shape by changing the design variables. The optimum values of the design variables are determined in order to minimize the total resistance of the ship subject to a number of geometrical constraints. The general optimization code ALIBABA, which is based on the dual technique of mathematical programming, is used to find an optimum hull form in combination with a shape description module ALADDIN.

This system of computer programs can be used to develop mathematically faired and hydrodynamically desirable hull forms starting from an existing ship. The method has been applied to the bow shape optimization of a fine-form, high speed ship and to the entire hull form optimization for a canoe type of vessel.

Footnote: The term "hydrodynamic performance" used in this paper identifies "resistance performance".

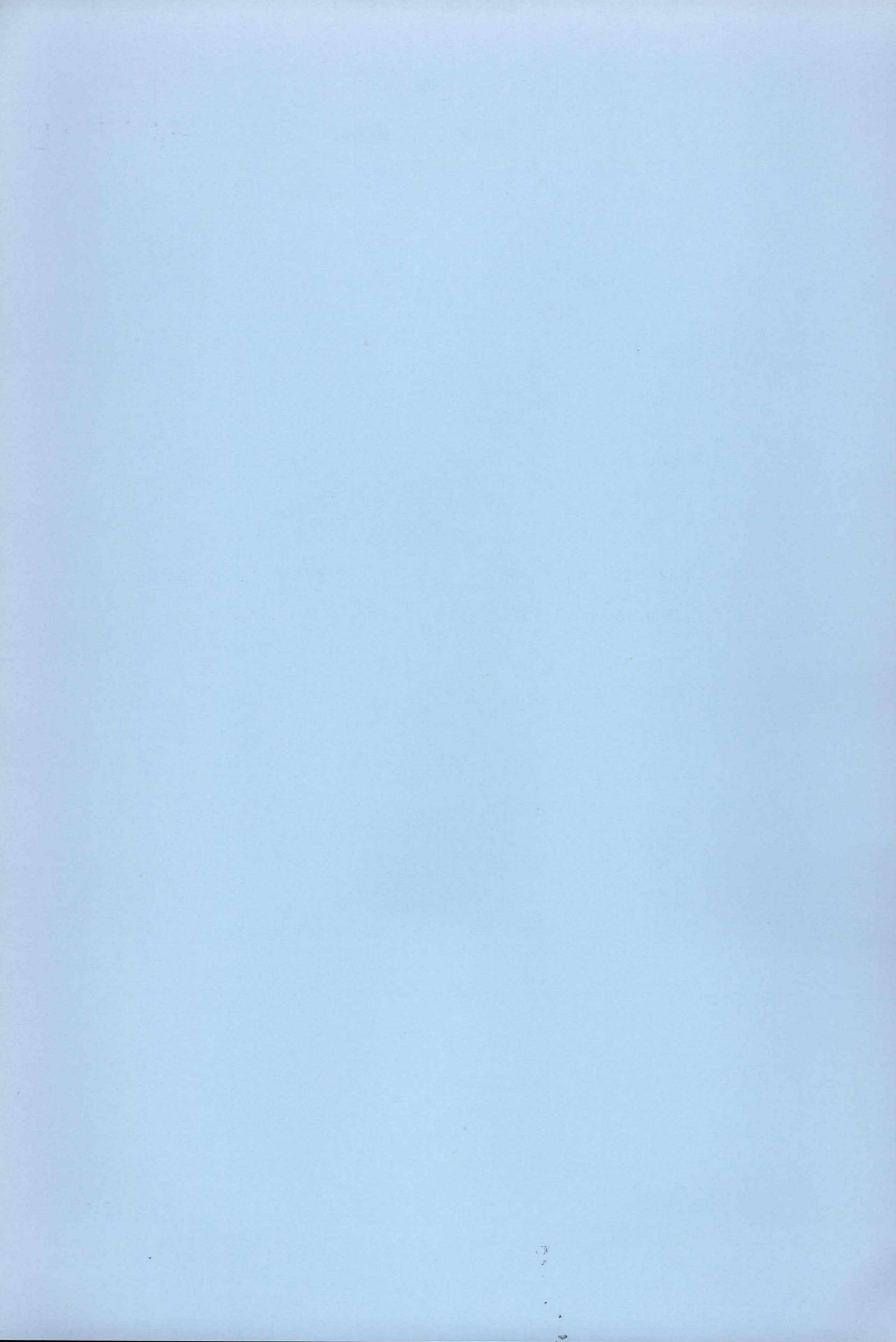
SSPA Report No 2964-1

A Numerical Method for Minimizing Ship Resistance

by

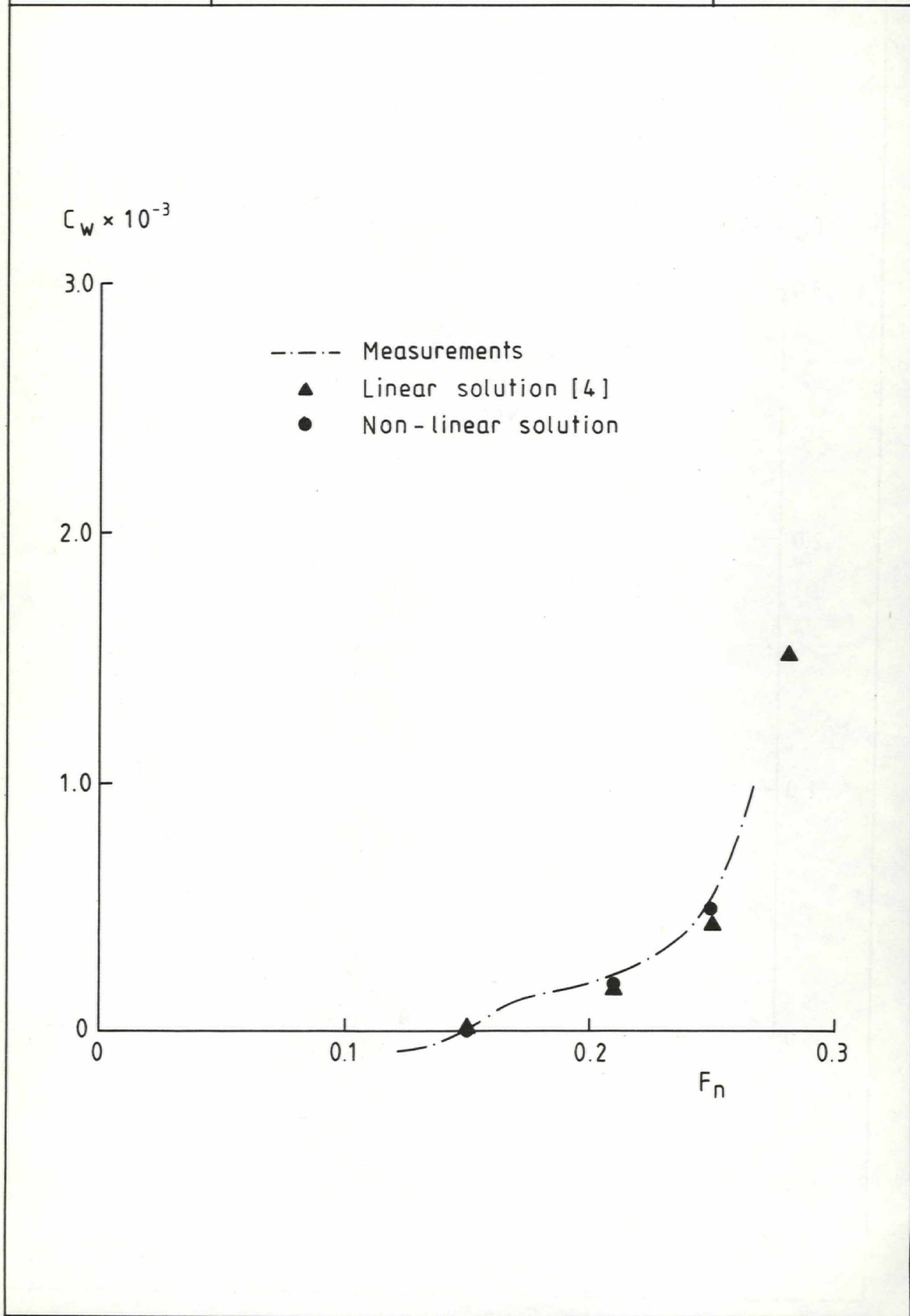
**Keun Jae Kim, SSPA Maritime Consulting AB, Gothenburg
Björn Esping, ALFGAM Optimizing AB, Stockholm
Dan Holm, ALFGAM Optimizing AB, Stockholm**

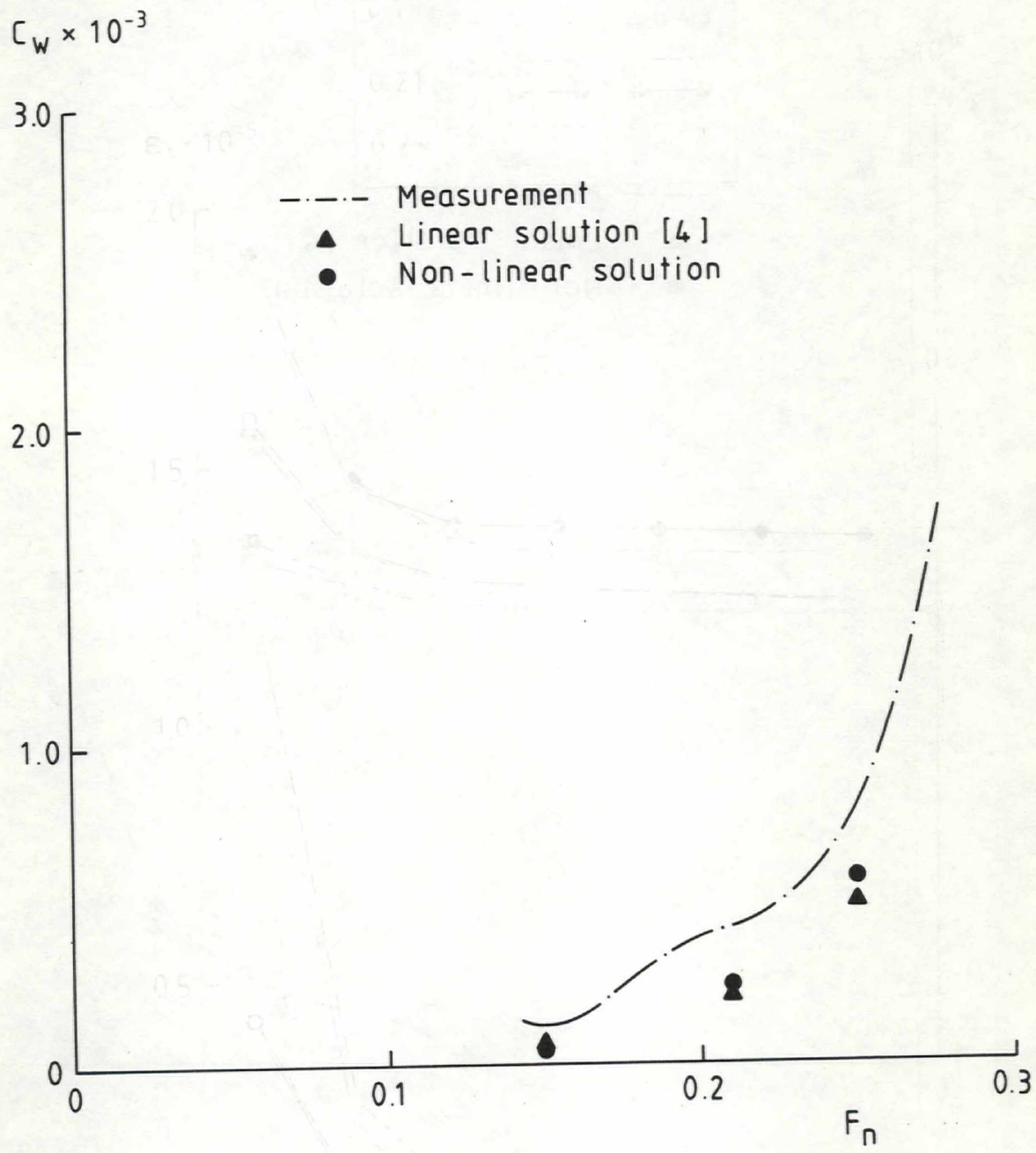
1989-08-08

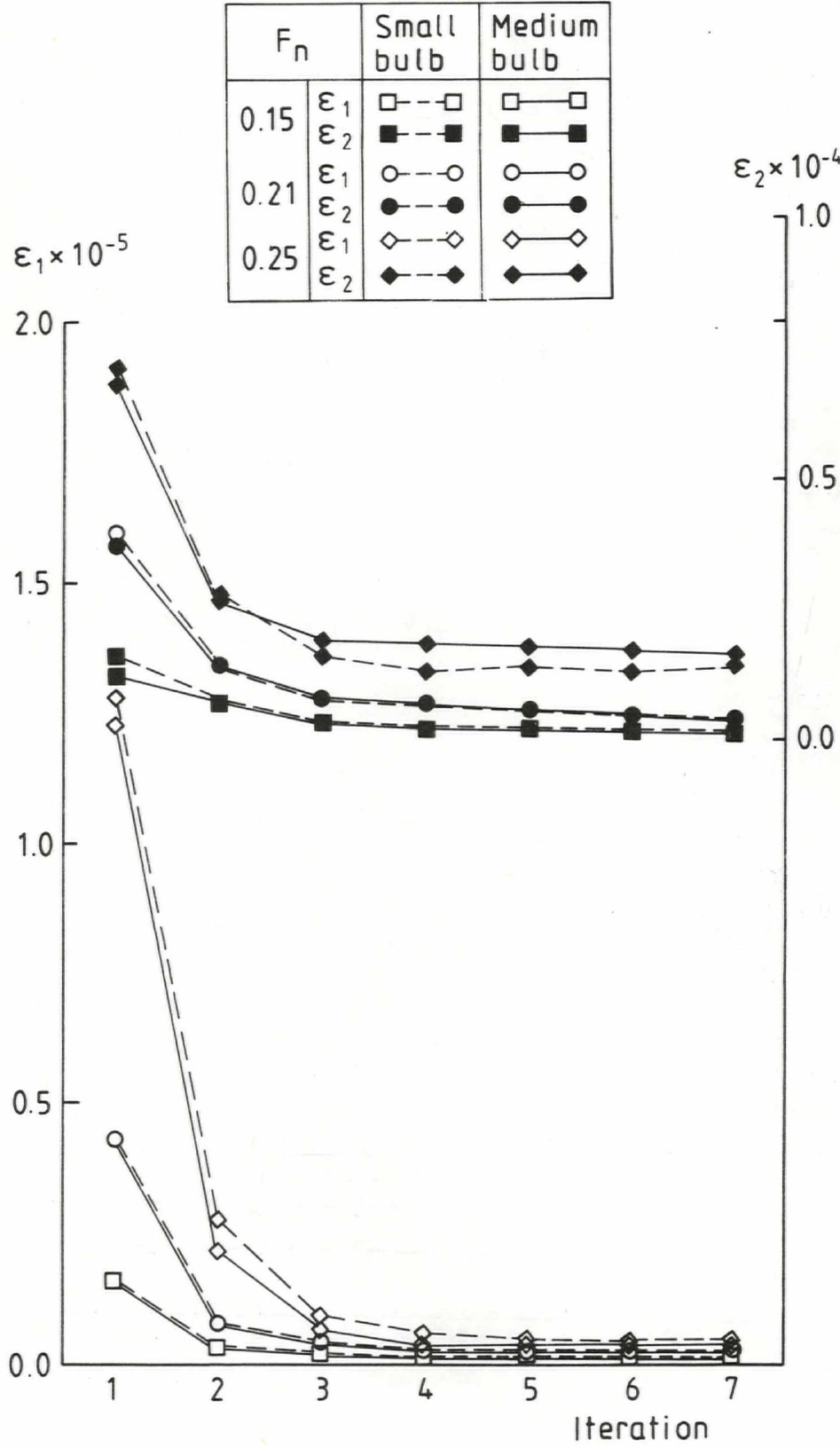


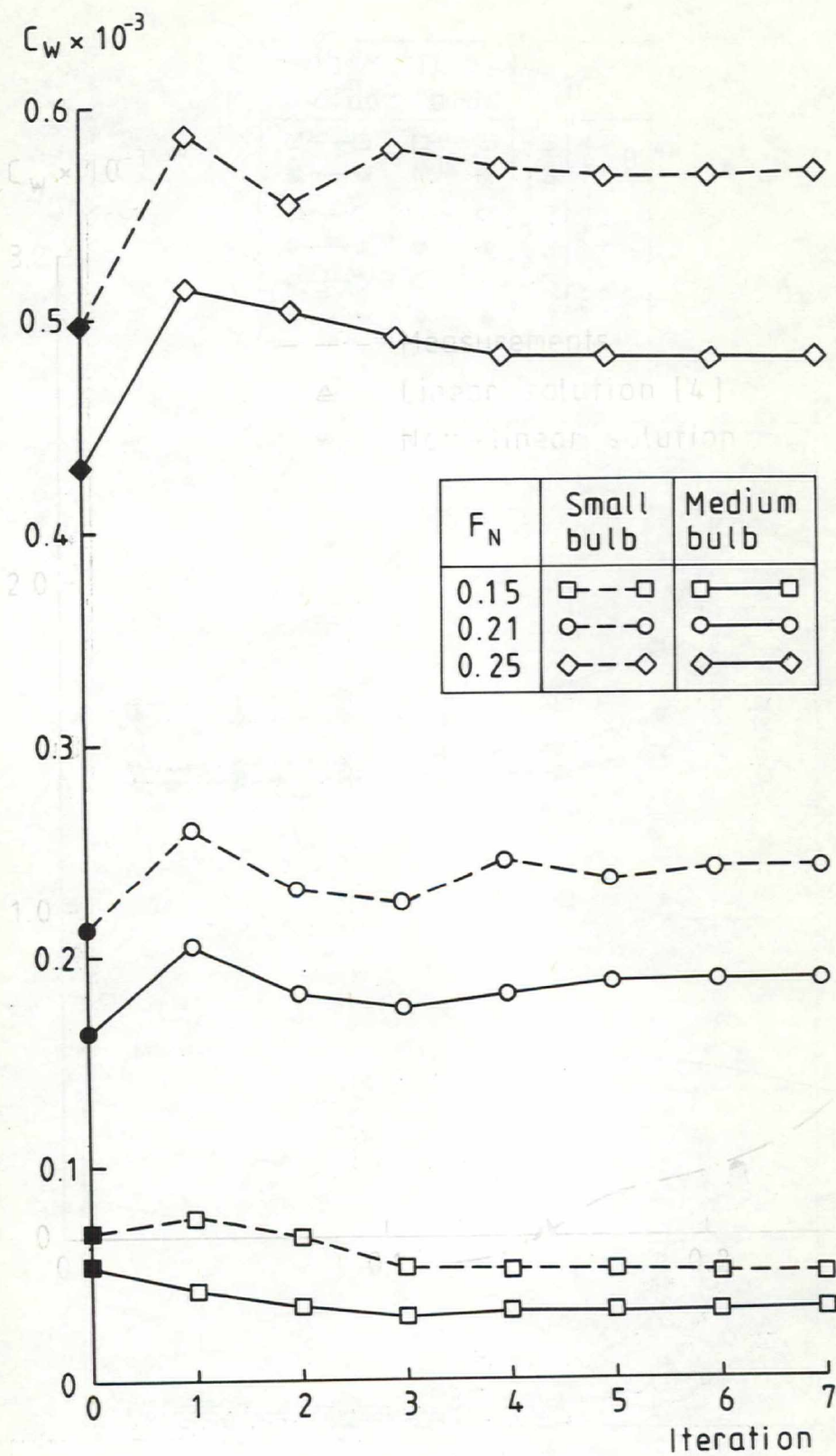
PAPER D

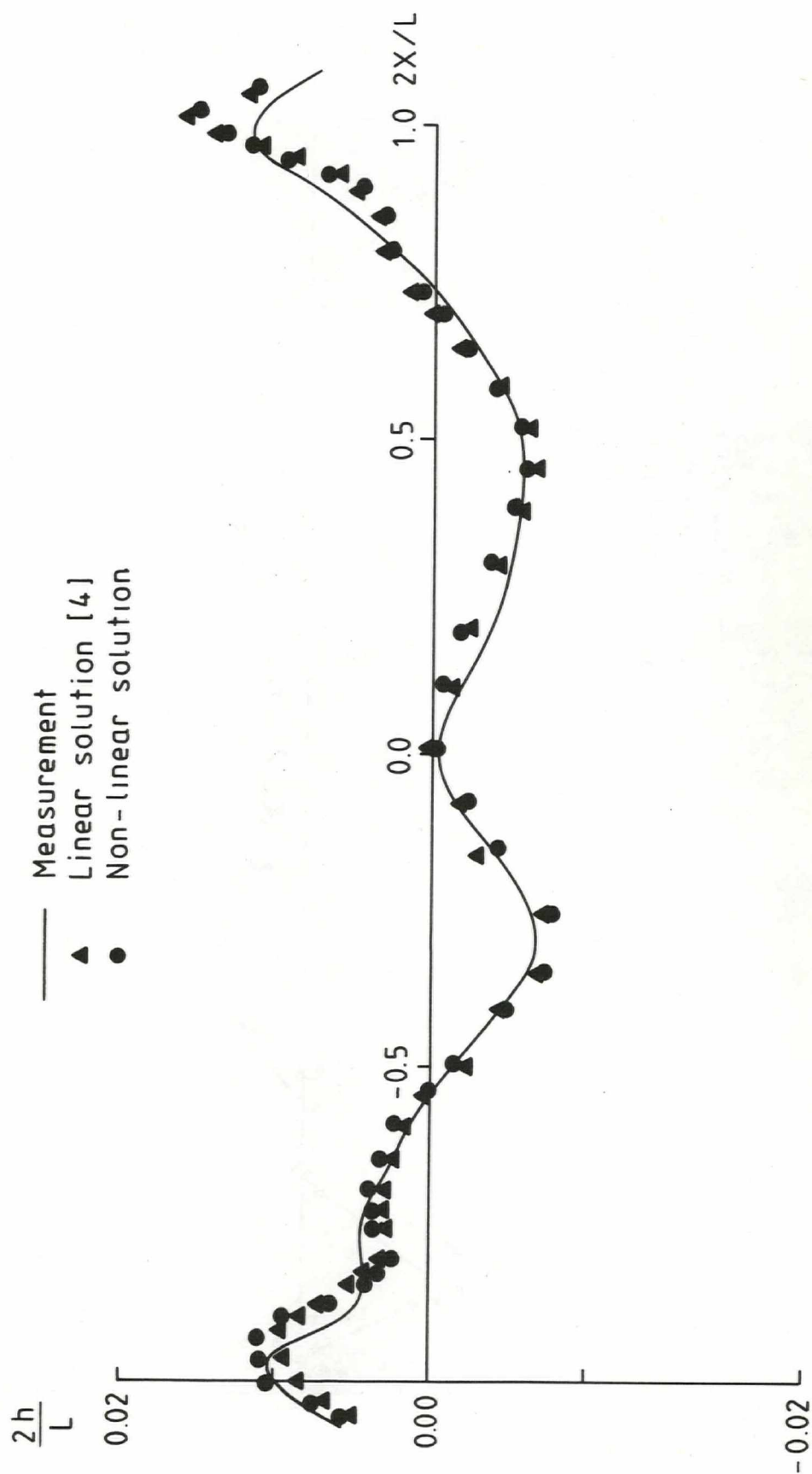
SSPA & CTH	Wave resistance the SSPA Ro-Ro ship (medium bulb)	FIG. 15

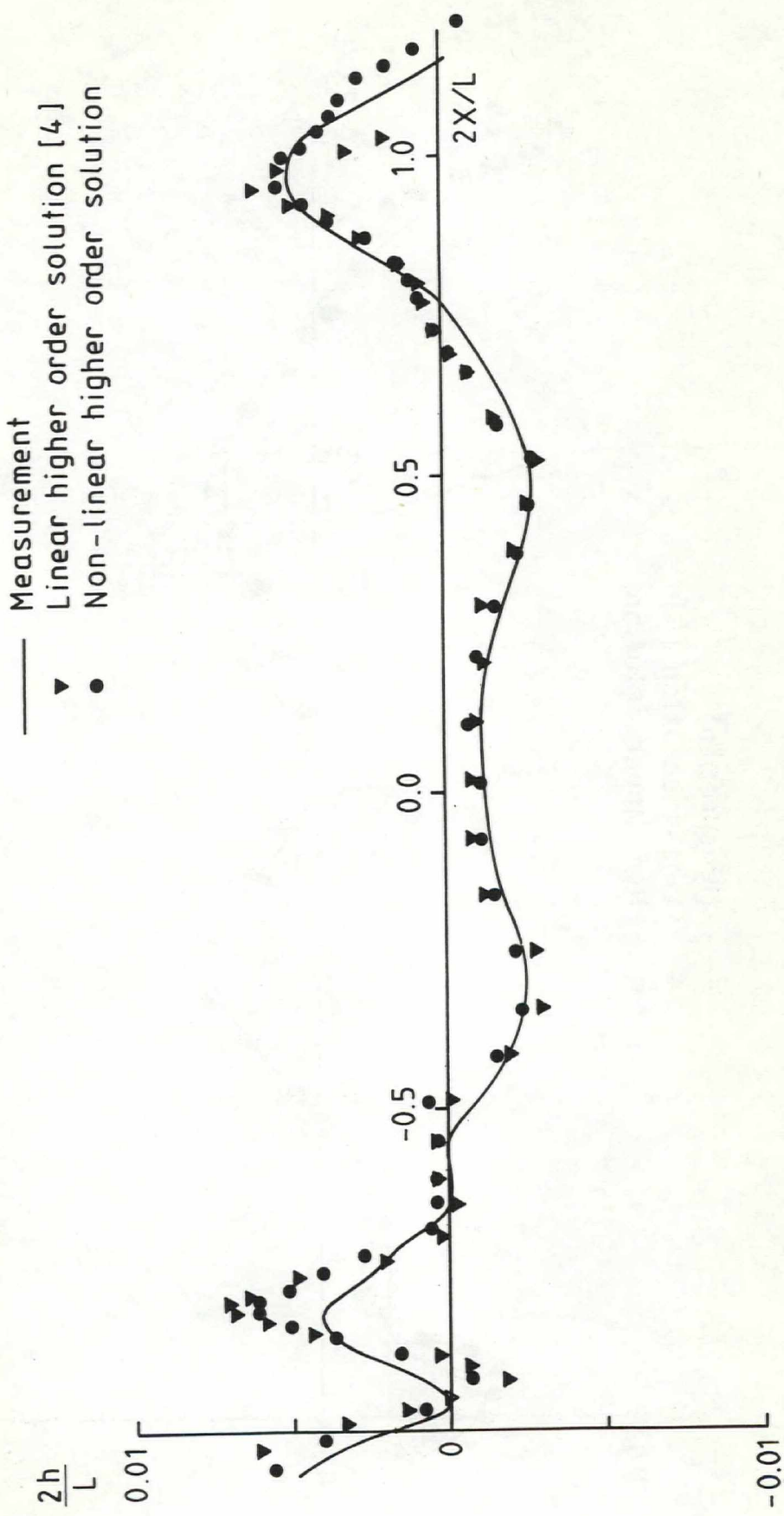


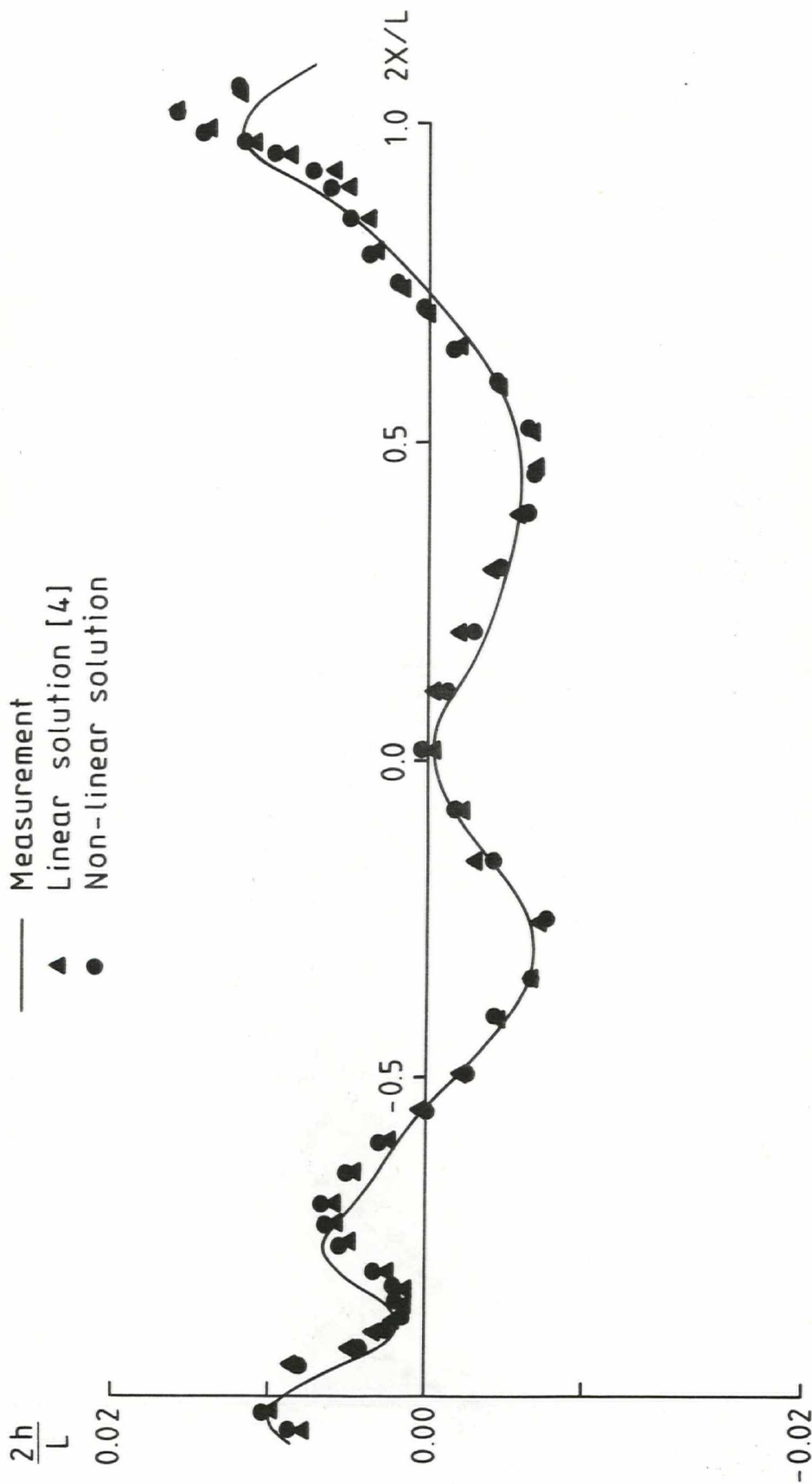


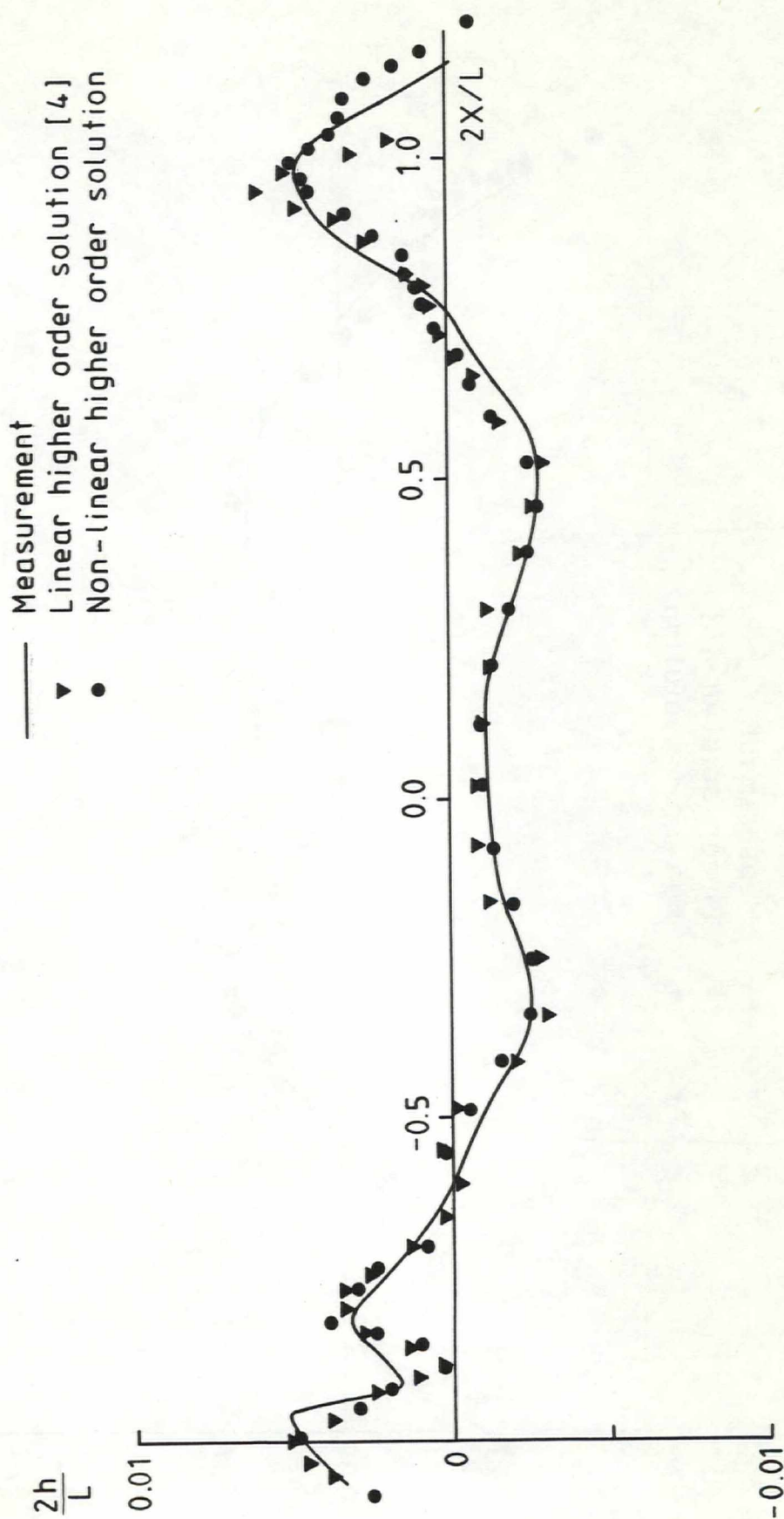




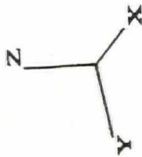








SSPA & CTH	Panel distribution the SSPA Ro-Ro ship (medium bulb)	FIG. 9

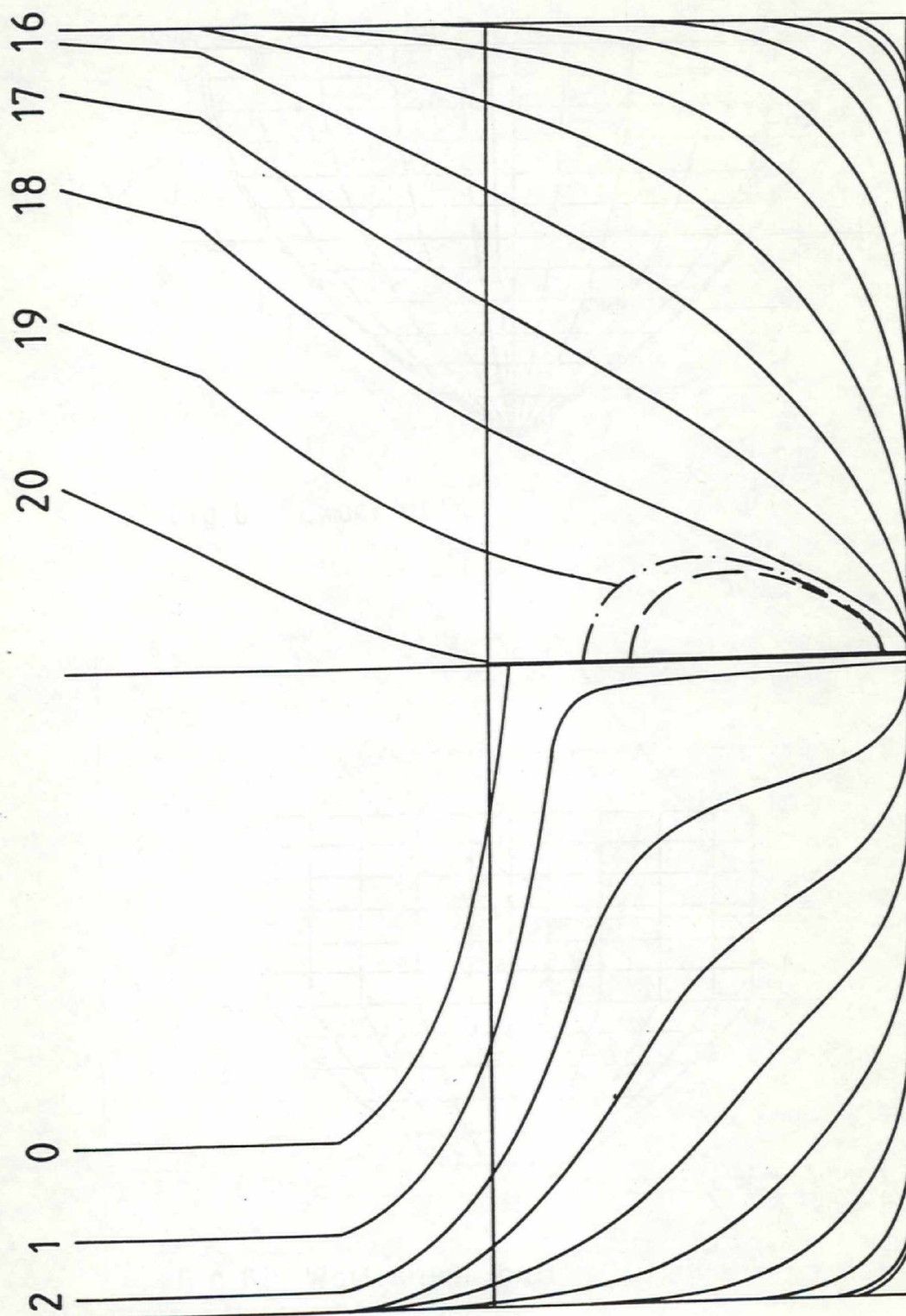


SSPA
&
CTH

Body plan with bulbs

the SSPA Ro-Ro ship

FIG. 8



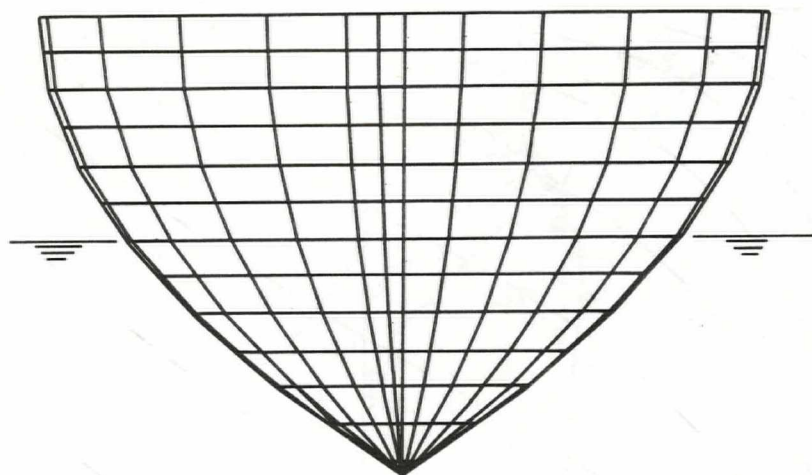


Fig 8a. Exact hull

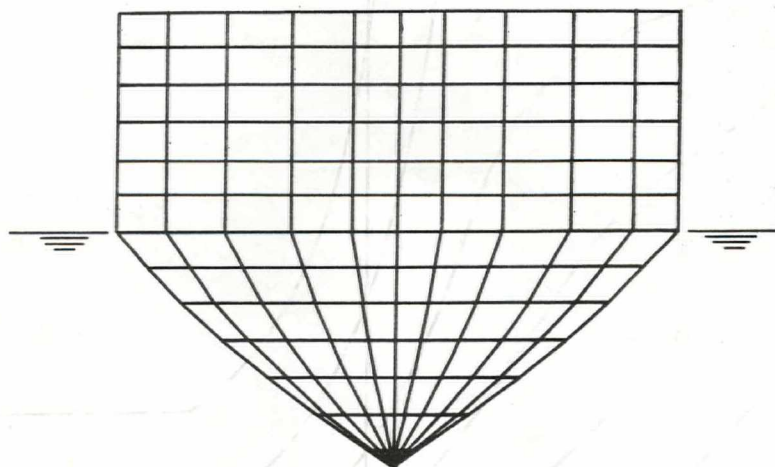
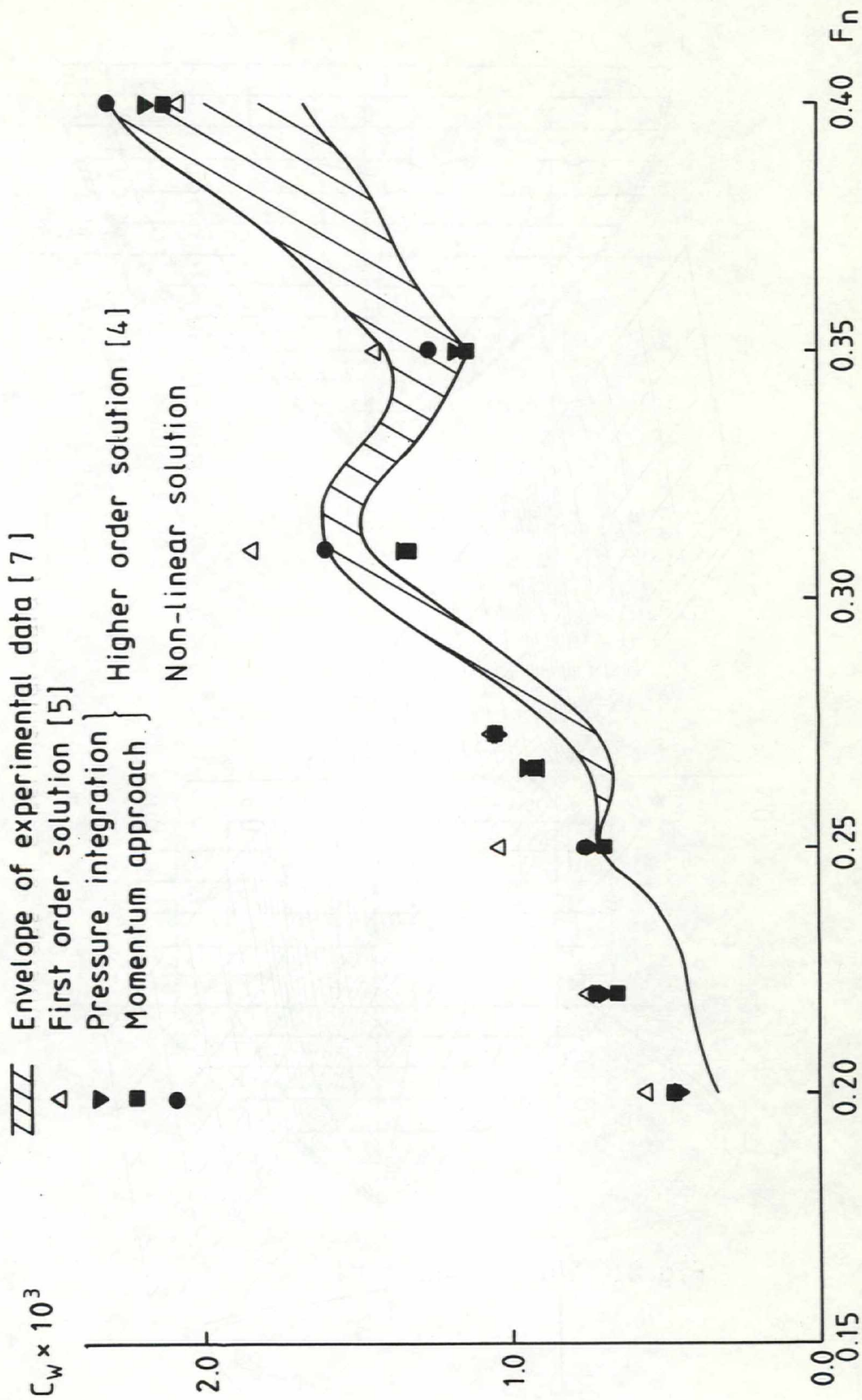
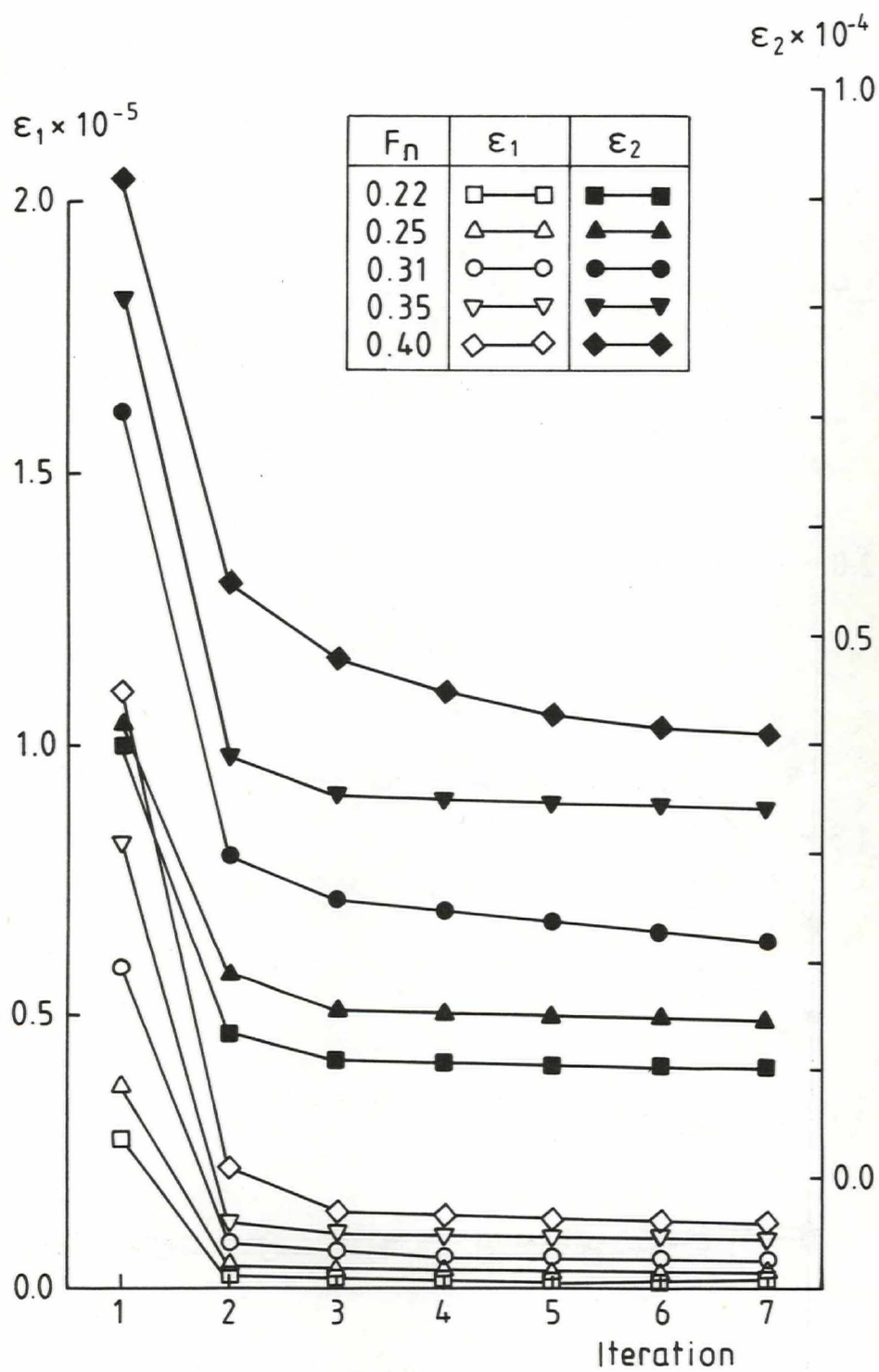
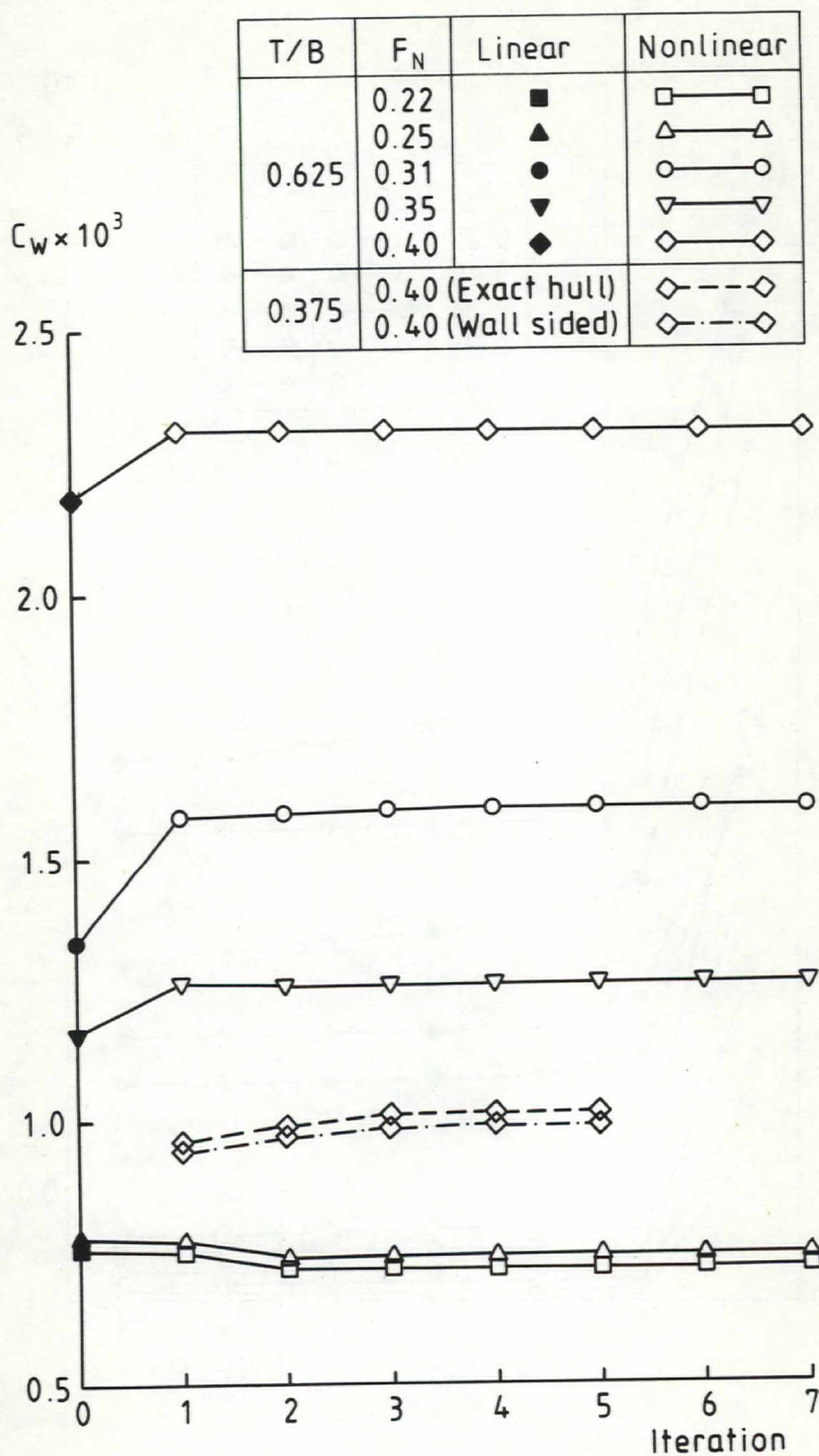
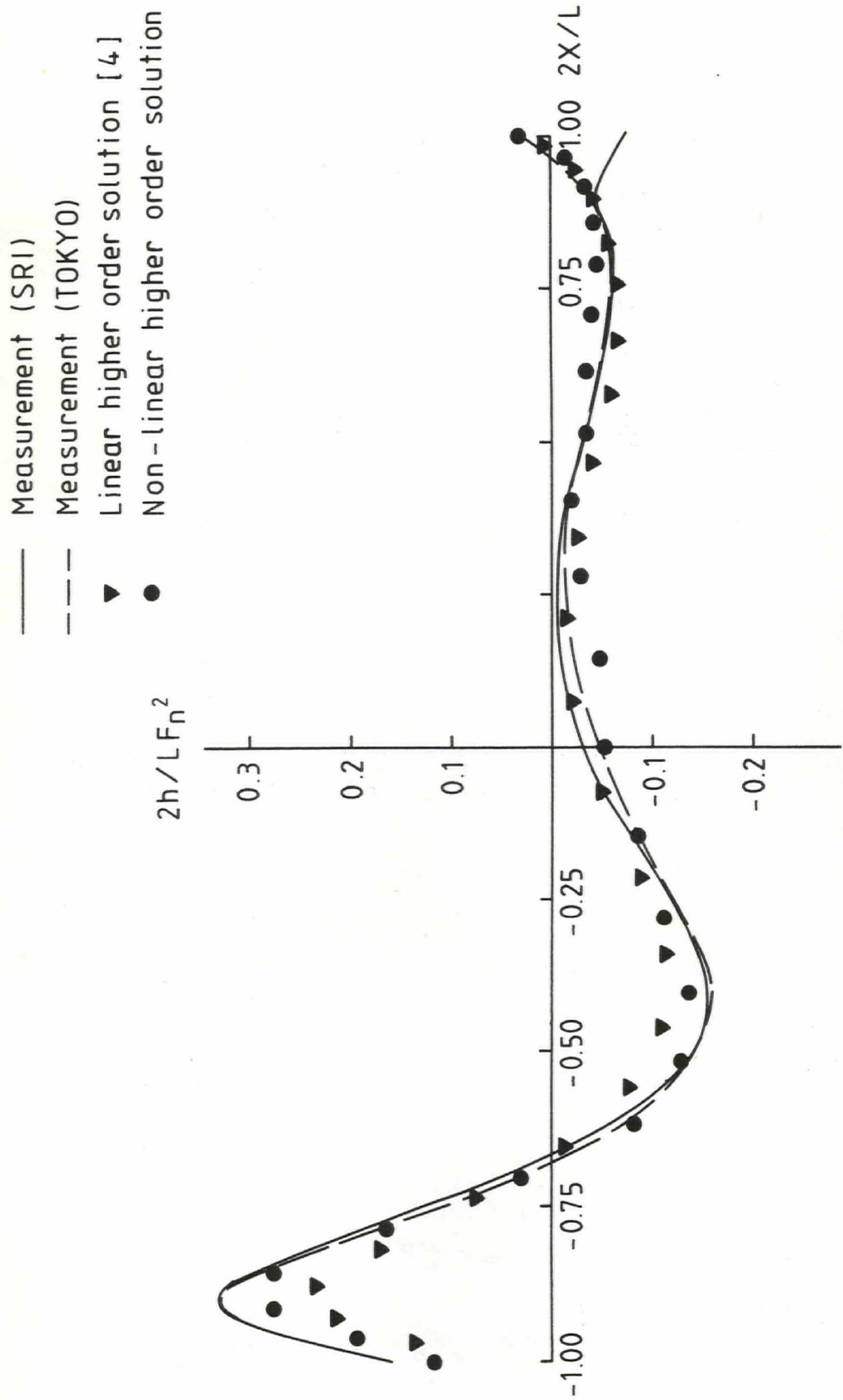


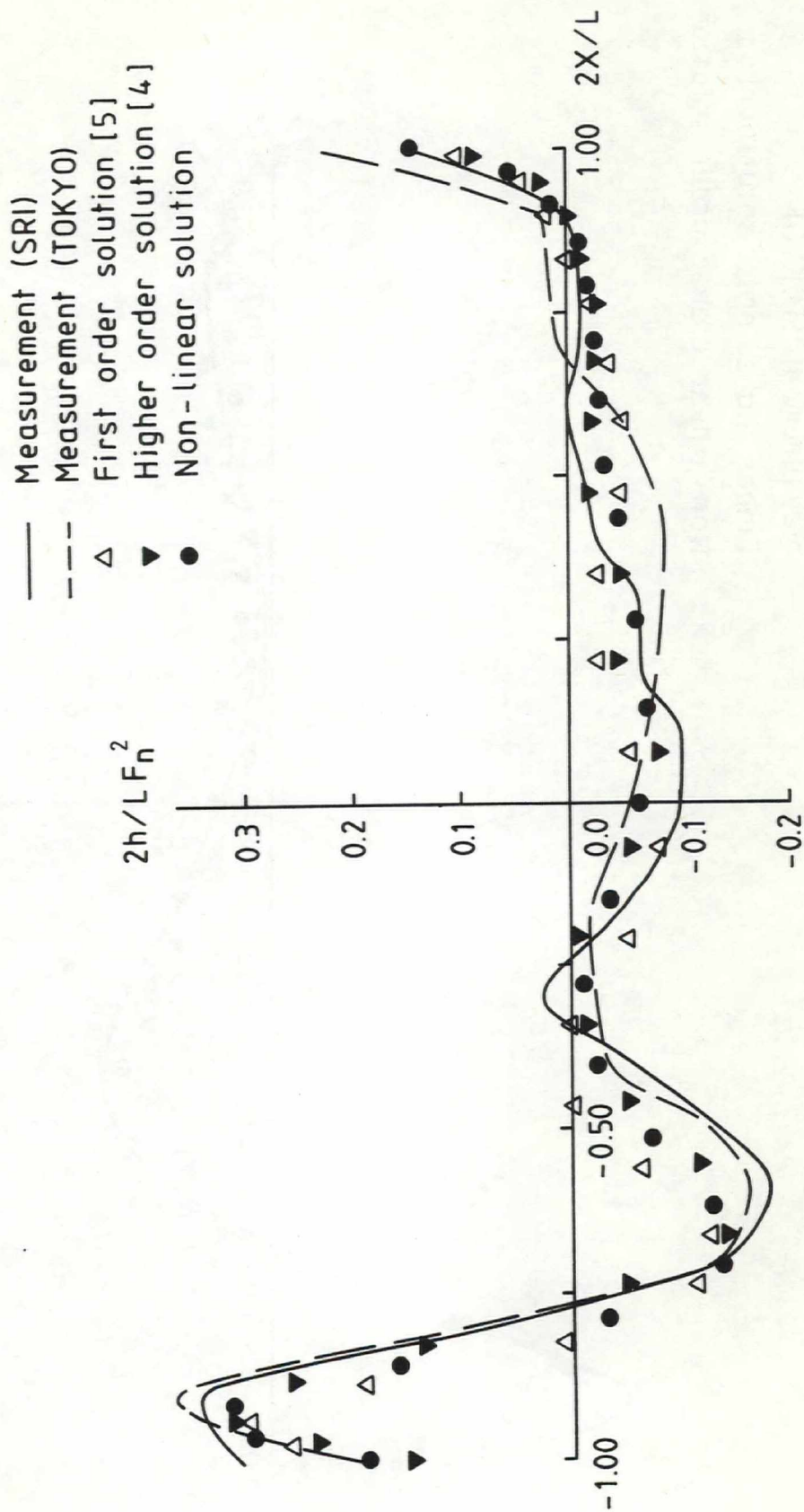
Fig 8b. Wall sided hull



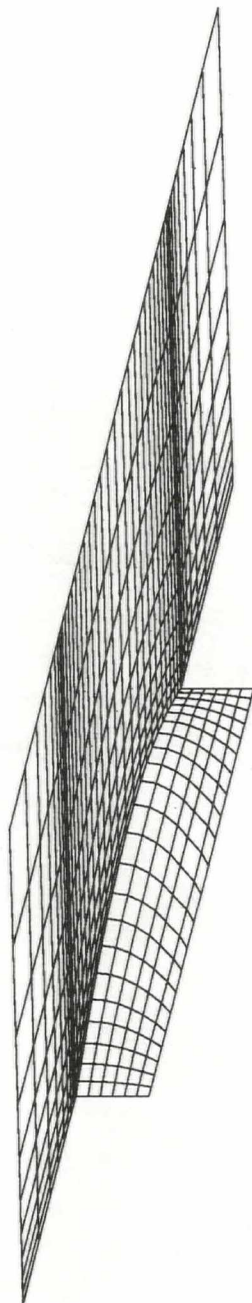
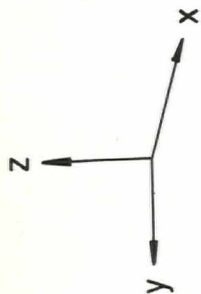


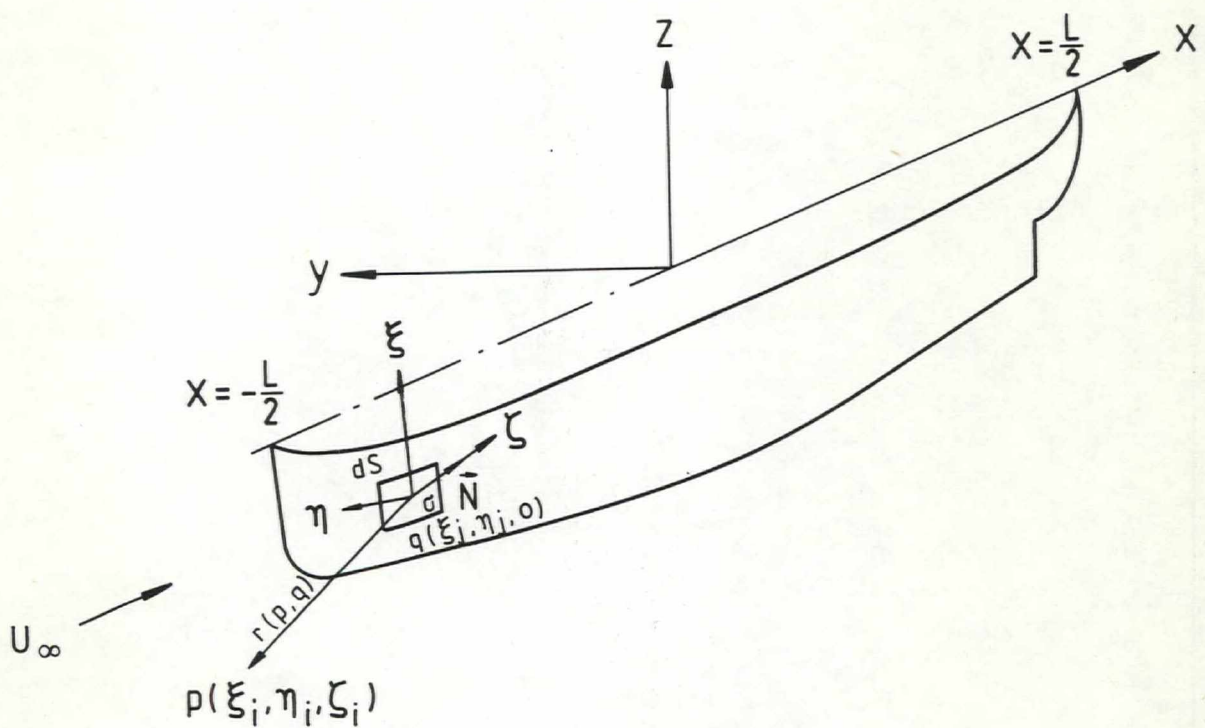






SSPA & CTH	Panel distribution on the hull (22*6) and free surface (40*10) The Wigley hull	FIG. 2





LIST OF FIGURES

- Figure 1 : Coordinate system
- 2 : Panel distribution for the Wigley hull
- 3 : Wave profiles along the Wigley hull
- 4 : Convergence history of the calculated wave resistance for the Wigley hull
- 5 : Convergence history of the calculated wave profile for the Wigley hull
- 6 : Calculated wave resistance for the Wigley hull
- 7 : Comparison test with exact and wall-sided hull
- 8 : Body plan with bulbs for the SSPA Ro-Ro ship
- 9 : Panel distribution for the SSPA Ro-Ro ship (medium bulb)
- 10 : Calculated wave profiles for the SSPA Ro-Ro ship (small bulb)
- 11 : Calculated wave profiles for the SSPA Ro-Ro ship (medium bulb)
- 12 : Convergence history of the calculated wave resistance for the SSPA Ro-Ro ship
- 13 : Convergence history of the calculated wave profile for the SSPA Ro-Ro ship
- 14 : Calculated wave resistance for the SSPA Ro-Ro ship (small bulb)
- 15 : Calculated wave resistance for the SSPA Ro-Ro ship (medium bulb)

REFERENCES

- [1] OGIWARA, S & MARUO, H: "A Numerical Method of Non-Linear Solution for Steady Waves around Ships". Journal of the Society of Naval Architects of Japan, Vol 157, 1985.
- [2] XIA, F: "A Study on the Numerical Solution of Fully Non-Linear Ship Wave Problems". SSPA Report No 2912-3, 1986
- [3] NI, S Y: "A Method for Calculating Non-Linear Free Surface Potential Flows Using Higher Order Panels". SSPA Report No 2912-6, 1987
- [4] KIM, K J: "A Higher Order Panel Method for Calculating Free Surface Potential Flows with Linear Free Surface Boundary Conditions". SSPA Report No 2966-2, 1989
- [5] XIA, F: "Numerical Calculation of Ship Flows, with Special Emphasis on the Free Surface Potential Flow". PhD thesis, Chalmers University of Technology, 1986
- [6] HESS, J L: "A Higher order Panel Method for Three-Dimensional Potential Flow". Douglas Report N62269-77-C-0437, 1979.
- [7] NORRBIN, N H (Editor): "The Proceedings of the 17th International Towing Tank Conference", SSPA, Göteborg, 1984

- d. Additional studies are required to improve the convergence of the iterative procedure. A large shift between the initial wave and the first iteration wave profile might cause some convergence problem, due to the fact that the change of the panel location may be large enough to violate the validity of the small perturbation principle.

One possible way is to compute the initial condition using the present method for a given design speed. This can be done by repeating the calculation of the first iteration wave profile for increasing speed condition by small steps, starting from the known non-linear wave profile. If the step is small the initial wave profile will not differ much from the actual one; as a result, the iterative calculation should be convergent.

Another way to improve convergence is the introduction of an under-relaxation factor. However, special investigations have to be made to ensure that only one converged solution is obtained, although different values for the under-relaxation factor are used in the iterative procedure.

V. CONCLUDING REMARKS AND FUTURE WORK

A more accurate prediction of the wave resistance and wave pattern around ships has been made by solving the normal velocity boundary condition on the wetted hull surface and the non-linear form of the free surface boundary condition on the wavy surface. An exact solution is obtained through iterations. In each iteration, an exact hull surface boundary condition and linearized free surface boundary conditions, which are obtained from the first order Taylor series expansion around the previous solution are solved simultaneously. In the new solution the hull and free surface panels are adjusted according to the new wavy surface and the sources are moved accordingly to simulate the boundary condition more exactly.

The present method has been applied to two hull forms and the results are compared with experiment. According to these studies the following conclusions can be drawn:

- a. Converged solutions are obtained after 5-6 iterations for the two test cases and they generally give better agreement with measurements than the linear method.
- b. To get better convergence, a higher order global algorithm with an initial linear wave profile is recommended.

The present method provides a possibility of obtaining more accurate results for relatively simple hull forms. There are, however, additional studies and problem areas that need to be considered and investigated before the present method can become a more effective tool in the design of ships. They are briefly described below.

- c. Further investigations of the numerical procedure should be made in order to achieve a convergence solution for more complicated hull forms, such as transom stern ships and sailing boats.

yielded $C_w = 0.990 \times 10^{-3}$ for the wall-sided case and $C_w = 1.012 \times 10^{-3}$ for the exact hull. The difference is only 0.22×10^{-4} or 2.2% of C_w . The relatively small differences may be due to the fact that the hulls are very thin. Large differences may be expected for bluff hulls.

As a more practical study the present method was applied in an investigation of the importance of non-linearity on the effect of a bow bulb on the free surface flow for the SSPA Ro-Ro ship model 2062 with small and medium size bulbs. A body plan with a small bulb and the panel representation for a medium bulb with 1 250 effective panel elements are presented in Figs 8 and 9.

Comparison between computed and measured wave profiles is made in Fig 10 for the small bulb and in Fig 11 for the medium bulb. The wave pattern predicted by the present method is better than the one from the linear method. Similar wave resistance convergence tendencies as for the Wigley case can be observed in Figs 12 and 13. It can be seen from Figs 14 and 15 that the predicted wave resistance is still lower than the measured residual resistance at all speeds, but better agreement with the measured one that with that of the linear method can be observed.

IV. RESULTS AND DISCUSSION

The solution of the wavy potential, which satisfies the exact boundary condition on the hull and the free surface was obtained by the iterative method and an extensive convergence study was performed using the Wigley hull and the SSPA Ro-Ro ship model 2062 with a small and a medium size bulb.

The panel representation for the Wigley hull with 532 effective panel elements is presented in Fig 2. The computed wave profiles at $F_n = 0.22$ and $F_n = 0.31$ are presented in Fig 3 and compared with the corresponding linear solutions and measurements. The iteration procedure started from the linear wave and converged after seven iterations. It can be seen from the figures that no great difference can be observed between linear and non-linear wave profiles. This might be explained by the fact that the non-linear effect does not seem to be very significant for such a fine hull at low speed. However, a small but distinctive improvement is achieved by the present method in the prediction of bow and stern wave profiles. Fig 4 shows the convergence history of the calculated wave resistance obtained from a higher order pressure integration method [4]. It is interesting to note that the change from linear wave resistance to the first iteration resistance is most significant and the successive changes are not large. A similar trend can be observed in the convergence history of the calculated wave profiles (Fig 5). The converged wave resistance coefficient versus ship speed is presented in Fig 6 and compared with the linear and measured ones.

In order to investigate the influence of the sources on the panels just below the free surface, a comparison study was performed at draught condition $T = 0.375 B$. One calculation was performed with a wall-sided hull and one with the exact hull at $F_n = 0.40$ (see Fig 7). For comparison, the wave resistance was computed from an integration of the pressure distribution. This

$$\epsilon_H = \phi_x h_x + \phi_y h_y - \phi_z \approx 0 \quad (31)$$

$$\epsilon_F = gh + \frac{1}{2}(\nabla\phi \cdot \nabla\phi - U_\infty^2) \approx 0$$

The iteration procedure is continued until the following convergence criterion is satisfied

$$\epsilon_1^{(k)} = \sqrt{\epsilon_H^2 + \epsilon_F^2} \leq \delta_1 \quad (32)$$

and

$$\epsilon_2^{(k)} = \sqrt{\sum_{i=1}^{NF} \delta h_i^2} / NF \leq \delta_2 \quad (33)$$

δh_i is the small change of wave elevation at the i -th control point on the free surface and k is the iteration number.

In the present calculation, the convergence tolerance δ_1 and δ_2 are specified as 1.0×10^{-6} and 1.0×10^{-5} respectively.

The equations (29) and (30) are more complicated than the corresponding linear ones. the second derivatives of the velocity potential ($\phi_{xz}, \phi_{yz}, \phi_{zz}$) appear due to the inclusion of non-linearity in the free surface boundary conditions. These terms are zero in the linear method assuming symmetry about the fault free surface.

III-4. Iterative Procedure and Convergence

The major difficulty of an iterative solution procedure is that of convergence. Several types of panel distributions and iteration techniques were tested by Xia [2]. One of the important findings was that in order to achieve convergence of the iterative process, the wave height change and the new source distribution must be computed simultaneously and also a three point finite difference operator should be used to calculate the derivative terms in free surface equation. It was possible for him to get a converged solution only for one simple hull (the Wigley hull) within a limited ship speed range. Ni [3] improved the convergence stability by introducing higher order panels and two under-relaxation factors in the non-linear iterations.

In the present work, the iteration start from a linear solution [4]. In each iteration the hull and free surface panels are adjusted according to new wavy surface and the sources are moved correspondingly to simulate the boundary condition more exactly. In the new solution the kinematic and dynamic boundary conditions are satisfied simultaneously, i.e. the new source strength as well as the new wave elevation are obtained from (28) at the same time. However, the new solution σ and h does not satisfy the exact boundary conditions (5) and (6) due to the nature of the first order (linear) approximation involved in the derivation of (12) and (13).

where

$$\begin{aligned}
 CK_{1i} &= \{ ax_1 h_t^i - ax_2 h_L^i \}_i / 2F_n^2 \\
 CK_{2i} &= \{ -ay_1 h_t^i + ay_2 h_L^i \}_i / 2F_n^2 \\
 CK_{3i} &= -ax_1 \phi_{xi} + ay_1 \phi_{yi} \\
 CK_{4i} &= ax_2 \phi_{xi} - ay_2 \phi_{yi} \\
 CK_{5i} &= 2F_n^2 (CK_{1i} \phi_{xzi} + CK_{2i} \phi_{yzi}) - \phi_{zzi} \\
 CK_{6i} &= 1 + 2F_n^2 (\phi_{xi} \phi_{xzi} + \phi_{yi} \phi_{yzi} + \phi_{zi} \phi_{zzi}) \\
 CK_{7i} &= 1 + \phi_{xi}^2 + \phi_{yi}^2 + \phi_{zi}^2 - 2\phi_{xi} - h_i^i / F_n^2 \\
 CK_{8i} &= CK_{1i} - CK_{5i} \phi_{xi} / CK_{6i} \\
 CK_{9i} &= CK_{2i} - CK_{5i} \phi_{yi} / CK_{6i} \\
 CK_{10i} &= -1/2F_n^2 - CK_{5i} \phi_{zi} / CK_{6i} \\
 AV_{ij} &= (\phi_{xi} X_{ij} + \phi_{yi} Y_{ij} + \phi_{zi} Z_{ij}) / CK_{6i}
 \end{aligned}$$

A similar procedure is followed in the generation of the right-hand side arrays of Eq (25), i e

For the upper part

$$B_i = N_{xi} \quad i = 1, \dots, NH \quad (30a)$$

For the lower part

$$\begin{aligned}
 B_i &= -CK_{1i} + CK_{11i} \\
 &+ CK_{3i} (GA_i BV_i + GB_i BV_{i+1} + GC_i BV_{i+2}) \\
 &+ CK_{4i} (CA_i BV_i + CB_i BV_{i-NL} + GC_i BV_{i-2NL})
 \end{aligned} \quad (30b)$$

where

$$\begin{aligned}
 CK_{11i} &= -0.5 \cdot CK_{5i} \cdot CK_{7i} / CK_{6i} \\
 BV_i &= 0.5 (\phi_{xi}^2 + \phi_{yi}^2 + \phi_{zi}^2 - 2\phi_{xi} - h_i^i / F_n^2) / CK_{6i}
 \end{aligned}$$

array.

The upper part (corresponding to the hull boundary condition) of the A matrix is easily generated by setting

$$A_{ij} = \bar{V}_{ij} \cdot \bar{N}_i = X_{ij}N_{xi} + Y_{ij}N_{yi} + Z_{ij}N_{zi} \quad (29a)$$

$$i = 1, \dots, NH$$

$$j = 1, \dots, NE$$

where NH is again the number of panels on the hull surface.

X_{ij} , Y_{ij} and Z_{ij} are the components of velocity influence coefficient. V_{ij} is induced at the control point of the i -th panel by a linearly varying source density at the j -th panel. N_{xi} , N_{yi} and N_{zi} are the components of the unit normal vector to the hull surface at i -th panel element. These are the only source equations to be solved in the double model case.

For the free surface, the lower part (corresponding to the free surface boundary condition) is generated in a more complicated form as

$$A_{ij} = CK_{8i}X_{ij} + CK_{9i}Y_{ij} + CK_{10i}Z_{ij}$$

$$+ CK_{3i}\{ GA_iAV_{ij} + GB_iAV_{i+1,j} + GC_iAV_{i+2,j} \} \quad (29b)$$

$$+ CK_{4i}\{ CA_iAV_{ij} + CB_iAV_{i-NL,j} + CC_iVA_{i-2NL,j} \}$$

Integration of the higher order derivative terms of (23) leads to an expression even more complicated than (24). To avoid complicated computations, the magnitude of the second derivative terms related to the curvature and linear variation of source density are assumed to be small and vanish rapidly during the iteration. In the present paper the second order derivative terms are calculated from a source velocity which corresponds to the flat panel with constant source density.

$$\begin{bmatrix} \Phi_{xz} \\ \Phi_{yz} \\ \Phi_{zz} \end{bmatrix}_i = \sum_{j=1}^{NE} \begin{bmatrix} a_{13} \\ a_{23} \\ a_{33} \end{bmatrix}_j^T \begin{bmatrix} a_{11} & a_{21} & a_{31} \\ a_{12} & a_{22} & a_{32} \\ a_{13} & a_{23} & a_{33} \end{bmatrix} \begin{bmatrix} \Phi_{\xi\xi} & \Phi_{\xi\eta} & \Phi_{\xi\zeta} \\ \Phi_{\eta\xi} & \Phi_{\eta\eta} & \Phi_{\eta\zeta} \\ \Phi_{\zeta\xi} & \Phi_{\zeta\eta} & \Phi_{\zeta\zeta} \end{bmatrix}_{ij} \quad (27)$$

NE is here again the total number of panels.

III-3. The Linear Equations for the source strength

From a purely mathematical point of view, the problem considered here is well defined. The mathematical solution of (4), (12) and (13) considering the radiation condition is a unique and continuous function for source density and wave elevation. The boundary condition is satisfied at all the points on the fluid boundary.

In the numerical computation, the flow boundary is taken into account in a discrete manner and the boundary condition is satisfied at only a finite number of control points. Through a numerical discretization procedure, eq. (12) and (13) can be transformed into a set of algebraic equations in σ as

$$[A] \{ \sigma \} = \{ B \} \quad (28)$$

where $[A]$ is a $NE \times NE$ matrix and $\{B\}$ is the right-hand side

velocities in Eq (24) can be obtained analytically.

Then the velocity in the reference coordinate can be calculated from the coordinate transformation

$$\begin{Bmatrix} \Phi_x \\ \Phi_y \\ \Phi_z \end{Bmatrix} = \begin{bmatrix} a_{11} & a_{21} & a_{31} \\ a_{12} & a_{22} & a_{32} \\ a_{13} & a_{23} & a_{33} \end{bmatrix} \begin{Bmatrix} \Phi_\xi \\ \Phi_\eta \\ \Phi_\zeta \end{Bmatrix} \quad (25)$$

These velocities may also be written as

$$\begin{aligned} \Phi_{xi} &= \sum_{j=1}^{NE} X_{ij} \sigma_j + U_\infty \\ \Phi_{yi} &= \sum_{j=1}^{NE} Y_{ij} \sigma_j \\ \Phi_{zi} &= \sum_{j=1}^{NE} Z_{ij} \sigma_j \end{aligned} \quad (26)$$

Here the velocity influence coefficients X_{ij} , Y_{ij} and Z_{ij} are the velocity components in the reference coordinate system (x, y, z) at the i -th control point, induced by a source density which is unity at the control point of the j -th panel. In the first order method the velocity induced by a panel depends only on the panel itself. The essentially new feature of the higher order method is that the velocity induced by a panel depends on the values of source densities also at the control points of adjacent elements. Thus the influence coefficients for a panel depend not only on the geometry of that panel but also on the geometry of adjacent panels. The assembly of the influence coefficient matrix is more complicated and special care must be taken in obtaining them.

The second derivative terms $(\Phi_{xzi}, \Phi_{yzi}, \Phi_{zzi})$ can be calculated in a similar way. Unfortunately they are much more complicated.

variation of the source density. All these terms only depend on the geometry of the j -th panel, but the curvature terms P , Q , R and the source derivative coefficients $C_k^{(\xi)}$ and $C_k^{(\eta)}$ depend on the surrounding panels. For more details see Ref [4, 6].

The individual Φ 's in Eq (22) are

$$\begin{aligned}
 \Phi_{ij}^{(0)} &= \int_{A_j} \frac{1}{r_f} d\xi d\eta \\
 \Phi_{ij}^{(P)} &= \int_{A_j} \zeta_i \xi_j^2 / r_f^3 d\xi d\eta \\
 \Phi_{ij}^{(Q)} &= \int_{A_j} \zeta_i \xi_j \eta_j / r_f^3 d\xi d\eta \\
 \Phi_{ij}^{(R)} &= \int_{A_j} \zeta_i \eta_j^2 / r_f^3 d\xi d\eta \\
 \Phi_{ij}^{(1\xi)} &= \int_{A_j} \xi_j / r_f d\xi d\eta \\
 \Phi_{ij}^{(1\eta)} &= \int_{A_j} \eta_j / r_f d\xi d\eta
 \end{aligned} \tag{23}$$

where r_f is the distance between (ξ_i, η_i, ζ_i) and the j -th control point $(\xi_j, \eta_j, 0)$ on the flat panel (see Fig 2 in [4]). Then the velocity induced by the panel is obtained by taking the gradient of the corresponding potential.

$$\begin{aligned}
 \Phi_\xi &= \Phi_\xi^* \sigma_j + \sum_{k=1}^{M-1} \{C_k^{(\xi)} \Phi_\xi^{(1\xi)} + C_k^{(\eta)} \Phi_\xi^{(1\eta)}\} \sigma_k \\
 \Phi_\eta &= \Phi_\eta^* \sigma_j + \sum_{k=1}^{M-1} \{C_k^{(\xi)} \Phi_\eta^{(1\xi)} + C_k^{(\eta)} \Phi_\eta^{(1\eta)}\} \sigma_k \\
 \Phi_\zeta &= \Phi_\zeta^* \sigma_j + \sum_{k=1}^{M-1} \{C_k^{(\xi)} \Phi_\zeta^{(1\xi)} + C_k^{(\eta)} \Phi_\zeta^{(1\eta)}\} \sigma_k
 \end{aligned} \tag{24}$$

Notice that subscript ij is omitted in the equation (24) for simplicity and new velocity terms $(\Phi_\xi^*, \Phi_\eta^*, \Phi_\zeta^*)$ are introduced. They are velocity components induced at the i -th control point by a unit source density on the j -th panel. All the induced

calculated from the distance between the successive points on the free surface panels, see [5].

As pointed out by Dawson, upstream waves are prevented by the use of upstream finite difference operators.

III-2. Initial condition and velocity potential

The numerical computation of Eq. (12) and (13) requires as a starting point a very accurate velocity potential and its first (Φ_x, Φ_y, Φ_z) and second derivative values ($\Phi_{xz}, \Phi_{yz}, \Phi_{zz}$) at the exact boundary control points. A slight error in these terms gives a magnified error in final solution. For instance a small error near the bow leads to a non-realistic set of waves bouncing along the ship hull. A linear solution is adapted as the initial condition and considerable care has been taken to compute the associated velocity gradients accurately in order to improve the convergency.

The velocity potential Φ_{ij} at the i -th control point induced by the j -th panel on which the source density at the control point is σ is given by the following equation in a panel element co-ordinate system (ξ, η, ζ).

$$\begin{aligned}\Phi_{ij} &= \Phi_{ij}^{(0)}\sigma_j + \{ P\Phi_{ij}^{(P)} + 2Q\Phi_{ij}^{(Q)} + R\Phi_{ij}^{(R)} \}\sigma_j \\ &+ \Phi_{ij}^{(1\xi)}\sigma_\xi + \Phi_{ij}^{(1\eta)}\sigma_\eta \\ &= \Phi_{ij}^*\sigma_j + \sum_{k=1}^{M-1} \{ C_k^{(\xi)}\Phi_{ij}^{(1\xi)} + C_k^{(\eta)}\Phi_{ij}^{(1\eta)} \}\sigma_k\end{aligned}\quad (22)$$

Here M is the number of the adjacent panel.

All the Φ terms in (22) can be calculated numerically and they may be interpreted as follows: $\Phi_{ij}^{(0)}$ corresponds to a flat panel with a constant source density, $\Phi_{ij}^{(P)}$, $\Phi_{ij}^{(Q)}$ and $\Phi_{ij}^{(R)}$ are caused by the parabolic panel shape, $\Phi_{ij}^{(1\xi)}$ and $\Phi_{ij}^{(1\eta)}$ come from the

previous work [4]. As can be seen from the Figs 2 and 10, the longitudinal lines are smooth arbitrary boundary fitted curves $y = f_L(x)$ and the transverse lines are parallel to the y -axis ($y=f_t(x)$). Then the derivative terms in the free surface boundary condition (12) and (13) may be expressed by finite differences in the two directions of the grid.

$$\begin{aligned} h_x^\circ &= ax_1 h_T^\circ - ax_2 h_L^\circ \\ h_y^\circ &= h_T^\circ \end{aligned} \quad (18)$$

and

$$\begin{aligned} \delta h_x &= ax_1 \delta h_T - ax_2 \delta h_L \\ \delta h_y &= - \delta h_T \end{aligned} \quad (19)$$

where

$$\begin{aligned} ax_1 &= f_L' \\ ax_2 &= - \sqrt{1 + f_L'^2} \end{aligned}$$

Three point finite difference operators are used to calculate the derivative terms in Eqs (12), (13) along the L and T directions.

$$\begin{aligned} h_{Li}^\circ &= CA_i h_i^\circ + CB_i h_{i-NL}^\circ + CC_i h_{i-2NL}^\circ \\ h_{Ti}^\circ &= GA_i h_i^\circ + GB_i h_{i+1}^\circ + GC_i h_{i+2}^\circ \end{aligned} \quad (20)$$

$$\begin{aligned} \delta h_{Li} &= CA_i \delta h_i + CB_i \delta h_{i-NL} + CC_i \delta h_{i-2NL} \\ \delta h_{Ti} &= GA_i \delta h_i + GB_i \delta h_{i+1} + GC_i \delta h_{i+2} \end{aligned} \quad (21)$$

where NL is the number of the longitudinal strips on the free surface.

The coefficient of the upstream three point operator (CA_i , CB_i and CC_i) and the downstream operator (GA_i , GB_i and GC_i) are

$$\begin{aligned}
 \text{Point P: } \{ & \begin{aligned} g(x_{FP}, 0) - h(x_{FP}, 0) &= 0 \\ z_{FP} &= g(x_{FP}, 0) = h(x_{FP}, 0) \end{aligned} \\
 \text{Point Q: } \{ & \begin{aligned} g(x_{AP}, 0) - h(x_{AP}, 0) &= 0 \\ z_{AP} &= g(x_{AP}, 0) = h(x_{AP}, 0) \end{aligned}
 \end{aligned} \tag{15}$$

The x-position of the original stations is adjusted according to the intersection points P and Q. The new hull definition points at the x_1^i -station can be interpolated by a cubic spline function. The expression for the hull surface at the new station ($x_1^i = \text{const}$) may be written

$$\begin{aligned}
 F &= y' - f(x_1^i, z') \\
 &= z' - g(x_1^i, y') = 0
 \end{aligned} \tag{16}$$

The intersection point R of the hull and wave surface at each x_1^i -station is the solution of the following equation

$$\begin{aligned}
 g(x_1^i, y_{Ri}^i) - h(x_1^i, y_{Ri}^i) &= 0 \\
 z_{Ri}^i &= g(x_1^i, y_{Ri}^i) \\
 &= h(x_1^i, y_{Ri}^i)
 \end{aligned} \tag{17}$$

Once the intersection point R_i is determined, the girthline between the keel and the intersection point R_i may be divided in some regular way to generate the quadrilateral panel on the hull surface. The rearrangement of the panels on the free surface can also be generated in a similar way.

Unlike most other panel methods the present one employs a free surface grid, which is boundary fitted and independent of double model streamlines. A much better resolution at the bow and stern was obtained in the boundary fitted grid as described in the

surrounding the hull due to computer storage limitations. The neglect of the panel distribution outside this region must inevitably cause a certain amount of errors. In the present calculation, the disturbance outside this region due to the existence of the hull is assumed to be small and only a small portion of the free surface between $-2.0 \leq x \leq 2.0$ and $-0.750 \leq y \leq 0$ is used as a boundary domain, as recommended by Xia [5].

The solution of the integral equation (1) subject to the boundary conditions (4), (12) and (13) requires an initial definition of the integral domain where the panel should be distributed. (The boundary conditions should be satisfied.) In principle, this is unknown a priori and must be computed as part of the solution through iterations. To start the calculation an initial panel arrangement is made, based on linear wave profiles. In the following iteration the hull and free surface panels are adjusted according to the new wavy surface and the sources are moved correspondingly. For this reason, a repanning routine has to be incorporated in the solution procedure and the details of the panel generation procedure will be described below.

First the hull geometry including the part above the waterline has to be defined as a family of points in the $x = \text{const}$ planes (x_i stations) to approximate the hull surface by the cubic spline function

$$\begin{aligned} F &= y - f(x_i, z) \\ &= z - g(x_i, y) = 0 \end{aligned} \quad (14)$$

With known wave profiles $z=h(x,y)$, the intersection points $P(x_{FP}, 0, z_{FP})$ and $Q(x_{AP}, 0, z_{AP})$ of the hull and wave surface at FP and AP in the $y=0$ plane are obtained by solving the following equations:

III. NUMERICAL METHOD

The central problem of the present method of flow calculation is the numerical solution of the boundary conditions (4), (12) and (13). The problem is highly non-linear since the free surface boundary condition itself is non-linear and should be exactly satisfied on the wavy surface, which is unknown a priori, and must be computed as a part of the solution. Thus numerical methods which have been applied to solve the problem usually entail some kind of linearization procedure. In the present method, an exact solution is obtained through iterations and in each iteration the free surface boundary condition is linearized about the previous solution based on the small perturbation principle. Upon convergence, which is obtained after 5-6 iterations, the non-linear terms left out in the equations go to zero and the solution is exact with respect to boundary conditions.

Once the final source density σ and wave height h are determined the flow velocity and pressure may be calculated at any point. With known pressure and velocity distributions, the wave pattern and the wave resistance can be predicted. The details of the numerical procedure for the prediction of ship wave resistance are described in the following sections.

III-1. Panel Arrangement

In the numerical implementation of the present method the first step is to discretize the integral domain S in (1) into a large number of small panels. In the wave resistance problem, the integration domain S consists of the hull surface and part of the free surface. In principle the free surface panel distribution should extend over the entire region where there are significant waves. In numerical computation, however, the region of free surface panels has to be severely limited to the region

$$\Delta D_2 (\sigma, h^\circ) = \frac{1}{g} (\phi_x \delta \phi_x + \phi_y \delta \phi_y + \phi_z \delta \phi_z) \quad (11)$$

$$\Delta D_2 (\sigma^\circ, h) = \delta h + \frac{1}{g} (\phi_x \phi_{xz} + \phi_y \phi_{yz} + \phi_z \phi_{zz}) \delta h$$

Therefore the linearized free surface boundary conditions are

$$\phi_x h_x^\circ + \phi_y h_y^\circ - \phi_z + \phi_x \delta h_x + \phi_y \delta h_y + (\phi_{xz} h_x^\circ + \phi_{yz} h_y^\circ - \phi_{zz}) \delta h = 0 \quad (12)$$

$$\left\{ 1 + \frac{1}{g} (\phi_x \phi_{xz} + \phi_y \phi_{yz} + \phi_z \phi_{zz}) \right\} \delta h = \quad (13)$$

$$\frac{1}{2g} \{ U_\infty^2 - \phi_x^2 - \phi_y^2 - \phi_z^2 - 2(\phi_x \delta \phi_x + \phi_y \delta \phi_y + \phi_z \delta \phi_z) \} - h^\circ$$

$$D_1(\sigma, h) \approx D_1(\sigma^0, h^0) + \Delta D_1(\sigma, h^0) + \Delta D_1(\sigma^0, h) \approx D_1(\sigma^0, h^0) + \frac{\partial}{\partial \sigma} D_1(\sigma, h^0) \cdot \delta \sigma + \frac{\partial}{\partial h} D_1(\sigma^0, h) \cdot \delta h \approx 0 \quad (8)$$

$$D_2(\sigma, h) \approx D_2(\sigma^0, h^0) + \Delta D_2(\sigma, h^0) + \Delta D_2(\sigma^0, h) \approx D_2(\sigma^0, h^0) + \frac{\partial}{\partial \sigma} D_2(\sigma, h^0) \delta \sigma + \frac{\partial}{\partial h} D_2(\sigma^0, h) \cdot \delta h \approx 0$$

It is a fundamental assumption of the present method that the perturbations of source ($\delta\sigma$) and wave elevation (δh) are small in certain senses. In a Taylor series, higher order terms in these quantities then become very small and can be neglected.

Here the superscript, 0, corresponds to the previous solution which is assumed to be known a priori. In the first iteration this may be either a double model solution, which gives the Bernoulli wave or a linear solution [4].

$$D_1(\sigma^0, h^0) = \Phi_x h_x^0 + \Phi_y h_y^0 - \Phi_z = 0 \quad (9)$$

$$D_2(\sigma^0, h^0) = h^0 - \frac{1}{2g} [U_\infty^2 - (\Phi_x^2 + \Phi_y^2 + \Phi_z^2)] = 0$$

where Φ_x , Φ_y and Φ_z mean the velocity components induced by σ^0 on the free surface $z = h^0(x, y)$.

The partial increments of D_1 and D_2 should be found in such a way that a new velocity potential $\phi = \Phi + \delta\phi$ induced by introducing small perturbations $\delta\sigma$ and δh should satisfy Eqs (5) and (6) on the new wave surface $h = h^0 + \delta h$. ΔD_1 and ΔD_2 can be linearly expanded based on σ^0 and h^0

$$\Delta D_1(\sigma, h^0) = \delta\phi_x h_x^0 + \delta\phi_y h_y^0 - \delta\phi_z \quad (10)$$

$$\Delta D_1(\sigma^0, h) = \Phi_x \delta h_x + \Phi_y \delta h_y + (\Phi_{xz} h_x^0 + \Phi_{yz} h_y^0 - \Phi_{zz}) \delta h$$

where n denotes the outward normal to the hull surface. At the free surface, two boundary conditions must be imposed, i.e. the flow must be tangent to the free surface

$$\phi_x h_x + \phi_y h_y - \phi_z = 0 \quad (5)$$

and the pressure should be constant

$$gh + \frac{1}{2} (\nabla \phi \cdot \nabla \phi - U_\infty^2) = 0 \quad (6)$$

Further, no upstream waves should be generated.

The exact problem described above is nonlinear, since the free surface boundary condition itself is nonlinear and should be exactly satisfied on the wavy surface $z=h(x,y)$, which is unknown, and must be computed as a part of the solution. Thus, numerical methods, which have been applied to solve the problem usually entail some kind of linearization procedure. In the present paper an iteration procedure is applied and the free surface boundary condition in each iteration is linearized about the previous solution.

Unknown sources σ on the hull and wavy surface $z=h(x,y)$ will induce a potential ϕ and a wave elevation h which satisfy the boundary conditions (5) and (6).

$$\begin{aligned} D_1(\sigma, h) &= \phi_x h_x + \phi_y h_y - \phi_z = 0 \\ D_2(\sigma, h) &= h - \frac{1}{2g} [U_\infty^2 - (\phi_x^2 + \phi_y^2 + \phi_z^2)] = 0 \end{aligned} \quad (7)$$

These non-linear forms of the free surface boundary conditions can be linearized by introducing small perturbations $\delta\sigma$ and δh with respect to the previous solution in a first order Taylor expansion.

II. MATHEMATICAL FORMULATION OF THE PROBLEM

As in the usual analysis, the flow is considered steady, inviscid, irrotational and incompressible and a right-handed coordinate system $Oxyz$ is employed with the origin on the mean free surface, x positive in the direction of the uniform flow, and z positive in the upward direction. A ship, piercing the free surface, is assumed to be in a uniform onset flow of velocity U_∞ . (See Fig 1.) Then the flow field around the ship may be described by a velocity potential ϕ which is generated by a certain distribution of sources on a surface S and by the uniform onset flow in the x -direction.

$$\phi(x, y, z) = \int \sigma(q)/r(p, q) dS + U_\infty x \quad (1)$$

where $\sigma(q)$ is the source density on the surface element dS and $r(p, q)$ is the distance from the point q to the field point $p(x, y, z)$ where the potential is being evaluated.

The potential ϕ given in Eq (1) is governed by the Laplace equation.

$$\nabla^2 \phi = 0 \quad (2)$$

in the fluid domain and satisfies the regularity condition at infinity

$$\nabla \phi \rightarrow (U_\infty, 0, 0) \text{ as } r \rightarrow \infty \quad (3)$$

The source density σ should be determined from the boundary conditions on the hull and free surface. On the wetted hull surface the solid boundary condition is

$$\phi_n = 0 \quad (4)$$

based on the earlier work by Xia [2] and Ni [3]. One of the major improvements is that the hull panels just below the wavy surface are generated in a more accurate way by considering the hull shape above the designed load waterline. In the early work on this method by Ni the hull was considered wall sided. This simplification may lead to some limitation in its application to ships with barge type stern sections, or inclined bows and sterns. This restriction is now removed.

It is believed that this is important for wave pattern prediction since the influence of the sources on hull panels just below the free surface is considerably larger than sources on the other parts of the hull. On the other hand, this might cause some convergence problems due to the fact that the change of the panel location may be large enough to violate the validity of the small perturbation principle. In order to improve the convergence, special care has been taken to select the initial condition and also to compute the velocity potential and the associated derivative terms in the free surface equation.

The present method has been applied to compute the wave pattern, pressure distribution over the hull surface and wave resistance for two different hull forms. The importance of non-linearity is discussed in more detail with relation to the effect of a bow bulb on the free surface flow and wave resistance in comparison with experiment.

Ogiwara took the non-linear effect into account iteratively by using relaxation factors in 1985, [1] and Xia proposed an iterative procedure in 1986, [2]. In his method the free surface boundary condition is linearized about the initial wavy surface, using the small perturbation principle and new wave elevations and source distributions are solved in the next iteration. It was found that the convergence problem for the iterative procedure is quite severe.

A higher order global algorithm was applied to the non-linear three-dimensional free-surface problem by Ni [3]. The results of the test computations were always convergent if a relaxation factor was used for the wave elevation modification. A single model with a new panelling to fit the wavy free surface was used and the vertical derivatives of the induced velocity were kept in the free surface boundary condition.

In the present paper, the solution of the wavy potential, which satisfies the exact boundary condition on the hull and the free surface is obtained through iterations and in each iteration the free surface boundary condition is linearized, based on the small perturbation principle, about the previous solution. The iteration start from the linear solution. In each iteration the hull and free surface panels are adjusted according to the new wavy surface and the sources are moved accordingly to simulate the boundary condition more exactly. In the new solution the kinematic and dynamic boundary conditions are satisfied simultaneously, i.e. the new source strength as well as the new wave elevation are obtained at the same time. Upon convergence, which is usually obtained after 5-6 iterations, the non-linear terms go to zero and the solution is exact with respect to the boundary conditions.

In order to fulfill the basic requirements of generality, economy and accuracy for the application to practical hull form design, some of improvements and modifications have been made

I. INTRODUCTION

An accurate prediction of ship wave resistance is extremely important not only for the analysis of ships' hydrodynamic performance but also to improve the hull forms. There are several different types of wave theories applicable to practical hull forms which can be found in the literature. These include largely linear types of theoretical methods, such as thin ship or slender ship theory, Guilloton's theory, and methods based on a numerical discretization using the surface singularity approach (panel method). The methods for calculating free surface potential flows with linear surface boundary conditions has been applied frequently to predict the wave pattern and ship wave resistance. Successful predictions have been made for idealized mathematical forms and simple types of hull forms without bulbous bows and bluff stern sections. However, the accuracy for more complex ship forms (very blunt bow and stern) is relatively poor. The most significant inaccuracy can be found in the prediction of the wave patterns near the bow and stern region. The poor resolution may result partially from the fact that the wave pattern near the bow and stern region is strongly influenced by the non-linear terms and the linearized free surface condition cannot simulate the exact boundary condition properly.

Further attempts to improve the accuracy have been made by taking the non-linear effects into account in the free surface boundary condition. In contrast to the linear wave theory, in this nonlinear method an exact boundary condition is satisfied both on the hull and on the free surface. This problem is highly non-linear since the free surface boundary condition itself is non-linear and should be exactly satisfied on the wavy surface, which is unknown a priori, and must be computed as a part of the solution. The numerical methods which have been applied to solve the problem usually entail some kind of linearization procedure.

Subscripts and Superscripts

i, j	Subscripts referring to the i -th or j -th panel
ij	Double subscript referring to the effect of the j -th panel at the i -th control point
o	Superscript referring to the double model solution
(o)	Superscript referring to a constant source density
$(P), (Q)$	Superscript referring to a panel curvature
(R)	
$(1\xi)(1\eta)$	Superscript referring to a varying source density

LIST OF SYMBOLS

[A]	Coefficient matrix for the linear equation system
{B}	Right hand side vector for the linear equation system
$A_0, B_0,$ Z_0	Coefficients of linear terms in the expression for the curved panel
CA,CB, CC,CD	Coefficients of the finite difference upstream operator
C_p	Pressure coefficient
C_w	Wave resistance coefficient
F_n	Froude number
GA,GB, GC,GD	Coefficients of the finite difference downstream operator
g	Acceleration of gravity
$h=z(x,y)$	Wave elevation
M	Number of adjacent panels
NH	Number of panels on the body
NF	Number of panels on the free surface
NE	Total number of panels
\bar{N}	Unit normal vector with components (N_x, N_y, N_z) in reference co-ordinates
\bar{N}^E	Unit normal vector with components (N_ξ, N_η, N_ζ) in panel co-ordinates
p	Static pressure
$P, Q, R,$ P_0, Q_0, R_0	Coefficients of quadratic terms in the expression for the curved panel
t	Maximum ζ value of a panel
U_∞	Magnitude of the uniform onset flow velocity
V	Flow velocity with components (ϕ_x, ϕ_y, ϕ_z) or (u, v, w)
[X],[Y]	Matrices of induced velocities
[Z]	
x, y, z	Global reference co-ordinates (see Fig 1)
ϕ	Total velocity potential
Φ	Velocity potential from previous solution
σ	Source density

CONTENTS

	Page
ABSTRACT	C2
ACKNOWLEDGEMENTS	C3
CONTENTS	C4
LIST OF SYMBOLS	C5
I. INTRODUCTION	C7
II. MATHEMATICAL FORMULATION OF THE FLOW PROBLEM	C10
III. NUMERICAL METHOD	C14
III-1. Panel Arrangement	C14
III-2. Initial Condition & Velocity Potential	C18
III-3. The Linear Equations for the Source Strengths	C21
III-4. Iterative Procedure and Convergence	C23
IV. RESULTS AND DISCUSSION	C25
V. CONCLUDING REMARKS AND FUTURE WORK	C28
REFERENCES	C30
LIST OF FIGURES	C31

ACKNOWLEDGEMENTS

I am greatly indebted to Professor Lars Larsson, whose informative discussions on the subject are highly valued, and to Dr Leif Broberg for his interest and help in the implementation of the program on the IBM 3090 super computer.

I would also like to thank Mr Hasse Olofsson for his contributions in the generation of input data by the NAPA system and Mr John Olofson for providing good working environment in SSPA's computer.

Thanks are expressed to Mrs Brita Svanberg, Mrs Barbara Karsberg and Mrs Elisabeth Algar, who helped in the plotting and typing of the manuscript.

The financial support from the Swedish Board for Technical Development and the Defence Material Administration of Sweden is gratefully acknowledged. Financial support for K-J Kim was provided by Daewoo Shipbuilding & Heavy Machinery Ltd in Korea.

ABSTRACT

In the present paper a method for calculating the potential flow about ships is described. The problem is discretized by covering the hull and part of the free surface with a large number of source singularities and the variable strengths of these source distributions are adjusted to satisfy the normal velocity boundary condition on the wetted hull surface and the non-linear form of the free surface boundary condition on the wavy surface.

An exact solution is obtained through iterations and in each iteration the free surface boundary condition is linearized, based on the small perturbation principle, about the previous solution.

In contrast to a linear method, a single model with higher order panels both on the hull and the free surface is used and special care has been taken in the generation of panels above the designed load water line to simulate more exact boundary conditions and also in the computation of the velocity potential and the associated derivative terms in the free surface equation.

Converged solutions are obtained after 5-6 iterations for two different hull forms and are compared with measurement data available.

SSPA Report No 2966-1

**A Higher Order Panel Method for Calculating Free
Surface Potential Flows with Non-Linear
Free Surface Boundary Conditions**

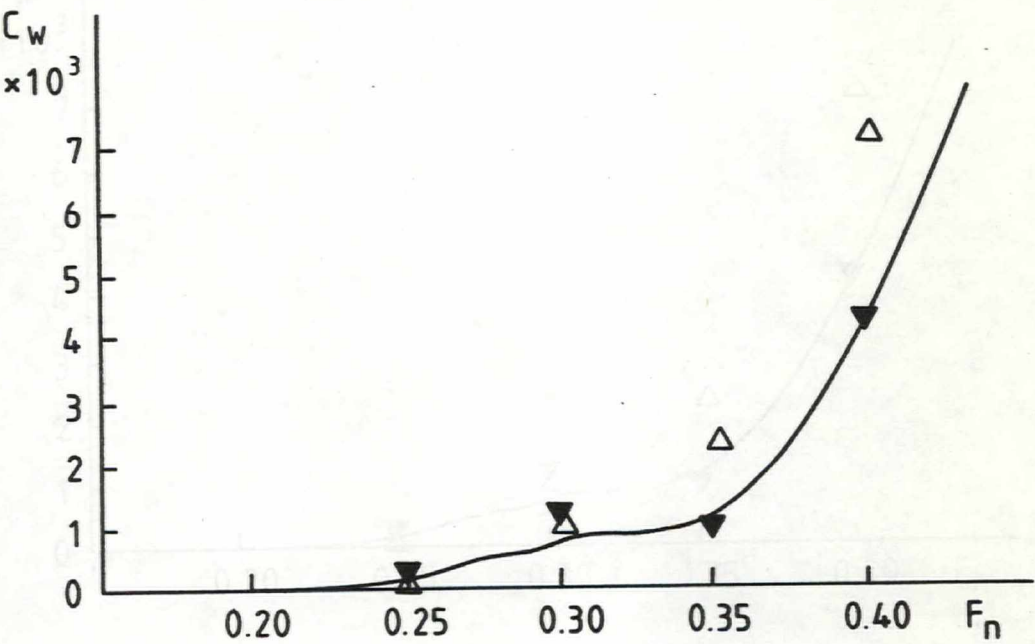
by

Keun Jae Kim

1989-07-07

PAPER C

- Measurement
- △ First order solution
- ▼ Higher order solution

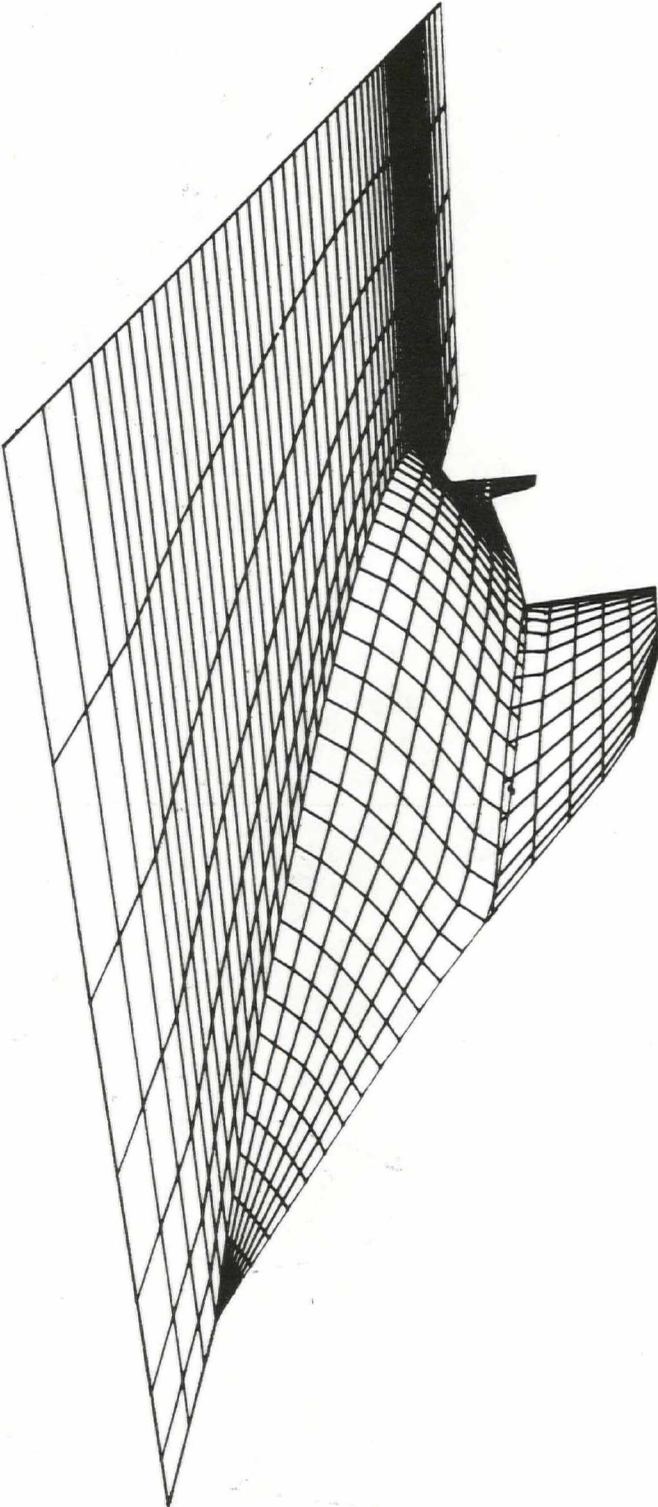


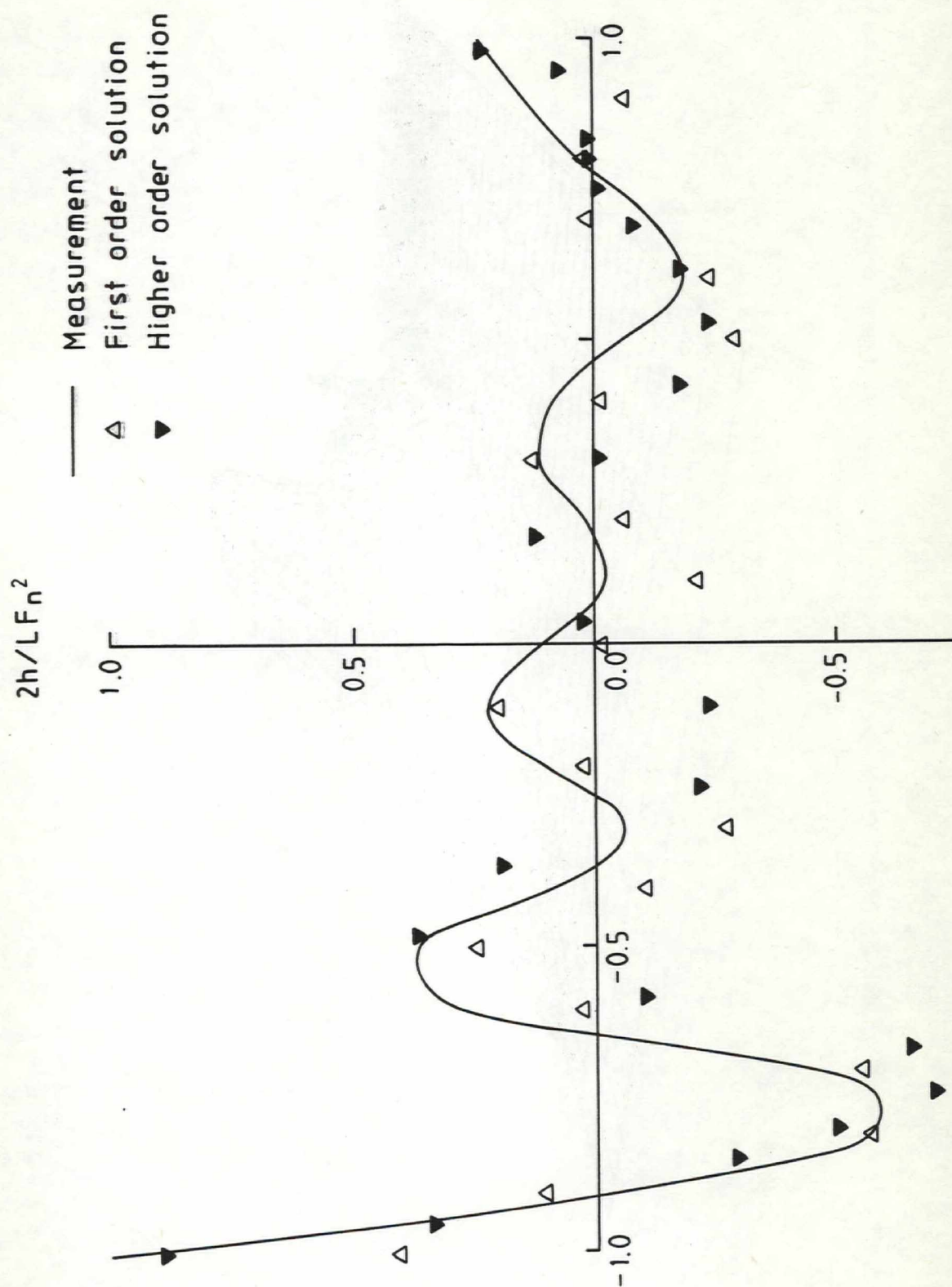
SSPA
&
CTH

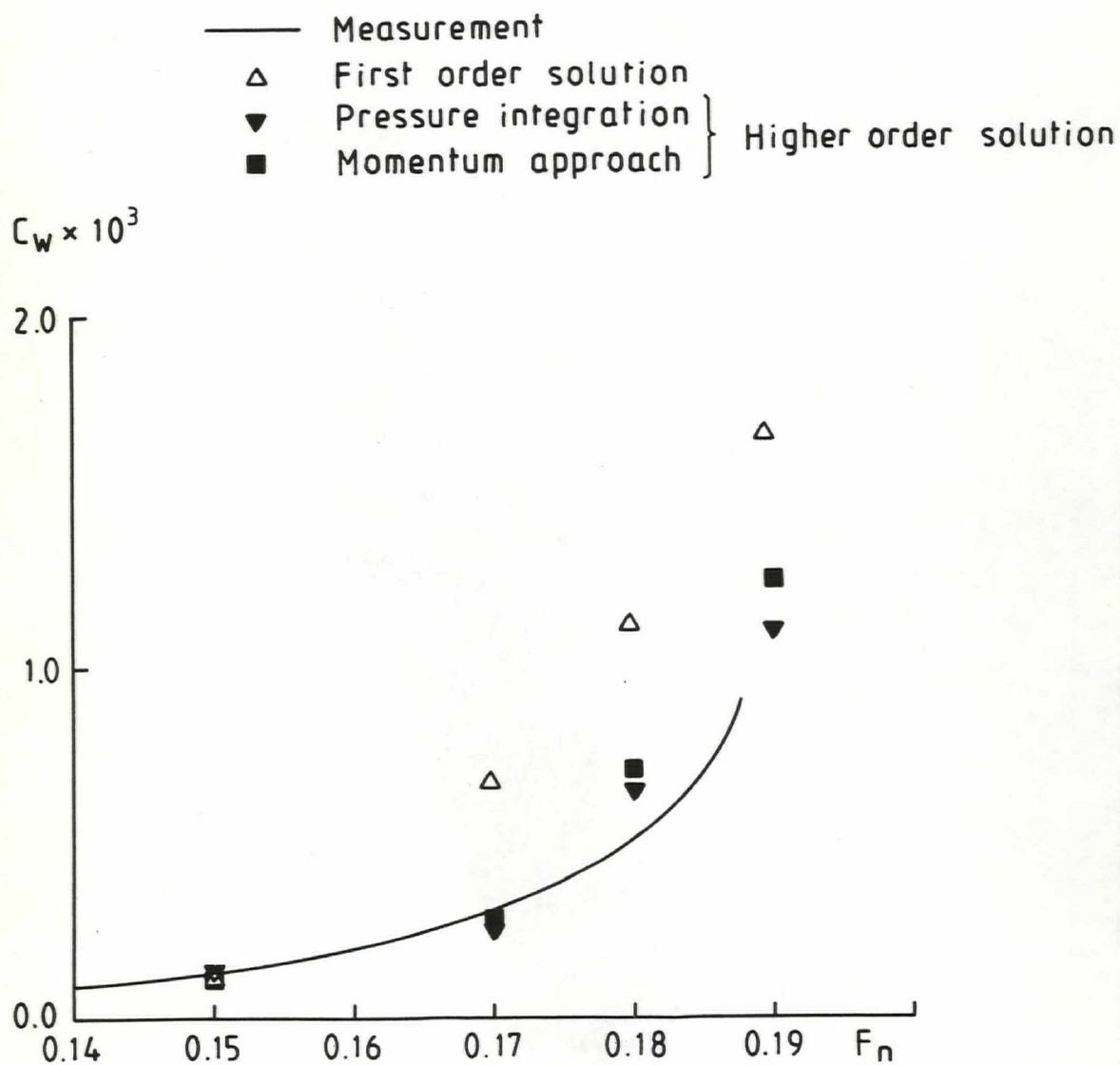
Panel distribution

the 12 M yacht

FIG. 17



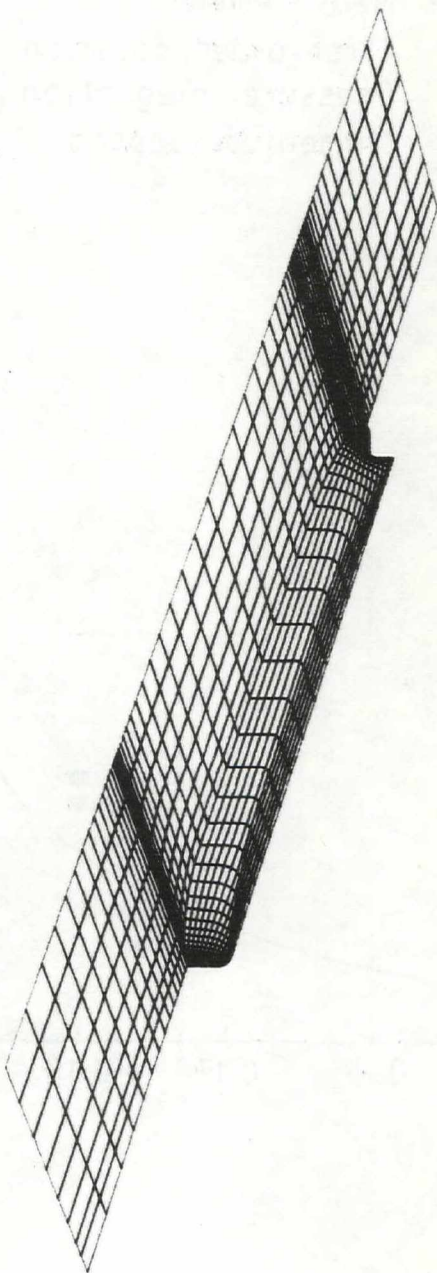


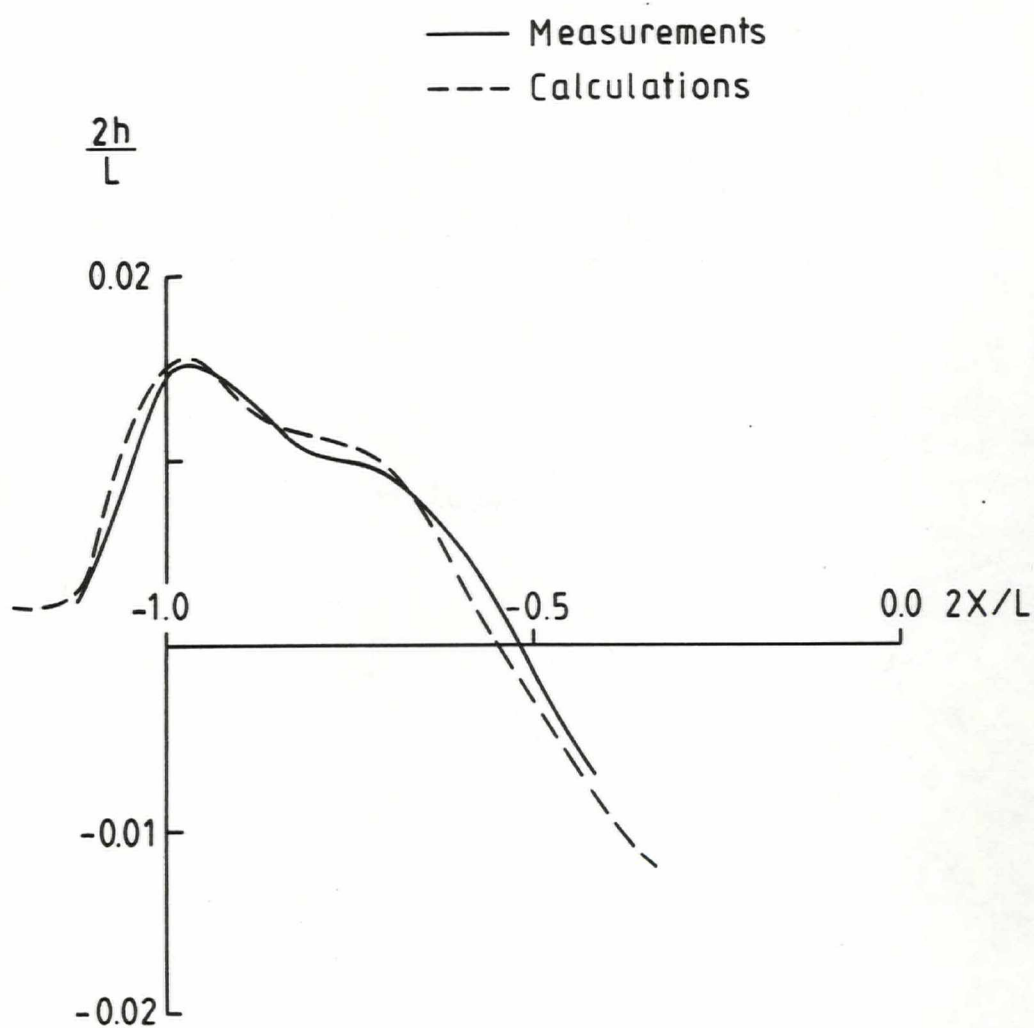


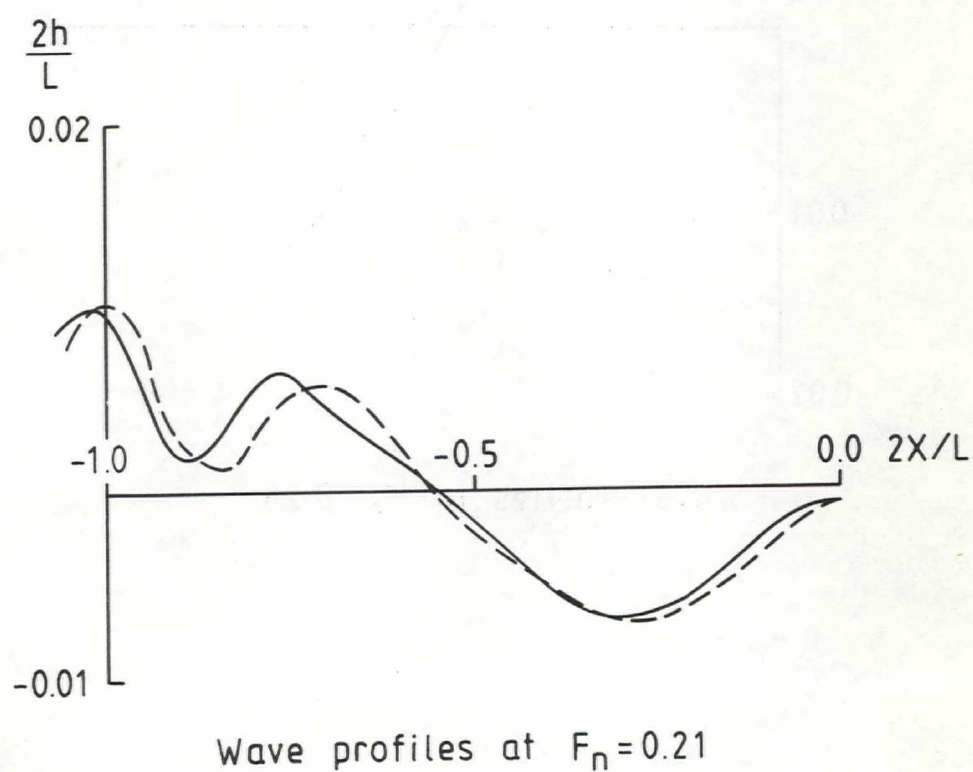
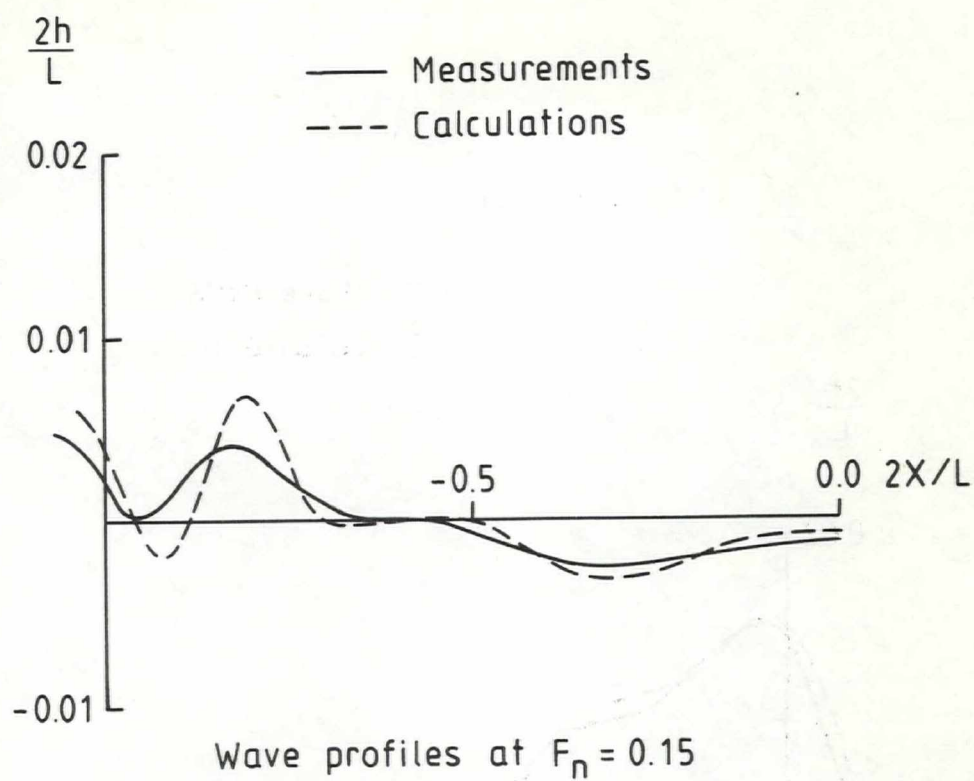
**SSPA
&
CTH**

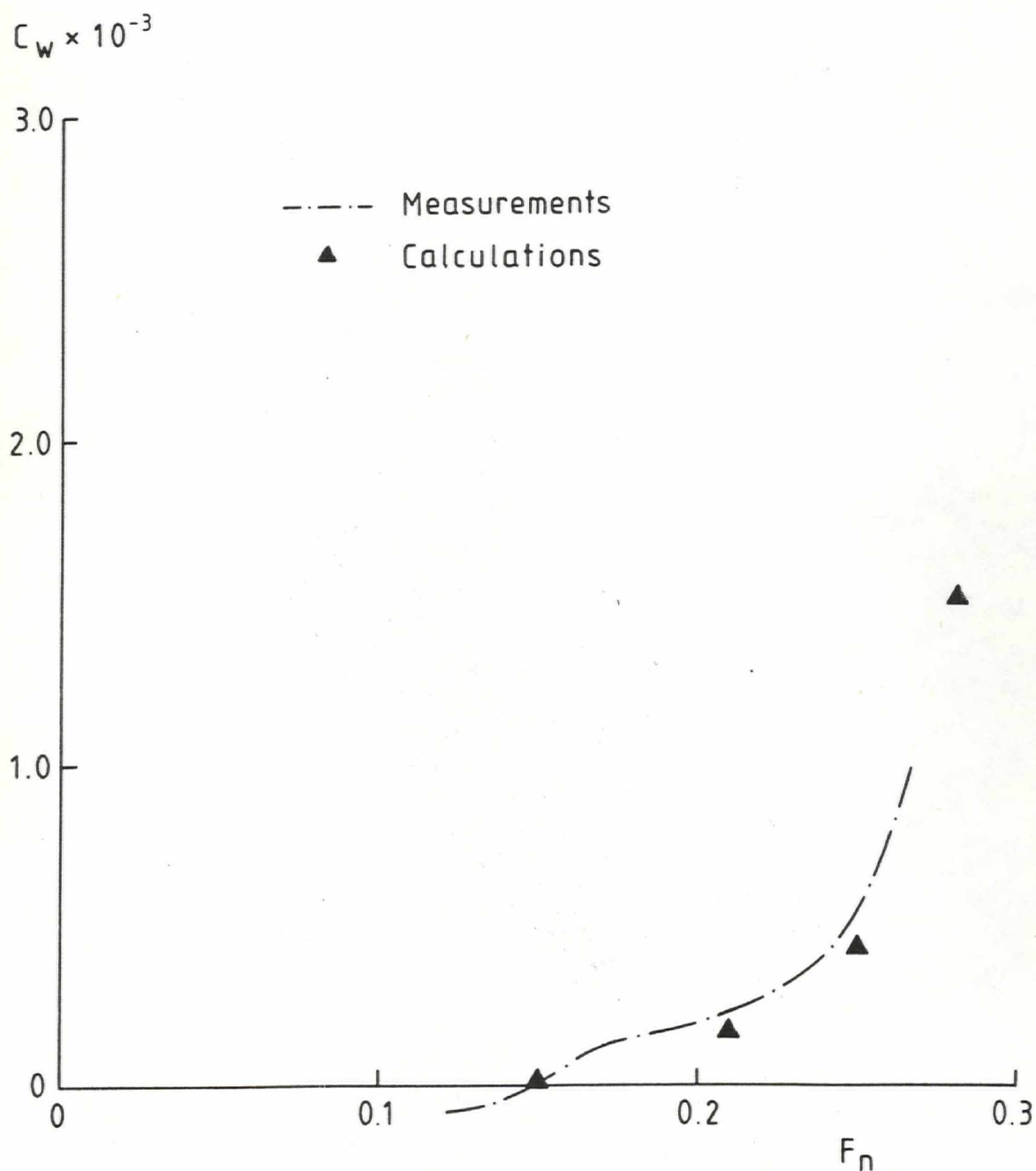
Panel distribution
the HSVA tanker

FIG. 14



Wave profiles at $F_n = 0.28$



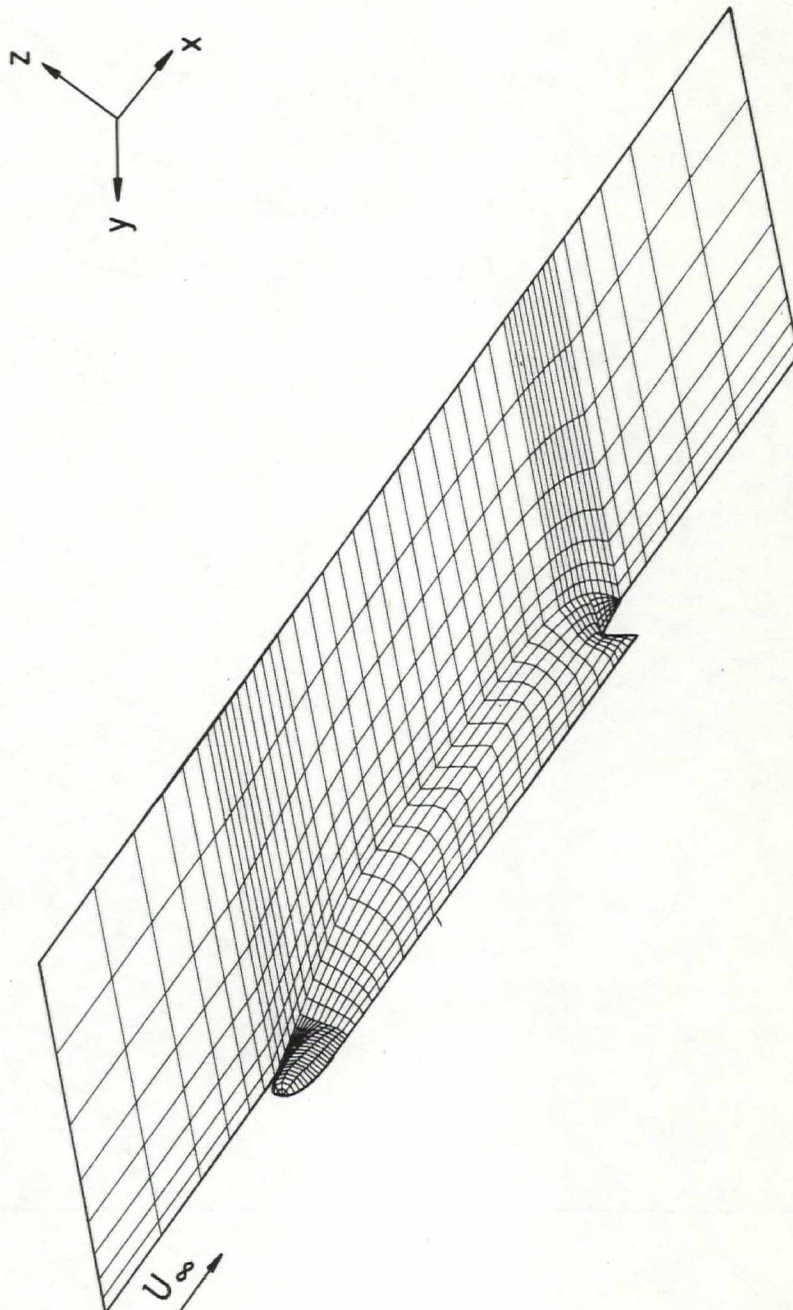


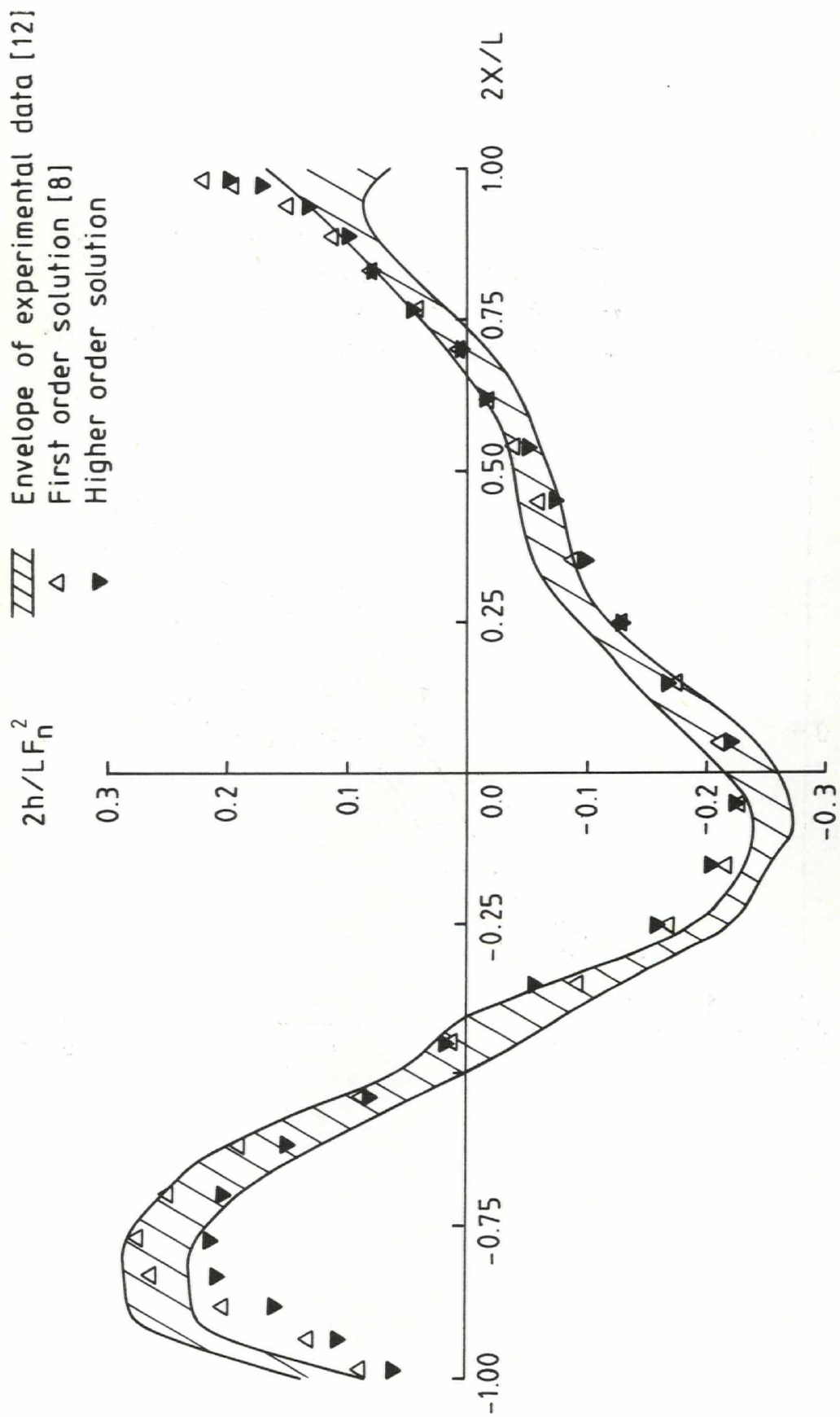
SSPA
&
CTH

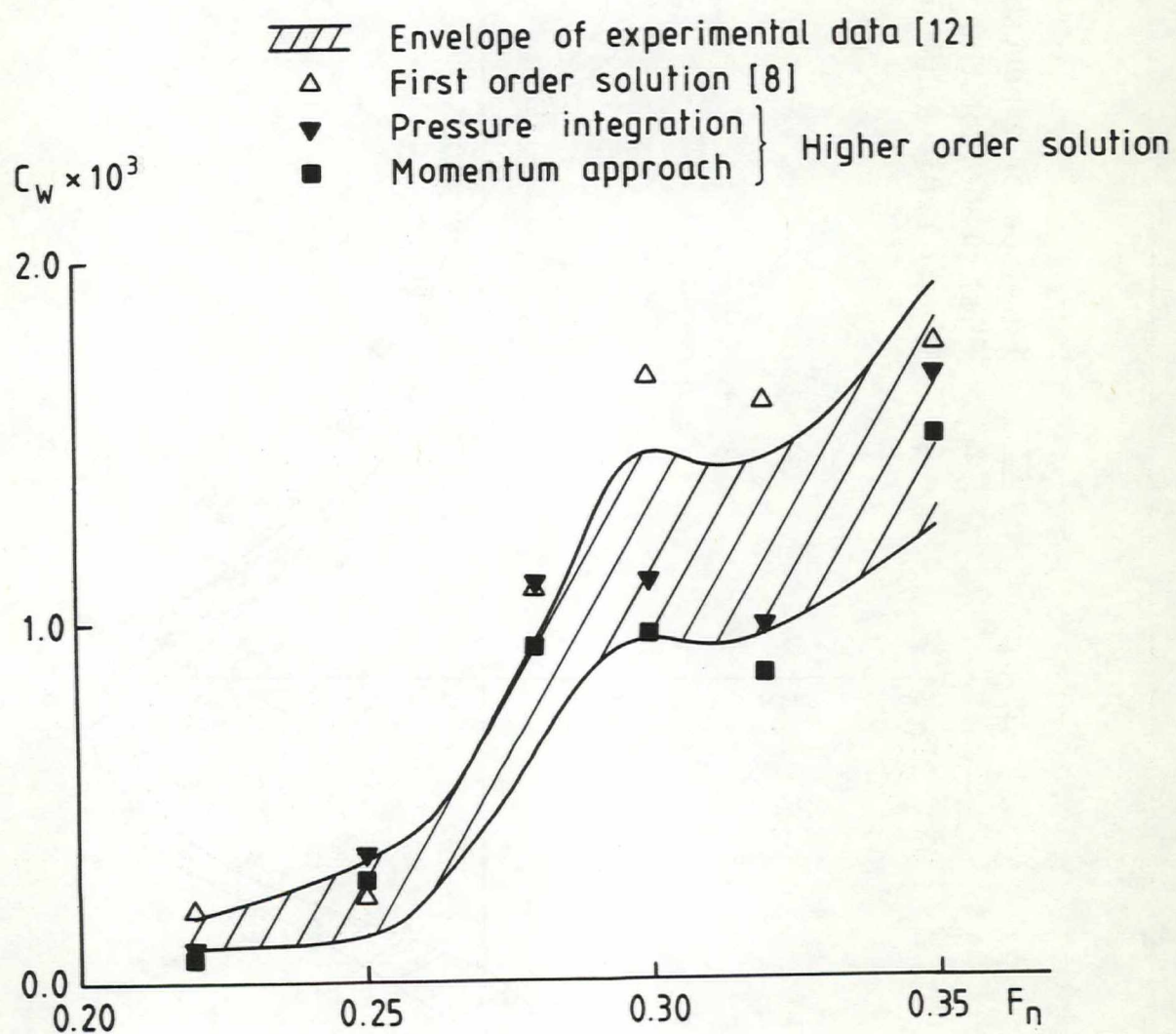
Panel distribution

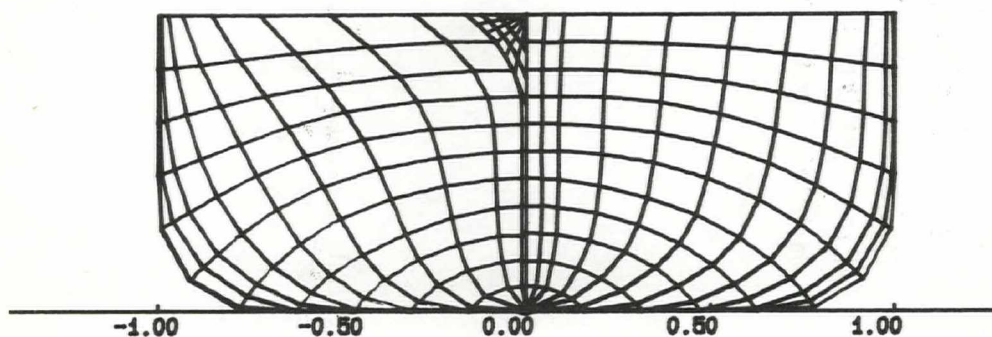
the SSPA Ro-Ro ship (medium bulb)

FIG. 11

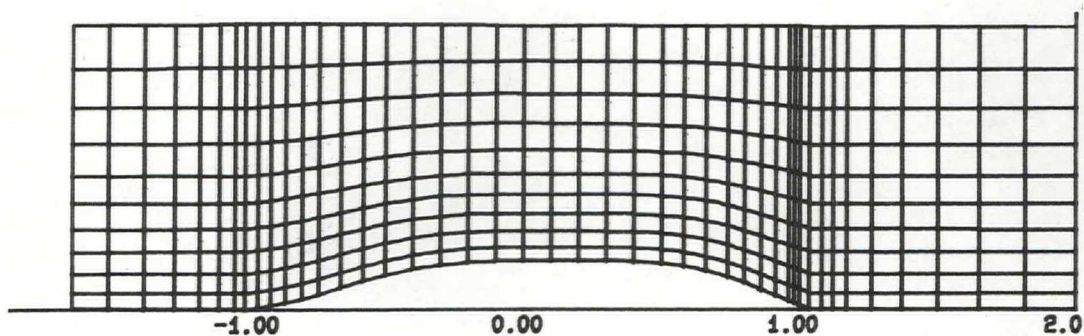




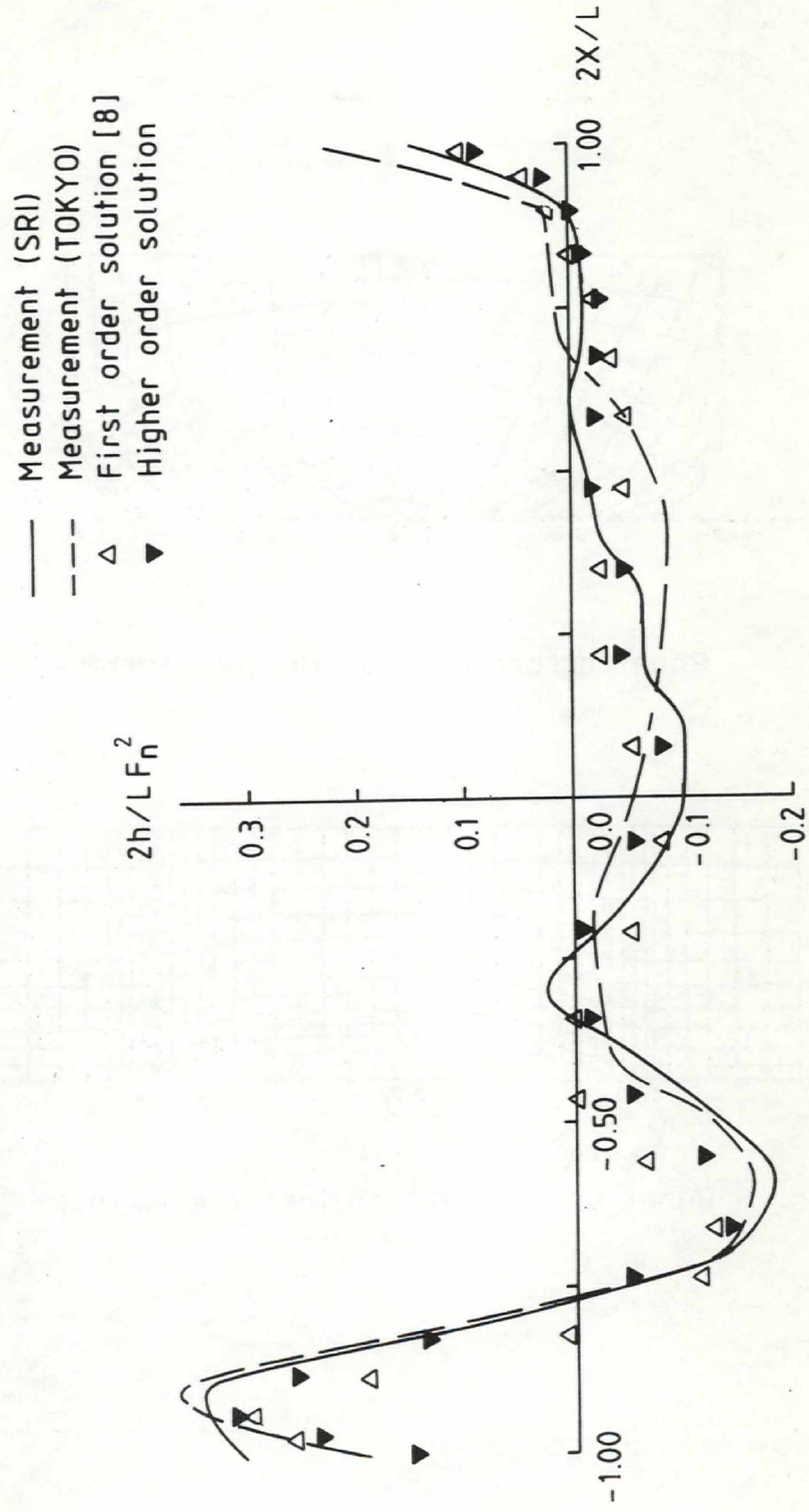


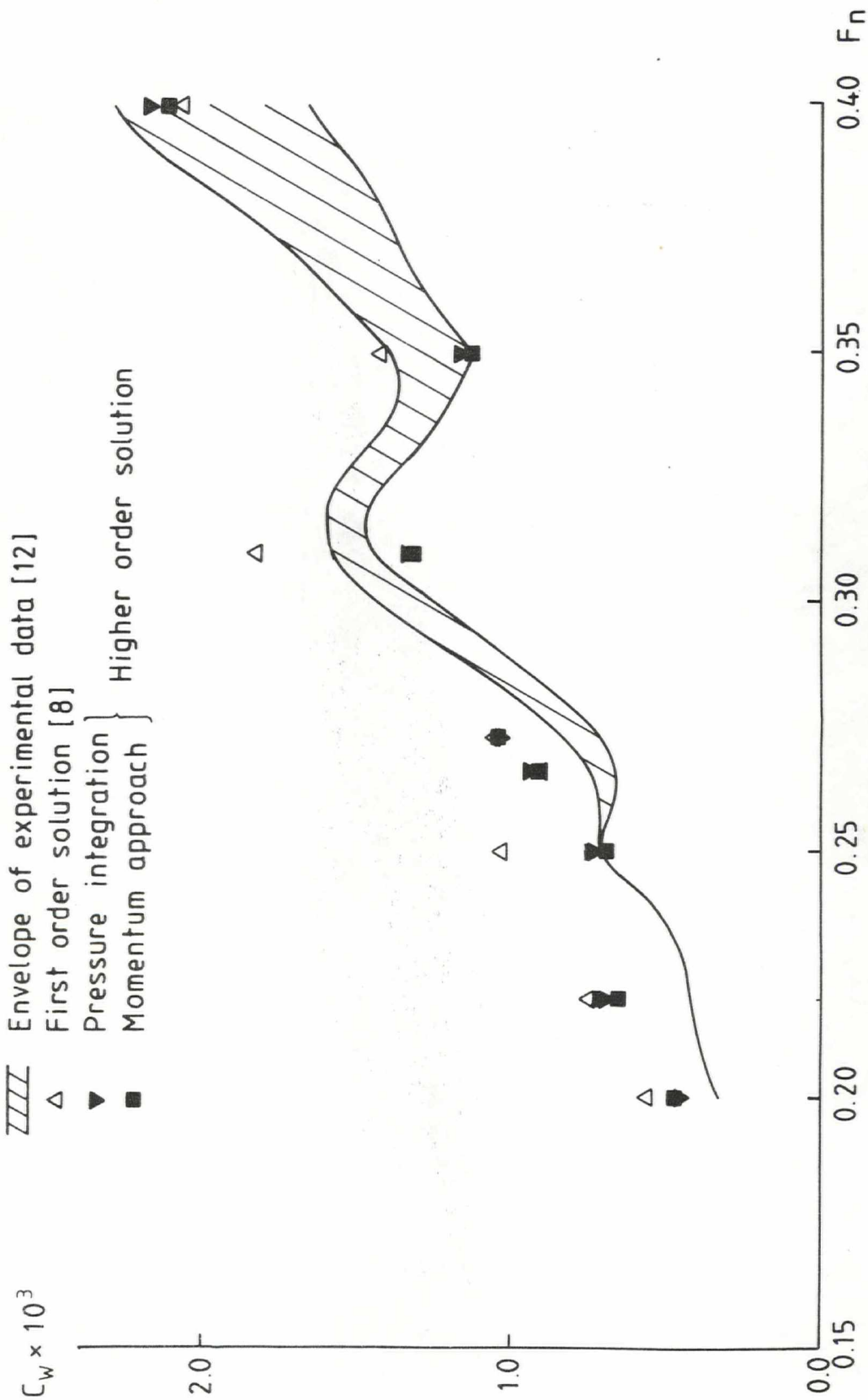


Panel arrangement on the hull surface



Panel arrangement on the free surface

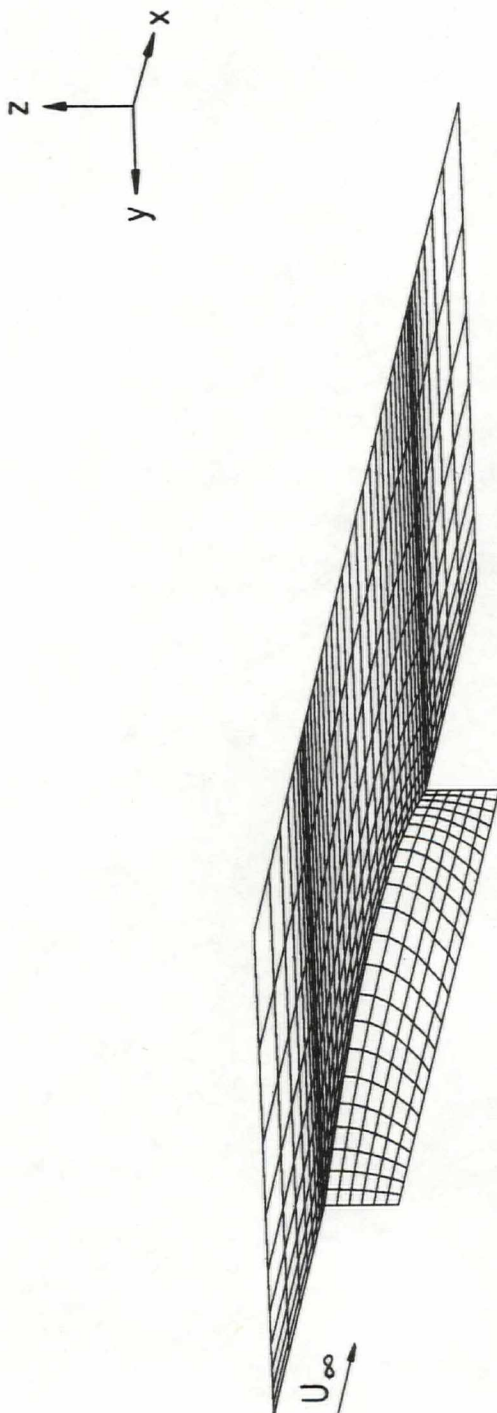


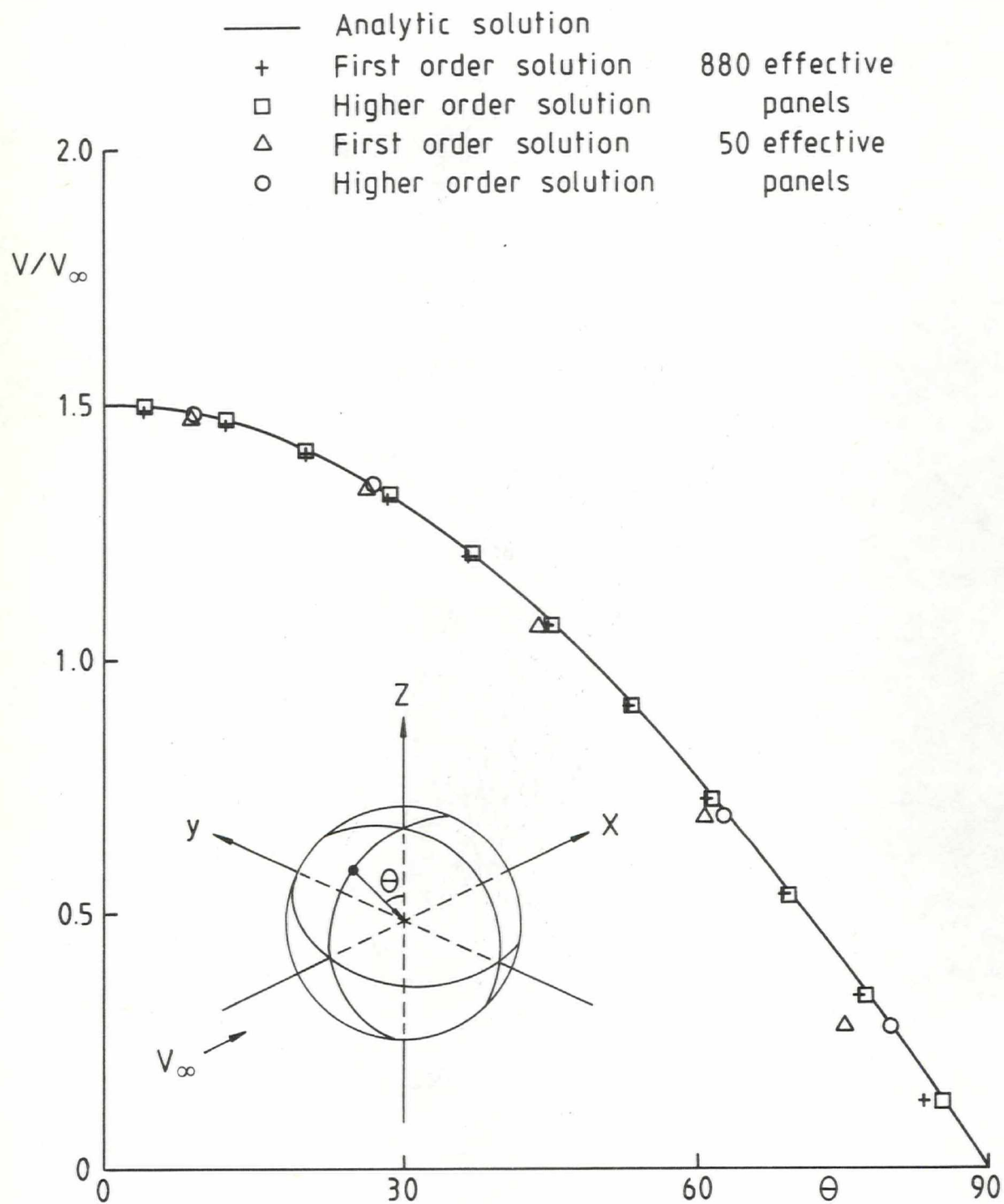


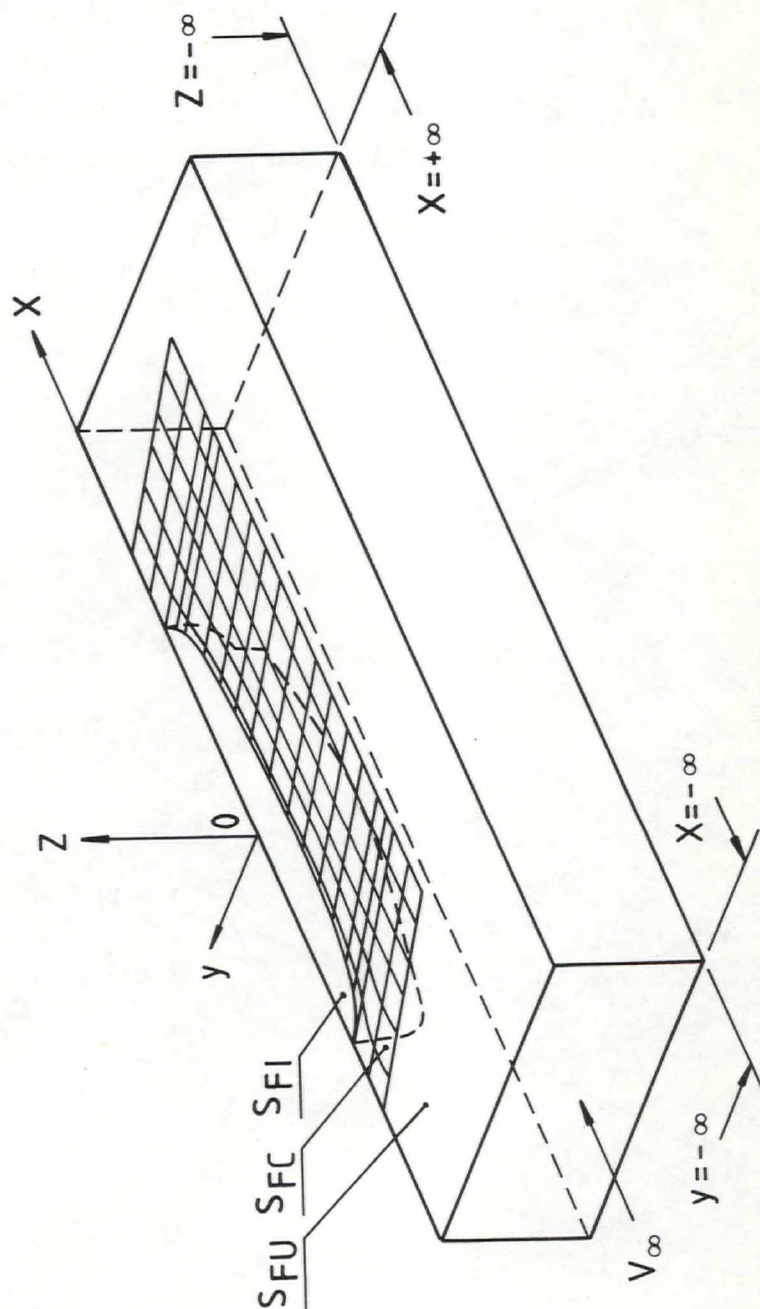
SSPA
&
CTH

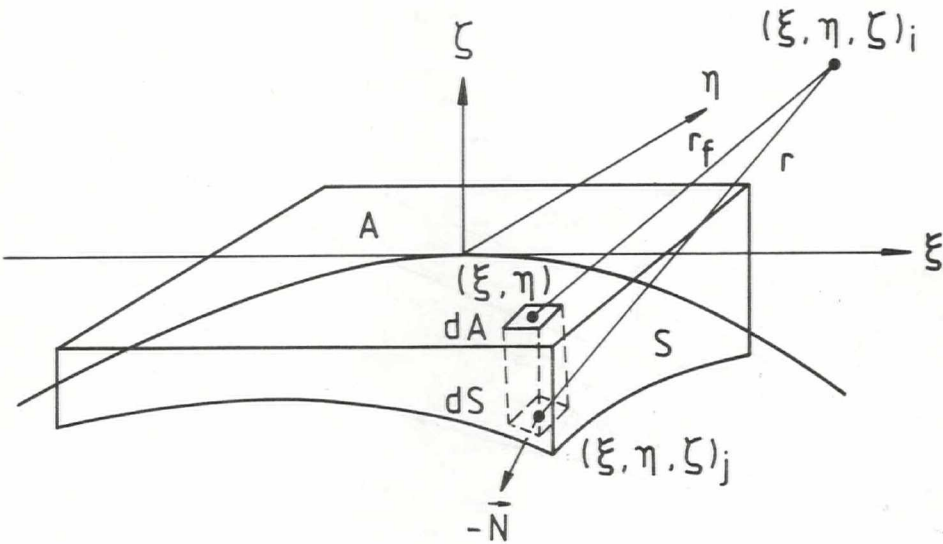
Panel distribution on the hull (22x8)
and free surface (40x10)
The Wiegley hull

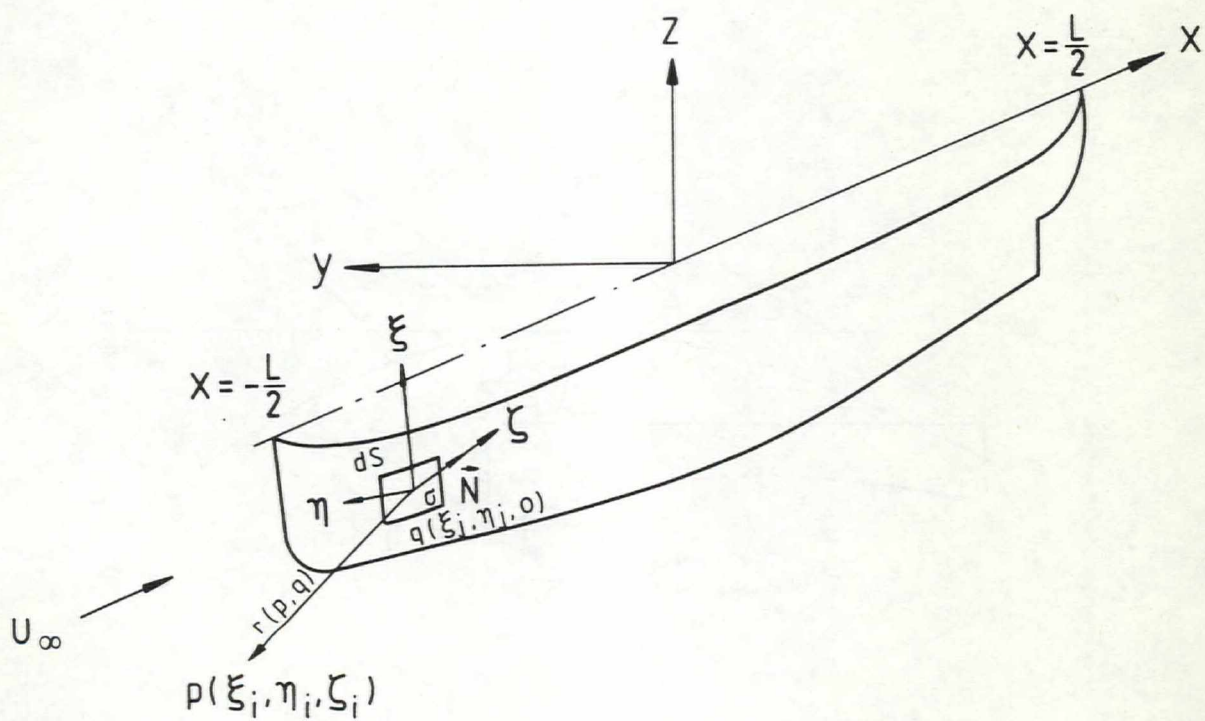
FIG. 5











LIST OF FIGURES

- Fig 1. Co-ordinate systems
- Fig 2. A general curved surface panel and its projection in the tangential plan
- Fig 3. The control volume in the momentum approach
- Fig 4. Comparison of calculated and analytic surface velocities on a sphere
- Fig 5. Panel arrangement for the Wigley hull
- Fig 6. Wave resistance for the Wigley hull
- Fig 7. Wave profile along the Wigley hull at $F_n = 0.22$
- Fig 8. Panel arrangement for the Series 60 hull
- Fig 9. Wave resistance for the Series 60 hull
- Fig 10. Wave profile along the Series 60 hull at $F_n = 0.35$
- Fig 11. Panel arrangement for the SSPA Ro-Ro 2062 with medium bulb
- Fig 12. Wave resistance for the SSPA Ro-Ro 2062 with medium bulb
- Fig 13. Wave profile for the SSPA Ro-Ro 2062 with medium bulb
- Fig 14. Panel arrangement for the HSVA Tanker
- Fig 15. Wave resistance for the HSVA Tanker
- Fig 16. Wave profile along the HSVA Tanker at $F_n = 0,19$
- Fig 17. Panel arrangement for the 12 M yacht
- Fig 18. Wave resistance for the 12 M yacht

Table 1. Dynamic force coefficient of half sphere in uniform flow

Method	First order solution	Higher order solution	Analytic solution
C_x Error %	0.550 12	0.622 0.5	0.625 -

- [9] NI, SHAO-YU: "Higher Order Panel Methods for Potential Flows with Linear or Non-Linear Free Surface Boundary Conditions". PhD Thesis, Chalmers University of Technology, 1987.
- [10] XIA, F., and LARSSON, L.: "A Calculation Method for the Lifting Potential Flow Around Yawed, Surface-Piercing 3-D Bodies". Proceedings of the 16th Symposium on Naval Hydrodynamics, University of California, Berkeley, June, 1986.
- [11] HESS, J.L.: "A Higher Order Panel Method for Three-Dimensional Potential Flow". Douglas Report N62269-77-C-0437, 1979.
- [12] NORRBIN, N.H. (Editor): "The Proceedings of the 17th International Towing Tank Conference", SSPA, Göteborg, 1984.

REFERENCES

- [1] DAWSON, C.W.: " A Practical Computer Method for Solving Ship-Wave Problems". Proceedings of the Second International Conference on Numerical Ship Hydrodynamics, 1977.
- [2] GADD, G.E.: "A Method of Computing the Flow and Surface Wave Pattern around Full Forms". Transactions of the Royal Institution of Naval Architects, 1976.
- [3] BAI, K.J., & MACARTHY, J.H. (Editors): "Proceedings of the First Workshop on Ship Wave Resistance Computations". David W. Taylor Naval Ship Research and Development Center, 1979.
- [4] NOBLESSE, F., & MACARTHY, J.H. (Editors): "Proceedings of the Second Workshop on Ship Wave Resistance Computations". David W. Taylor Naval Ship Research and Development Center, 1983.
- [5] OGIWARA, S.: "A Method to Predict Free Surface Flow around Ship by Means of Rankine Sources". Journal of the Kansai Society of Naval Architects, Japan, Vol 190, 1983.
- [6] RAVEN, H.C.: "Variations on a Theme by Dawson". Proceedings of the Seventeenth Symposium on Naval Hydrodynamics, 1988.
- [7] MUSKER, A.J.: "A Panel Method for Predicting Ship Wave Resistance". Proceedings of the Seventeenth Symposium on Naval Hydrodynamics, 1988.
- [8] XIA, F.: "Numerical Calculation of Ship Flows, with Special Emphasis on the Free Surface Potential Flow". PhD Thesis, Chalmers University of Technology, 1986.

VI. CONCLUSIONS

An effort has been made in the present work to investigate the improvements of panel methods for calculating the double model linearized free surface potential flow around ships. A higher order method which uses curved panels of the second degree with linearly varying source density, has been developed. Numerical calculations have been made for five test cases and compared with experiments. According to these studies the following conclusions can be drawn:

- a. The calculations of the flow around a sphere have shown that for a given accuracy a much fewer number of panels are needed in the higher order method.
- b. A small but distinctive improvement over first order method is achieved by the present method in the prediction of the wave pattern and wave resistance for the Wigley hull and Series 60 ($C_B=0.6$) ship hulls in the Froude number range of 0.20 to 0.40.
- c. For the SSPA Ro-Ro, the HSVA Tanker and the 12 M yacht, the agreement between the wave pattern and wave resistance predicted by the present method and experimental data is much better than for the first order method.

The second test case is the Series 60 hull ($C_B=0.6$) with 249 effective panels on the hull surface and 440 body-fitted panel arrangements on the free surface (see Fig 8). The same tendencies as for the Wigley case can be observed in Figs 9 and 10. The relatively small differences between the first and higher order methods in the two cases may be due to the fact that the hulls are very thin or simple. Larger differences may be expected for more complicated hulls. A more practical study was performed therefore using the SSPA Ro-Ro ship model 2062 with a medium size bulb, the HSVA Tanker and a 12 M yacht.

The panel representation for the SSPA Ro-Ro ship with 1250 effective panel elements is presented in Fig 11. The computed wave resistance coefficient versus ship speed is presented in Fig 12 and compared with the measured residual resistance coefficient. As can be seen from the figure the present method predicted lower wave resistance than measured residual resistance at all speeds. This might be explained by the fact that the residual resistance contains other components like the viscous pressure resistance. However, a good agreement between measured and predicted bow wave profiles can be observed in Fig 13.

Another test case is the HSVA tanker with 1064 effective panel elements shown in Fig 14. It also can be seen in Fig 15 that a much better agreement in wave resistance prediction is obtained, especially when using higher order panel method with the momentum approach. The computed wave profiles (Fig 16) at $F_n = 0,19$ around the bow and stern region are improved considerably but still more improvements are desired.

The 12 M yacht was also tested in the upright position and the panel representations with 805 effective panels is presented in Fig 17. A better agreement with measurement than the first order one [8] can be observed in wave resistance results presented in Fig 18.

IV. RESULTS AND DISCUSSIONS

To illustrate the improvements in accuracy due to the inclusion of higher order effects in the present method, some cases have been tested for which analytic solutions or experimental data are available.

In order to obtain a comparison with an analytic case, the flow around a sphere in an unbounded flow was computed first. One calculation was performed with the higher order method and one with the first order method of reference [8]. Calculated and analytic surface velocities along the curve in the xz plane are compared in Fig 4. The total flow is axisymmetric and a high accuracy solution was obtained by both methods with 880 effective panels. The results of the two methods using a greatly reduced number of panels (50 effective panels) are also shown in Fig 4. In Table I the force coefficient on one half of the sphere is compared with the analytical one. A considerable improvement in accuracy is noted for the higher order method. The first order solution is quite inaccurate in certain regions while the higher order solution is scarcely distinguishable from the exact one.

To investigate the prediction of the wave pattern and wave resistance, a mathematical hull due to Wigley was tested first. A body plan with effective panels (22×6) and the body-fitted panel arrangement (40×10) on the free surface are shown in Fig 5. It can be seen from Fig 6 that the wave resistance obtained by the higher order method generally agrees better with measurements than that of the first order method, especially using the momentum approach.

Comparison between calculations and measurements of the wave profile is made in Fig 7. The wave pattern predicted by the present method is better than the one from the first order method.

In the practical calculation the wave resistance coefficient can be expressed as

$$C_w = - \frac{\sum_{i=1}^{N_F} u_{Bi} w_{Fi} \Delta S_i}{\sum_{i=1}^{N_B} U_\infty^2 \Delta S_i} \quad (48)$$

If it is noted that $w_{Fi} = -2\pi\sigma_i$ Eq (48) can be written

$$C_w = \frac{\sum_{i=1}^{N_F} 4\pi u_{Bi} \sigma_i \Delta S_i}{\sum_{i=1}^{N_B} U_\infty^2 \Delta S_i} \quad (49)$$

Furthermore,

$$u_i = \sum_{j=1}^{N_B+N_F} X_{ij}\sigma_j = \sum_{j=1}^{N_B} X_{ij}\sigma_j + \sum_{j=N_B+1}^{N_F} X_{ij}\sigma_j = u_{Bi} + u_{Fi}$$

$$w_i = \sum_{j=1}^{N_B+N_F} Z_{ij}\sigma_j = \sum_{j=1}^{N_B} Z_{ij}\sigma_j + \sum_{j=N_B+1}^{N_F} Z_{ij}\sigma_j = w_{Bi} + w_{Fi}$$

where index B refers to the hull sources and their images, F to the free surface sources. Because of the double model linearization $w_B=0$ on free surface S_F . Eq (44) now becomes

$$D_w = -\rho \iint_{S_{FC}} u_B w_F dS - \rho \iint_{S_{Fu}} u_B w_F dS - \rho \iint_{S_F} u_F w_F dS \quad (45)$$

If it is imaged that the fictitious flow is generated by the source distribution only on the free surface S_{FC} the conservation of momentum holds also

$$-\rho \iint_{S_F} u_F w_F dS - \rho \iint_{S_{Fi}} u_F w_F dS = 0 \quad (46)$$

where S_{Fi} is the part of the plane $z = 0$ inside the hull. Then it is deduced that

$$w_F = 0 \text{ on } S_{Fu} \text{ and } S_{Fi}$$

because no source is distributed on the two parts S_{Fu} and S_{Fi} . Finally, Eq (45) is reduced to the following expression

$$D_w = -\rho \iint_{S_{FC}} u_B w_F dS \quad (47)$$

The mass conservation equation for the control volume is

$$\iint_S \bar{\mathbf{v}} \cdot \bar{\mathbf{n}} dS = 0 \quad (42)$$

Eq (41) minus Eq (42) multiplied by ρU_∞ yields

$$\iint_S \rho u \bar{\mathbf{v}} \cdot \bar{\mathbf{n}} dS + \iint_S (p + \rho g z) \mathbf{n}_x dS = 0 \quad (43)$$

The free surface S_F consists of two parts: S_{FC} which refers to the part covered by source panels, and S_{Fu} which refers to the rest of the free surface outside S_{FC} . It can be assumed that the front plane, aft plane, both side planes and the lower plane are located infinitely far from the hull. The velocity in these planes is equal to the onset flow U_∞ . Since

$$\iint_S \rho g z \mathbf{n}_x dS = 0$$

and

$$\iint_S p \mathbf{n}_x dS = \iint_{S_B} p \mathbf{n}_x dS = -D_w$$

Equations (8-3) can be simplified as

$$D_w = - \iint_{S_B} p \mathbf{n}_x dS = \rho \iint_{S_F} u \bar{\mathbf{v}} \cdot \bar{\mathbf{n}} dS = - \rho \iint_{S_F} u w dS \quad (44)$$

$$C_w = \int_E (C_{p0} + C_{p\xi} + C_{p\eta}) (a_{11}N_\xi^E + a_{21}N_\eta^E + a_{31}N_\zeta^E) (1+2\psi_z) d\xi d\eta / \int_E (1+2\psi_z) d\xi d\eta \quad (40)$$

2. Momentum Approach

The momentum conservation equation in the x-direction is applied to the control volume within the surface S shown in Fig 3. Note that the interior of the hull is outside the control volume.

$$\iint_S \rho \phi_x \bar{V} \cdot \bar{n} dS + \iint_S (p + \rho g z) n_x dS = 0 \quad (41)$$

where

$$\phi_x = u + U_\infty = \sum_{j=1}^{N_B + N_F} X_{ij} \sigma_j + U_\infty$$

$$\phi_y = v = \sum_{j=1}^{N_B + N_F} Y_{ij} \sigma_j$$

$$\phi_z = w = \sum_{j=1}^{N_B + N_F} Z_{ij} \sigma_j$$

and

$$\bar{V} = (\phi_x, \phi_y, \phi_z)$$

$$C_{p\xi} = \sum_{k=0}^M C_k^{(\xi)} C_{pk}$$

$$C_{p\eta} = \sum_{k=0}^M C_k^{(\eta)} C_{pk}$$

Note here that the wave resistance formula (36) is defined in the reference co-ordinate, while the pressure coefficient (37) is represented in terms of panel element co-ordinates. A transformation between the two co-ordinates thus is required. The elements of this transformation matrix are the components of the three unit vectors along the ξ, η, ζ directions, \bar{T}_1, \bar{T}_2 and \bar{N} .

$$[T] = \begin{bmatrix} a_{11} & a_{12} & a_{13} \\ a_{21} & a_{22} & a_{23} \\ a_{31} & a_{32} & a_{33} \end{bmatrix} = \begin{bmatrix} \bar{T}_1 & T_1 & T_1 \\ T_2 & T_2 & T_2 \\ N_\xi & N_\eta & N_\zeta \end{bmatrix} \quad (38)$$

From Eq (18) the x-component of the unit normal vector in the reference co-ordinate system can be found

$$N_x^R = a_{11}N_\xi^E + a_{21}N_\eta^E + a_{31}N_\zeta^E \quad (39)$$

where the superscripts R and E denote the reference and panel co-ordinate system, respectively. Finally the wave resistance coefficient C_w is

IV-3. Calculation of Wave Resistance

The most common way to obtain the wave resistance is to integrate the x-components of the pressure forces acting on the hull panels.

$$C_w = \int C_p N_x ds / \int ds \quad (36)$$

Application of this approach to a number of full slow ships showed large differences with measurements and the wave resistance for the double model case was often far from zero. To improve the numerical accuracy of the resistance calculation, two different approaches have been tested for a given source density on the hull and the free surface.

1. Higher Order Pressure Integration Method

In the first order panel method, the pressure integration is performed based on the assumption that the pressure and normal direction are constant over each panel. But in practice the pressure coefficient is often found to vary considerably between neighbouring panels. In the present method the pressure and normal direction on each panel are assumed not to be constant but vary continuously. With an analogy to the source density the pressure coefficient on the panel in question is assumed to have the following distribution

$$C_p(\xi, \eta) = C_{p0} + C_{p\xi}\xi + C_{p\eta}\eta \quad (37)$$

where

$$\begin{aligned}
CK_{1i} &= \{ ax_1(GA_i h^\circ_i + GB_i h^\circ_{i+1} + GC_i h^\circ_{i+2} + GD_i h^\circ_{i+3}) \\
&\quad - ax_2(CA_i h^\circ_i + CB_i h^\circ_{i-NL} + CC_i h^\circ_{i-2NL} + CD_i h^\circ_{i-3NL}) \} / 2F_n^2 \\
CK_{2i} &= \{ GA_i h^\circ_i + GB_i h^\circ_{i+1} + GC_i h^\circ_{i+2} + GD_i h^\circ_{i+3} \} / 2F_n^2 \\
CK_{3i} &= - ax_1 \phi_{xi} + \phi_{yi} \\
CK_{4i} &= ax_2 \phi_{xi} \\
VA_{ij} &= \phi_{xi} X_{ij} + \phi_{yi} Y_{ij}
\end{aligned}$$

A similar procedure is followed in the generation of the right-hand side arrays of Eq (33), i e.

For the upper part

$$B_i = - N_{xi} \quad i = 1, \dots, NB \quad (35a)$$

For the lower part

$$\begin{aligned}
B_i &= - CK_{1i} + CK_{1i} \phi_{xi} + CK_{2i} \phi_{yi} \\
&\quad + \frac{CK_{3i}}{2} (GA_i VB_i + GB_i VB_{i+1} + GC_i VB_{i+2} + GD_i VB_{i+3}) \\
&\quad + \frac{CK_{4i}}{2} (CA_i VB_i + CB_i VB_{i-NL} + CC_i VB_{i-2NL} + CD_i VB_{i-3NL})
\end{aligned} \quad (35b)$$

$$i = NB+1, \dots, NE$$

where

$$VB_i = \phi_{xi}^2 + \phi_{yi}^2 - 2\phi_{xi}$$

The complete set of equations (34) and (35) compose a system of NE equations in NE unknown values of σ that is solved by Crout's factorization method. Iterative procedures may not be used, since the matrix of coefficients is not diagonally dominant.

$$[A]\{\sigma\} = \{B\} \quad (33)$$

where $[A]$ is a $NE \times NE$ matrix and $\{B\}$ is the right-hand side array.

The upper part (corresponding to the hull boundary condition) of the A matrix is easily generated by setting

$$A_{ij} = \bar{V}_{ij} \cdot \bar{N}_i = X_{ij}N_{xi} + Y_{ij}N_{yi} + Z_{ij}N_{zi} \quad (34a)$$

$$i = 1, \dots, NB$$

$$j = 1, \dots, NE$$

where NB is again the number of panels on the hull surface. N_{xi} , N_{yi} and N_{zi} are the components of the unit normal vector to the hull surface at i -th panel element. These are the only source equations to be solved in the double model case, in which $NB=NE$.

For the free surface case, the lower part (corresponding to the free surface boundary condition) is generated as follows

$$\begin{aligned} A_{ij} = & CK_{1i}X_{ij} + CK_{2i}Y_{ij} \\ & + CK_{3i}\{ GA_iVA_{ij} + GB_iVA_{i+1j} + GC_iVA_{i+2j} + GD_iVA_{i+3j} \} \\ & + CK_{4i}\{ CA_iVA_{ij} + CB_iVA_{i-NLj} + CC_iVA_{i-2NLj} + CD_iVA_{i-3NLj} \} \\ & + \begin{cases} \pi/F_n^2 & \text{as } i = j \quad i = NB+1, \dots, NE \\ 0 & \text{as } i = j \quad j = 1, \dots, NE \end{cases} \end{aligned} \quad (34b)$$

where

and

$$\begin{aligned}\delta h_x &= ax_1 \delta h_T - ax_2 \delta h_L \\ \delta h_y &= - \delta h_T\end{aligned}\tag{31}$$

where

$$\begin{aligned}ax_1 &= f_L' \\ ax_2 &= - \sqrt{1 + f_L'^2}\end{aligned}$$

Four-point finite difference operators are used to calculate the derivative terms in Eqs (30), (31) along the L and T directions.

$$\begin{aligned}h^{\circ}_{Li} &= CA_i h^{\circ}_i + CB_i h^{\circ}_{i-NL} + CC_i h^{\circ}_{i-2NL} + CD_i h^{\circ}_{i-3NL} \\ h^{\circ}_{Ti} &= GA_i h^{\circ}_i + GB_i h^{\circ}_{i+1} + GC_i h^{\circ}_{i+2} + GD_i h^{\circ}_{i+3} \\ \delta h_{Li} &= CA_i \delta h_i + CB_i \delta h_{i-NL} + CC_i \delta h_{i-2NL} + CD_i \delta h_{i-3NL} \\ \delta h_{Ti} &= GA_i \delta h_i + GB_i \delta h_{i+1} + GC_i \delta h_{i+2} + GD_i \delta h_{i+3}\end{aligned}\tag{32}$$

where NL is the number of the longitudinal strips on the free surface.

The coefficient of the upstream four-point operator (CA_i, CB_i, CC_i and CD_i) and the downstream operator (GA_i, GB_i, GC_i and GD_i) are calculated from the distance between the successive points on the free surface panels, see [8].

As pointed out by Dawson, upstream waves are prevented by the use of upstream finite difference operators.

IV-2. The Linear Equations for the Source Strength

The central problem of the present method of flow calculation is numerical solution of the boundary conditions (4), (12) and (13). These boundary conditions can be transformed into a set of linear algebraic equations in σ as

IV. NUMERICAL METHOD

In the numerical implementation of the present method the first step is to discretize the integration domain S (hull surface + free surface) into a large number of small panels. On the hull, curved panels are employed, while on the free surface $z = 0$ the panels are obviously flat. Over each panel the value of the source density is assumed vary linearly. A double model solution is obtained first by discretizing Eq (4). The free surface is assumed to be a symmetry plane so only the hull panels are considered. This solution yields a set of source strengths, σ_0 , and velocities ϕ_x , ϕ_y , ϕ_z . Thereafter, the free surface solution is obtained by solving the same equation in combination with equations (12) and (13). This yields the final source strength, σ , velocities, ϕ_x , ϕ_y , ϕ_z , and wave height, h . Once the source density is determined the flow velocity and pressure may be calculated at any point. With known pressure and velocity distributions, the wave pattern and the wave resistance can be predicted.

IV-1. Panel Arrangement on the Free Surface

Unlike most other double model linearized free surface methods the present one employs a surface grid, which is independent of the streamlines. A much better resolution at the bow and stern is obtained in the body-fitted grid shown in Fig 5. As can be seen from the figure, the longitudinal lines are smooth arbitrary body-fitted curves $y=f_L(x)$ and the transverse lines are parallel to the y -axis ($y=f_T(x)$). Then the derivative terms in the free surface boundary conditions (12) and (13) may be expressed by finite differences in the two directions of the grid.

$$\begin{aligned} h_x^\circ &= ax_1 h_T^\circ - ax_2 h_L^\circ \\ h_y^\circ &= h_T^\circ \end{aligned} \tag{30}$$

where each individual velocity is the gradient of the corresponding potential, Eq (27).

$$\begin{aligned}
 \bar{V}(\circ) &= \nabla \phi(\circ) \\
 \bar{V}(P) &= \nabla \phi(P) \\
 \bar{V}(Q) &= \nabla \phi(Q) \\
 \bar{V}(R) &= \nabla \phi(R) \\
 \bar{V}(1\xi) &= \nabla \phi(1\xi) \\
 \bar{V}(1\eta) &= \nabla \phi(1\eta)
 \end{aligned}
 \tag{29}$$

All the induced velocities in Eq (29) can be calculated numerically and they may be interpreted as follows: $\bar{V}(\circ)$ corresponds to a flat panel with a constant source density, $\bar{V}(P)$, $\bar{V}(Q)$ and $\bar{V}(R)$ are caused by the parabolic panel shape, $\bar{V}(1\xi)$ and $\bar{V}(1\eta)$ come from the linear variation of the source density.

Special care must be taken in obtaining influence coefficients X_{ij} , Y_{ij} and Z_{ij} , which are the velocity components in the reference co-ordinate system (x,y,z) at the i -th control point, induced by a unit source density on the j -th panel. In the first order method the velocity induced by a panel depends only on the panel itself. The essentially new feature of the higher order method is that the velocity induced by a panel depends on the values of source densities also at the control points of adjacent elements. Thus the influence coefficients for a panel depend not only on the geometry of that panel but also on the geometry of adjacent panels and the assembly of the influence coefficients matrix is more complicated.

Thus the potential of the parabolic panel can be expressed as follows

$$\begin{aligned}
 \phi_{ij} &= \int_{A_j} \frac{1}{r_f} (\sigma_j + \sigma_\xi \xi_j + \sigma_\eta \eta_j) \left\{ 1 + \frac{\zeta_i}{r_f^2} (P \xi_j^2 + 2Q \xi_j \eta_j + R \eta_j^2) \right\} \\
 &\quad (1 + 2\psi_2) d\xi d\eta + \dots \quad (26) \\
 &= \sigma_j \phi(^{\circ}) + \sigma_j \{ p\phi(P) + 2Q\phi(Q) + R\phi(R) \} + \sigma_\xi \phi(1\xi) + \sigma_\eta \phi(1\eta)
 \end{aligned}$$

The individual potentials in Eq (26) are

$$\begin{aligned}
 \phi(^{\circ}) &= \int_{A_j} \frac{1}{r_f} d\xi d\eta \\
 \phi(P) &= \int_{A_j} (\zeta_i \xi_j^2 / r_f^3) d\xi d\eta \\
 \phi(Q) &= \int_{A_j} (\zeta_i \xi_j \eta_j / r_f^3) d\xi d\eta \\
 \phi(R) &= \int_{A_j} (\zeta_i \eta_j^2 / r_f^3) d\xi d\eta \quad (27) \\
 \phi(1\xi) &= \int_{A_j} (\xi_j / r_f) d\xi d\eta \\
 \phi(1\eta) &= \int_{A_j} (\eta_j / r_f) d\xi d\eta
 \end{aligned}$$

The velocity induced by the panel is obtained as

$$\begin{aligned}
 \bar{V} &= \bar{V}(^{\circ}) \sigma_o + [P\bar{V}^{(P)} + 2Q\bar{V}^{(Q)} + R\bar{V}^{(R)}] \sigma_o \\
 &\quad + \bar{V}^{(1\xi)} \sigma_\xi + \bar{V}^{(1\eta)} \sigma_\eta \quad (28)
 \end{aligned}$$

$$\text{where } r^2 = (\xi_i - \xi_j)^2 + (\eta_i - \eta_j)^2 + (\zeta_i - \zeta_j)^2$$

and S is the surface area of the parabolic panel. It is very difficult to carry out direct integration along the curved panel surface. Therefore it is desired to express ϕ in terms of a series of integrals over the projected flat panel. The distance r can be written

$$\begin{aligned} r^2 &= (\xi_i - \xi_j)^2 + (\eta_i - \eta_j)^2 + \zeta_i^2 - 2\zeta_i\zeta_j + \zeta_j^2 \\ &= r_f^2 \{ 1 + (-2\zeta_i\zeta_j + \zeta_j^2)/r_f^2 \} \end{aligned} \quad (23)$$

where r_f is the distance between (ξ_i, η_i, ζ_i) and the point $(\xi_j, \eta_j, 0)$ on the flat panel (Fig 2). Thus

$$\frac{1}{r} = \frac{1}{r_f} \left[1 + \frac{\zeta_i}{r_f} \frac{\zeta_j}{r_f} + \left\{ \frac{3}{2} \frac{\zeta_i^2}{r_f^2} - \frac{1}{2} \right\} \frac{\zeta_j^2}{r_f^2} + \dots \right] \quad (24)$$

Some simpler expressions are obtained in the derivation above by dropping higher order terms than second order of ζ_j which is assumed to be small everywhere on the panel in question.

The elementary surface dS on the parabolic panel is related to the element area $dA = d\xi d\eta$ in the tangent plane by

$$dS = \frac{1}{N_\zeta^E} dA = (1 + 2\psi_2) d\xi d\eta \quad (25)$$

$$\text{where } \psi_2 = (p^2 + Q^2)\xi^2 + 2(pQ + QR)\xi\eta + (Q^2 + R^2)\eta^2$$

and N_ζ^E is the ζ component of the unit normal vector defined in Eq (18).

III-2. Source Distribution

The source density distribution is assumed to be linear on the panel in question

$$\sigma(\xi, \eta) = \sigma_0 + \sigma_\xi \xi + \sigma_\eta \eta \quad (19)$$

This is fitted in the least squares sense to the values of source density at the control points of the M adjacent panels. Thus the source derivatives on the panel in question may be expressed in terms of the unknown values of the source density on the adjacent panels in the form

$$\begin{aligned} \sigma &= \sum_{k=0}^M C_k^{(\xi)} \sigma_k \\ \sigma &= \sum_{k=0}^M C_k^{(\eta)} \sigma_k \end{aligned} \quad (20)$$

The desired source density coefficients $C_k^{(\xi)}$ and $C_k^{(\eta)}$ are obtained by minimizing the error function ϵ

$$\text{Min } \epsilon = \text{Min}_{C_k^{(\xi)} C_k^{(\eta)}} \sum_{k=0}^M [\sigma_k - (\sigma_0 + \sigma_\xi \xi_k + \sigma_\eta \eta_k)]^2 \quad (21)$$

III-3. The Velocity Induced by a Curved Panel

As seen from Eq (1) the perturbation potential ϕ_{ij} at the i-th field point (ξ_i, η_i, ζ_i) induced by the j-th panel on which the source density σ is distributed is

$$\phi_{ij} = \int_{A_j} (\sigma/r) ds \quad (22)$$

control point is characterized by the condition that the vector from the origin is parallel to the local normal vector

$$[\xi' \hat{e}_i + \eta' \hat{e}_j + \zeta'(\xi', \eta') \hat{e}_k] \times [-\zeta'_\xi \hat{e}_i - \zeta'_\eta \hat{e}_j + \hat{e}_k] = \bar{0} \quad (15)$$

This is equivalent to the two scalar equations

$$G(\xi', \eta') = \xi' + \zeta'(\xi', \eta') \zeta'_\xi, (\xi', \eta') = 0 \quad (16)$$

$$H(\xi', \eta') = \eta' + \zeta'(\xi', \eta') \zeta'_\eta, (\xi', \eta') = 0$$

These nonlinear equations are solved by Newton-Ralphson iteration.

Once the control point is determined, the panel co-ordinate system (ξ', η', ζ') is transformed to a new projected flat panel which is tangent to the parabolic panel and the tangent point is both the control point and the origin of new panel co-ordinate system (ξ, η, ζ) see Fig 2. The equation of the panel may be written

$$F(\xi, \eta, \zeta) = \zeta - [P\xi^2 + 2Q\xi\eta + R\eta^2] = 0 \quad (17)$$

There are no constant or linear terms in (17) because the origin is at the tangent point. The normal vector at any point is

$$\begin{aligned} N^E(\xi, \eta) &= N_\xi^E \hat{e}_i + N_\eta^E \hat{e}_j + N_\zeta^E \hat{e}_k \\ &= \{-2(P\xi + Q\eta) \hat{e}_i - 2(Q\xi + R\eta) \hat{e}_j + \hat{e}_k\} / |\text{grad } F| \end{aligned} \quad (18)$$

where \hat{e}_i, \hat{e}_j and \hat{e}_k are the unit vectors of the panel co-ordinate system.

III. HIGHER ORDER PANEL METHOD

The first order method [8] has been applied frequently to investigate the linearized free surface potential flow around the ship and to predict the wave resistance. Most three dimensional ship flow problems, however, need a very large number of panels to represent complicated configurations accurately and long computational time is required. Moreover, the accuracy obtained is not always what is desired. The inaccuracy of the first order method may result partially from the fact that the body surface is represented by flat panels with constant source density and that the pressure and normal direction are assumed to be constant over each panel. In order to increase speed and accuracy a higher order method, using curved panels with varying source density, has been developed. A similar method for flows without a free surface was proposed by Hess [11].

III-1. Definition of the Curved Panel

A parabolic panel is defined in following form

$$\zeta' = Z_0 + A_0 \xi' + B_0 \eta' + P_0 \xi'^2 + 2Q_0 \xi' \eta' + R_0 \eta'^2 \quad (14)$$

where a panel element co-ordinate system (ξ', η', ζ') is constructed using the four corner points. Thus, the origin is defined as the average of the corner points, while the ζ' -direction is normal to the two diagonal vectors. The six parameters $(Z_0, A_0, B_0, P_0, Q_0$ and $R_0)$ are determined from: (a) requiring the panel to pass through the corner points of the panel (four conditions), and (b) requiring the panel to pass as closely as possible, in a least squares sense, to the eight additional input points for the adjacent panels (two additional conditions).

In the present method the control point is the point on curved panel closest to the average point of the four input points. This

In the present calculation, the terms containing the second derivative of velocity potential (ϕ_{xz} , ϕ_{yz} , ϕ_{zz}) are assumed to be small and neglected.

Therefore the linearized boundary conditions are

$$\phi_x h_x^\circ + \phi_y h_y^\circ - \phi_z + \phi_x \delta h_x + \phi_y \delta h_y = 0 \quad (12)$$

$$\delta h = \{ U_\infty^2 + \phi_x^2 + \phi_y^2 - 2(\phi_x \phi_x + \phi_y \phi_y) \} / 2g - h^\circ \quad (13)$$

These conditions are to be applied at $z=0$.

$$\begin{aligned}
D_1(\sigma, h) &\approx D_1(\sigma^\circ, h^\circ) + \Delta D_1(\sigma, h^\circ) + \Delta D_1(\sigma^\circ, h) \approx \\
D_1(\sigma^\circ, h^\circ) + \frac{\partial}{\partial \sigma} D_1(\sigma, h^\circ) \delta\sigma + \frac{\partial}{\partial h} D_1(\sigma^\circ, h) \delta h &\approx 0
\end{aligned} \tag{8}$$

$$\begin{aligned}
D_2(\sigma, h) &\approx D_2(\sigma^\circ, h^\circ) + D_2(\sigma, h^\circ) + D_2(\sigma^\circ, h) \approx \\
D_2(\sigma^\circ, h^\circ) + \frac{\partial}{\partial \sigma} D_2(\sigma, h^\circ) \delta\sigma + \frac{\partial}{\partial h} D_2(\sigma^\circ, h) \delta h &\approx 0
\end{aligned}$$

It is a fundamental assumption of the present method that the perturbations of source ($\delta\sigma$) and wave elevation (δh) are small in certain senses. In a Taylor series, higher order terms in these quantities then become very small and can be neglected.

Here the superscript, $^\circ$, corresponds to the double model solution which is assumed to be known a priori.

$$\begin{aligned}
D_1(\sigma^\circ, h^\circ) &= \phi_x h_x^\circ + \phi_y h_y^\circ - \phi_z = 0 \\
D_2(\sigma^\circ, h^\circ) &= h^\circ - \frac{1}{2g} [U_\infty^2 - (\phi_x^2 + \phi_y^2 + \phi_z^2)] = 0
\end{aligned} \tag{9}$$

where ϕ_x , ϕ_y and ϕ_z mean the velocity components induced by σ° on the undisturbed free surface.

The partial increments of D_1 and D_2 should be found in such a way that a new velocity potential $\phi = \phi + \delta\phi$ induced by introducing small perturbations $\delta\sigma$ and δh should satisfy Eqs (5) and (6) on the new wave surface $h = h^\circ + \delta h$. D_1 and D_2 can be lineary expanded based on σ° and h°

$$\Delta D_1(\sigma, h^\circ) = \delta\phi_x h_x^\circ + \delta\phi_y h_y^\circ - \delta\phi_z \tag{10}$$

$$\Delta D_1(\sigma^\circ, h) = \phi_x \delta h_x + \phi_y \delta h_y + (\phi_{xz} h_x^\circ + \phi_{yz} h_y^\circ - \phi_{zz}) \delta h$$

$$\begin{aligned}
\Delta D_2(\sigma, h^\circ) &= \frac{1}{g} (\phi_x \delta\phi_x + \phi_y \delta\phi_y + \phi_z \delta\phi_z) \\
\Delta D_2(\sigma^\circ, h) &= \delta h + \frac{1}{g} (\phi_x \phi_{xz} + \phi_y \phi_{yz} + \phi_z \phi_{zz}) \delta h
\end{aligned} \tag{11}$$

At the free surface, two boundary conditions must be imposed, i e the flow must be tangent to the free surface

$$\phi_x h_x + \phi_y h_y - \phi_z = 0 \quad (5)$$

and the pressure should be constant

$$gh + \frac{1}{2}(\nabla\phi \cdot \nabla\phi - U_\infty^2) = 0 \quad (6)$$

Further, no upstream waves should be generated.

II-2. Linearization of the Free Surface Condition

The exact problem described in the previous section is nonlinear, since the free surface boundary condition itself is nonlinear and should be exactly satisfied on the wavy surface $z=h(x,y)$, which is unknown, and must be computed as a part of the solution. Thus, numerical methods, which have been applied to solve the problem usually entail some kind of linearization procedure. In the present paper linearization of the free surface condition is performed with respect to the flow at zero Froude number, i e the flow with an undisturbed free surface.

Unknown sources σ on the hull and flat free surface $z=0$ will induce a potential ϕ and a wave elevation h which satisfy the boundary conditions (5) and (6).

$$\begin{aligned} D_1(\sigma, h) &= \phi_x h_x + \phi_y h_y - \phi_z = 0 \\ D_2(\sigma, h) &= h - \frac{1}{2g} [U_\infty^2 - (\phi_x^2 + \phi_y^2 + \phi_z^2)] = 0 \end{aligned} \quad (7)$$

These non-linear forms of the free surface boundary conditions can be linearized by introducing small perturbations $\delta\sigma$ and δh with respect to the double model solution in a first order Taylor expansion.

II. THEORY

II-1. Mathematical Formulation of the Flow Problem

A ship, piercing the free surface, is assumed fixed in a uniform onset flow of velocity U_∞ and the flow is considered inviscid, irrotational and incompressible. Then the flow field around the ship may be described by a velocity potential ϕ which is generated by a certain distribution of sources on a surface S and by the uniform onset flow in the x -direction (see Fig 1).

$$\phi(x,y,z) = \int \sigma(q)/r(p,q)dS + U_\infty x \quad (1)$$

where $\sigma(q)$ is the source density on the surface element dS and $r(p,q)$ is the distance from the point q to the field point $p(x,y,z)$ where the potential is being evaluated.

The potential ϕ is given in Eq (1) is governed by the Laplace equation.

$$\nabla^2 \phi = 0 \quad (2)$$

in the fluid domain and satisfies the regularity condition at infinity

$$\nabla \phi \Rightarrow (U_\infty, 0, 0) \quad \text{as } r \rightarrow \infty \quad (3)$$

The source density σ should be determined from the boundary conditions on the hull and free surface. On the wetted hull surface the solid boundary condition is

$$\phi_n = 0 \quad (4)$$

where n denotes the outward normal to the hull surface.

1. INTRODUCTION

Although research in wave resistance has been a major interest among theoretical ship hydrodynamicists for almost a century it is not until fairly recently that predictions, useful for arbitrary hulls, have become possible. A major break-through was the paper presented by C.W. Dawson at the Second Conference on Numerical Hydrodynamics in 1977 [1]. As had been suggested by Gadd two years earlier [2] the free surface boundary condition could be approximately satisfied by covering part of the undisturbed surface close to the hull by sources. In Dawson's method the boundary condition is linear and the linearization is made about the so called double model solution, obtained assuming a flat free surface. This is a major improvement, as compared to thin ship theory, where the linearization is made about the undisturbed flow.

Since 1977 many organizations have adopted Dawson's method and several papers have been published, see i e [3], [4], [5], [6] and [7]. A considerable effort has been made also at SSPA in the past five years to extend and improve the theory. Much of the work is described in the two PhD theses by Xia in 1986 [8] and Ni in 1987 [9]. Xia investigated the original Dawson method in several respects and extended it to include lifting surfaces [10]. He also started investigations on the inclusion of nonlinear effects in the free surface boundary condition. This work was continued by Ni, who found that higher order accuracy improved the convergence of the nonlinear iterations, so he introduced the higher order technique, first in the linear method and later in the nonlinear method.

In the present paper the extension of the linear Dawson method to include higher order panels and source distributions is described. An improvement in the panelization on the free surface is also presented, as are two alternatives for calculating the wave resistance, knowing the pressure and velocities.

Subscripts and Superscripts

i, j	Subscripts referring to the i -th or j -th panel
ij	Double subscript referring to the effect of the j -th panel at the i -th control point
o	Superscript referring to the double model solution
(o)	Superscript referring to a constant source density
$(P), (Q)$	Superscript referring to a panel curvature
(R)	
$(1\xi)(1\eta)$	Superscript referring to a varying source density

LIST OF SYMBOLS

[A]	Coefficient matrix for the linear equation system
{B}	Right hand side vector for the linear equation system
$A_0, B_0,$ Z_0	Coefficients of linear terms in the expression for the curved panel
CA, CB, CC, CD	Coefficients of the finite difference upstream operator
C_p	Pressure coefficient
C_w	Wave resistance coefficient
F_n	Froude number
GA, GB, GC, GD	Coefficients of the finite difference downstream operator
g	Acceleration of gravity
$h=z(x,y)$	Wave elevation
M	Number of adjacent panels
NB	Number of panels on the body
NF	Number of panels on the free surface
NE	Total number of panels
\bar{N}	Unit normal vector with components (N_x, N_y, N_z) in reference co-ordinates
$\frac{E}{N}$	Unit normal vector with components (N_ξ, N_η, N_ζ) in panel co-ordinates
p	Static pressure
P, Q, R, P_0, Q_0, R_0	Coefficients of quadratic terms in the expression for the curved panel
t	Maximum ζ value of a panel
U_∞	Magnitude of the uniform onset flow velocity
V	Flow velocity with components (ϕ_x, ϕ_y, ϕ_z) or (u, v, w)
[X], [Y]	Matrices of induced velocities
[Z]	
x, y, z	Global reference co-ordinates (see Fig 1)
ϕ	Total velocity potential
Φ	Double model flow velocity potential
σ	Source density

CONTENTS	Page
ABSTRACT	B2
ACKNOWLEDGEMENTS	B3
CONTENTS	B4
LIST OF SYMBOLS	B5
I. INTRODUCTION	B7
II. THEORY	B8
II-1. Mathematical Formulation of the Flow Problem	B8
II-2. Linearization of the Free Surface Condition	B9
III. HIGHER ORDER PANEL METHOD	B12
III-1. Definition of the Curved Panel	B12
III-2. Source Distribution	B14
III-3. The Velocity Induced by a Curved Panel	B14
IV. NUMERICAL METHOD	B18
IV-1. Panel Arrangement of the Free Surface	B18
IV-2. The Linear Equations for the Source Strength	B19
IV-3. Calculation of Wave Resistance	B22
V. RESULTS AND DISCUSSIONS	B28
VI. CONCLUSIONS	B30
REFERENCES	B31
LIST OF TABLES	B33
LIST OF FIGURES	B34

ACKNOWLEDGEMENTS

I wish to express my deep gratitude to Prof Lars Larsson for his guidance and encouragement.

Thanks are also due to Dr. Fei Xia and Dr. Shao Yu Ni who have worked on the subject. Their previous work was highly valued.

Thanks are expressed to Mrs Elisabeth Algar, Mrs Barbara Karsberg and Mrs Brita Svanberg who helped in plotting and typing the manuscript.

The financial support from the Swedish Board for Technical Development and the Defence Material Administration of Sweden is gratefully acknowledged. Financial support for living expense was provided by Daewoo Shipbuilding & Heavy Machinery Ltd in Korea.